Development and Design of Membrane Gas Absorption Processes

P.S. Kumar

2002

Ph.D. thesis
University of Twente

Twente University **Press**

Also available in print:
http://www.tup.utwente.nl/catalogue/book/index.jsp?isbn=9036517486

Development and Design of Membrane Gas Absorption Processes

Samenstelling promotiecommissie:

Prof. dr. A. Brand, voorzitter	Universiteit Twente
Prof. dr. ir. G.F. Versteeg, promotor	Universiteit Twente
Dr. ir. J.A. Hogendoorn, assistent-promotor	Universiteit Twente
Dr. P.H.M. Feron, Referent	TNO-MEP, Nederland
Prof. dr. ir. J.A.M. Kuipers	Universiteit Twente
Prof. dr. Ing. M.H.V. Mulder	Universiteit Twente
Prof. dr. V.G. Pangarkar	University of Mumbai, India
Prof. dr. D.W. Agar	University of Dortmund, Duitsland
Prof. dr. R. Taylor	Universiteit Twente & Clarkson University, VS

The research in this thesis was financially supported by the Centre for Separation Technology, a cooperation between the University of Twente and TNO, the Netherlands Organisation for Applied Scientific Research.

Kumar, P.S.

Development and Design of Membrane Gas Absorption Processes

Thesis, University of Twente, The Netherlands

ISBN 90-36517486

Twente University Press

Publisher: Twente University Press, P.O. Box. 217, 7500 AE Enschede, the Netherlands, www.tup.utwente.nl

Print: Océ Facility Services, Enschede

DEVELOPMENT AND DESIGN OF MEMBRANE GAS ABSORPTION PROCESSES

PROEFSCHRIFT

ter verkrijging van
de graad van doctor aan de Universiteit Twente,
op gezag van de rector magnificus,
prof.dr. F.A. van Vught,
volgens besluit van het College voor Promoties
in het openbaar te verdedigen
op donderdag 6 juni 2002 te 15.00 uur

door

Paramasivam Senthil Kumar
geboren op 9 februari 1974
te Velur (India)

Dit proefschrift is goedgekeurd door de promotor

Prof. dr. ir. G.F. Versteeg

en de assistent-promotor

Dr. ir. J.A. Hogendoorn

To my parents…

Contents

Introduction

Separation of a gas from a mixture by means of absorption in a liquid, either physically or chemically, is an important and economically vital mass transfer operation in the chemical process industry. Though a wide range of gases is removed or separated using the absorption process, their role in the bulk or selective removal of acid gases like CO_2, H_2S, SO_2, etc., commonly known as acid gas treating, is growing at a phenomenal rate. This is partly related to the tremendous increase in the manufacturing capacity of gas based industrial processes (such as natural gas purification, synthesis gas manufacture for chemicals, hydrogen manufacture, refinery fuel gas treating, etc.) and partly due to the stringent environmental regulations towards the emission of acidic gases, over the last few decades.

Most of the gas-liquid contactors used in the industrial absorption processes can be classified into the following three categories.

1. Contactors in which the liquid flows as a thin film (e.g. packed columns, rotating disc contactors)
2. Contactors with dispersion of gas into liquids (e.g. plate columns, bubble columns)
3. Contactors with dispersion of liquid in the gas (e.g. spray columns, venturi scrubbers)

The above classification is rather broad and there are many contactors that overlap the features of more than one category. The mass transfer rate in a gas-liquid contactor depends among others on the mass transfer coefficients (k_L, k_g) as well as the interfacial area available for gas-liquid mass transfer (a). For physical or reactive gas absorption in traditional contactors, the principle resistance to mass transfer usually (except at very low concentrations of the absorbed species in the gas phase) lies in the liquid phase. This is especially true for the absorption of CO_2 in physical or reactive solvents, which is the absorption system of interest in the present research work. Therefore accurate information on the liquid side mass transfer characteristics of the contactors is very critical in the absorber design.

Depending upon the gas-liquid contactor type and operating conditions, there can be a wide variation (several orders of magnitude) in the values of k_L (3.0×10^{-5}-1.0×10^{-3} m s^{-1}) and “a” (20-1000 m^2 m^{-3}; Doraiswamy & Sharma, 1984). Mostly, the gas-liquid contacting becomes unstable at the extreme operating conditions of the contactor (like flooding and loading in packed columns). This means that k_L and “a” cannot be varied over a wide range by merely changing the operating conditions. Moreover, due to the interpenetration of phases, the mass transfer coefficients and interfacial area cannot be varied in isolation, as they are strongly dependent on each other. For a reliable design of the absorber, this necessitates laborious experimental measurements of the above parameters for the different type of contactors and at different operating conditions.

Microporous Membranes in Gas-Liquid Contacting

Microporous membranes can be conveniently used for gas-liquid contacting, in which the membrane does not function as a species selective barrier (as in gas separation using dense membranes); instead the membrane facilitates the generation of the interfacial area for gas-liquid mass transfer. By a suitable choice of the membrane and operating conditions, the phase boundaries are kept stabilised at the pore mouth of the membrane. The resulting

configuration provides a dispersionless gas-liquid contacting in which the interfacial area for mass transfer is essentially the membrane surface area. This offers the following significant advantages over conventional contactors:

1. The mass transfer coefficients and interfacial area for mass transfer can be varied independently;
2. There are no operational limitations like flooding, loading, weeping, etc, which are encountered in various conventional gas-liquid contactors. Also, there are no operational difficulties like foaming which occur during the dispersive contacting of a gas with a viscous liquid;
3. The density difference of the contacting phases, which is a necessity in conventional contactors for the separation of the phases after contacting, is irrelevant for membrane contactors. Consequently, the orientation of the contactor is not an important criterion in the design and it offers tremendous opportunities in offshore applications and life support systems;
4. The interfacial area per unit contactor volume can be an order of magnitude higher than conventional contactors. This is possible with hollow fiber membrane modules where a large number of small diameter (of a few hundred microns) fibers are densely packed in an extremely small volume. Commercially available membrane modules can provide interfacial areas as high as 3000 m^2 m^{-3} (Kreulen et al., 1993a). In these very small diameter hollow fibers, the liquid flows in the laminar regime. Consequently, the mass transfer coefficient is lower than in conventional contactors. Nevertheless, the product of k_L and "a", which is the contactor specific design parameter that influences the absorption rate in a membrane contactor to a large extent, is a few times higher than in conventional contactors;
5. The scale-up of the membrane contactor is linear due to its modular nature;
6. The membrane modules are light in weight, making it ideally suitable for offshore applications.

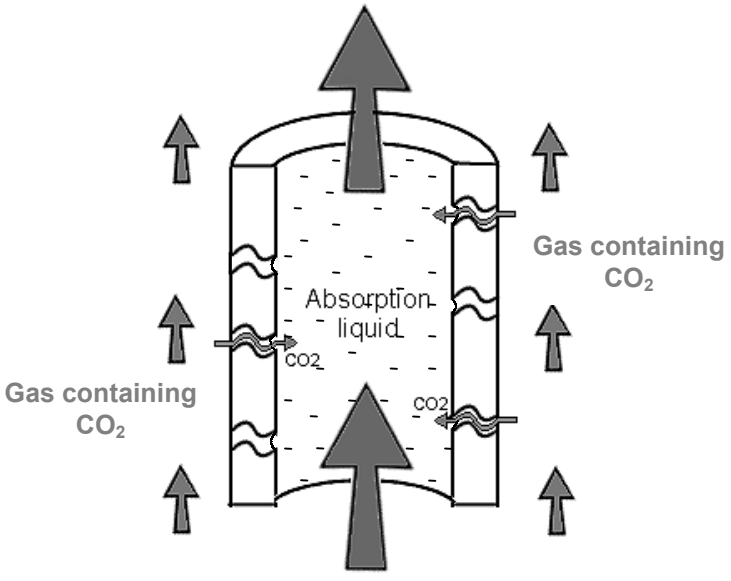

Schematic diagram of CO_2 removal in a hollow fiber membrane contactor

The schematic diagram of a membrane hollow fiber used in gas-liquid contacting is shown above. It can be observed that the liquid is present at the pore mouth of the microporous membrane and the pores are gas filled. This feature is an important criterion for an efficient operation of the contactor, which will be discussed a little later.

Mass Transport in Membrane Contactors

The mass transfer of a chemical species from the gas phase to the liquid flowing inside a hollow fiber membrane can be related to the resistances to mass transfer due to gas phase, membrane and liquid phase respectively. The absorption flux of a species is traditionally defined as,

$$J = K_{ov} \Delta C$$

For well-known reasons, absorption of a gaseous species in the liquid accompanied by chemical reaction is preferred over physical absorption (Kohl & Nielsen, 1997). The overall mass transfer coefficient (K_{ov}) can be related to the individual mass transfer resistance due to gas phase ($1/k_g$), membrane ($1/k_m$) and liquid phase ($1/mk_LE$) respectively, using the traditional "resistances in series" model (Kreulen et al., 1993b).

$$\frac{1}{K_{ov}} = \frac{1}{k_g} + \frac{1}{k_m} + \frac{1}{mk_LE}$$

Here E is the enhancement factor that quantifies the increase in the absorption rate due to chemical reaction and m is the physical solubility of the gaseous species in the absorption liquid. The mass transfer coefficients associated with the gas and liquid phase depend on the respective hydrodynamics. The fiber side hydrodynamics can be accurately described using a mass transfer theory analogous to Leveque's heat transfer problem (laminar flow of a liquid through a circular duct). However the shell side mass transfer characteristics have to be described empirically and is very membrane module specific (Gabelman & Hwang, 1999).

In a porous membrane, two types of diffusive mass transport can be identified: the continuum diffusion, which is determined by the interaction of the different molecules present in the gas and the Knudsen diffusion, when interactions of the molecules with the walls of the pores are dominating. The role of the Knudsen diffusion (smaller than the bulk diffusion coefficient) is important only for gas filled pores having a diameter less than 0.1 micron. The membranes used for gas absorption are microporous (pore diameter: 0.1-1 μm) and therefore the mass transfer of gaseous species through the membrane should be predominantly by bulk diffusion through a stagnant gas (non-wetted) or liquid (wetted membranes) film. Non-wetted membranes are generally preferred for gas-liquid contacting because of the significant difference in the bulk diffusion coefficients of the chemical species in liquid and gas phase. The porosity of the microporous membranes used is very high (70-80%) and therefore the mass transfer resistance due to the membrane is usually negligible.

Therefore, the primary focus of the present investigation is on the liquid side mass transfer with chemical reaction that occurs during the absorption of a gas in a liquid flowing through a membrane hollow fiber. This also necessitates determination of the physico-chemical properties related to the third term ($1/mk_LE$) in the above equation.

CO_2 Removal using Membrane Gas Absorption (MGA)

The application of microporous membranes for gas absorption was explored as early as 1975 for the oxygenation of blood (artificial lung) and is being successfully used today (Sirkar, 1992). However, the thrust to introduce membrane contactors for industrial gas absorption was initiated later by Cussler & his coworkers (Qi & Cussler, 1985a,b). Since then, a number of research groups investigated MGA and numerous processes based on MGA were successfully commercialised. Initial developments of the MGA processes were mostly focussed on using traditional absorption liquids in combination with commercially attractive membrane materials. Only a few important developments in MGA that are related to the removal of CO_2 will be discussed here and more information can be obtained from extensive reviews available in literature (Gabelman & Hwang, 1999; Sirkar, 1997).

A significant amount of the published research work on MGA is related to CO_2 removal, due to the enormous scope for application in the high volume gas treating processes (e.g. offshore natural gas processing) as well as low volume cyclical CO_2 removal/supply processes (e.g. life support systems, supply of CO_2 to green houses). Most of the published information on CO_2 removal is related to the use of liquids of high surface tension such as water, aqueous alkali or alkaline salt solutions, in combination with hydrophobic microporous membranes. However, aqueous alkanolamine solutions are the commonly used absorption liquids in the conventional CO_2 absorption processes. While Qi and Cussler (1985b) had successfully used porous polypropylene membranes (pore diameter: 0.03 μm) for aqueous alkanolamine solutions, Kreulen et al. (1993b) reported wetting by aqueous methyl diethanolamine (MDEA) solutions with microporous polypropylene membranes having a somewhat larger pore diameter (0.2 μm). Nii and Takeuchi (1994) showed that more hydrophobic microporous polytetraflouroethylene (PTFE/Teflon) hollow fibers (maximum pore diameter: 2.0 μm) can be used for various primary, secondary and tertiary aqueous alkanolamines, to overcome wetting of the membrane.

Till date, large scale testing or commercial exploitation of MGA in CO_2 removal has been attempted only by very few. Kvaerner Oil & Gas and W.L. Gore & Associates GmbH are developing a membrane gas absorption process for the removal of acid gases from natural gas and exhausts of the offshore gas turbines (Hanisch, 1999). In this process, PTFE hollow fiber membranes are used in combination with physical (Morphysorb®) or chemical solvents (alkanolamines). TNO Environment Energy and Process Innovation (The Netherlands) is currently developing a MGA process for the removal of CO_2 from flue gases using commercially available and cheaper polypropylene hollow fiber membrane modules. As conventional absorption liquids like alkanolamines have proven to be unsuitable for polypropylene microporous membranes because of wetting, alternative reactive absorption liquids have been developed by them (Feron & Jansen, 1995).

Wetting of Microporous Membranes

A suitable combination of absorption liquid and membrane is critical for the stability of gas-liquid contacting in membrane contactors. For most applications, aqueous solutions are

used as absorbents and therefore, the hydrophobicity as well as pore characteristics of the membrane should be so chosen to ensure gas filled pores under all operating conditions of the membrane contactor. In general, the wettability of a microporous membrane is determined by the interaction between the liquid and polymeric material; with no wetting occurring at low affinity. In simple terms, the contact angle of the liquid with the membrane material should be larger than 90° (Mulder, 1996). For a porous membrane, the minimum pressure required for the liquid to penetrate into the pores of a membrane is dependent on the maximum pore diameter (d_{max}), the surface tension of the liquid (γ_L) and surface energy of the membrane material (θ), and is given by the Laplace equation.

$$\Delta p = - \frac{4\gamma_L \cos\theta}{d_{max}}$$

Below are several possible strategies to overcome membrane wetting using more or less traditional absorption liquids, some of them being already explored by various researchers.

1. Selection of *membrane materials compatible with the absorption liquid* used. For example, PTFE/Teflon membranes can be used in combination with aqueous alkanolamines (Nii & Takeuchi, 1994). However, PTFE hollow fibers are more expensive than polyolefin fibers and very small diameter (< 500 μm) hollow fibers are not commercially available.
2. Reduction of the *maximum pore diameter* of the membrane. Though the critical entry pressure of the liquid is inversely related to the maximum pore diameter, beyond a certain limit, the increase in Δp can be achieved only at the cost of the reduced transport of the gas through the membrane due to the Knudsen flow. This can be calculated beforehand rather accurately, as described in Mulder (1996).
3. Use of absorption liquids having a *high surface tension* for a given hydrophobic membrane. Traditional absorption liquids like aqueous alkanolamines are organic substances dissolved in water. Consequently, these liquids have a surface tension significantly lower than that of water and they wet polyolefin membranes. Therefore, new non-wetting absorption liquids with comparable absorption qualities as alkanolamines can be developed.
4. *Surface treatment* of the membrane. Nishikawa et al. (1995) increased the hydrophobicity of the polyethylene membrane by pretreatment with a fluorocarbonic material. However, the improvement was found to be a temporary phenomenon only.
5. Controlling the *transmembrane pressure difference* (Δp). The wetting can be avoided by controlling the gas side pressure with reference to the liquid side pressure or *vice-versa*. However, this is difficult to implement in practice due to the significant pressure drop across the length of the fiber. Any malfunction in the pressure control has the serious risk of one of the phases being dispersed in the other.
6. The liquids can be physically prevented from entering the pores of the membrane by *coating a very thin layer of dense membrane* (say polydimethylsiloxane or silicone skin) on the liquid side of the microporous membrane. This strategy could be advantageous only if the resistance to mass transport of a gas (this basically depends on the permeability of the gas through the dense membrane) through the dense membrane is

much lower than the mass transfer resistance associated with transport through the liquid filled pores. This also necessitates ultra thin coating of a desired polymer on the desired side of the microporous hollow fiber, which can become a challenging and expensive task if it is to be done on the inner side of the hollow fiber.

Poddar et al. (1996) made an investigation on the removal of volatile organic compounds from gas streams using hydrocarbon absorption liquids and microporous polypropylene membrane coated with a thin silicone skin, on the liquid side of the membrane. Based on the experimental results, the authors concluded that the additional mass resistance of the liquid filled pores (in the absence of a silicone skin) was less than that of a highly (selective) gas permeable, but absorbent blocking dense membrane skin on the porous fiber.

This thesis titled "*Development and Design of Membrane Gas Absorption Processes*" is focussed on the development of stable membrane gas-liquid contactors for the removal of CO_2 from industrial gas streams (preferably flue gas). Of the various strategies discussed above to overcome wetting, concept 3 was explored in detail by developing and studying new reactive absorption liquids that can be used in combination with relatively cheap and commercially available polypropylene membranes. In the present work, the CORAL (CO_2 Removal Absorption Liquid) liquids, based on the alkaline salts of amino acids (developed and patented by TNO; Feron & Jansen, 1998) was investigated in detail to explore their scope for application in acid gas treating processes in general and membrane contactors in particular. The potassium salt of Taurine (2-aminoethansulfonicacid) was used as a model amino acid salt in the present investigation.

In chapter **one**, the physico-chemical and transport properties of CO_2 in aqueous potassium salts of taurine and glycine, measured indirectly using N_2O as a model gas, are given over a wide range of amino acid salt concentrations and temperatures. The physico-chemical and transport data are important in the interpretation of the kinetic measurements of the reaction between CO_2 and aqueous amino acid salts as well in the design of membrane contactors.

The information in the literature on the kinetics of the reaction between CO_2 and aqueous alkaline salts of amino acids is very limited and only available in the range of very low amino acid salt concentrations; a range not particularly suited for acid gas treating applications. Chapter **two** deals with the measurement of the reaction kinetics in a stirred cell with a flat gas-liquid interface, for aqueous potassium salts of taurine and glycine over a wide range of amino acid salt concentrations. The temperature influence on the reaction kinetics was studied for taurine at near absorber conditions. The traditional reaction mechanisms, such as the zwitterion mechanism proposed for the reaction of CO_2 with amines, were used to analyse the experimental kinetic data and develop the reaction rate expression.

Absorption of CO_2 in certain amino acid salts results in crystallisation of reaction product(s), as reported recently by Hook (1997). However, the relation between CO_2 loading (mole CO_2 per mole of Amino acid salt) at which crystallisation occurs and the type and concentration of amino acid salt is not known clearly. Crystallisation was also encountered during the

absorption of CO_2 in aqueous potassium salt solutions of taurine, which was studied in detail and is discussed in Chapter **three**. The identity of the crystallising solid was determined and a semi-quantitative study on the influence of various process parameters that affect crystallisation was carried out. The influence of the formation of crystals on the liquid side mass transfer characteristics of the gas-liquid contactor (stirred vessel in the present case) was also investigated.

Information on the vapor-liquid equilibria of CO_2-aqueous amino acid salts is very important in the design of membrane gas absorbers. In Chapter **four**, experimental data on the solubility of CO_2 in aqueous potassium taurate solutions are presented for 298 and 313 K over a wide range of amino acid salt concentrations. The favorable influence of crystallisation of a reaction product on the CO_2 absorption capacity was quantitatively studied. This phenomenon can form the basis for the development of a new range of reactive absorption liquids for the CO_2 removal, where crystallisation can be advantageously used in enhancing both bulk CO_2 absorption capacity and equilibrium driving force for mass transfer by many folds. The experimental equilibria data measured in the absence of crystallisation were fitted to the traditional CO_2-amine equilibrium models to obtain the equilibrium constants necessary for the design of the MGA process.

Chapter **five** deals with the performance of the new absorption liquids for CO_2 removal in the MGA process. The wetting and non-wetting characteristics of aqueous alkanolamines and aqueous amino acid salt solutions respectively were quantified by measuring the surface tension of the liquid and critical entry pressure (Δp) of the absorption liquids in a flat sheet, microporous polypropylene membrane. The performance of the new absorption liquids developed for CO_2 removal in membrane contactors was studied in a single hollow fiber membrane contactor. A numerical model to describe the mass transfer accompanied with multiple chemical reactions occurring in the liquid phase, during the absorption of CO_2 in aqueous amino acid salt solutions flowing through the hollow fiber was developed. The model was used to indirectly validate the kinetic, physico-chemical and equilibrium data measured experimentally in the earlier chapters and also to compare the predictions to a limited number of experimental data from a pilot MGA unit.

The approximate solutions for the enhancement factor (E) required to predict the influence of a chemical reaction on the mass transfer rate, developed originally for a gas-liquid system with a liquid bulk was adopted in Chapter **six**, to the reactive absorption of a gas in a liquid flowing through the hollow fiber (where no liquid bulk is present; but a velocity gradient is present in the mass transfer zone). The explicit approximate solution of DeCoursey (1974) for an irreversible second order reaction was used as a case study. The limitations of the approximate solutions and their accuracy in comparison to the exact numerical solution for the enhancement factor and experimentally measured values were investigated. It is shown that the approximate solutions in combination with a single fiber membrane contactor (as applied in Chapter five) can be conveniently used as a model gas-liquid contactor to measure various physical, chemical and kinetic properties of reactive gas-liquid systems in general.

References

DeCoursey, W.J. (1974). Absorption with chemical reaction: development of a new relation for the Danckwerts model. *Chemical Engineering Science*, **29**, 1867-1872.

Doraiswamy, L.K., & Sharma, M.M. (1984). *Heterogeneous Reactions: Analysis, Examples, and Reactor Design. Volume 2: Fluid-Fluid-Solid Reactions*. Singapore: John Wiley.

Feron, P.H.M., & Jansen, A.E. (1995). Capture of carbon dioxide using membrane gas absorption and reuse in the horticultural industry. *Energy Conversion & Management*, **36(6-9)**, 411-414.

Feron, P.H.M. & Jansen, A.E. (1998). Method for gas absorption across a membrane. US Patent No. US5749941.

Gabelman, A., & Hwang, S.T. (1999). Hollow fiber membrane contactors. *Journal of Membrane Science*, **159**, 61-106.

Hanisch, C. (1999). Exploring options for CO_2 capture and management. *Environmental Science & Technology*, **33(3)**, 66A-70A.

Hook, R.J. (1997). An Investigation of some sterically hindered amines as potential carbon dioxide scrubbing compounds. *Industrial & Engineering Chemistry Research,* **36(5)**, 1779-1790.

Kohl, A. L., & Nielsen, R.B. (1997). *Gas Purification*: 5th ed. Houston: Gulf Publishing Company.

Kreulen, H., Versteeg, G.F., Smolders, C.A., & van Swaaij, W.P.M. (1993a). Microporous hollow fiber membrane modules as gas-liquid contactors. 1. Physical mass transfer processes - A specific application – Mass transfer in highly viscous liquids. *Journal of Membrane Science*, **78(3)**, 197-216.

Kreulen, H., Versteeg, G.F., Smolders, C.A., & van Swaaij, W.P.M. (1993b). Microporous hollow fiber membrane modules as gas-liquid contactors. 2. Mass transfer with chemical reaction. *Journal of Membrane Science*, **78(3)**, 217-238.

Mulder, M. (1996). *Basic Principles of Membrane Technology*. 2nd Ed., Dordrecht: Kluwer Academic.

Nii, S., & Takeuchi, H. (1994). Removal of CO_2 and SO_2 from gas streams by a membrane absorption method. *Gas Separation & Purification*, **8(2)**, 107-114.

Nishikawa, H., Ishibashi, M., Ohta, H., Akutsu, N., Matsumoto, H., Kamata, T., & Kitamura, H. (1995). CO_2 removal by hollow fiber gas-liquid contactors. *Energy Conversion & Management*, **36(6-9)**, 415-418.

Poddar, T.K., Majumdar, S., & Sirkar, K.K. (1996). Membrane-based absorption of VOCs from a gas stream. *AIChE Journal*, **11**, 3267-3282.

Qi, Z., & Cussler, E.L. (1985a). Microporous hollow fibers for gas absorption I. Mass transfer in the liquid. *Journal of Membrane Science*, **23**, 321-332.

Qi, Z., & Cussler, E.L. (1985b). Microporous hollow fibers for gas absorption II. Mass transfer across the membrane. *Journal of Membrane Science*, **23**, 333-345.

Sirkar, K.K. (1992). Other New Membrane Processes in *Membrane Handbook* (Edited by W.S. Winston Ho and K.K. Sirkar). New York: Chapman and Hall.

Sirkar, K.K. (1997). Membrane separation technologies: Current developments. *Chemical Engineering Communications*, **157**, 145-184.

Chapter 1

Density, Viscosity, Solubility and Diffusivity of N_2O in Aqueous Amino Acid Salt Solutions

Abstract

Solubility and diffusivity of N_2O in aqueous solutions of potassium taurate are reported over a wide range of concentration and temperature. Also, the solubility of N_2O in aqueous potassium glycinate solution is reported at 295 K. The ion specific constants, based on the model of Schumpe (Schumpe, 1993; Weisenberger & Schumpe, 1996) are reported for taurate and glycinate anions. A modified Stokes-Einstein relationship is proposed for the diffusivity of N_2O in aqueous potassium taurate solution in the temperature range of 293-308 K.

1.0 Introduction

Aqueous solutions of amines are extensively used in the removal of acid gas components like CO_2 and H_2S from a variety of industrial gas streams (Kohl & Nielsen, 1997). In particular, alkanolamines and blends of alkanolamines are widely used amines in the gas treating industry. Alkanolamines undergo degradation in oxygen rich atmosphere, usually encountered in the treatment of flue gases, resulting in very toxic degradation products (Hook, 1997). Amino acid salts can be a possible alternative to alkanolamines in certain areas of gas treating, although they are more expensive than alkanolamines. The ionic nature of these salt solutions makes them more stable to oxidative degradation along with certain other desirable properties such as low volatility, higher surface tension, etc. Salts of amino acids have been of considerable interest in the development of hybrid solvents, especially as promoters to conventional solvents. Some of the amino acids used commercially are Glycine, Alanine, and diethyl or dimethyl glycine (Kohl & Nielsen, 1997). Numerous processes based on the use of sterically and non-sterically hindered amino acids have been reported in the recent past (Hook, 1997). Amino acids containing a sulfonic acid group have greater stability to degradation and are less corrosive than alkanolamines and amino acids with a carboxylic acid group. Taurine (2-aminoethansulfonicacid) is one such compound and its potential for use in gas treating is being explored.

Design of gas-liquid contactors, to be used in acid gas treating processes requires information on mass transfer coefficients, interfacial area, reaction kinetics and physico-chemical properties such as solubility and diffusivity of the relevant gases in the solvents. As the acid gases react with the solvents mentioned above, properties like diffusivity and solubility need to be estimated by an indirect way, using gases with similar properties. In case of alkanolamines, N_2O is often used as non-reacting gas to estimate the physico-chemical properties of CO_2 in a reactive liquid (Laddha et al., 1981). As the aqueous salt solutions of amino acids are ionic in nature, the "N_2O analogy" proposed by Laddha et al. (1981), for the estimation of the solubility of CO_2 in aqueous alkanolamine solutions, can not be simply extended for the present situation. Instead, the experimental data on the solubility of N_2O in amino acid salt solutions can be interpreted using the van Krevelen-Hoftijzer model (van Krevelen & Hoftijzer, 1948) or the model of Schumpe (Schumpe, 1993; Weisenberger & Schumpe, 1996). Applying these models to the N_2O solubility data, the ion specific constants as defined by these models can be estimated. Using these constants, the solubility of CO_2 in amino acid salt solutions can now be reliably estimated for the amino acid salt solution (Joosten & Danckwerts, 1972). Gubbins et al. (1966) suggest that the ratio of diffusivity of the solute gas in an aqueous electrolyte solutions to the diffusivity in water is marginally affected by the species of the diffusant. As the properties of N_2O are very similar to CO_2 with regard to configuration, molecular volume, and electronic structure, the diffusivity of N_2O in aqueous amino acid salt solutions can be used to estimate the diffusivity of CO_2 in these solutions (Joosten & Danckwerts, 1972). In the present work, the density, viscosity, solubility and diffusivity of N_2O in aqueous potassium taurate solutions are reported at various temperatures. Also, the solubility of N_2O in aqueous potassium glycinate solutions at 295 K is reported.

2.0 Experimental Setup & Procedure

The potassium salt of a selected amino acid was prepared by neutralising the amino acid (99.9 % purity, Merck) dissolved in deionised, distilled water, with an equimolar quantity of potassium hydroxide (Merck) in a standard flask. The neutralisation reaction was carried out with constant cooling. The amino acid dissolved in water exists as a zwitterion, with the amino group completely protonated. The ionic equilibria of the amino acids exists as follows:

$$HO_2C\text{-}R\text{-}NH_3^+ \overset{-H^+}{\rightleftharpoons} {}^-O_2C\text{-}R\text{-}NH_3^+ \overset{-H^+}{\rightleftharpoons} {}^-O_2C\text{-}R\text{-}NH_2$$

Addition of KOH results in deprotonation of the amino group, corresponding to the second equilibrium. Only the deprotonated amine species can react with the acid gases. The concentration of the deprotonated amine (amino acid salt) was estimated potentiometrically, by titrating with standard HCl solutions. The endpoint is the isoelectric point of the chosen amino acid. The experimentally determined amine concentrations were accurate to within 0.5 percent.

2.1. Density and Viscosity

The density was measured using a commercial density meter (DMA 58, Anton Paar GmbH) and the viscosity using a Haake Microviscometer (Haake MessTechnik GmbH). In both cases, the measurement temperature could be controlled within ± 0.05 K.

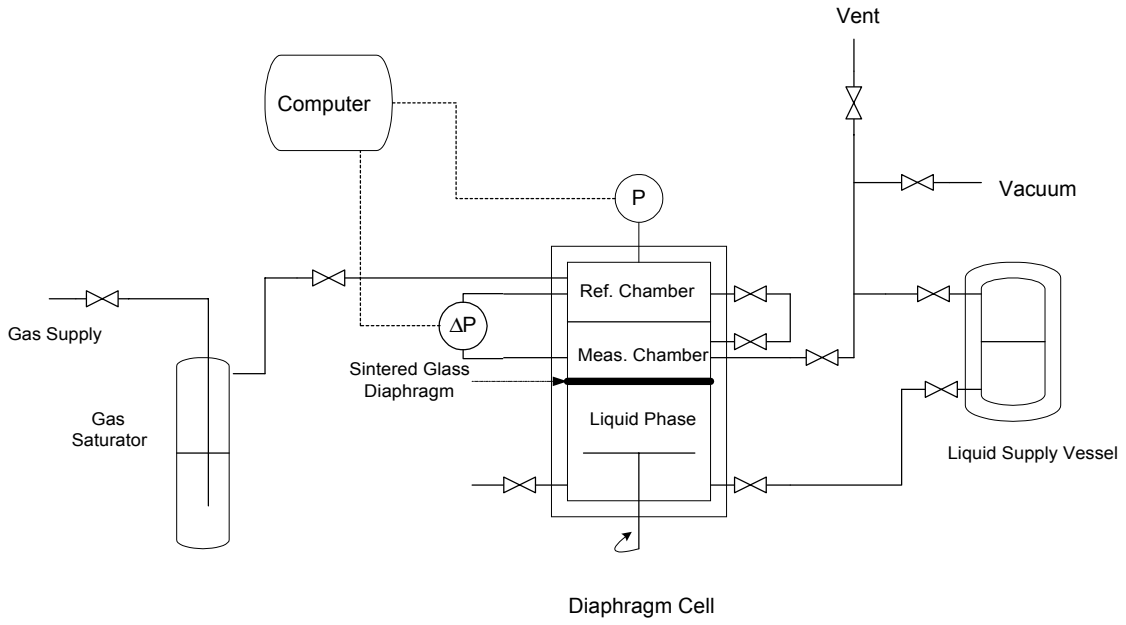

Figure (1) *Diaphragm diffusion cell to determine the diffusion coefficient of N_2O in aqueous potassium taurate solutions*

2.2. Solubility

The solubility was measured in a thermostatic stirred vessel, provided with a pressure transducer (0-1500 mbar, Druck) and gas inducing impeller. A known volume of

solution was transferred into the vessel. The temperature of the solution was allowed to adjust to the temperature at which the measurement had to be done. The contents of the vessel above the liquid as well as the dissolved gas in the solution were removed by the application of vacuum, until the gas bubbles ceased to evolve and vapor-liquid equilibrium was attained. The vapor pressure of the liquid was recorded. The gas was fed into the stirred vessel, until a desired pressure was attained and the pressure was recorded. The vessel was closed and the agitator was turned on. The equilibrium was attained in around 30 minutes when the pressure inside the vessel remains constant. The final equilibrium pressure value was recorded. From the values of pressures and volumes recorded, the solubility of the gas in the liquid could be calculated. The reliability of the experimental data was verified by measuring the solubility of CO_2 and N_2O in water. The measured values were in agreement with those reported in the literature (Versteeg & van Swaaij, 1988) and the accuracy of the experiments was within ± 2%.

2.3. Diffusivity

The diffusion coefficient of N_2O in aqueous potassium taurate solutions was determined using a diaphragm diffusion cell. In the diaphragm cell, a porous, non-permselective sintered glass membrane separates the liquid and gas phase. The pores of the glass membrane are completely filled with the liquid in which the diffusion coefficient is to be measured [Figure 1]. The liquid phase is stirred at sufficiently high speed to avoid mass transfer resistance in the liquid phase. The liquid inside the pore is stagnant except at very high stirring speeds. If the resistance due to mass transfer in the liquid phase is negligible (at higher stirring speeds) and pure gas is used for absorption, the gas absorption flux through the stagnant liquid film inside the pores of the diaphragm can be related to the diffusion coefficient, using the film theory. From the experimental time versus gas phase pressure data, the diffusion coefficient can be calculated using overall and gas phase mass balances as given below,

Overall mass balance:

$$V_G \frac{P_o}{RT} + V_L C_{L,o} = V_G \frac{P(t)}{RT} + V_L C_L(t) \tag{1}$$

Gas phase balance:

$$\frac{V_G}{RT}\frac{dP}{dt} = -k_L A\left(m\frac{P}{RT} - C_L\right) \tag{2}$$

Initial condition:

$$t = 0: \quad P = P_o,\ C_L = C_{L,o} = 0 \tag{3}$$

where A is the interfacial area for mass transfer, C_L and $C_{L,o}$ are the concentration of gas in the liquid at time, t and at t = 0 respectively, k_L is the mass transfer coefficient, m is dimensionless solubility defined as the ratio of the liquid-phase concentration to the gas phase concentration of the solute at equilibrium conditions, P(t) and P_o are the gas phase pressures at time, t and t = 0 respectively, R is the universal gas constant, T is the

temperature of the diaphragm cell, V_G and V_L are the volume of gas and liquid phase respectively of the diaphragm cell. The k_L in eq (2) can be defined using the film theory by,

$$k_L = \frac{D}{\delta} \tag{4}$$

Here D is the diffusion coefficient of gas in the liquid. For the case where the entire mass resistance is located inside the diaphragm, the effective film thickness (δ) depends on the thickness of the membrane (d_m), its porosity (ε) and the tortuosity of the pores (τ). As the values of these properties are not known beforehand, a membrane calibration factor (f) as defined in the equation below has to be determined experimentally,

$$k_L A = \frac{D}{d_m} A \frac{\varepsilon}{\tau} = Df \tag{5}$$

The calibration factor, f can be determined by absorbing gas into a liquid, for which the diffusion coefficient is known accurately. In the present case, the absorption of N_2O and CO_2 in water was used as calibration system, as for these systems, a considerable amount of information on diffusion coefficients is available in literature (Versteeg & van Swaaij, 1988).

Solving the mass balance eqs (1) and (2) with the initial condition (3), the following equation can be obtained.

$$\ln\left[\frac{(V_G + mV_L)\frac{P(t)}{P_o} - V_G}{mV_L}\right] = -k_L A\left(\frac{1}{V_L} + \frac{m}{V_G}\right)t \tag{6}$$

A plot of eq (6) yields the value of k_LA. Using eq (5), the diffusion coefficient can be calculated if the calibration factor, f is known or vice versa.

2.4. Diffusion Cell

The diaphragm diffusion cell used for the measurements is shown in Figure 1. The liquid chamber (volume: 282.5 ml) was equipped with a magnetic stirrer. The gas chamber was divided into two parts. The upper chamber (170.5 ml) was the reference chamber and consisted of a pressure transducer (0-1000 mbar, Druck) connected to the lower measuring chamber (187.5 ml) by two valves. The valves can be used to disconnect the two gas chambers. A differential pressure transducer (range: 0-0.305m H_2O, accuracy: 1% of full scale, Druck 600DP series) was connected between the reference and measuring chamber. It was used to measure the pressure drop in the measuring chamber, with respect to the constant pressure in the reference chamber. This method of measuring the pressure drop during gas absorption significantly reduces the duration of the experiment, in comparison to earlier version of instrument containing a gas chamber without partition (Little et al., 1992). The whole apparatus was thermostated and the temperature was controlled within $\pm$ 0.1 K.

Calibration of Diaphragm

The calibration factor, f for the diaphragm [P4 type; pore diameter: (10-16) μm; Area: (33 ± 0.5) cm^2; thickness: 4 mm] was determined by carrying out experiments on the absorption of N_2O and CO_2 in water in the temperature range of 292-310 K, using different liquid stirrer speeds. The values of diffusion coefficient of N_2O and CO_2 in water obtained from literature (Versteeg & van Swaaij, 1988) was used to determine the calibration factor, f. The f factor of the diaphragm used for the measurements was 0.48. The accuracy of the estimated calibration factor was within ± 3% for the two gases studied and over the temperature range mentioned above. There was no influence of the stirrer speed between 30 and 60 rpm. At temperatures above 310 K, this operational window reduced and considerable scatter of the estimated f values occurred at the higher and lower end of the stirrer speed. Therefore, no experiments above 308 K are presented on the diffusivity.

3.0 Results and discussion

The measured values of density and viscosity of the aqueous salt solutions studied are given in the Table 1 of Appendix. The estimated accuracy of the density and viscosity measurements is within 0.01% and 0.5% respectively.

3.1. Solubility

Table 2 and Table 3 (see Appendix) gives the experimental data of the solubility of N_2O in aqueous potassium taurate and potassium glycinate solutions respectively. The data show typical “salting out effect” observed in electrolyte solutions for N_2O. For moderately high concentrations, the effect can be best described by the Sechenov relation,

$$\log (m_w/m) = K C_s \qquad (7)$$

Here m_w and m denote the solubility of N_2O in water and salt solution respectively and C_s is the molar salt concentration. Several empirical models have been proposed in the past to predict the Sechenov constant (K). The most widely used models are the van Krevelen-Hoftijzer model (van Krevelen & Hoftijzer, 1948) and the one proposed by Schumpe (Schumpe, 1993; Weisenberger & Schumpe, 1996). For a single salt, the Sechenov constant, based on the Schumpe model is given by the following relation,

$$K = \Sigma (h_i + h_G) n_i \qquad (8)$$

The Sechenov constant as defined in the van Krevelen-Hoftijzer model, for a single salt is,

$$K = (h_+' + h_-' + h_G') n_i \qquad (9)$$

n_i being the index of the ion i in the formula of the salt. The parameter K is specific to the gas and the salt. h_i and h_G are the ion and gas specific constants. Based on extensive study by Schumpe (Weisenberger & Schumpe, 1996) on the solubility of various gases in different salt solutions, it was found that the standard deviation of the experimentally determined Sechenov constant by the model of Schumpe was half as compared to the

constant determined with the van Krevelen-Hoftijzer model. So, the model proposed by Schumpe was adopted for the present system.

The plot of eq (7) for the experimental data yields the Sechenov constants and they are given in Table 4 (see Appendix). The experimental data were found to be well fitted by eq (7) (R^2 > 0.985). From the Sechenov constants, the anion specific constant (h_-) can be estimated using eq (8) as the information on cation specific constant (h_+) as well as gas specific constant (h_G) and its dependence on temperature are available in literature (Weisenberger & Schumpe, 1996). The value of the constant corresponding to the anion is given at various temperatures in Table 4. The average value of h_- for taurate and glycinate ions are 0.0249 (std. dev.: 0.0026) and 0.0276 respectively. A parity plot between the experimental data and estimated values using eq (7) and (8) is shown in Figure 2.

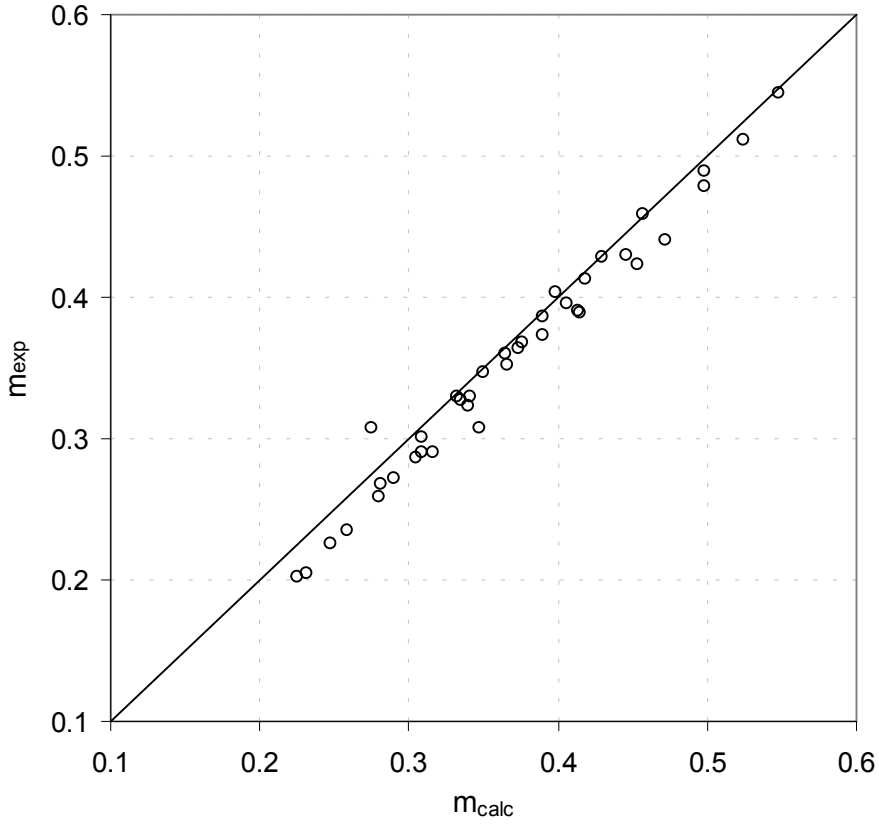

Figure (2) *Parity plot for the Sechenov model for N_2O-aq. potassium taurate system. The average value of h_- (0.025) was used to estimate the solubility of N_2O.*

3.2. Diffusivity

The experimental data for the diffusivity of N_2O in potassium taurate solutions are given in Table 5 (see Appendix). The values provided here are the arithmetic mean of 3-4 identical measurements. The standard deviation of the measured values was within ± 5 percent of the mean value. The dependence of diffusion coefficient on the concentration and temperature can be described in terms of viscosity of the solution (μ), using a modified Stokes-Einstein equation. In case of alkanolamines, the dependence has been reported as

$D\mu^{0.6}$ = constant for various amines in aqueous solutions (Brilman et al., 2001). Similarly, gas diffusion in electrolyte solutions can be reasonably correlated with the modified Stokes-Einstein equation (Gubbins et al., 1966; Brilman et al., 2001). Figure 2 shows the plot of (D/D_w) versus (μ/μ_w). The data fit to the following equation within ±10 % accuracy as shown in Figure 3.

$$(D/D_w) = (\mu/\mu_w)^{-0.74} \qquad (10)$$

Here D_w is the diffusion coefficient of the gas in water and μ_w is the viscosity of water. The values of viscosity used to calculate (μ/μ_w) in Table 5 at various concentrations and temperatures were interpolated from the experimental data given in Table 1.

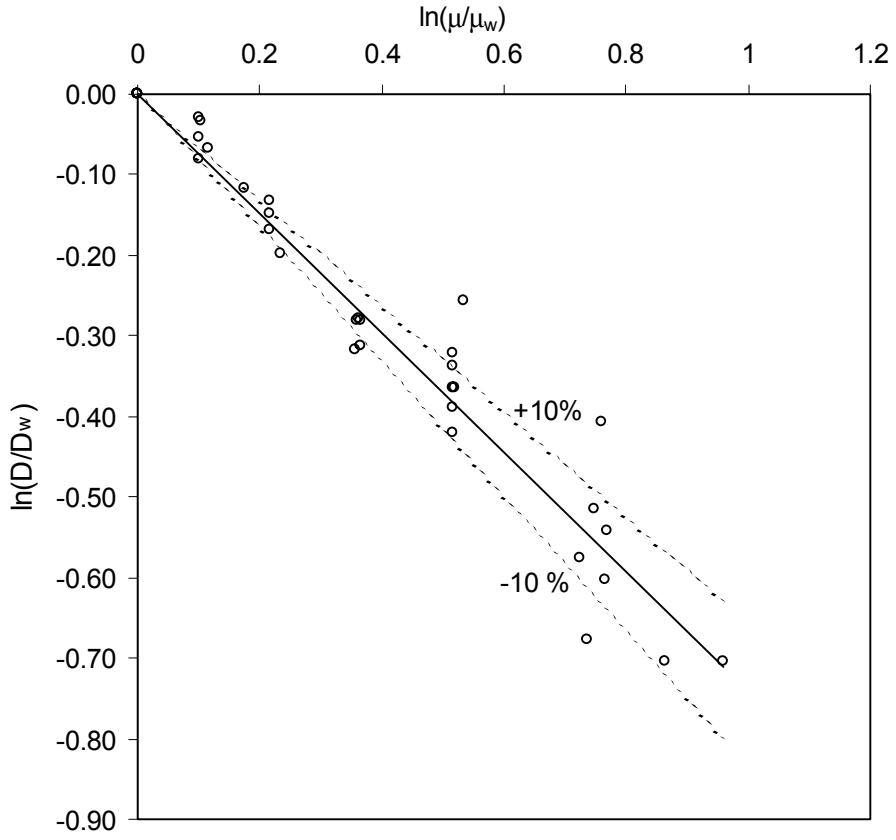

Figure (3) *Parity plot for Eq (10) for N_2O-aq. potassium taurate system.*

4.0 Conclusions

1. The solubility of N_2O in aqueous potassium glycinate and taurate has been experimentally determined. The effect of temperature and concentration of the salt on the solubility of N_2O can be expressed by the Sechenov equation. The anion specific constant (h_-) in the Sechenov equation has been determined for Taurate and Glycinate ions.

$^-O_3S\text{-}CH_2\text{-}CH_2\text{-}NH_2$	(h_-)	-	0.0249
$^-O_2C\text{-}CH_2\text{-}NH_2$	(h_-)	-	0.0276

2. The diffusivity of N_2O in aqueous potassium taurate solution is reported in the range of 0-3.5 M and 293-308 K. As expected, the modified Stokes-Einstein equation can be used for the estimation of the diffusion coefficient of N_2O in aqueous potassium taurate solution.

$$D\mu^{0.74} = \text{constant}$$

Acknowledgement

This research is part of the research programme carried out within the Centre for Separation Technology, a cooperation between the University of Twente and TNO, the Netherlands Organisation for Applied Scientific Research. We acknowledge Pieter Derksen for his assistance to the experimental work and Wim Leppink for the construction of experimental setups.

5.0 Nomenclature

A	Interfacial area for mass transfer, m^2
C	Concentration, mol m^{-3}
D	Diffusion coefficient, m^2 s^{-1}
d_m	Thickness of the Diaphragm/membrane, m
f	Diaphragm specific calibration factor, m
h_-	Anion specific constant, m^3 $kmol^{-1}$
h_G	Gas specific constant, m^3 $kmol^{-1}$
h_I	Cation specific constant, m^3 $kmol^{-1}$
h_I	Ion specific constant, m^3 $kmol^{-1}$
K	Sechenov constant, m^3 $kmol^{-1}$
k_L	Liquid side mass transfer coefficient, m s^{-1}
m	Physical solubility of gas in liquid, $(C_{A,l}/C_{A,g})_{eq}$, dimensionless
n_I	Valency of the ion, dimensionless
P	Pressure, N m^{-2}
P(t)	Pressure at time, t, N m^{-2}
R	Universal gas constant, 8.314 J $gmole^{-1}$ K^{-1}
T	Temperature, K
t	time, s
V	Volume, m^3

Greek

μ	Liquid viscosity, kg m^{-1} s^{-1}
τ	Tortousity of the membrane, dimensionless
δ	Film thickness, m
ε	Porosity of the membrane, dimensionless

Subscript

G	Gas phase
L	Liquid phase
o	At time, t = 0
s	Salt
w	Water

6.0 References

Brilman, D.W.F., van Swaaij, W.P.M., & Versteeg, G.F. (1998). Diffusion coefficient and solubility of isobutene and trans-2-butene in aqueous sulfuric acid solutions. *Journal of Chemical & Engineering Data*, **46(5)**, 1130-1135.

Gubbins, K.E., Bhatia, K.K., & Walker, R.D. (1966). Diffusion of gases in electrolyte solutions. *AIChE Journal,* **12**, 548-552.

Hook, R.J. (1997). An investigation of some sterically hindered amines as potential carbon dioxide scrubbing compounds. *Industrial & Engineering Chemistry Research,* **36(5)**, 1779-1790.

Joosten, G.E.H., & Danckwerts, P.V. (1972). Solubility and diffusivity of nitrous oxide in equimolar potassium carbonate-potassium bicarbonate Solutions at 25°C and 1 atm. *Journal of Chemical & Engineering Data,* **17**, 452-454.

Kohl, A.L., & Nielsen, R.B. (1997). *Gas Purification*: 5th ed. Houston: Gulf Publishing Company.

Laddha, S.S., Diaz, J.M., & Danckwerts, P.V. (1981). The analogy: The solubilities of CO_2 and N_2O in aqueous solutions of organic compounds. *Chemical Engineering Science,* **36**, 228-229.

Littel, R.J, Versteeg, G.F., & van Swaaij, W.P.M. (1992). Solubility and diffusivity data for the absorption of COS, CO_2 and N_2O in amine solutions. *Journal of Chemical & Engineering Data*, **37**, 49-55.

Schumpe, A. (1993). The estimation of gas solubilities in salt solutions. *Chemical Engineering Science,* **48**, 153-158.

Snijder, E.D., te Riele, M.J.M., Versteeg, G.F., & van Swaaij, W.P.M. (1993). Diffusion coefficients of several aqueous alkanolamine solutions. *Journal of Chemical & Engineering Data*, **38**, 475-480.

van Krevelen, D.W., & Hoftijzer, P.J. (1948). *Chimie et Industrie: Numero Speciale du XXI^{e} Congress International de Chimie Industrielle*, Bruxelles, Belgium.

Versteeg, G.F., & van Swaaij, W.P.M. (1988). Solubility and diffusivity of acid gases (CO_2, N_2O) in aqueous alkanolamine solutions. *Journal of Chemical & Engineering Data,* **33**, 29-34.

Weisenberger, S., & Schumpe, A. (1996). Estimation of gas solubilities in salt solutions at temperatures from 273K to 363K. *AIChE Journal,* **42**, 298-300.

Appendix

Table (1) *Density, ρ, and Viscosity, μ, of aqueous potassium taurate solution.*

T (K)	C_s (kmol m^{-3})	ρ x 10^{-3} (kg m^{-3})	μ (mPa. s)
293	0	0.9982	0.974
	0.498	1.0375	1.083
	0.996	1.0756	1.217
	1.987	1.1505	1.624
	2.990	1.2240	2.046
	3.979	1.2966	3.446
303	0.498	1.0345	0.925
	0.996	1.0722	1.042
	1.987	1.1463	1.389
	2.990	1.2194	1.729
	3.979	1.2915	2.652
313	0.498	1.0309	0.806
	0.996	1.0683	0.915
	1.987	1.1419	1.204
	2.990	1.2142	1.649
	3.979	1.2862	2.052
323	0.498	1.0274	0.698
	0.996	1.0645	0.788
	1.987	1.1379	1.043
	2.990	1.2102	1.455
	3.979	1.2817	1.601
328	0.498	1.0239	0.636
	0.996	1.0609	0.716
	1.987	1.1242	0.945
	2.990	1.2062	1.332
	3.979	1.2775	1.449

Table (2) *Solubility, m, of N_2O in aqueous potassium taurate solutions*

C_s (kmol m^{-3})	T (K)	m (mole.$mole^{-1}$)
0.499	285	0.712
0.492	295	0.548
0.492	300	0.498
0.498	306	0.429
0.501	308.6	0.398
0.496	313	0.376
0.496	314	0.365
0.499	318	0.333
0.744	295	0.524
0.744	300	0.457
0.741	305	0.418
0.738	308	0.389
0.744	313	0.349
1.001	285	0.675
1.002	295	0.498
1.002	300	0.445
0.998	304	0.406
0.992	308	0.373
1.005	312.5	0.340
0.999	313	0.334
0.990	317	0.309
1.479	295	0.452
1.485	293	0.471
1.479	299	0.413
1.488	308	0.339
1.492	313	0.308
1.492	317	0.281
2.060	285	0.516
1.967	293	0.415
1.972	295	0.389
1.972	298	0.365
1.985	308	0.305
1.985	313	0.279
1.976	318	0.258
2.480	285	0.459
2.992	285	0.401
2.971	295	0.315
2.952	298.6	0.290
2.964	308	0.247
2.986	313.8	0.225
3.460	285	0.347
3.985	285	0.275

Table (3) *Solubility, m, of N_2O in aqueous potassium glycinate solutions at 295 K*

C_s (kmol m^{-3})	m (mole.$mole^{-1}$)
0	0.605
0.507	0.549
0.998	0.476
1.550	0.432
2.006	0.362
2.583	0.329
2.996	0.285
3.505	0.262
3.965	0.226

Table (4) *Sechenov constants, K, for solubility of N_2O in aqueous potassium taurate and glycinate solutions*

Amine salt	T (K)	K (m^3 $kmol^{-1}$)	h_+ (m^3 $kmol^{-1}$)	h_G (m^3 $kmol^{-1}$)	h_- (m^3 $kmol^{-1}$)
Potassium Taurate	285	0.1117	0.0922	-0.0022	0.0239
	295	0.0999	0.0922	-0.0070	0.0217
	300	0.0975	0.0922	-0.0094	0.0241
	308	0.0937	0.0922	-0.0132	0.0279
	313	0.0883	0.0922	-0.0156	0.0273
Potassium Glycinate	295	0.1058	0.0922	-0.0070	0.0276

Table (5) *Diffusivity, D, of N_2O in aqueous potassium taurate solutions*

C_s (kmol m^{-3})	T (K)	D x 10^9 (m^2 s^{-1})	μ/μ_w*	D/D_w
0.487	293	1.533	1.123	0.934
0.748	293	1.460	1.191	0.890
0.991	293	1.346	1.266	0.820
1.474	293	1.240	1.442	0.756
1.972	293	1.141	1.675	0.695
3.039	293	0.897	2.154	0.547
3.469	293	0.812	2.610	0.495
0.489	296	1.700	1.108	0.967
0.991	296	1.484	1.243	0.844
1.474	296	1.280	1.428	0.728
1.972	296	1.220	1.681	0.694
3.039	296	0.988	2.067	0.562
3.469	296	0.870	2.370	0.495
0.489	299	1.846	1.108	0.981
0.995	299	1.622	1.243	0.862
1.477	299	1.420	1.433	0.755
1.969	299	1.275	1.679	0.678
3.031	299	0.957	2.090	0.509
0.477	305	1.980	1.107	0.922
0.995	305	1.898	1.243	0.884
1.477	305	1.570	1.439	0.731
1.975	305	1.530	1.676	0.713
3.031	305	1.430	2.136	0.666
0.477	308	2.170	1.107	0.948
1.469	308	1.770	1.708	0.774
1.971	308	1.662	1.675	0.726
3.031	308	1.320	2.160	0.577

* Derived from Table 1

Chapter 2

Kinetics of the Reaction of Carbon Dioxide with Aqueous Potassium Salt Solutions of Taurine and Glycine

Abstract

The kinetics of the reaction between CO_2 and aqueous potassium salts of taurine and glycine was measured at 295 K in a stirred cell reactor with a flat gas-liquid interface. For aqueous potassium taurate solutions, the reaction kinetics were also measured at 285 and 305 K. Unlike aqueous primary alkanolamines, the partial reaction order in amino acid salt changes from one at low salt concentration to approximately 1.5 at salt concentrations as high as 3000 mol m^{-3}. At low salt concentrations, the measured apparent rate constant (k_{app}) for potassium glycinate is comparable to the earlier reported work of Penny and Ritter (1983). In the absence of reliable information in the literature on the kinetics as well as mechanism of the reaction, the applicability of the zwitterion and termolecular mechanism (proposed originally for alkanolamines) was explored. For the zwitterion mechanism, the forward second order reaction rate constant (k_2) of the reaction of CO_2 with the amino acid salt seems to be much higher than for alkanolamines of similar basicity. This indicates that the Brønsted plot for amino acid salts might be different from that of alkanolamines. Also, the contribution of water to the deprotonation of zwitterion seems to be significantly higher in comparison to reported values for aqueous secondary alkanolamines.

1.0 Introduction

The removal of acid gases (like CO_2, H_2S, COS) from industrial and natural gas streams is an important operation in the process industry and reactive absorption has been the most widely used method for their removal. Aqueous alkanolamine solutions are the commonly used reactive solvents in the gas treating industry and numerous alkanolamines are available with widely varying reactivity towards CO_2 (while H_2S reacts instantaneously with all amines) and CO_2/H_2S absorption capacity. Thus the choice of the alkanolamine among primary, secondary and tertiary sterically or non-sterically hindered amine depends on the process requirements. For the bulk removal of CO_2 or removal of H_2S from a gas stream containing both H_2S and CO_2, information on the mechanism and kinetics of the reaction between CO_2 and the reactive component in the solvent are necessary for the design of the gas-liquid contactor. This information can also be used to improve the overall selectivity towards absorption of H_2S from a gas stream containing CO_2 and H_2S. Incase of alkanolamines, considerable information is available in literature and has been recently summarised by Versteeg et al. (1996). Besides alkanolamines, carbonate-bicarbonate buffers are used in the bulk removal of CO_2 owing to the low steam requirement for their regeneration (hot carbonate process, Astarita et al., 1983). In actual modern industrial practice, additives (which act as rate promoters) to the carbonate solution are nearly always used. Kohl and Nielsen (1997) have summarised the list of chemicals found to enhance the rate of CO_2 absorption.

Amino acids are a class of chemical species used commercially (Giammarco-Vetrocoke Process) as promoters in carbonate solutions (Kohl & Nielsen, 1997). Also, aqueous solutions of amino acid salts alone have also been used in the past for the (selective) removal of H_2S or CO_2 from a variety of gas streams. The industrially tested Alkacid process uses three absorption liquids, namely Alkacid “M”, Alkacid “dik” and Alkacid “S” depending on the acid gas component (H_2S, CO_2) to be removed and the composition of the gas stream (Kohl & Nielsen, 1997). Of the three mentioned above, the “M” and “dik” processes use amino acid salts. The most commonly encountered amino acids used in the gas treating solvents are glycine (Giammarco-Vetrocoke), alanine (Alkacid, BASF), dimethyl glycine (Alkacid, BASF), diethyl glycine (Alkacid, BASF) and a number of sterically hindered amino acids (Exxon). Though amino acids are more expensive than alkanolamines, they have certain unique advantages due to their physical and chemical properties. The amino acid salts solutions were found to have better resistance to degradation, especially in the removal of acid gases from oxygen rich gas streams like flue gas (Hook, 1997). Due to the ionic nature of the solutions, they also have negligible volatility and higher surface tension. Their reactivity and CO_2 absorption capacity are comparable to aqueous alkanolamines of related classes (Hook, 1997; Penny & Ritter, 1983).

Design of gas-liquid contactors for the removal of CO_2 using aqueous amino acid salt solutions requires information, among others, on the kinetics of the reaction between CO_2 and amino acid salts. Unlike aqueous alkanolamines, there is limited information in literature in general on the absorption of CO_2 in aqueous amino acid salt solutions and in particular on the mechanism and kinetics of the reaction between CO_2 and aqueous amino acid salts solutions. The available information is briefly summarised in section 2. In the present study,

the kinetics of the reaction between CO_2 and aqueous potassium salt of taurine (2-aminoethansulfonic acid) and glycine (aminoacetic acid) were investigated over a wide range of concentrations (100 - 4000 mol m^{-3}) and temperatures (285-305 K).

2.0 Literature Review

During the absorption of CO_2 in aqueous amino acid salt solutions, the following reactions can occur.

$$CO_2 + 2\,AmA \rightleftharpoons AmACOO^- + AmAH^+ \quad (1)$$

$$CO_2 + OH^- \rightleftharpoons HCO_3^- \quad (2)$$

$$CO_2 + H_2O \rightleftharpoons H_2CO_3 \quad (3)$$

The forward rate constants as well as the equilibrium constants of the reaction (2) and (3) are available in literature (Pohorecki & Moniuk, 1988; Pinsent et al., 1956; Edwards et al., 1978). However, the relative contribution of the reaction (2) and (3) to the overall absorption rate for most of the amino acid salts that can be possibly used in gas treating is not significant and hence the forward rate constant of reaction (1) needs to be determined accurately. Most of the experimental techniques used in the past to measure the kinetics of the reaction between CO_2 and amino acid salts were relatively inaccurate (with respect to the experimental procedure and the interpretation of the results) in comparison to the present day methods. Also, the amino acid salt concentration range over which the experiments were conducted was very low as they were used mainly as promoters. It may be highly inaccurate to extrapolate the data to higher concentrations, which is of more use in the gas treating process.

Table (1) *Kinetic data on the reaction between CO_2 and aqueous amino acid salts available in the literature*

Amino acid	T (K)	pKa -	k_{AmA} ($m^3\ mol^{-1}\ s^{-1}$)	Reference
α-Alanine	291	10.01	3.49	Jensen & Faurholt (1952)
β-Alanine	291	10.41	5.81	Jensen & Faurholt (1952)
Glycine	291	9.97	5.93	Jensen et al. (1952)
Glycine	283	10.17	1.65	Caplow (1968)
Glycine	278-303	9.80*	$k_2 = 8.51 \times 10^8 \exp(-5508/T)$	Penny & Ritter (1983)

* at 293 K

Jensen & Faurholt (1952): The reaction rates were determined by the "competitive" method. In this method, a given volume of an aqueous solution of alanine containing a known molar excess of sodium hydroxide was "shaken vigorously" with a gas phase containing CO_2 for 2 minutes. The initial partial pressure of CO_2 in the gas phase was 50 kPa. At the end of the reaction time, the carbamate content as well as the sum of carbamate and carbonate

content in the reaction mixture were determined immediately. The ratio of carbamate to carbonate in the reaction mixture was used to determine the relative rates of the reaction of CO_2 with OH^- and amino acid. The rate of formation of carbamate was assumed to be first order with respect to amino acid as given in Eq (4).

$$\frac{\%\ \text{Carbamate}}{\%\ \text{Carbonate}} = \frac{k_{AmA}\,[AmA]}{k_{OH^-}\,[OH^-]} \qquad (4)$$

Here $[OH^-]$ and [AmA] are the averaged values of the initial and final concentration of OH^- and AmA measured during the experiment. The maximum concentrations of amino acid and NaOH used in the measurements were 150 and 90 mol m^{-3} respectively for α-alanine and 200 and 200 mol m^{-3} respectively for β-alanine. As the gas-liquid mass transfer coefficient cannot be estimated from their description of the experimental conditions, it is not possible to determine the suitability of the process conditions for kinetic measurements (i.e., the absorption regime cannot be determined). Also the value of k_{OH-} used to predict k_{AmA} as per Eq (4) was inaccurate compared to present day values. The reported experimental values of k_{AmA} were recalculated using more accurate value of k_{OH-} (Pohorecki & Moniuk, 1988) and the resulting values are given in Table 1. The acidic dissociation constants of the amino acids as reported by Jensen and Faurholt (1952) are also given in Table 1.

Jensen et al. (1952): Using a similar experimental technique as mentioned above, the authors reported the rate constant for the carbamate formation reaction. The values of k_{AmA} as given in Table 1 have been recalculated because of the inaccuracy in the value of k_{OH-} as used by the authors.

Caplow (1968): The author studied the rates of reaction of CO_2 with glycine and a number of other amines at varying pH, using a sophisticated [but apparently not very accurate (Danckwerts, 1978)] version of the "competitive" method. As the calculated values of k_{AmA} [based on Eq (4)] increased with increasing pH of the solution for some amines, the author considered carbamate formation reaction to be catalysed by OH^- and modified Eq (4) as follows,

$$\frac{\%\ \text{Carbamate}}{\%\ \text{Carbonate}} = \frac{k_{AmA}\,[AmA] + k'_{AmA}\,[AmA]\,[OH^-]}{k_{OH^-}\,[OH^-]} \qquad (5)$$

However for glycine it was found that the contribution of the second term in the numerator of Eq (5) was not significant in comparison to the first term. The k_{AmA} as reported by Caplow has been corrected using more accurate value of k_{OH-} and is given in Table 1.

Penny and Ritter (1983): The kinetics of the reaction between CO_2 and aqueous primary amines (including amino acid salts) was measured using a relatively more accurate stopped flow technique, over the temperature range of 278-298 K. Due to limitations of the experimental technique, the maximum amine concentration that could be studied was 60 mol m^{-3}. Within this concentration range, the overall order of the reaction was found to be two. The authors used the zwitterion mechanism (Caplow, 1968; Danckwerts, 1979; see also

next section) to explain the reaction kinetics. The following Brønsted relationship was proposed between the rate constant (k_2) and acidic dissociation constant (pKa) of the amine used.

$$\log_{10} k_2 = 0.34\ pKa + 0.45 \qquad (6)$$

3.0 Reaction Mechanism

3.1. Zwitterion Mechanism: It can be expected that the aqueous alkaline salts of glycine, alanine and taurine exhibit a similar reactivity towards CO_2 as primary alkanolamines (say monoethanolamine, MEA) due to the similarity in the functional group ($-NH_2$) reacting with CO_2. Incase of primary and secondary alkanolamines, the reaction kinetics can be well described using the zwitterion mechanism proposed originally by Caplow (1968) and later reintroduced by Danckwerts (1979). As per the mechanism, CO_2 reacts with alkanolamines *via* the formation of a zwitterion, followed by the removal of a proton by a base B.

$$CO_2 + RR'NH \underset{k_{-1}}{\overset{k_2}{\rightleftharpoons}} RR'N^+HCOO^- \qquad (7)$$

$$RR'N^+HCOO^- + B \underset{k_{-b}}{\overset{k_b}{\rightleftharpoons}} RR'NCOO^- + BH^+ \qquad (8)$$

The second proton transfer step can be considered to be irreversible. With the assumption of a quasi steady-state condition for the zwitterion concentration, the overall forward rate of the reaction is given by,

$$R_{CO_2} = \frac{k_2 [CO_2][Am]}{1 + \frac{k_{-1}}{\sum k_b [B]}} = \frac{[CO_2][Am]}{\frac{1}{k_2} + \frac{k_{-1}}{k_2}\frac{1}{\sum k_b [B]}} \qquad (9)$$

where $\Sigma\ k_b\ [B]$ is the contribution of all the bases present in the solution for the removal of protons. In lean aqueous solutions, the species amine, water and OH^- can act as bases as shown by Blauwhoff et al. (1984). For a few asymptotic situations, Eq (9) can be simplified.

I. $k_{-1}/(\Sigma\ k_b\ [B]) << 1$: This results in simple second-order kinetics, as experimentally found for aqueous MEA and implies that the zwitterion is deprotonated relatively fast in comparison to the reversion rate to CO_2 and amine.

$$R_{CO_2} = k_2 [CO_2][Am] \qquad (10)$$

II. $k_{-1}/(\Sigma\ k_b\ [B]) >> 1$: This results in a somewhat more complex kinetic rate expression.

$$R_{CO_2} = k_2 [CO_2][Am]\left(\frac{\sum k_b [B]}{k_{-1}}\right) \qquad (11)$$

Depending on the relative contribution of various bases present in the aqueous solution to the deprotonation of the zwitterion, the above expression can explain any reaction order. If the deprotonation is mainly due to the amine, then the overall order of the reaction is three. It can also describe the shift in reaction order with a change

in amine concentration as has been experimentally observed for various secondary alkanolamines (Danckwerts, 1979; Versteeg & Oyevaar, 1989).

III. In the absorption of CO_2 in alkanolamines dissolved in non-aqueous solvents (e.g. alcohols), the deprotonation of the zwitterion is solely due to amine. For, this case, Eq (9) reduces to,

$$R_{CO_2} = \frac{k_2 [CO_2][Am]}{1 + \frac{k_{-1}}{k_{Am}[Am]}} \qquad (12)$$

Only at low concentrations of amine, the second term in the denominator becomes significant and the partial order in amine is higher than one (two being the limiting case when $k_{-1}/(k_{Am}\ [Am]) >> 1$) and this reduces to one at very high amine concentrations.

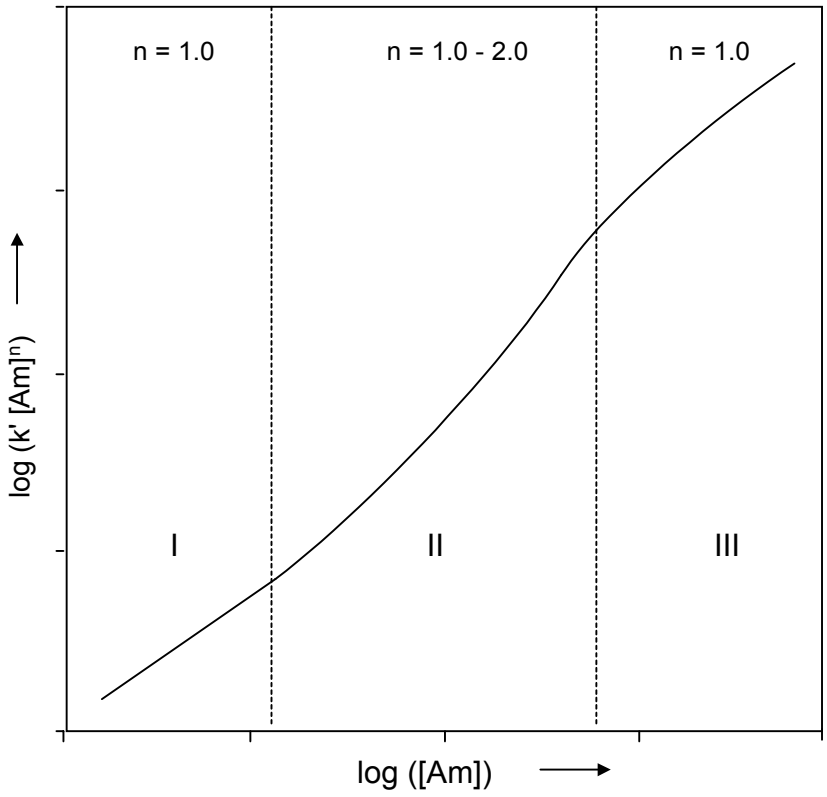

Figure (1) *Kinetic behavior of the reaction of CO_2 with alkanolamines & amino acid salts (trendline based on the Eq (9) of the zwitterion mechanism).*

In general, a plot of the apparent rate constant ($k'\ [Am]^n$) against the amine concentration ([Am]) gives the partial reaction order (n) in amine. The trend line for the Eq (9) of the zwitterion mechanism is shown in Figure 1, which gives a qualitative indication of the concentration range over which the individual mechanistic rate constants can possibly be explicitly measured or estimated. For very low amine concentration, Eq (9) will reduce to the following form and the partial reaction order in amine is one.

$$R_{CO_2} = k_2 [CO_2][Am]\left(\frac{k_{H_2O}[H_2O]}{k_{-1}}\right) \quad (13)$$

At moderately high amine concentrations, the contribution of amine and water to the zwitterion deprotonation are equally significant and hence Eq (9) in its complete form must be used to describe the experimental kinetic data. For very high amine concentrations at which the contribution of water to the overall deprotonation rate becomes negligible and also the numerical value of $k_{-1}/(k_{Am}[Am])$ is far less than 1, Eq (9) reduces to,

$$R_{CO_2} = k_2 [CO_2][Am] \quad (14)$$

In the above discussion, the contribution of the OH^- ions to the deprotonation step has been assumed to be negligible [which is the case for the most commonly used weakly basic amines (DEA, DIPA, MEA) and amino acids (glycine, taurine)]. From Eq (14) it is clear that k_2 can be explicitly measured independent of other constants at very high amine concentrations, provided the following condition is satisfied.

$$\frac{k_{H_2O}[H_2O]}{k_{-1}} << \frac{k_{Am}[Am]}{k_{-1}} >> 1 \quad (15)$$

For secondary alkanolamines in aqueous solutions (say DEA, DIPA), the value of k_{Am}/k_{-1} is approximately $1x10^{-4}$ m^3 mol^{-1} (Versteeg et al., 1996). This indicates that the k_2 can only be measured explicitly at amine concentrations far higher than 10^4 mol m^{-3}, which is a practically unrealistic amine concentration range. So the rate constants in Eq (9) need to be measured in the concentration range falling under zone II and I. It should be noted that some of the experimental techniques used in the kinetic measurements, like the stopped flow technique, can be mostly used for very low amine concentrations only, i.e., Zone I (Penny & Ritter, 1983). Under these situations, one can expect the partial order in amine to be one. However, the second order rate constant, k_2 (based on the zwitterion mechanism) obtained directly from the experimental kinetic data (k' $[Am]^n/[Am]$) may be underestimated if the contribution of k_{H2O} to the deprotonation as shown in Eq (13) is assumed to be negligible. For a good estimation of the zwitterionic rate constants, experimental measurements need to be done from very low (at which k_{H2O}/k_{-1} can be estimated accurately) to high (at which k_{Am}/k_{-1} can be obtained) concentrations of amine.

Applying the zwitterion mechanism to the reaction of CO_2 with aqueous amino (sulfonic or carboxylic) acid salts results in:

$$CO_2 + {}^+K\,{}^-O_3S - R - NH_2 \underset{k_{-1}}{\overset{k_2}{\rightleftharpoons}} {}^+K\,{}^-O_3S - R - NH_2{}^+COO^- \quad (16)$$

$${}^+K\,{}^-O_3S - R - NH_2{}^+COO^- + B \underset{k_{-b}}{\overset{k_b}{\rightleftharpoons}} {}^+K\,{}^-O_3S - R - NHCOO^- + BH^+ \quad (17)$$

It can be observed that the principle difference in applying the zwitterion mechanism to aqueous primary alkanolamines and amino acid salts seems to be the ionic charge associated with the reactant, product as well as the intermediate species. This difference may significantly influence the stability and deprotonation rate of the zwitterion and hence

the overall order of the reaction in aqueous amino acid salt solutions may differ from aqueous primary alkanolamines.

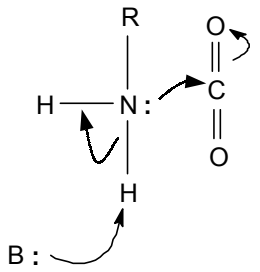

Figure (2) *Single step, termolecular reaction mechanism (Crooks & Donnellan, 1989)*

3.2. Termolecular Mechanism: Crooks and Donnellan (1989) questioned the validity of the zwitterion mechanism based on the argument that the number of fitting parameters required to describe the experimental data is too high (four) and the numerical values of the parameters (especially the deprotonation rate constants) in some cases seems to be physically unrealistic. The authors proposed a single step, termolecular mechanism (see Figure 2) and the reaction rate equation (18) to describe their experimental kinetic data which is infact similar to one of the limiting cases ($k_{-1}/(\Sigma\ k_b\ [B]) >> 1$) of the zwitterion mechanism.

$$R_{CO_2} = k'\ [RNH_2][RNH_2][CO_2] + k''\ [RNH_2][H_2O][CO_2] \qquad (18)$$

Though the termolecular mechanism can describe the fractional reaction orders for aqueous alkanolamine solutions, it fails to explain the occurrence of changing reaction orders with concentration of amine observed for non-aqueous alkanolamine solutions as was experimentally observed by many investigators (Versteeg et al., 1988a; Sada et al., 1985). For most purposes, Eq (9) and its various limiting cases serve as a good engineering model to describe all type of experimental kinetic behavior of amines. In the absence of insufficient kinetic data with regard to reaction of CO_2 with aqueous amino acid salt solutions, both the reaction mechanisms are considered in the present study.

4.0 Experimental

4.1. Chemicals

The potassium salt of a selected amino acid was prepared by neutralising (by titration) the amino acid (Merck) dissolved in deionised, distilled water, with an equimolar quantity of potassium hydroxide (Merck) in a standard flask. The neutralisation reaction was carried out with constant cooling. The amino acid dissolved in water exists as a zwitterion (form II in reaction 19), with the amino group completely protonated. The ionic equilibria of the amino acids in water exists as follows:

$$\underset{\text{I}}{HO_2C\text{-}R\text{-}NH_3^+} \overset{-H^+}{\rightleftharpoons} \underset{\text{II}}{{}^-O_2C\text{-}R\text{-}NH_3^+} \overset{-H^+}{\rightleftharpoons} \underset{\text{III}}{{}^-O_2C\text{-}R\text{-}NH_2} \qquad (19)$$

Addition of KOH results in deprotonation of the amino group, resulting in chemical species III. Only this deprotonated amine species (III) can react with acid gases. The concentration of the deprotonated amine (amino acid salt) was estimated potentiometrically, by titrating with standard HCl solutions. The experimentally determined amine concentrations were accurate to within 0.5 percent.

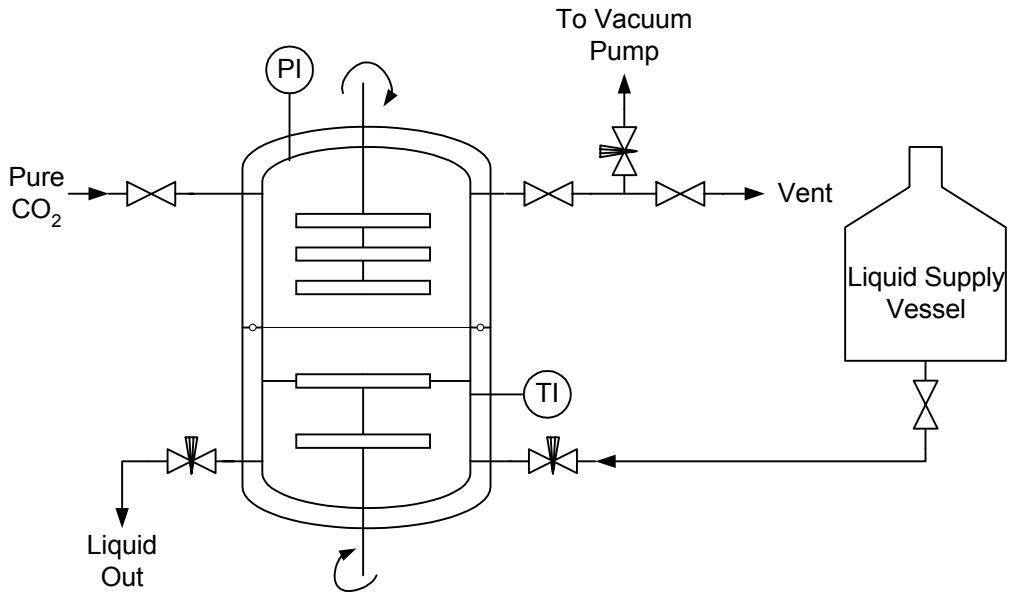

Figure (3) *Schematic diagram of the experimental set-up*

4.2. Experimental Set-up and Procedure

The experiments were carried in a stirred vessel with a smooth gas-liquid interface and the reactor was operated batchwise with respect to the gas and liquid phases (Figure 3). The reactor was all glass, thermostatted and consisted of upper and lower parts, sealed gas tight using an O-ring and screwed flanges. The reactor had magnetic stirrers in the gas (upper) and liquid phases (lower) and the stirring speed could be controlled independently of one another. The pressure in the gas phase was measured using a digital pressure transducer (Drück) and was recorded in the computer.

The experimental procedure is similar to the one described in detail by Blauwhoff et al. (1984) and will be only briefly summarised here. A freshly prepared amino acid salt solution was charged into the reactor from the liquid supply vessel and degassed under vacuum to remove dissolved gases. After degassing, the vapor-liquid equilibrium was allowed to establish. The gas phase pressure (P_{vap}) was noted down and pure CO_2 was introduced into the reactor. The initial CO_2 partial pressure of the reactor was adjusted for different amino acid salt concentrations to maintain a constant amine conversion or average CO_2 loading for all the experiments. In the present experiments, the initial CO_2 partial pressure was adjusted to have a final CO_2 loading of 0.03 ± 0.005 (mole CO_2/mole amine)

for all the experiments. For these low CO_2 loading and using amines with a relatively high value of the equilibrium constant for reaction (1), the influence of reversibility is negligible (Blauwhoff et al., 1984). The stirrer in both phases was turned on and the pressure ($P_{tot,t}$) decrease due to the absorption of CO_2 was recorded. The reaction kinetics can the determined if the following conditions are satisfied.

$$2 < Ha << E_{CO_2,\infty} \tag{20}$$

where

$$Ha = \frac{\sqrt{k_{ov}\, D_{CO_2}}}{k_L} \tag{21}$$

$$E_{CO_2,\infty} = \sqrt{\frac{D_{CO_2}}{D_{AmA}}} + \sqrt{\frac{D_{CO_2}}{D_{AmA}}}\ \frac{[AmA]\ R\ T}{\nu_{AmA}\ P_{CO_2,t}\ m_{CO_2}} \tag{22}$$

If the condition (20) is fulfilled, the reaction can be considered to be pseudo first order and the CO_2 absorption rate is given by,

$$J_{CO_2}\ A = \sqrt{k_{ov}\, D_{CO_2}}\ m_{CO_2}\ P_{CO_2,t} \left(\frac{A}{R\ T}\right) \qquad \text{mol s}^{-1} \tag{23}$$

The information on the solubility and diffusivity of CO_2 in aqueous amino acid salt solutions is given in Appendix. The actual partial pressure of CO_2 at any instant ($P_{CO2,t}$) was calculated according to the following relation:

$$P_{CO_2,t} = P_{tot,t} - P_{vap} \tag{24}$$

In aqueous amino acid salt solutions, the overall rate constant, k_{ov}, comprises mainly the contributions of the reactions (1) and (2).

$$k_{OV} = k_{OH^-}\,[OH^-] + k_{app} \qquad s^{-1} \tag{25}$$

The value of k_{OH-} was obtained from Pohorecki and Moniuk (1988) and the reaction between CO_2 and water (reaction 3) was neglected due to its negligible contribution to the overall reaction rate.

5.0 Results and Discussion

The kinetics of the reaction between CO_2 and aqueous potassium taurate solution was measured at 285, 295 and 305 K. For comparison, the kinetic measurements were also carried out for aqueous potassium glycinate solutions at 295 K.

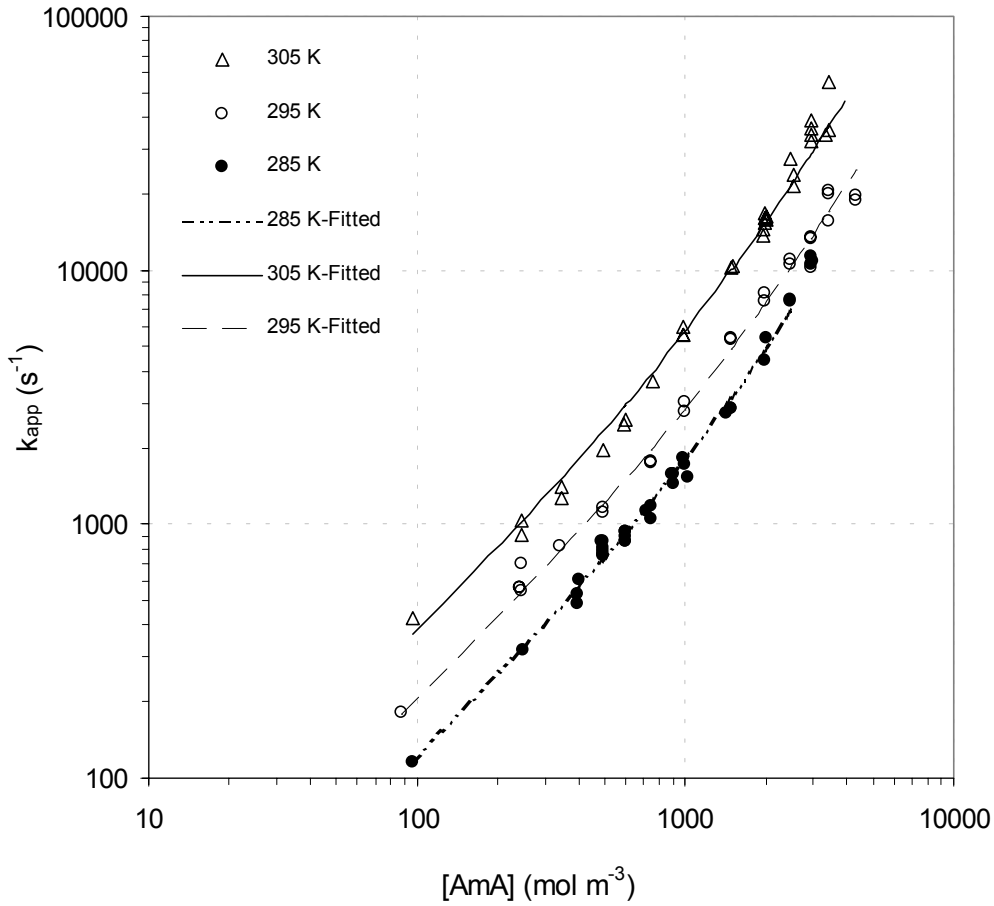

Figure (4) *Experimental results for aqueous potassium taurate at different temperatures*

5.1. Aqueous Potassium Taurate

The measured values of the apparent rate constants (k_{app}) in relation to the potassium taurate concentrations at 295 K are shown in Figure 4. In the calculation of the apparent rate constant using Eq (25), the contribution of the reaction between OH^- and CO_2 to the overall rate was found to be insignificant due to the low basic strength of taurine (pKa). At low taurate concentrations (less than 100 mol m^{-3}), it was practically difficult to measure the reaction kinetics in the 'E = Ha' absorption regime (Eq 20) due to diffusion limitations of the reactant species in the liquid phase. From Figure 4, it can be observed that the partial reaction order (n) in amino acid salt increases with the molar salt concentration. For salt concentrations less than 1000 mol m^{-3}, n approaches the value of 1 for the range of temperatures studied and it increases to approximately 1.5 at salt concentrations as high as 4000 mol m^{-3}. This seems similar to the behavior of aqueous diethanolamine (DEA) where the order with respect to the amine was found to change from 1 at very low amine concentration (< 100 mol m^{-3}) to 2 at high amine concentrations (Blauwhoff et al., 1984; Versteeg & Oyevaar, 1989). However, DEA is a secondary alkanolamine in contrast to the presently used amino acid salt, which has a primary amino functional group.

Table (2) *Zwitterion mechanism constants for the absorption of CO_2 in aqueous potassium taurate solutions*

Amine	T (K)	pKa -	k_2 (m^3 mol^{-1} s^{-1})	k_{AmA}/k_{-1} (m^3 mol^{-1})	k_{H2O}/k_{-1} (m^3 mol^{-1})	Reference
Potassium Taurate	295	9.14	12.60	1.30×10^{-4}	3.39×10^{-6}	Present Study
Monoethanolamine	295	9.62	4.94	-	-	Versteeg et al. (1996)
Diethanolamine	295	8.96	2.42	3.86×10^{-4}	5.31×10^{-7}	Littel et al. (1992)

The experimental k_{app} data was regressed to the reaction rate expression (9) by means of a Levenberg-Marquardt fitting procedure. It was found that the contribution of the OH^- ions to deprotonation of the zwitterion was not significant and was left out from Eq (9) in the fitting procedure. The fitted rate constants are summarised in Table 2 along with the zwitterionic constants of some selected primary and secondary alkanolamines, for which reasonably accurate information is available in the literature. For aqueous amino acid salt solutions, there seems to be a significant difference in the kinetic behavior as well as in the magnitude of the zwitterionic rate constants from the aqueous alkanolamines.

1. Contrary to primary aqueous alkanolamines (e.g. MEA), the partial reaction order in amino acid salt (containing primary amino group) changes with molar salt concentration. This indicates that the deprotonation step in the zwitterion mechanism is not much faster than the zwitterion formation step, a behavior typically exhibited by the secondary aqueous alkanolamines. Also, it indicates that the zwitterion of the amino acid salt is less stable compared to primary alkanolamines.

2. More significantly, the numerical value of k_{Am}/k_{-1} for amino acid salt is lower than that for aqueous alkanolamines (secondary alkanolamines) and that of k_{H2O}/k_{-1} is higher by almost an order of magnitude. This qualitatively indicates that water contributes significantly to the deprotonation even at moderately high amine concentrations. It should be noted that for secondary alkanolamines, there is a negative influence of the steric hindrance of the additional alkanol group to the deprotonation of the zwitterion by an amine in comparison to aqueous primary alkanolamine or amino acid salt. So, in contrast to the general expectation for the amino acid salt, the contribution of water to the deprotonation of the zwitterion is considerable.

3. The value of k_2 is much higher than that expected from the Brønsted plot of Penny and Ritter (1983). These authors have shown that a single Brønsted plot can be used to relate k_2 with the basicity of the amine (pKa) for both alkanolamines as well as amino acid salts. It should be noted that the k_2 measured by the authors was rather an apparent rate constant ($k_2^*=k_2k_{H2O}[H_2O]/k_{-1}$) as explained earlier using Eq (13). Even in the present case, the apparent second order rate constant (k_2^*) at 295 K is 2.96 m^3 mol^{-1} s^{-1}. This value falls in line with the Brønsted plot of Penny and Ritter (1983) at 295 K (Figure 5). In Figure 5, the values of k_2 at 295 K used in the plot were recalculated from the experimental data of Penny and Ritter (1983). It can be concluded that the Brønsted plot

for amino acid salts based on the intrinsic value of k_2 obtained over the complete range of concentrations may be different from that of alkanolamines. More experimental kinetic data for different amino acid salts are required to verify this hypothesis.

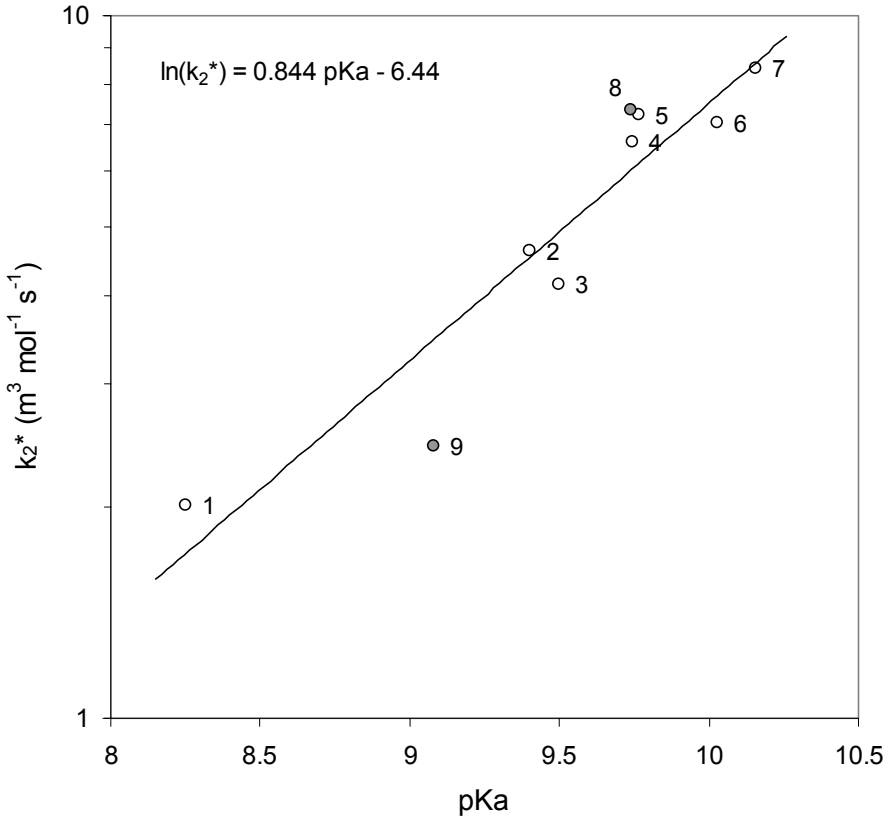

Figure (5) *Bronsted plot for the reaction of CO_2 with amines based on the experimental data of Penny and Ritter (1983) at 295 K, also includes the data obtained from the present work. 1. Glycylglycine salt; 2. Bezylamine; 3. 2-aminoethanol (DEA); 4. Glycine salt; 5. 2-phenethylamine; 6. 2-aminopropan-1-ol; 7. 3-phenyl-1-propylamine; 8. Glycine salt (present work); 9. Taurine salt. (present work). Here k_2* obtained from the work of Penny and Ritter (1983) is $k_{app}/[Am]$ and from the present study is $k_2 k_{H2O}[H_2O]/k_{-1}$.*

4. There is a unique problem associated with the absorption of CO_2 in aqueous amino acid salt solutions that can influence the experimental kinetic measurements. During the absorption of CO_2 in some aqueous amino acid salt solutions, precipitation of certain reaction products occurs. Hook (1997) has made a qualitative study of this phenomenon for different classes of amino acid salts. Independent of the present work, experiments on the vapor-liquid equilibria of CO_2-potassium taurate show that precipitation occurs in the liquid phase during CO_2 absorption in solutions having salt concentrations higher than 2000 mol m^{-3}, depending upon the liquid temperature. Precipitation was observed at reasonably high partial pressures of CO_2 (hence at higher CO_2 loading) and this critical loading or CO_2 partial pressure at which precipitation occurred decreased with an increase in the salt concentration in the liquid. In the kinetic experiments, the CO_2 loading has been kept low (~0.02 mole CO_2/ mole salt) and so there is no precipitation in

the liquid bulk. However, it can not be excluded that micro-particles can precipitate at the gas-liquid interface where the concentration of the reaction products is at its maximum. These miniscule particles might redissolve in the liquid bulk as they move away from the interface (due to stirring). The influence of precipitation (though not visually observed during the experiments) can result in an increase in the mass transfer coefficient due to interfacial turbulence (Westerterp et al., 1984). However, it should be noted that the kinetic experiments have been measured in the "E = Ha" regime ($2 < Ha << E_{CO2,\infty}$) and any marginal change in the value of k_L should not affect the resulting kinetic data. In the range of partial pressures in which the measurements were made, any influence of this phenomenon can be expected only for amino acid salt concentrations greater than approximately 2500 mol m^{-3}, for liquid temperature of 295 K or above. Even if the precipitation at the interface would occur, the effect should be negligible in the "E = Ha" regime and hence the difference in the kinetic behavior seems to be due to the mechanistic aspects of the reaction. Nevertheless, in the regression of the experimental kinetic data to obtain zwitterion mechanism constants, the experimental data in the range of amine concentrations where local precipitation can not be excluded have been neglected.

Mechanistically there can be a significant difference in the zwitterion mechanism applied to the primary or secondary alkanolamines and amino acid salts at the molecular or ionic level (see also section 3.1) This can have influence on the relative rates of the reverse reaction of the zwitterion to CO_2 and amine and deprotonation step ($k_{-1}/\Sigma k_b[B]$) and can possibly offer an explanation for the departure of the experimental results from the one expected for the primary amines.

1. *Stability of the Zwitterion*: The zwitterion of the amino acid salt could be inherently less stable than that of MEA due to the multiple charges associated with the amino acid salt zwitterion [see reaction (16)]. There may also be a negative influence of other charged species (reactant and products) on its stability.

2. *Deprotonation of the Zwitterion*: The zwitterion can be deprotonated by the amine, water and OH^- ions. As mentioned earlier, the contribution of the OH^- ions to the deprotonation is usually negligible. From the numerical value of the deprotonation constants (especially that of water) in comparison to alkanolamines, it seems to be relatively easy for the uncharged water molecules to form hydrogen bonding with the zwitterion (charged at both the ends) as compared to the charged amino acid salt. The mechanism of the deprotonation step has been explained in detail by Caplow (1968).

As an alternative to the zwitterion mechanism, the single step-termolecular reaction mechanism proposed by Crooks and Donnellan (1989) was considered and was assumed to occur in two steps (see Figure 2). In the first step, CO_2, amine and the base (may be amine) forms an intermediate product, which is a "loosely bound encounter complex". The complex can then break down back to reactant molecules or form final reaction products (carbamate).

$$CO_2 + {}^{+}K\,{}^{-}O_3S - R - NH_2 + B \underset{k'_{-1}}{\overset{k_3}{\rightleftharpoons}} [\text{Encounter Complex}] \xrightarrow{k_e} {}^{+}K\,{}^{-}O_3S - R - NHCOO^{-} + BH^{+} \qquad (26)$$

The overall forward reaction rate equation can be derived with the assumption of a quasi-steady state condition for the encounter complex concentration:

$$R_{CO_2,B} = \frac{k_{3,B}\, k_e}{k'_{-1} + k_e}[RNH_2][B][CO_2] \qquad \text{mol m}^{-3}\,\text{s}^{-1} \qquad (27)$$

Table (3) *Temperature influence on the Zwitterion (Eq 9) and Termolecular (Eq 30) reaction mechanism constants*

Amino acid Salt	T (K)	pKa* -	$k_2^{\#}$ ($m^3\ mol^{-1}\ s^{-1}$)	$k_{AmA}/k_{-1}^{\#}$ ($m^3\ mol^{-1}$)	$k_{H2O}/k_{-1}^{\#}$ ($m^3\ mol^{-1}$)	$k'_{AmA}{}^{\#\#}$ ($m^6\ mol^{-2}\ s^{-1}$)	$k'_{H2O}{}^{\#\#}$ ($m^6\ mol^{-2}\ s^{-1}$)
Potassium Taurate	285	9.38	6.78	1.86×10^{-4}	4.23×10^{-6}	7.20×10^{-4}	2.02×10^{-5}
Potassium Taurate	295	9.14	12.60	1.30×10^{-4}	3.39×10^{-6}	9.71×10^{-4}	3.69×10^{-5}
Potassium Taurate	305	8.91	25.20	1.41×10^{-4}	3.01×10^{-6}	2.24×10^{-3}	6.60×10^{-5}
Potassium Glycinate	295	9.67	49.68	6.04×10^{-5}	2.69×10^{-6}	2.09×10^{-3}	1.18×10^{-4}

$^{\#}$ Zwitterion mechanism constants
$^{\#\#}$ Termolecular mechanism constants
* Perrin (1965)

In the present case, the principle bases contributing to the deprotonation are the amino acid salt and water. Depending upon the deprotonating base B, the encounter complex will differ for each base and the net forward rate should be the sum of the individual reaction rates of the two reactions in which the amino acid salt and water act as base, B.

$$R_{CO_2} = R_{CO_2,AmA} + R_{CO_2,H_2O} \qquad \text{mol m}^{-3}\,\text{s}^{-1} \qquad (28)$$

$$R_{CO_2} = \frac{k_e}{k'_{-1} + k_e}\left\{k_{3,AmA}[RNH_2][RNH_2][CO_2] + k_{3,H_2O}[RNH_2][H_2O][CO_2]\right\} \qquad (29)$$

$$R_{CO_2} = k'_{AmA}[RNH_2][RNH_2][CO_2] + k'_{H_2O}[RNH_2][H_2O][CO_2] \qquad (30)$$

where,

$$k'_{AmA} = \frac{k_e}{k'_{-1} + k_e}\, k_{3,AmA} \;\; ; \;\; k'_{H_2O} = \frac{k_e}{k'_{-1} + k_e}\, k_{3,H_2O} \qquad m^6\,\text{mol}^{-2}\,\text{s}^{-1} \qquad (31)$$

Surprisingly, Eq (30) is similar to Eq (11) (though there are no assumptions like $k_{-1}/\Sigma k_b[B] >> 1$ as in the case of zwitterion mechanism). The experimental kinetic data was regressed for Eq (30) using the earlier mentioned numerical technique and the optimal solutions are given in Table 3.

5.2. Temperature dependence of Zwitterion and Termolecular Mechanism Constants

To understand the influence of temperature on reaction kinetics, experiments were conducted at 285 and 305 K as well. The measured apparent rate constants (k_{app}) are shown in Figure 4 and the trend is identical to the measurements at 295 K, i.e., an increase in the partial order in amino acid salt with an increase in salt concentration. The regressed value of the kinetic rate constants based on Eq. (9) and (30) are given in Table 3.

$$k_2 = 3.23 \times 10^9 \exp\left(-\frac{5700}{T}\right) \qquad m^3\,mol^{-1}\,s^{-1} \qquad (32)$$

$$\frac{k_{H_2O}}{k_{-1}} = 2.29 \times 10^{-8} \exp\left(\frac{1483}{T}\right) \qquad m^3\,mol^{-1} \qquad (33)$$

$$\frac{k_{AmA}}{k_{-1}} = 2.36 \times 10^{-6} \exp\left(\frac{1225}{T}\right) \qquad m^3\,mol^{-1} \qquad (34)$$

Of the zwitterion mechanism constants, only k_2 was found to be strongly temperature dependent, while the deprotonation constants were found to be less sensitive to temperature. Relatively accurate values of the taurate and water deprotonation constants can be obtained at very high and low taurate concentrations respectively. For example, at very low salt concentrations, the deprotonation of the zwitterion is mostly due to water. However in the present study, due to the limitations of the experimental technique at low taurate concentrations as well as scatter in the experimental data at very high taurate concentrations, it was practically difficult to do measurements in these ranges of salt concentrations.

5.3. Potassium Glycinate

The kinetics of the reaction between CO_2 and aqueous potassium glycinate solutions was studied at 295 K to compare it to the reaction mechanism proposed for aqueous potassium taurate solutions. It should be noted that taurine is an amino sulfonic acid whereas glycine is an amino carboxylic acid. However, during the reaction of CO_2 with amino acid salts, the acidic group probably has no direct influence on the reaction rate. During the absorption of CO_2 in aqueous potassium glycinate solutions, precipitation does not occur even at very high CO_2 loading (Hook, 1997). Therefore, with this experimental system, it is possible to ascertain whether the difference in the reaction mechanism observed for amino acid salts (in comparison to alkanolamines) can be attributed to the precipitation phenomenon that can occur for taurate solutions at high salt concentrations. Figure 6 shows the measured values of k_{app} as a function of the amino acid salt concentration. Though the pKa of glycine (9.85) is higher than that of taurine (9.14), the contribution of the reaction between OH^- ions and CO_2 to the overall rate was still negligible (less than one percent). Aqueous potassium glycinate solutions showed greater reactivity towards CO_2 over potassium taurate due to higher basic strength (pKa) of glycine.

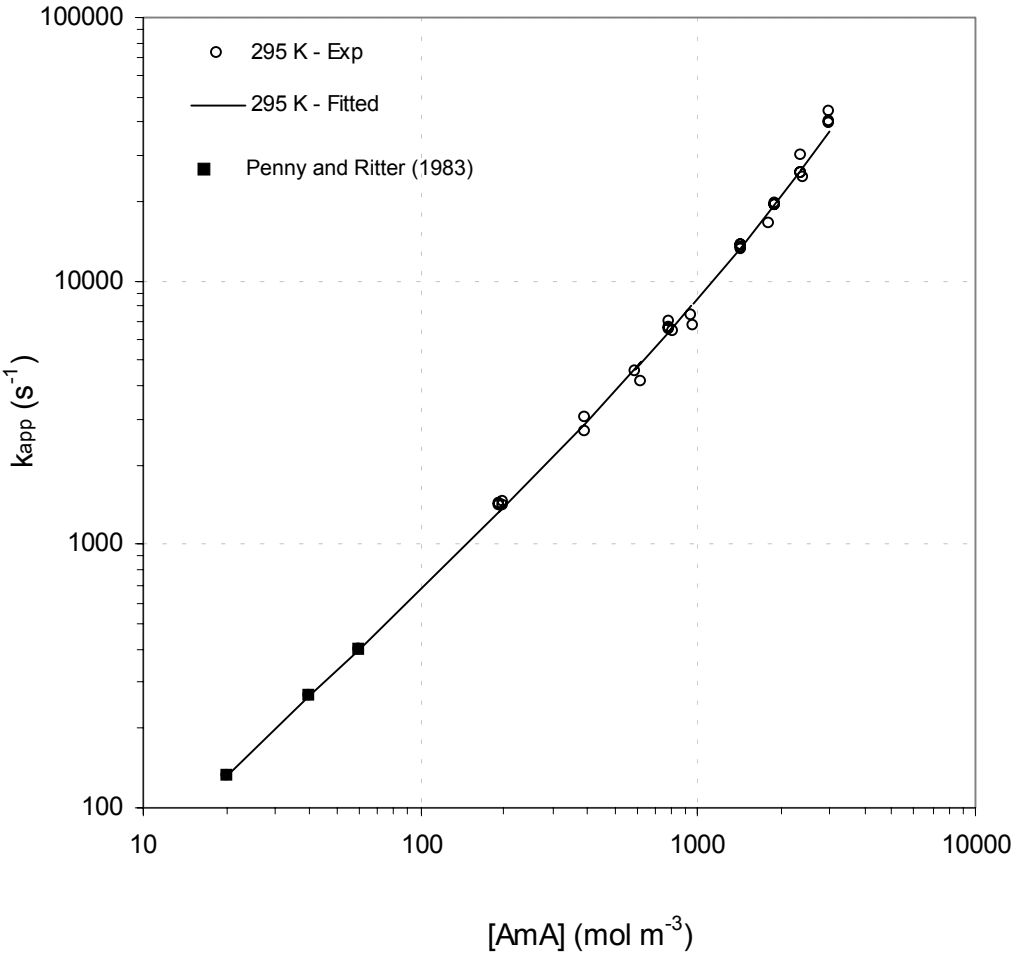

Figure (6) *Experimental results for aqueous potassium glycinate at 295 K.*

Like potassium taurate solutions, aqueous solutions of potassium salt of glycine also exhibit a change in partial reaction order in amino acid salt with the molar concentration of the salt. Again due to the limitations of the experimental technique, reliable measurements could not be conducted using potassium glycinate solutions having concentrations lower than 200 mol m^{-3}. The experimental k_{app} data was regressed to the rate equations of the two reaction mechanisms discussed earlier (Eq 9 and 30). Due to insufficient data at lower amine concentrations, it was found to be difficult to get a good optimal solution and hence the apparent rate constant (k_{app}) from the work of Penny and Ritter (1983) was used in the regression to supplement the k_{app} data from the present work. The resulting rate constants of the reaction mechanism are given in Table 3. As can be expected, the value of k_2 (49.68 $m^3mol^{-1}s^{-1}$) is very high in comparison to the published data (Penny & Ritter, 1983; Jensen et al., 1952) and is also greater than that of taurine. However, the calculated apparent k_2^* ($k_2k_{H2O}[H_2O]/k_{-1}$ = 7.3 $m^3mol^{-1}s^{-1}$) is in good agreement with the reported value (6.61 m^3mol^{-1} s^{-1}) of Penny and Ritter (1983) and is also shown in Figure 5 for comparison. It should be noted that even in the absence of the experimental data of Penny and Ritter, the calculated value of k_2^* obtained from the optimal value of the regressed zwitterionic constants were within $\pm$ 0.2 $m^3mol^{-1}s^{-1}$. Among the zwitterionic deprotonation constants, the value of k_{AmA} for

glycine is lower than for taurine at identical temperature, whereas the deprotonation constant corresponding to that of water are comparable within the accuracy of the estimation of the constants and in the range of amino acid salt concentrations studied. The termolecular mechanism constants are also given in Table 3 and the values of the two constants are higher than for taurine.

6.0 Conclusion

The kinetics of the reaction of CO_2 with aqueous potassium salt of taurine was investigated over a wide range of salt concentrations (100-4000 mol m^{-3}) and temperatures (285-305 K). Similarly, kinetic data for the reaction of CO_2 with aqueous potassium glycinate solutions were obtained at 295 K. Unlike primary aqueous alkanolamines, aqueous amino acid salts show an increase in the partial reaction order in amino acid salt from one at molar salt concentrations larger than approximately 1000 mol m^{-3}. This behavior was observed for both potassium taurate and potassium glycinate solutions. For potassium glycinate, the apparent second order rate constant ($k_2^* = k_2 k_{H2O}[H_2O]/k_{-1}$) obtained from the present study is in good agreement with literature.

The zwitterion mechanism can be conveniently used to describe the experimental kinetic data. However, the numerical value of the rate constants (especially k_2) is very different from that of aqueous alkanolamines. For both taurine and glycine salts, the value of k_2 is far higher than the values that can be expected, based on the Brønsted plot for aqueous amines reported in the literature (Versteeg et al., 1996; Penny & Ritter, 1983). This indicates that the Brønsted plot of amino acids might be different from that of aqueous alkanolamines. Based on the zwitterion mechanism, the role of water in the zwitterion deprotonation seems to be significantly larger than reported in the literature for aqueous alkanolamines. As with aqueous alkanolamines, the termolecular mechanism can also be used to describe the experimental kinetic data. However, more experimental kinetic data is required for different types of amino acid salts to conclude on the mechanistic aspects of the reaction kinetics.

Acknowledgement

This research is part of the research programme carried out within the Centre for Separation Technology, a cooperation between the University of Twente and TNO, the Netherlands Organisation for Applied Scientific Research. We also acknowledge H.B. Ongena for his assistance to the experimental work and Wim Leppink for the construction of experimental setups.

7.0 Nomenclature

A	Gas-liquid interfacial area, m^2
B	Base (H_2O, OH^-, AmA or Am)
D_i	Diffusion coefficient of component i, $m^2\ s^{-1}$
E	Enhancement factor, dimensionless
$E_{CO2,\infty}$	Infinite enhancement factor for the mass transfer of CO_2, dimensionless
Ha	Hatta Number, dimensionless
J_{CO2}	CO_2 absorption mole flux, mol $m^{-2}\ s^{-1}$
$k^{'}$, $k^{''}$	Rate constants, $(mol\ m^{-3})^{1-O}\ s^{-1}$
$k^{'}_{AmA}$	Termolecular mechanism rate constant for AmA, $m^6\ mol^{-2}\ s^{-1}$
$k^{'}_{H2O}$	Termolecular mechanism rate constant for H_2O, $m^6\ mol^{-2}\ s^{-1}$
k_{-1}	Zwitterion mechanism rate constant, s^{-1}
$k_{-1}^{'}$	Termolecular mechanism rate constant, s^{-1}
k_2	Second order rate constant, $m^3\ mol^{-1}\ s^{-1}$
k_2*	Apparent second order rate constant (k_{app}/[AmA]), $m^3\ mol^{-1}\ s^{-1}$
$k_{3,B}$	Termolecular mechanism rate constant, $m^6\ mol^{-2}\ s^{-1}$
k_{AmA}	Zwitterion mechanism deprotonation rate constant for AmA, $m^3\ mol^{-1}\ s^{-1}$
k_{app}	Apparent rate constant, s^{-1}
k_b	Zwitterion mechanism deprotonation rate constant by base B, $m^3\ mol^{-1}\ s^{-1}$
k_e	Termolecular mechanism rate constant, s^{-1}
k_{H2O}	Zwitterion mechanism deprotonation rate constant for H_2O, $m^3\ mol^{-1}\ s^{-1}$
k_L	Liquid phase mass transfer coefficient, m s^{-1}
k_{OH-}	Zwitterion mechanism deprotonation rate constant for OH^-, $m^3\ mol^{-1}\ s^{-1}$
k_{ov}	Overall rate constant, s^{-1}
m	Physical solubility $([CO_2]_{liq}/[CO_2]_{gas})_{eq}$, dimensionless
n	Partial order of the reaction in Amine acid salt, dimensionless
o	Overall order of the reaction, dimensionless
$P_{CO2,t}$	Instantaneous partial pressure of CO_2, Pa
$P_{Tot,t}$	Instantaneous total pressure of reactor, Pa
P_{vap}	Vapor pressure of the liquid, Pa
R	Universal gas constant (8.3143), J $mol^{-1}\ K^{-1}$
R_{CO2}	Rate of reaction of CO_2, mol $m^{-3}\ s^{-1}$
T	Temperature, K
ν	Stoichiometric coefficient, dimensionless
[ ]	Concentration, mol m^{-3}

Abbreviations

Am	Alkanolamine
AmA	Amino acid salt
MEA	Monoethanolamine
DEA	Diethanolamine
DIPA	Diisopropanolamine

8.0 References

Astarita, G., Savage, D.W., & Bisio, A. (1983). *Gas treating with chemical solvents*. New York: John Wiley.

Blauwhoff, P.M.M., Versteeg, G.F., & van Swaaij, W.P.M. (1984). A study on the reaction between CO_2 and alkanolamines in aqueous solutions. *Chemical Engineering Science*, **39(2)**, 207-225.

Caplow, M. (1968). Kinetics of carbamate formation and breakdown. *Journal of American Chemical Society*, **90(24)**, 6795-6803.

Crooks, J.E., & Donnellan, J.P. (1989). Kinetics and mechanism of the reaction between carbon dioxide and amines in aqueous solution. *Journal of the Chemical Society-Perkin Transactions II*, **4**, 331-333.

Danckwerts, P.V. (1979). The reaction of CO_2 with ethanolamines. *Chemical Engineering Science*, **34**, 443-446.

Edwards, T.J., Maurer, G., Newman, J., & Prausnitz, J.M. (1978). Vapour-liquid equilibria in multicomponent aqueous solutions of volatile weak electrolytes. *AIChE Journal*, **24**, 966-976.

Greenstein, J.P., & Winitz, M. (1961). *Chemistry of the amino acids*. New York: Wiley.

Gubbins, K.E., Bhatia, K.K., & Walker, R.D. (1966). Diffusion of gases in electrolytic solutions. *AIChE Journal*, **12**, 548-552.

Hook, R.J. (1997). An investigation of some sterically hindered amines as potential carbon dioxide scrubbing compounds. *Industrial & Engineering Chemistry Research,* **36(5)**, 1779-1790.

Jensen, A., & Faurholt, C. (1952). Studies on Carbamates V. The carbamates of α-Alanine and β-Alanine. *Acta Chemica Scandinavica*, **6**, 385-394.

Jensen, A., Jensen, J.B., & Faurholt, C. (1952). Studies on carbamates VI. The carbamate of Glycine. *Acta Chemica Scandinavica*, **6**, 395-397.

Kohl, A. L., & Nielsen, R.B. (1997). *Gas Purification*: 5th ed. Houston: Gulf Publishing Company.

Kumar, P.S., Hogendoorn, J.A., Feron, P.H.M., & Versteeg, G.F. (2001). Density, viscosity, solubility and diffusivity of N_2O in aqueous amino acid salt solutions. *Journal of Chemical & Engineering Data,* **46**, 1357-1361 (Chapter 1 of this thesis).

Littel, R.J., Versteeg, G.F., & van Swaaij, W.P.M. (1992). Kinetics of CO_2 with primary and secondary amines in aqueous solutions. 2. Influence of temperature on zwitterion formation and deprotonation rates. *Chemical Engineering Science*, **47(8)**, 2037-2045.

Penny, D.E., & Ritter, T.J. (1983). Kinetic study of the reaction between carbon dioxide and primary amines. *Journal of Chemical Society Faraday Society*, **79**, 2103-2109.

Perrin, D.D. (1965). *Dissociation of organic bases in aqueous solution*. London: Butterworth.

Pinsent, B.R.W., Pearson, L., & Roughton, F.J.W. (1956). The kinetics of combination of carbon dioxide with hydroxide ions. *Transactions Faraday Society*, **52**, 1512-1520.

Pohorecki, R., & Moniuk, W. (1988). Kinetics of the reaction between carbon dioxide and hydroxyl ion in aqueous electrolyte solutions. *Chemical Engineering Science*, **43**, 1677-1684.

Sada, E., Kumuzawa, H., Han, Z.Q., & Butt, M.A. (1985). Chemical kinetics of the reaction of carbon dioxide with ethanolamines in nonaqueous solvents. *AIChE Journal*, **31**, 1297-1303.

Schumpe, A. (1993). The estimation of gas solubilities in salt solutions. *Chemical Engineering Science*, **48**, 153-158.

Versteeg, G.F., & Oyevaar, M.H. (1989). The reaction between CO_2 and diethanolamine at 298 K. *Chemical Engineering Science*, **44(5)**, 1264-1268.

Versteeg, G.F., & van Swaaij, W.P.M. (1988a). On the kinetics between CO_2 and alkanolamines both in aqueous and non-aqueous solutions – I. Primary and secondary amines. *Chemical Engineering Science*, **43**, 573-585.

Versteeg, G.F., & van Swaaij, W.P.M. (1988b). Solubility and diffusivity of acid gases (CO_2, N_2O) in aqueous alkanolamine solutions, *Journal of Chemical & Engineering Data*, **33**, 29-34.

Versteeg, G.F., van Dijck, L.A.J., & van Swaaij, W.P.M. (1996). On the kinetics between CO_2 and alkanolamines both in aqueous and non-aqueous solutions. An overview. *Chemical Engineering Communications,* **144**, 113-158.

Weisenberger, S., & Schumpe, A. (1996). Estimation of gas solubilities in salt solutions at temperatures from 273K to 363K. *AIChE Journal,* **42**, 298-300.

Westerterp, K.R., van Swaaij, W.P.M., & Beenackers, A.A.C.M. (1984). *Chemical reactor design and operation*. New York: Wiley and Sons.

Appendix: Physico-Chemical Parameters used in the Determination of Kinetic Constants

The solubility and diffusivity of CO_2 in aqueous amino acid salt solutions are required for the estimation of kinetic parameters from the basic experimental data (P_{CO2} Vs t). Since there is no published information in open literature, they were experimentally determined independently of the present study (Kumar et al., 2001). As CO_2 reacts with the aqueous amino acid salt solutions, the physical solubility (m) and diffusivity (D_{CO2}) of CO_2 were indirectly estimated from the solubility and diffusivity of N_2O respectively in aqueous salt solutions.

Physical solubility

A model similar to that of Schumpe (1993) was used to describe the experimental data on the solubility of N_2O (m) in aqueous potassium taurate solutions (Kumar et al., 2001).

$$\log (m_w/m) = K C_s \qquad (1)$$

where C_s is the salt concentration in kmol m^{-3}. For a single salt, the Sechenov constant, K based on the Schumpe model is given by the following relation,

$$K = \Sigma (h_i + h_G) n_I \qquad m^3\ kmol^{-1} \qquad (2)$$

The temperature independent anion (h_-) and cation specific constants (h_+) for potassium taurate are,

$$h_+: \quad 0.0922 \qquad m^3\ kmol^{-1} \qquad (3)$$
$$h_-: \quad 0.0249 \qquad m^3\ kmol^{-1} \qquad (4)$$

For the solubility of N_2O in aqueous potassium glycinate solutions, the anion specific constant is given by

$$h_-: \quad 0.0276 \qquad m^3\ kmol^{-1} \qquad (5)$$

The temperature dependent gas (CO_2) specific constant (h_G) was obtained from the database of Schumpe (1993; also Weisenberger & Schumpe, 1996) and the solubility of CO_2 in aqueous potassium taurate solution was estimated using Eq (20). The solubility of CO_2 and N_2O in water (m_w) was obtained from the work of Versteeg and van Swaaij (1988b).

Diffusion Coefficient

The diffusion coefficient of N_2O (D_{N2O}) in aqueous potassium taurate solution was obtained from Kumar et al. (2001). A modified Stokes-Einstein equation was used for the estimation of the diffusion coefficient of N_2O in aqueous potassium taurate solutions.

$$D_{N2O}\ \mu^{0.74} = \text{constant} \qquad (6)$$

The information on the dependence of viscosity (μ) on the amino acid salt concentration is available in Kumar et al. (2001). The diffusion coefficient of CO_2 in aqueous potassium taurate solutions was estimated according to Gubbins et al. (1966):

$$\left(\frac{D}{D_W}\right)_{N_2O} = \left(\frac{D}{D_W}\right)_{CO_2} \quad (7)$$

The diffusion coefficients of CO_2 ($D_{CO2,W}$) and N_2O ($D_{N2O,W}$) in water were obtained from the published work of Versteeg and van Swaaij (1988b). The diffusion coefficient of CO_2 in aqueous potassium glycinate was estimated similarly.

Chapter 3

Crystallisation in CO_2 Loaded Aqueous Alkaline Salt Solutions of Amino Acids

Abstract

Crystallisation of a reaction product was observed during the absorption of CO_2 in aqueous potassium taurate solutions at 298 K. The crystallising solid was found to be the protonated amine. The critical CO_2 loading value at which crystallisation occurs has been measured for various amino acid salt concentrations. A simple relation between the critical CO_2 loading value, initial amino acid salt concentration and solubility of amino acid in water has been established. This relation seems to hold well in predicting the critical CO_2 loading value for salts of amino acids other than taurine for which Hook (1997) had recently published some qualitative experimental data. The influence of the formation of solid reaction product during the absorption of CO_2 in aqueous potassium taurate solutions on the mass transfer characteristics of gas-liquid contactor has been semi-quantitatively investigated for a stirred reactor. In particular, the effect of the presence and absence of crystals in the CO_2 loaded solutions on the liquid side volumetric mass transfer coefficient has been studied; by carrying out physical absorption experiments with CO_2 loaded solutions.

1.0 Introduction

Aqueous solutions of amines, more in particular alkanolamines are extensively used in the removal of acid gases like CO_2 and H_2S from a variety of industrial gas streams (Kohl & Nielsen, 1997). It has been widely reported that alkanolamines undergo degradation in oxygen rich atmosphere, usually encountered in the treatment of flue gases, resulting in very toxic degradation products apart from the loss of solvent (Poldermann et al., 1955; Kim & Saratori, 1984). Aqueous alkaline salts of amino acids can be a good alternative for alkanolamines in certain areas of gas treating, though they are more expensive than alkanolamines. The ionic nature of these liquids makes them more stable to oxidative degradation along with certain other desirable physical properties such as low volatility, higher surface tension, etc. Salts of amino acids have been of considerable interest in the development of hybrid solvents, especially as rate promoters to conventional gas treating solvents. Numerous processes based on sterically and non-sterically hindered amino acid salts have been reported in the literature or patented (Kohl & Nielsen, 1997).

Inspite of the above mentioned positive features of amino acid salts over alkanolamines, many salts undergo crystallisation during the absorption of CO_2, especially for solutions of high amino acid salt concentration and at high CO_2 loading (Hook, 1997). The occurrence of crystallisation during absorption offers certain interesting opportunities as well as drawbacks. The opportunities are related to the fact that crystallisation of reaction product(s) in an equilibrium limited liquid phase reaction results in an increase of the equilibrium conversion of the limiting liquid phase reactant or equilibrium CO_2 loading capacity (as in the present case, usually expressed as mole CO_2 per mole amine) over a situation where no crystallisation of the reaction product(s) occurs. The negative aspects are the plugging and fouling of the gas-liquid contactors and heat transfer surfaces. Also, the presence of micro/macro particles of the reaction product in the liquid phase can significantly influence the mass transfer characteristics of the gas-liquid contactors (Beenackers & van Swaaij, 1993). In the past, the amino acid salts have been used mostly in low concentrations (as rate promoters) along with conventional gas treating solvents and hence the crystallisation problems have probably not been encountered. Consequently, there is not much information on this in the open literature. Recently, Hook (1997) presented an extensive (but qualitative) investigation on the absorption of CO_2 in many sterically and non-sterically hindered aqueous amino acid salt solutions and found that many amino acid salts undergo crystallisation at various values of CO_2 loading. Due to limited experimental data, especially on crystallisation, no significant conclusions can be drawn on the relation between the critical CO_2 loading value or point (at which crystallisation occurs) and the type of amino acid. For situations where crystallisation of the reaction product(s) is undesirable, the critical CO_2 loading point is very important as it indicates the operational width (cyclic loading) for the maximum loading in absorber and regeneration of the solvent in stripper.

The present work was done within a project to develop new reactive absorption liquids for the removal of CO_2 using membrane gas-liquid contactors. In this work, a detailed study has been made on the crystallisation phenomenon that occurs during the absorption of CO_2 in amino acid salt solutions and its influence on the mass transfer. Taurine (2-Amino

ethanesulfonic acid) was used as a model amino acid compound to understand the crystallisation phenomenon.

2.0 Literature Review

Alkaline salts of amino acids react with CO_2 similar to alkanolamines and the reactions that occur in the liquid phase are given below.

$$2\,RNH_2 + CO_2 \Leftrightarrow RNHCOO^- + RNH_3^+ \quad (1)$$
$$RNHCOO^- + H_2O \Leftrightarrow RNH_2 + HCO_3^- \quad (2)$$
$$HCO_3^- \Leftrightarrow CO_3^{2-} + H^+ \quad (3)$$
$$RNH_3^+ \Leftrightarrow RNH_2 + H^+ \quad (4)$$
$$H_2O \Leftrightarrow H^+ + OH^- \quad (5)$$

An amino acid salt (represented as RNH_2) reacts with carbon dioxide and the primary products are carbamate and protonated amine. In aqueous solutions, the carbamate undergoes hydrolysis, resulting in the formation of amine and bicarbonate/carbonate (depending upon the pH of the liquid). The deprotonated amine can then react with CO_2. Hook (1997) observed crystallisation during the absorption of CO_2 in a wide variety of amino acid salt solutions. For all amino acids, except glycine, crystallisation was observed at moderate to high CO_2 loading. The author used a batch experimental set-up, in which pure CO_2 was absorbed in a 2.5 molar amino acid salt solution, from a constant pressure (100 kPa) gas "reservoir". From the change in the volume of the gas reservoir, the CO_2 loading of the liquid was estimated. After crystallisation had occurred in the liquid and the liquid had reached equilibrium with the gas phase, water was added to the contents (liquid as well as precipitate) of the reactor to redissolve the solids. The analysis of the resulting liquid using ^{13}C NMR indicated that there were 2 moles of amine per mole of the carbon dioxide species. Hence, the precipitate was concluded to be a carbonate salt of doubly charged protonated amine [$(KO_2CR'NH_2R^+)_2CO_3^{2-}$]. It should be noted that the equilibration time in the experiments was long enough (approximately 20 hrs) for the hydrolysis of the carbamate to occur and hence, it is natural to expect carbonate/bicarbonate salts in the liquid. Since crystallisation was observed at very high CO_2 loading (α > 0.9 mol CO_2/mol AmA) for some amino acids (for example α-alanine), the dissolved CO_2 should be present predominantly as bicarbonate species rather than carbonate. At such high CO_2 loading, the pH of the solution is low enough to overrule the presence of carbonate (see also Figure 4). More clear information about the composition of the solids could have been obtained if the crystals would have been separated from the liquid and analysed independently.

3.0 Experimental

A clear idea of the composition of the precipitate can possibly aid in controlling or overcoming the crystallisation problem. To understand the crystallisation phenomenon, an experimental study on the absorption of CO_2 in aqueous amino acid salt solutions was carried out at near absorber conditions (298 K). The objective was to predict some process parameters that control the onset of crystallisation and identify the nature of the solids

formed. From the reaction scheme discussed earlier, the precipitate should be one (or more) of the reaction products: i.e., carbamate, carbonate, bicarbonate and/or protonated amine. In the present study, taurine was used as a model compound as already some information was available on the salts of amino carboxylic acids (Hook, 1997). For an aqueous potassium salt of taurine, the reaction scheme is,

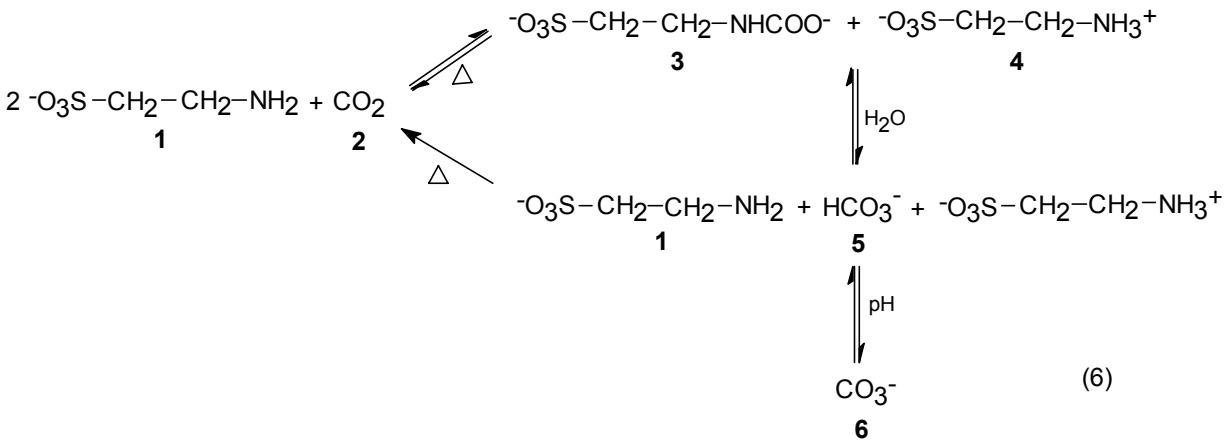

Figure (1) *Reaction scheme for the absorption of CO_2 in aqueous potassium salt of taurine.*

For primary amines, the reaction between amine and CO_2 is very fast in comparison to the secondary carbamate hydrolysis reaction (Sharma & Danckwerts, 1966). From the reaction scheme, it can be observed that the theoretical maximum CO_2 loading of the solution is 0.5, if the hydrolysis reaction is neglected. Depending upon the residence time of the liquid in the gas-liquid contactor, some degree of carbamate hydrolysis always occurs and this results in maximum CO_2 loading values greater than 0.5. From the reaction scheme (Figure 1), it should be noted that component (4) is identical to the zwitterionic form of taurine.

3.1 Chemicals

The potassium salt of Taurine (2-amino ethanesulfonic acid, 99.9 % pure, Merck) was prepared by neutralising the amino acid dissolved in deionised, distilled water, with an equimolar quantity of potassium hydroxide (Merck) in a standard flask. The neutralisation reaction was carried out with constant cooling. The amino acid dissolved in water exists as a zwitterion (form II in reaction 7), with the amino group completely protonated. The ionic equilibria of the amino acids exists as follows:

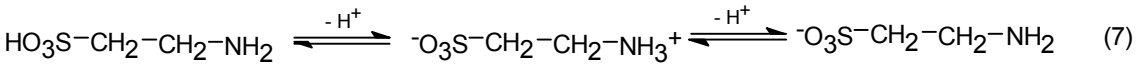

Addition of KOH results in deprotonation of the amino group, corresponding to the second equilibrium. Only the deprotonated amine species III can react with the acid gases. The

concentration of the deprotonated amine (amino acid salt) was estimated potentiometrically, by titrating with standard HCl solutions.

3.2 Experimental Setup

The experimental setup consisted of a double walled stirred reactor (1660 ml) as shown in Figure 2. The stirrer used was a gas inducing impeller to enable a high mass transfer rate and thereby reduce possible liquid side mass transfer limitations. The reactor was provided with a temperature and pressure indicator. The reactor was connected to a calibrated gas supply vessel through a pressure controller, to control the pressure in the reactor side. The gas supply vessel was also provided with a pressure and temperature indicator. The reactor was connected to a vacuum pump for the evacuation of inert gases from the reactor as well as to remove the dissolved gases in the liquid, prior to the actual experiments. To analyse the CO_2 loading in the liquid, an analytical method similar to the one reported by Blauwhoff (1982) was used.

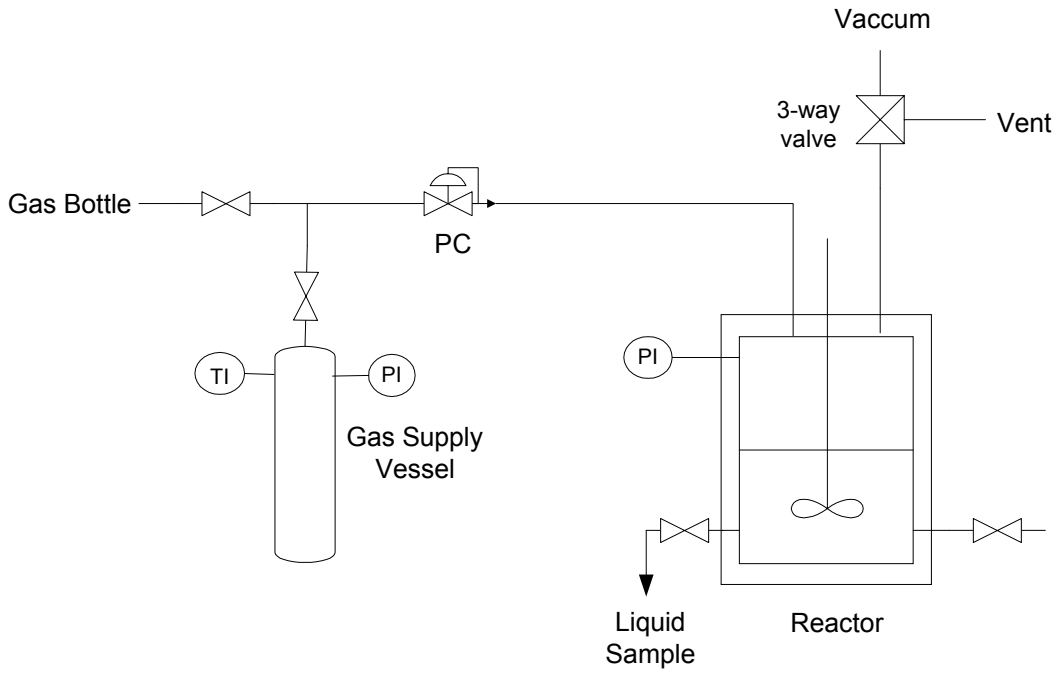

Figure (2) *Experimental Setup*

3.3 Procedure

A known volume of the prepared salt solution was transferred to the reactor and vacuum was applied to the reactor till the liquid started boiling. The application of vacuum to the reactor was stopped and gas-liquid equilibrium was allowed to establish in the reactor. The pressure in the reactor was noted down. The gas supply vessel was subsequently filled with pure CO_2 (99.999 % purity) to a desired initial pressure. The stirrer was started and the gas flow into the reactor was regulated by the pressure controller. After admitting a known amount of CO_2 to the reactor, a small known volume of the liquid sample was taken from the reactor and analysed immediately for pH. Also a known volume of liquid sample was collected in a sample bottle to determine the CO_2 loading analytically. The samples in the

sealed bottles were allowed to stay overnight in a water bath maintained at 298 ± 0.5 K, to verify for crystallisation in the liquid. From the initial and final values (at the time of sampling) of the pressure in the gas supply vessel and reactor, the total number of moles of CO_2 transferred into the liquid was calculated. This gives the value of CO_2 loading (mol CO_2/mol amine) in the liquid. This value was cross-checked with the analytically determined CO_2 loading (according to method of Blauwhoff) and they were in agreement within ± 4%. For certain salt concentrations and CO_2 loading of the solution, crystallisation occurred in the reactor itself. However, the stepwise loading of the liquid was continued until it was difficult to collect reliable samples. At the end of experiment, the slurry of the liquid and solids (if it was formed during the experiment) was collected in a vessel for further investigation (discussed in section 4.1).

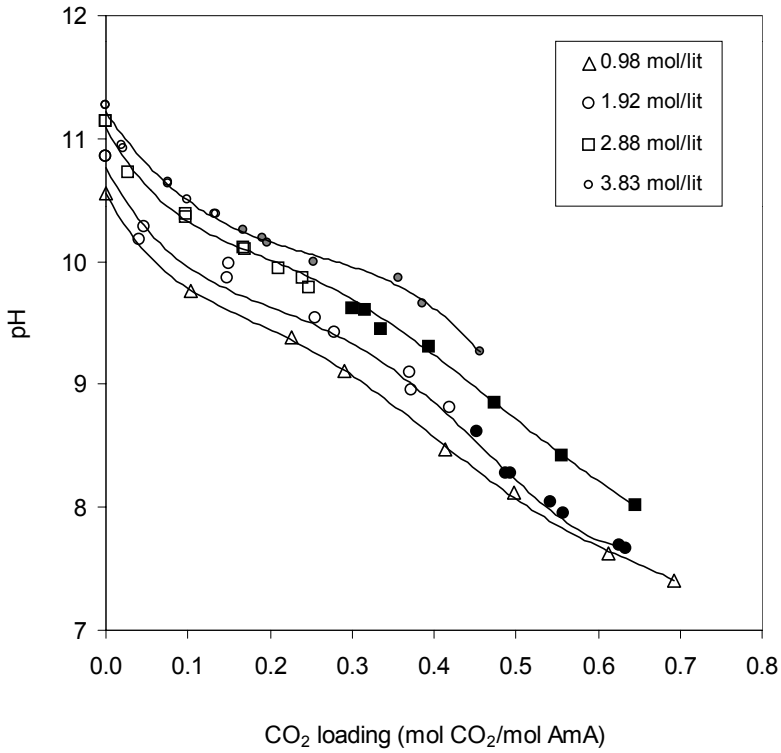

Figure (4) *Effect of CO_2 loading on pH of the aqueous potassium salt of taurine (at 298 K). The dark points in the figure denote the presence of solids in the solution.*

4.0 Results and Discussion

4.1 Analysis of the Solids/Crystals

The slurry containing the crystals was filtered to recover the solids. The liquid and a small amount of the crystals dissolved in deionised water was analysed using ^{13}C NMR (Varian Unity 400 MHz) for identification of the constituent species. The sample preparation and conditions for the ^{13}C NMR analysis were similar to those described by Hook (1997). A small amount of the solids was washed with distilled water for 5-6 times and subsequently analysed using ^{13}C NMR. Figure 3 shows the ^{13}C NMR spectra of the CO_2 loaded liquid, washed crystals and pure amino acid (Figure 3 is in the Appendix I). In case of the liquid, the

^{13}C NMR spectra showed peaks corresponding to CO_3^{2-} (6)/HCO_3^- (5), $RNHCOO^-$ (3), RNH_2 (1) and RNH_3^+ (4). The numbers within the parenthesis are the one assigned to the various chemical species in the reaction scheme as shown in Figure 1. For the unwashed crystals, there were no peaks corresponding to the carbamate or bicarbonate. The ^{13}C NMR spectra of the washed crystals showed exactly identical peaks corresponding to the spectra of the pure amino acid, indicating that the crystallised material is the protonated amine (4) which is one of the reaction products as shown in the reaction scheme. The crystals washed with water were dissolved in deionised water and the pH of the resulting solution was measured. The pH of the solution was acidic (5.7) and this is close to the isoelectric point of taurine (5.3).

4.2 Crystallisation in Loaded Solutions

Figure 4 shows the plot of the pH of a loaded solution against CO_2 loading (α). As can be expected, the shape of the curve is typical for the absorption of acid gases in aqueous amine solutions. The plateau in the curve is due to the buffering action of the amine, corresponding to the basic strength (pKa) of taurine. The dark points in the curve indicate the visual presence of crystals in the solution (during the experiment in the reactor or afterwards in the sample bottles). The first dark experimental data point from the origin of the abscissa for each amino acid salt concentration indicates the onset of crystallisation. For a 1 molar solution, no crystallisation occurred in the loaded salt solution. Crystallisation was observed for solutions of 2 molar salt concentration and above. It can be observed from Figure 4 that with an increase in molar salt concentration, crystallisation occurs at lower CO_2 loading (critical CO_2 loading, α_{crit}). Although the actual time for the completion of the experiments was high (approximately 140 minutes), the critical CO_2 loading point was always reached relatively fast (less than 40 minutes). For high salt concentrations, the critical CO_2 loading at which crystallisation occurred was low and the time to reach this point was relatively short. For very large absorption times, the contribution of the secondary carbamate hydrolysis reaction to the overall absorption capacity or CO_2 loading of the liquid can become significant and this explains for the experimentally observed final CO_2 loading values higher than 0.5.

Table (1) *Carbamate hydrolysis reaction rate and equilibrium constants*

Amine	Temperature K	k_{carb} s^{-1}	K_{carb} mol m^{-3}	Reference
Monoethanolamine	291	6.0×10^{-6}	19.5	Jensen et al. (1954)
α-alanine	291	3.3×10^{-5}	107.2	Jensen & Faurholt (1952)
β-alanine	291	1.3×10^{-5}	30.9	Jensen & Faurholt (1952)
Glycine	291	2.0×10^{-5}	33.1	Jensen et al. (1952)
Taurine	298	-	50.9	Kumar et al. (2002)
Diethanolamine	291	4.0×10^{-5}	206.5	Jensen et al. (1954)

Table 1 gives the values of the carbamate hydrolysis reaction rate and equilibrium constants for various alkanolamines and amino acid salts. The carbamate hydrolysis equilibrium constant is defined as follows.

$$K_{carb} = \frac{C_{HCO_3^-}\, C_{AmA}}{C_{AmACOO^-}} \qquad (8)$$

While there is a large amount of accurate information available on the equilibrium constants, the data on the carbamate hydrolysis reaction rate constants are relatively scarce and old. The experimental data of Faurholt and coworkers are given in Table 1 for a few important primary alkanolamines and amino acids. The equilibrium constant of taurine was obtained experimentally from an independent study (Kumar et al., 2002). From these data, it is clear that the carbamates of the primary amines are in general more stable than that of secondary amines. Similarly, the hydrolysis reaction rates for the primary amine carbamates are relatively slower than that of secondary amine carbamates and much slower than the preceding reaction of CO_2 with the unreacted amine to form the carbamate (reaction 1; second order rate constant, $k_2 \cong 10^3$ m^3 mol^{-1} s^{-1}). It should be noted that the above constants are dependent on the ionic strength of the solution (Chan & Danckwerts, 1981) and the values provided here are the ones determined for low amine concentrations. Assuming that the k_{carb} of taurine is comparable to that of glycine, the maximum contribution of carbamate hydrolysis reaction to the CO_2 loading can be 4 percent. This value corresponds to a reaction/absorption time of 40 minutes, the time needed to reach α_{crit} for the unloaded 2 molar amino acid salt solution. In the above analysis, an Arrhenius temperature dependence of k_{carb} was assumed to estimate its value at the absorption temperature (298 K) and the highest possible carbamate concentration of (α_{crit}. $C_{AmA,0}$) was assumed to be present (hypothetically) at the beginning of the reaction. Hence, it is unlikely that there is a significant concentration of carbamate hydrolysis products (like bicarbonate or carbonate) at the critical CO_2 loading point. For the present system, the rapid onset of crystallisation and the analysis of the precipitate itself makes clear that the crystallised product is not likely to be a bicarbonate/carbonate salt and instead has to be the protonated amine or zwitterionic form of taurine.

Table (2) *Estimated concentration of amino acid (species 4 in Figure 1) in the loaded solutions at the critical CO_2 loading point. S_w is the solubility of taurine in water at 298K (109 kg m^{-3})*

$C_{AmA,0}$ x 10^{-3} (mol m^{-3})	α_{crit} (mol CO_2/mol AmA)	C_{AmAH+} (kg m^{-3})	(C_{AmAH+}/S_w) -
0.98	-	-	-
1.92	0.450	108.0	0.99
2.48	0.366	114.4	1.05
2.91	0.301	108.8	1.00
3.46	0.202	89.3	0.82
3.83	0.170	81.5	0.75

Due to the discrete addition of CO_2 during the absorption experiments, it was not practically possible to accurately find the critical CO_2 loading point and so experiments were repeated to reach α_{crit} as close as possible. The concentration of the amino acid (species 4 in Figure 1) at the critical loading point was calculated as the product of α_{crit} and initial amino acid salt concentration ($C_{AmA,0}$), again with the assumption that there is no hydrolysis of the carbamate till the critical CO_2 loading point.

Using the above assumption, Table 2 shows the concentration of the zwitterionic form of the amino acid (component 4) at the critical CO_2 loading point as a function of the initial amino acid salt concentration in the solution. In the fourth column of Table 2, the ratio of the concentration of component 4 to the solubility of taurine in pure water (C_{AmAH+}/S_w) is given. As can be seen, the ratios (C_{AmAH+}/S_w) at which crystallisation of component 4 occurs are quite close to 1, which is to be expected if the crystallising substance is taurine. With the above assumptions, the concentration of taurine at the critical CO_2 loading can be approximated by the product of the initial salt concentration and CO_2 loading, according to $C_{AmAH+} = (\alpha_{crit} \, . \, C_{AmA,0})$. The fact that $C_{AmAH+} \cong S_w$ (within ~25%, See Table 2) also means that the critical CO_2 loading is more or less inversely proportional to the initial amino acid salt concentration. The initial increase of C_{AmAH+}/S_w with amino acid salt concentration and subsequent drop below that of water (See Table 2) can be attributed to the influence of different ionic species present in the solution on the solubility of taurine. In the section 4.3, the experimental results of the solubility of taurine in the presence of different ionic species are given.

Table (3) *Absorption of pure CO_2 in 2.5 M aqueous potassium salts of amino acids at 295.5 K (Hook, 1997). The solubility data was obtained from Greenstein & Winitz (1961).*

Amino acid	Carbamate (%)	CO_3^{2-}/HCO_3^- (%)	α_{crit} (mol mol^{-1})	t_{crit} (min)	C_{AmAH+} (mol m^{-3})	$S_{m,w}$ (mol m^{-3})
Glycine	31	69	-	-	-	3310
α-Alanine	10	90	0.94	>> 200	2115	1810

Analysis of the experimental data of Hook (1997)

Hook (1997) qualitatively studied the CO_2 absorption rate and capacity of aqueous potassium salts of sterically and non-sterically hindered amino acids. In the present discussion, experimental data of Hook, related to the primary amino acids (glycine, α-alanine, 2-methyl alanine) alone will be considered for comparison with taurine and they are summarised in Table 3. During CO_2 absorption, crystallisation was encountered for potassium salts of α-alanine and 2-methyl alanine. However, no such phenomenon was observed for glycine. As the duration of the experiments was relatively long ($\cong$ 20 hrs), there should be a significant contribution of the hydrolysis reaction to the CO_2 absorption capacity, even for primary amines. The distribution of the absorbed CO_2 between carbamate and carbonate/bicarbonate species is shown in Table 3 and was measured at the end of the equilibration time ($\cong$ 20 hrs). Considering the time to reach α_{crit} for α-alanine, the carbamate

formation reaction (reaction 1) would be almost complete in comparison to the carbamate hydrolysis reaction (reaction 2) and therefore concentration of protonated species can be related to the α_{crit} as given below.

$$C_{AmAH^+} = C_{AmA,0}\ \alpha_{crit}\ \frac{100 - \%\ Carbamate}{100} \quad \text{for \% Carbamate} < 100 \quad (9)$$

In arriving at the above equation, carbamate formation reaction (1) was assumed to be irreversible as the equilibrium constant for the primary amines is high (Sharma & Danckwerts, 1966) and the dissociation reactions (3) to (5) were neglected. For glycine, the maximum concentration of the amino acid (assuming a complete hydrolysis of carbamate) could be 2500 mole m^{-3} and this is still smaller than the solubility of glycine (3310 mol m^{-3}) in water at 295.5 K. Incase of alanine, the concentration of the protonated species at the critical loading point is significantly larger than the molar solubility of alanine in water. Consequently, the protonated species should crystallise out of the solution for alanine, which was also observed experimentally.

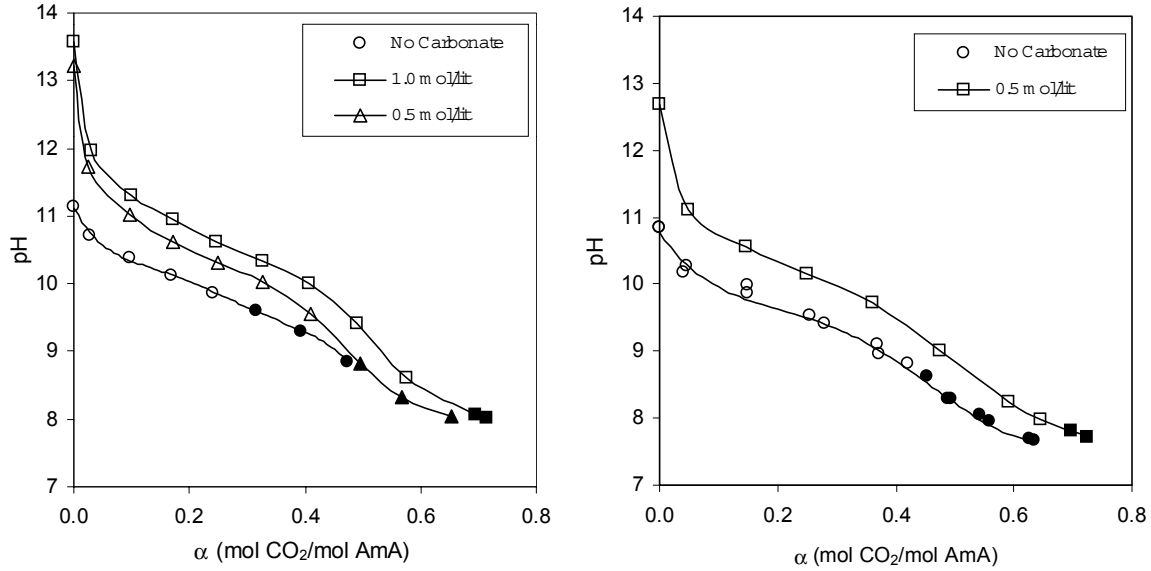

$C_{AmA,0}$: 3000 mol m^{-3} $C_{AmA,0}$: 2000 mol m^{-3}

Figure (5) *Influence of the addition of potassium carbonate on the absorption capacity and α_{crit} of 3.0 and 2.0 molar potassium taurate solution at 298 K. The dark points in the figure denote the presence of solids in the solution. The legends indicate the initial concentration of carbonate in the liquid.*

A simple way of increasing the α_{crit} is by the addition of another base or buffer to the amino acid salt solution. Though it does not change the intrinsic absorption capacity of the amino acid salt solution, the added base or buffer simply increases the overall absorption capacity of the liquid. This modification of the process is in principle similar to the promoted carbonate process, in which amino acids or alkanolamines are used as rate promoters to the conventional hot carbonate process (Kohl & Nielsen, 1997). In the present case, the addition of carbonate to the aqueous solution of amino acid salt is to increase the absorption capacity of the liquid. This could lead to a higher cyclical loading in the actual absorption process and

thereby avoid crystallisation in the absorber. Figure 5, as an example, shows the effect of the addition of potassium carbonate on the critical CO_2 loading point for the aqueous solutions of two different salt concentrations. The dark points in the figure indicate the presence of solids in the liquid. As can be expected, α_{crit} increases with the initial carbonate concentration and this increase in absorption capacity is solely due to the following reaction.

$$CO_3^{2-} + CO_2 + H_2O \Leftrightarrow 2\,HCO_3^- \qquad (10)$$

For a 3 molar potassium taurate solution containing 1000 mol m^{-3} of potassium carbonate, the incremental increase in absorption capacity is 0.359 mol CO_2/mol AmA. This corresponds to an additional 1080 mol m^{-3} of CO_2 absorbed in the liquid, which is the approximately equal to the amount that should have been absorbed by 1000 mol m^{-3} of carbonate solution, as per reaction stoichiometry. This is logical if one considers the acidic dissociation constant (pKa) of the amino acid (9.14) as well as that of carbonate (10.34); the reaction (10) should have gone to completion in comparison to the reaction between CO_2 and amino acid salt, at α_{crit}.

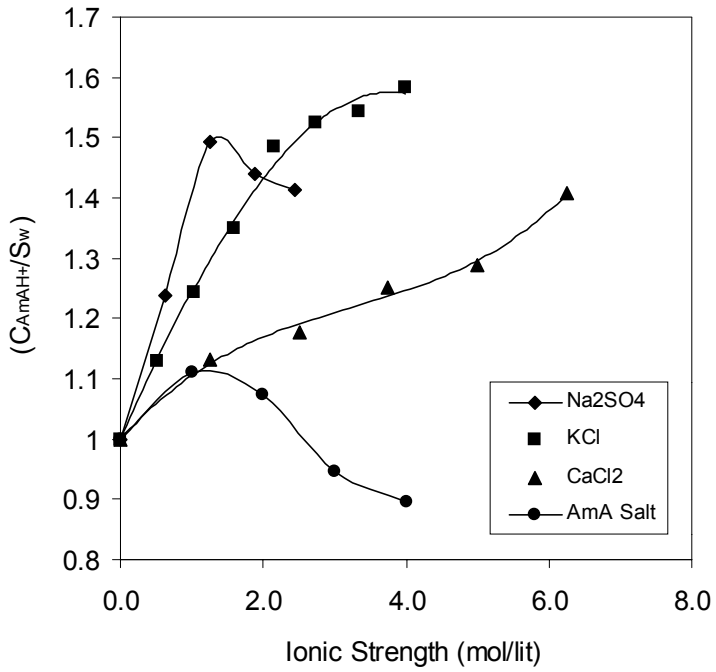

Figure (6) *Effect of ionic species on the solubility of Taurine in water at 298 °C*

4.3 Solubility of amino acid in salt solutions

The deviation of (C_{AmAH+}/S_w) from unity, as given in Table 2 could be due to the influence of the ionic species present in the loaded solution on the solubility of the protonated amine. Considerable information is available in literature on the solubility of amino acids in different salt solutions (Greenstein & Winitz, 1961). In general, there is no clear or general rule to predict the solubility behavior of amino acids in the presence of salts or as a function of ionic strength. However, it can be observed in literature that salts with monovalent ions increase the solubility of amino acids in water and salts with polyvalent ions (like sodium sulfate) increase solubility upto a certain salt concentration and then solubility

drops drastically with further increase in salt concentration. It should be noted that this behavior does not hold good for all amino acids. Due to this and because of the absence of information on the influence of electrolytes on the solubility of taurine, experiments were carried out to study the solubility of taurine in different salt solutions at 295 K. The results are shown in Figure 6. In this figure, the solubility is given in a dimensionless form (C_{AmAH+}/S_w). For KCl and $CaCl_2$, the solubility increases monotonically with ionic strength of the solution. Incase of sodium sulfate, the solubility increases and then drops. More importantly, Figure 6 also shows the solubility of taurine (component 4) in aqueous potassium taurate (component 1 in Figure 1) solutions. The trend follows that of aqueous sodium sulfate solutions, but the solubility of the amino acid drops below the value for pure water ($C_{AmAH+}/S_w<1.0$) at higher concentrations of potassium taurate. This is similar to the behavior observed during the CO_2 absorption experiments described in section 4.2 (see table 2).

Generally, it can be seen that the values of C_{AmAH+}/S_w are again within ± 20% to unity for aqueous potassium taurate solutions, indicating that the absolute solubility of taurine in these solutions does not differ significantly from the solubility in pure water. Of course one should note that in the loaded solutions, other ions like carbamate, bicarbonate, etc., are also present which might influence the solubility differently. Additionally, the initial concentration of potassium taurate as given in Table 1 is not the same as the concentration of potassium taurate at the critical loading point. Nevertheless, this finding again supports the view that the precipitate is the zwitterionic form of taurine and it gives some qualitative explanation for the behavior of C_{AmAH+}/S_w as observed in Table 2.

5.0 Influence of Crystallisation on the Gas-Liquid Mass Transfer In Loaded Aqueous Amino Acid Salt Solutions

The effect of the presence of a third phase (solid or immiscible liquid phase) on gas-liquid mass transfer has been widely investigated in the recent past and also extensively reviewed by Beenackers & van Swaaij (1986; 1993). In particular, emphasis has been given to those gas-liquid-solid systems, in which the presence of small particles in the liquid phase enhances the mass transfer at the gas-liquid interface. The enhancement is usually due to the favorable physical or chemical interaction of the small particles with the dissolved gas phase. However, some authors have shown that the presence of inert solid particles in the liquid phase have a negligible or negative influence on the gas-liquid mass transfer (Quicker et al., 1989; Godbole et al., 1990). For detailed information, the reader is referred to the above-mentioned original or review articles published in open literature.

In the present context also, crystallisation of the reaction products during the absorption of CO_2 in aqueous potassium taurate solutions, for CO_2 loading values beyond that of α_{crit} may significantly influence the gas-liquid mass transfer characteristics (k_La) of the contactor. So, a semi-quantitative study was carried out on the influence of the presence/formation of solids on k_La in a stirred vessel. It is clear from the earlier discussions that for amino acid salt concentrations larger than approximately 2000 mol m^{-3}, the critical CO_2 loading point is inversely related to the amino acid salt concentration in the liquid. In the current investigation, the physical absorption of N_2O in unloaded and loaded aqueous

potassium taurate solutions was studied to determine the effect of CO_2 loading (α) on the volumetric mass transfer coefficient, k_La.

5.1 Experimental

An aqueous solution of potassium taurate with a concentration of 2000 mol m^{-3} was prepared using the procedure mentioned in section 3.1. The solution was loaded with pure CO_2 in a stirred vessel to a predetermined value, using the method given in section 3.3. The loaded solution was collected in a gas tight vessel and a known volume (615 ml) of this liquid was transferred to an another stirred reactor (volume: 2060 ml, i.d.: 0.11 m) provided with a high intensity, gas-inducing stirrer in the liquid phase and four symmetrically mounted stainless steel baffles. The stirred reactor was also provided with digital temperature, stirred speed and pressure indicators and these data were recorded by a data acquisition system. Two gas phase stirrers (propeller type) were provided on the shaft of the high intensity stirrer. The reactor was connected to a vacuum pump and gas supply vessel by a two-way valve.

After the transfer of unloaded or loaded solution to the stirred reactor, mild vacuum was applied to reduce the gas phase pressure to approximately 0.48 bar. The stirring was started and the liquid was allowed to equilibrate with the gas phase for approximately 60 minutes. This also provided sufficient time to adjust the temperature of the contents of the reactor to the desired absorption temperature. The gas phase contained air, water vapor as well as CO_2 [the (equilibrium) partial pressure of which depends mainly on the α, salt concentration and temperature]. After this period, stirring was stopped and the gas phase pressure was noted down (p_{inert}). The reactor was filled with pure N_2O from the gas supply vessel to a pressure of approximately 1.2 bar (p_o). The stirrer was started and the pressure (p) in the reactor was recorded in the computer as a function of time. A stirrer speed of 800 rpm was used in all the experiments reported here. The liquid phase mass transfer coefficient was calculated from the following equation, obtained from the mass balance of N_2O in the gas phase.

$$\frac{k}{k+1}\ln\left[\frac{p_{N_2O,0}}{(k+1)\,p_{N_2O} - k\,p_{N_2O,0}}\right] = k_L a\, t \qquad (11)$$

where,

$$k = \frac{V_G}{m\,V_L} \qquad (12)$$

$$p_{N2O,\,0} = p_o - p_{inert} \qquad (13)$$

$$p_{N2O} = p - p_{inert} \qquad (14)$$

A linear regression of equation (11) can be used to obtain the value of k_La. The physical solubility (m) of N_2O in loaded potassium taurate solution was considered to be identical to that of the unloaded solutions of similar concentration and was obtained from the experimental data of Kumar et al. (2001).

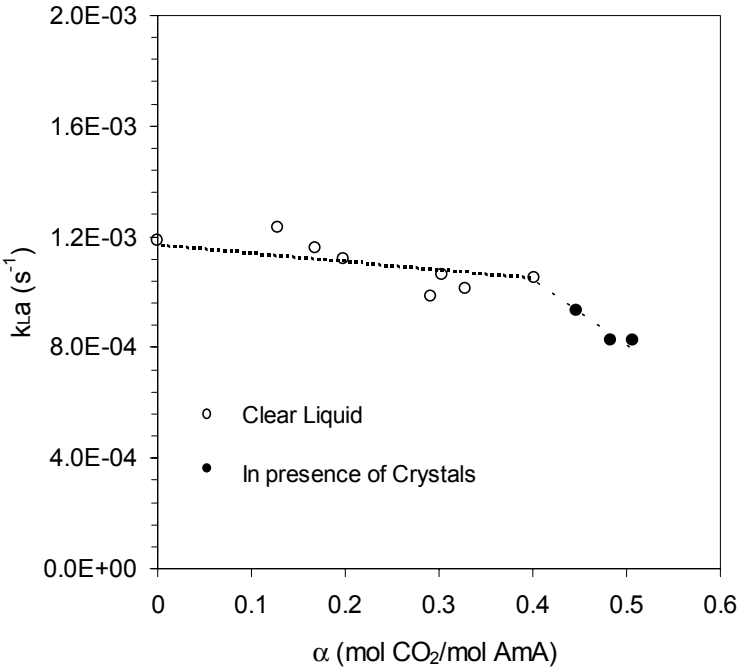

Figure (7) *Influence of solid reaction products on the volumetric mass transfer coefficient (k_La), during the absorption of N_2O in unloaded and CO_2 loaded aqueous potassium taurate solutions at 298 K. The concentration of the amino acid salt is 2000 mol m^{-3}.*

5.2 Results and Discussion

The reactor was operated at a stirrer speed slightly less than the value at which the induction of the gas into the liquid occurred. Therefore, the interfacial area for the gas-liquid mass transfer is mainly the surface of the liquid, though it is very turbulent at the liquid surface. At the same time, the stirrer speed was high enough to keep all the solids suspended in the liquid. In the absence of gas induction, the influence of solids on coalescence or break up of gas bubbles (hence on interfacial area, a) can be neglected. Figure 7 shows the effect of CO_2 loading on the volumetric mass transfer coefficient (k_La). The dark points in the figure indicate the measurements done in the absence of crystals in the loaded solution. In the absence of solids, there seems to be no numerically significant (within the experimental accuracy) influence of α on k_La, though one could see a clear, but marginal decrease in k_La with CO_2 loading. As sufficient time was provided for the equilibration of the loaded solution with the gas phase in the stirred reactor prior to the actual experiment with N_2O (to avoid errors due to possible mass transfer of CO_2 from the liquid to the gas phase during the absorption of N_2O), the decrease in k_La must probably be attributed to the marginal increase in the viscosity of the solution due to CO_2 loading. However in the presence of crystals, a clear and sharp decrease in the k_La with CO_2 loading can be observed. The decrease in the k_La due to the presence of solid particles that are inert to the dissolved solute at the gas-liquid interface is due to the following widely accepted reasons.

1. Increase in the apparent slurry viscosity due to the presence of solids in relation to the solid free liquid. Due to this, the k_L can be reduced due to the lowering of the effective diffusivity of gas in the liquid (Joosten et al., 1977).

2. Blockage of the gas-liquid interface by the solid particles (Beenackers & van Swaaij, 1993).

It should be noted that beyond the α_{crit} value, the solid fraction (hold-up) in the solution increases proportionally with the CO_2 loading and there seems to be a definite relationship between the CO_2 loading and k_La. For solids particles of size greater than the film thickness (> ~ 200 μm), a number of studies have correlated their experimental data of k_La and solid holdup (ε_s) using relations similar to the one given below (Schmitz et al., 1987; Kojima et al., 1987).

$$\frac{k_La}{(k_La)_o} = A - B\,\varepsilon_s \qquad (15)$$

Here A and B are constants. For the present case where there is most probably a distribution in the size of solid particles, the actual mechanism behind the decrease in k_La beyond α_{crit} could be quite complex and it is beyond the scope of the present work to investigate this in detail.

It can be concluded that for solutions of higher amino acid salt concentration (say 4000 mol m^{-3}), the solid fraction in the slurry will be very high even for moderately high CO_2 loading. This example study shows that this can significantly affect the volumetric mass transfer coefficient of the gas-liquid contactor.

6.0 Conclusions

A semi-quantitative investigation on the crystallisation phenomenon that occurs during the absorption of CO_2 in aqueous amino acid salt solutions has been carried out, using the potassium salt of taurine as a model amino acid salt. The ^{13}C NMR analysis of the crystallised solid product showed that it was protonated amine (the zwitterionic form of taurine), which is one of the reaction products.

From the experiments conducted to study the relation between the critical CO_2 loading point (at which crystallisation occurs) and the initial amino acid salt concentration, it was found that the critical CO_2 loading point (α_{crit}) was more or less inversely proportional to the initial amino acid salt concentration ($C_{AmA,0}$).

$$\alpha_{crit} = \frac{S}{C_{AmA,0}}$$

As the estimated concentration of taurine at α_{crit}, in the loaded solution was found to differ (though not significantly) from the solubility of taurine in water, the solubility behavior of taurine in water, in the presence of different types of inorganic salts and potassium taurate was studied. Though the solubility behavior of taurine in water in the presence of different types of ions seems to be complex, its behavior in the presence of potassium taurate follows the same trend as that of the estimated concentration of taurine at the critical CO_2 loading point. This can only be regarded as a qualitative indication as the ionic strength of the model solution differs from that of loaded potassium taurate solution.

The crystallisation of the reaction product beyond the α_{crit} value in the loaded potassium taurate solution can have a significant effect on the gas absorption rate. The presence/formation of solids in the liquid phase during CO_2 absorption seems to have a significant effect on the volumetric mass transfer coefficient at the gas-liquid interface, for a stirred vessel. As the solids have no interaction (either physical or chemical) with the gas absorbed, the k_La was found to decrease significantly with CO_2 loading beyond the α_{crit} value. It is mostly attributed to the decrease in the effective interfacial area for mass transfer, due to the physical blockage of the gas-liquid interface by the solid particles.

Acknowledgement

This research is part of the research programme performed within the Centre for Separation Technology (CST), which is a co-operation between the Netherlands Organisation for Applied Scientific Research (TNO) and the University of Twente. We also acknowledge H.J. Moed and Wim Leppink for the construction of experimental setups.

7.0 Nomenclature

A	Constant, dimensionless
a	Interfacial area for mass transfer, $m^2\ m^{-3}$
B	Constant, dimensionless
C	Concentration, mol m^{-3}
k	Constant, $V_G/(V_L.m)$, dimensionless
K_{carb}	Carbamate hydrolysis reaction equilibrium constant, mol m^{-3}
k_{carb}	Carbamate hydrolysis reaction rate constant, s^{-1}
k_L	Liquid side mass transfer coefficient, m s^{-1}
m	Physical solubility, $(C_{N2O,l}/C_{N2O,g})_{eq}$, dimensionless
p	Partial pressure, N m^{-2}
S	Solubility of amino acid, kg m^{-3}
S_m	Molar solubility of amino acid, mole m^{-3}
t	time, s
t_{crit}	time at which crystallisation occurred during absorption, s
V_G	Volume of gas phase, m^3
V_L	Volume of liquid phase, m^3

Symbol

ε_s	Solid holdup, dimensionless
α	CO_2 loading, mol CO_2 mol AmA^{-1}
α_{crit}	Critical CO_2 loading, mol CO_2 mol AmA^{-1}

Subscript

0	at time, t = 0
AmA	Amino acid salt

$AmACOO^-$	Carbamate
$AmAH^+$	Amino acid
g	gas
inert	Inerts
l	liquid
N_2O	Nitrous oxide
o	Absence of solids
w	Water

8.0 References

Beenackers, A.A.C.M., & van Swaaij, W.P.M. (1986). Slurry reactors, fundamentals and application in *Chemical Reactor Design and Technology* (Ed. by H. de Lasa), NATO ASI, pp.463-538. Martinus Nijhoff, The Hague.

Beenackers, A.A.C.M., & van Swaaij, W.P.M. (1993). Mass transfer in gas-liquid slurry reactors. *Chemical Engineering Science*, **48(18)**, 3109-3139.

Blauwhoff, P.M.M. (1982). Selective absorption of hydrogen sulfide from sour gases by alkanolamine solutions, Ph.D. Thesis, University of Twente, The Netherlands.

Chan, H.M., & Danckwerts, P.V. (1981). Equilibrium of MEA and DEA with bicarbonate and carbamate. *Chemical Engineering Science*, **36**, 229-231.

Godbole, S.P., Schumpe, A., & Shah, Y.T. (1990). The effect of solid wettability on gas-liquid mass transfer in a slurry bubble column. *Chemical Engineering Science*, **45**, 3593-3595.

Greenstein, J.P., & Winitz, M. (1961). *Chemistry of the Amino Acids*. London: John Wiley & Sons.

Hook, R.J. (1997). An Investigation of some sterically hindered amines as potential carbon dioxide scrubbing compounds. *Industrial & Engineering Chemistry Research*, **36**, 1779-1790.

Jensen, A., & Faurholt, C. (1952). Studies on carbamates V. The carbamates of α-Alanine and β-Alanine. *Acta Chemica Scandinavica*, **6**, 385-394.

Jensen, A., Jensen, J.B., & Faurholt, C. (1952). Studies on carbamates VI. The carbamate of Glycine. *Acta Chemica Scandinavica*, **6**, 395-397.

Jensen, M.B., Jorgensen, F., & Faurholt, C. (1954). Reaction between CO_2 and amino alcohols – I. Monoethanolamine and diethanolamine. *Acta Chemica Scandinavica*, 8, 1137-1141.

Joosten, G.E.H., Schilder, J.G.M., & Jansen, J.J. (1977). The influence of suspended solid material on the gas-liquid mass transfer in stirred gas-liquid contactors. *Chemical Engineering Science*, **32**, 563-566.

Kim, C.J., & Saratori, G. (1984). Kinetics and mechanism of DEA degradation in aqueous solutions containing Carbon dioxide. *International Journal of Chemical Kinetics*, **16**, 1257-1266.

Kohl, A.L., and & Nielsen, R.B. (1997). *Gas Purification*, Fifth Edition, New York: Gulf Publishing Company.

Koijma, H., Uchida, T., Ohsawa, T., & Iguchi, A. (1987). Volumetric liquid phase mass transfer coefficient in gas sparged three phase stirred vessel. *Journal of Chemical Engineering of Japan*, **20**, 104-106.

Kumar, P.S., Hogendoorn, J.A., Feron, P.H.M., & Versteeg, G.F. (2001). Density, viscosity, solubility and diffusivity of N_2O in aqueous amino acid salt solutions. *Journal of Chemical & Engineering Data,* **46**, 1357-1361 (Chapter 1 of this thesis).

Kumar, P.S., Hogendoorn, J.A., Feron, P.H.M., & Versteeg, G.F. (2002). Equilibrium solubility of CO_2 in aqueous potassium taurate solutions. (To be published; Chapter 4 of this thesis).

Polderman, L.D., Dillion, C.P., & Steele, A.B. (1955). Why MEA solution breaks down in gas treating service. *Oil and Gas Journal*, **54**, 180-186.

Quicker, G., Alper, E., & Deckwer, W.D. (1989). Gas absorption rates in a stirred cell with plane interface in the presence of fine particles. *Canadian Journal of Chemical Engineering*, **67**, 32-38.

Schmitz, M., Steiff, A., & Weinspach, P.M. (1987). Gas-liquid interfacial area per unit volume and volumetric mass transfer coefficient in stirred slurry reactors. *Chemical Engineering & Technology*, **10**, 204-215.

Sharma, M.M., & Danckwerts, P.V. (1966). The absorption of carbon dioxide into solutions of alkalis and amines. *Chemical Engineer*, CE244-CE280.

Appendix I: ^{13}C NMR spectra of the loaded liquid, unwashed and washed crystals

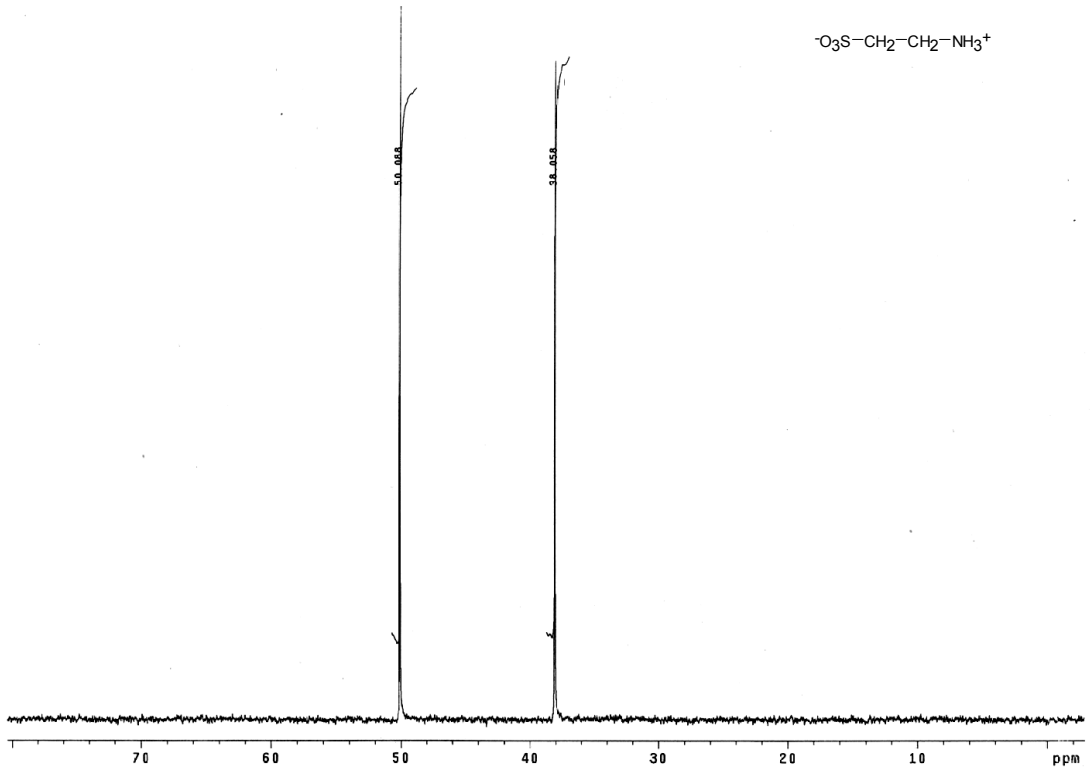

Figure (3a) *^{13}C NMR spectra of the pure amino acid dissolved in water*

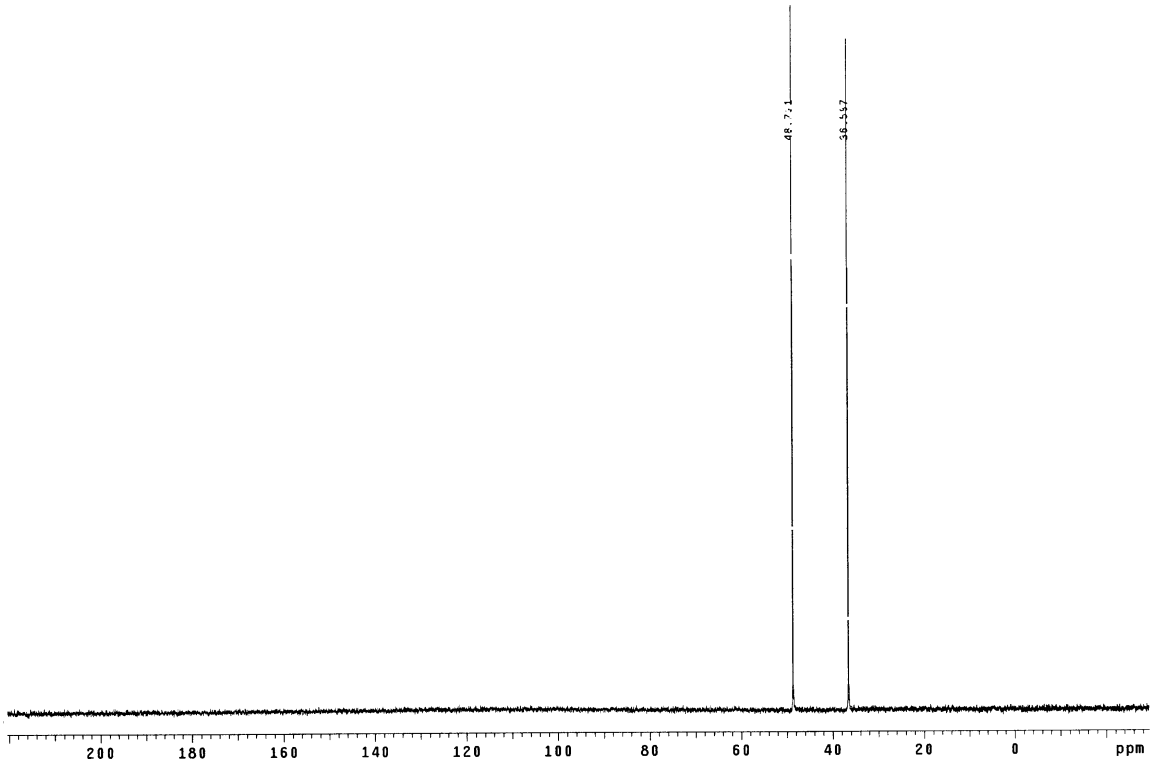

Figure (3b) *^{13}C NMR spectra of the crystals washed with water*

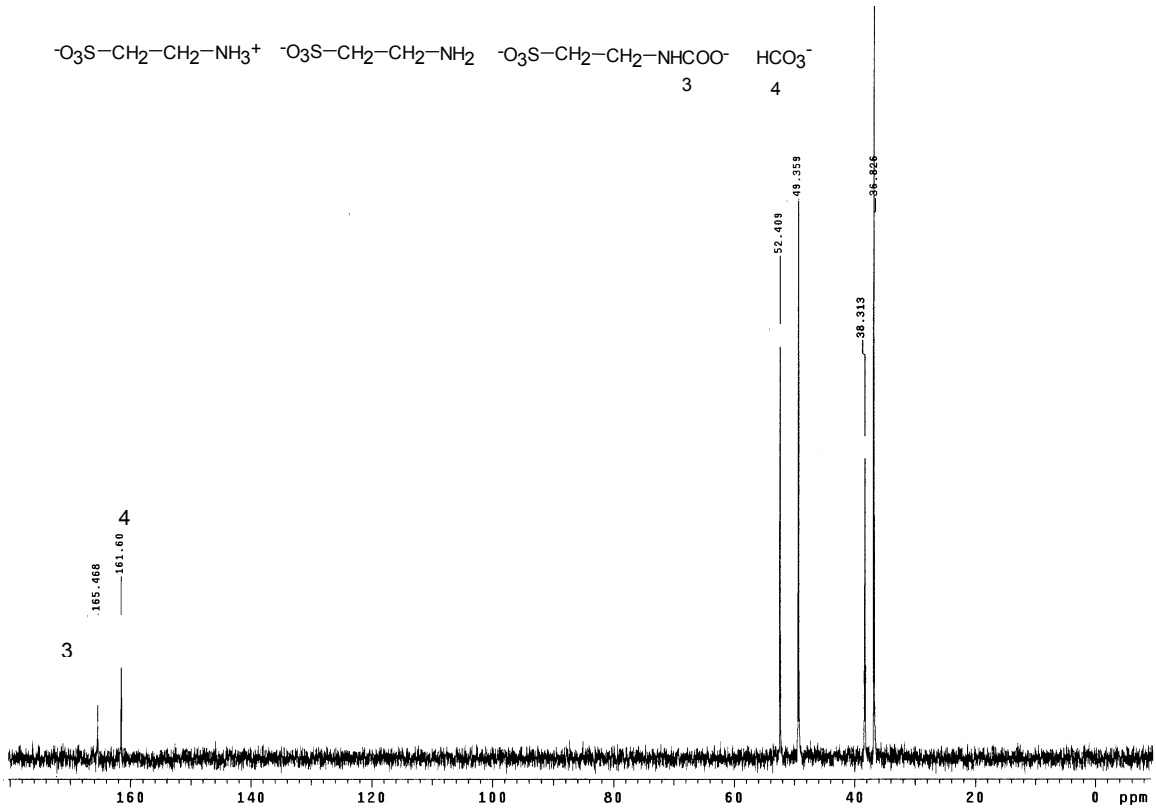

Figure (3c) *^{13}C NMR spectra of the CO_2 loaded aqueous potassium taurate solution*

Chapter 4

Solubility of Carbon Dioxide in Aqueous Potassium Taurate Solutions

Abstract

The solubility of CO_2 in aqueous potassium taurate solutions has been measured at 298 and 313 K. Crystallisation of the protonated amine (one of the reaction products) was observed during the absorption of CO_2 in concentrated amino acid salt solutions. The influence of crystallisation on the equilibrium CO_2 absorption capacity of the amino acid salt solution has been investigated. The difference in the thermodynamic characteristics of the aqueous amino acid salt solution and aqueous alkanolamines has been discussed using the Deshmukh-Mather model. Due to a limited change in the ionic strength of the solution in the range of the measured CO_2 loading, a simplified model similar to the one proposed by Kent and Eisenberg (1976) has been used to interpret the solubility data. In addition to this, the equilibrium constant of the carbamate hydrolysis reaction has been experimentally measured for monoethanolamine and the potassium salt of taurine at 298 K.

1.0 Introduction

Removal of acid gases, such as CO_2 and H_2S, by absorption in reactive solvents is a vital mass transfer operation in a number of industrial activities such as the processing of natural gas or refinery gas and the gas from coal gasification. Due to the increasingly stringent environmental regulations, it is also used in the removal of CO_2 from effluent gas streams such as flue gas from a power generation plant. The widely used chemical solvents in the bulk or selective removal of CO_2 are aqueous solutions of alkanolamines and amine promoted alkaline salt solutions (Kohl & Nielsen, 1997). Some of the practical problems associated with alkanolamines in acid gas treating processes are a high volatility (especially for primary amines like monoethanolamine; leading to vaporisation losses in the stripper) and degradation of the solvent in COS or oxygen bearing gas streams. Aqueous alkaline salt solutions of amino acids can be a possible alternative for aqueous alkanolamines. The amino acids have been primarily used in the past in minor quantities as “rate promoters” in the conventional gas treating processes such as the hot carbonate process. However, there were also a few commercial processes (such as Alkacid M and Alkacid dik from BASF) which exclusively use amino acid salt solutions for the selective removal of acid gases. The ionic nature of these liquids offer many advantages over alkanolamines such as negligible volatility (consequently negligible loss of solvent in the stripper), better resistance to degradation, especially in oxygen rich atmospheres, and a low viscosity (resulting in a lower pressure drop in solvent circulation). The surface tension of these liquids is comparable to that of water, which is of tremendous advantage for their use in some of the latest generation gas-liquid contactors such as membrane contactors. In membrane contactors, wetting of the microporous membranes by aqueous alkanolamines is a major technical bottleneck in their use for CO_2 removal (Kumar et al., 2002a). Currently, there is a renewed interest in the use of amino acids for acid gas treating, especially in removal of CO_2 from gas streams also containing oxygen such as flue gas.

Design of gas-liquid contactors for CO_2 removal using aqueous alkaline salts of amino acids requires information, among others, on the vapor-liquid equilibria (VLE) of the CO_2-aqueous amino acid salt system. Unlike aqueous alkanolamine-CO_2 systems where there is a large amount of experimental VLE data available in the literature, the published data on CO_2-aqueous amino acid salt systems is scarce. Recently, Hook (1997) made a qualitative study on the CO_2 absorption rate and capacity of the aqueous alkaline salt of some sterically and non-sterically hindered amino acids and found them to be comparable to that of aqueous alkanolamines of a similar class. A unique phenomenon associated with certain amino acids is the crystallisation of a reaction product during CO_2 absorption, especially at high CO_2 loading (mole CO_2 per mole amino acid salt) and amino acid salt concentrations (Hook, 1997; Kumar et al., 2002b). Kumar et al. (2002b) gave a relationship between the critical CO_2 loading value at which crystallisation of the reaction product occured for potassium taurate solutions. However, its influence on the solubility of CO_2 in the aqueous amino acid salt solutions is not known. So, there is a real need for experimental data on the equilibrium solubility of CO_2 in aqueous amino acid salt solutions to understand the behavior of these absorption liquids qualitatively as well as quantitatively. Fortunately, substantial knowledge accumulated from the research in developing rigorous VLE models

for alkanolamines (or aqueous electrolytes in general) can be conveniently extended to CO_2-aqueous amino acid salts systems.

The objective of the present work is to provide experimental solubility data for CO_2 in aqueous potassium salt solutions of taurine (2-aminoethansulfonic acid). The experimental measurements were performed for the range of partial pressures of CO_2 typically encountered in the treatment of flue gases (0.1- 6.0 kPa) and for amino acid salt concentrations between 500 and 4000 mol m^{-3} at 298 K. A limited number of experimental data is also presented for 313 K as well. The influence of crystallisation of a reaction product on the equilibrium absorption capacity of the aqueous salt solutions was studied quantitatively. The extended Debye-Hückel model (Deshmukh-Mather model) which was found to be accurate and convenient in describing the single acid gas-amine equilibria is used to analyse the experimental VLE data (Deshmukh & Mather, 1981). Experimental data is also provided on the carbamate hydrolysis equilibrium constant (K_{carb}), which is usually an important fit parameter in the VLE model.

2.0 Theory

Amino acids are amphoteric electrolytes i.e., they behave as both acid and base due to the presence of at least one carboxyl or sulphonyl group and one amino group. Amino acids exist in water as zwitterion or dipolar ion (form II in reaction 1), with the amino group completely protonated. The zwitterion is considered to be electrically neutral, since the number of positive charges is equal to the number of negative charges (Greenstein & Winitz, 1961). In water and in the absence of other solutes, the pH of the solution is equal to the isoelectric point of the amino acid. In salt solutions or solutions containing ions other than those derived from amino acids, some of the ionisable groups of the ampholyte may be electrically neutralised by other ions present. The ionisation equilibria of amino acids in aqueous solutions are described below:

$$\underset{\text{I}}{HO_2C\text{-}R\text{-}NH_3^+} \overset{-H^+}{\rightleftharpoons} \underset{\text{II}}{{}^-O_2C\text{-}R\text{-}NH_3^+} \overset{-H^+}{\rightleftharpoons} \underset{\text{III}}{{}^-O_2C\text{-}R\text{-}NH_2} \qquad (1)$$

Addition of a base to the zwitterionic amino acid solution removes a proton from the ammonium group, leaving the molecule with a net negative charge (anion: form III in reaction 1). It is the anion with a deprotonated amino group, which can react with acid gases like CO_2 and H_2S. Amino acids are weak electrolytes and there are atleast two dissociation constants corresponding to the dissociation equilibria of the two functional groups present in the amino acids. However, for the present study the second acid dissociation constant (pKa) is the only one of interest and its values at various temperatures are available in literature (Perrin, 1965). In the present work, the zwitterionic form of an amino acid in water was neutralised with a strong base and the resulting aqueous amino acid salt solutions were used.

2.1 Chemical Reactions

The alkaline salts of amino acids having a primary amino functional group react with CO_2 similar to primary amines, forming a water soluble and relatively stable carbamate as described by reaction (2) (Jensen & Faurholt, 1952).

$$2\ {}^{-}O_3S\text{-}R\text{-}NH_2 + CO_2 \Leftrightarrow {}^{-}O_3S\text{-}R\text{-}NHCOO^{-} + {}^{-}O_3S\text{-}R\text{-}NH_3^{+} \quad (2)$$

Detailed information on the above reaction (like reaction kinetics) can be obtained elsewhere (Jensen & Faurholt, 1952; Penny & Ritter, 1983; Kumar et al., 2002c). Already at moderately high amino acid salt conversions the carbamates of amino acids undergo hydrolysis to bicarbonate/carbonate (depending on the pH of the solution) and free amine to a certain extent (reaction 3). The free amine can further react with CO_2, resulting in actual CO_2 loadings much higher than the theoretical value of 0.5 mole CO_2 per mole of amino acid salt as would seem obvious from the stoichiometry of reaction (2).

$${}^{-}O_3S\text{-}R\text{-}NHCOO^{-} + H_2O \Leftrightarrow {}^{-}O_3S\text{-}R\text{-}NH_2 + HCO_3^{-} \quad (3)$$

The other reactions that occur in the liquid phase along with the above two reactions are, Dissociation of protonated amine:

$${}^{-}O_3S\text{-}R\text{-}NH_3^{+} \Leftrightarrow {}^{-}O_3S\text{-}R\text{-}NH_2 + H^{+} \quad (4)$$

Hydrolysis of carbon dioxide:

$$CO_2 + H_2O \Leftrightarrow HCO_3^{-} + H^{+} \quad (5)$$

Dissociation of bicarbonate:

$$HCO_3^{-} \Leftrightarrow H^{+} + CO_3^{2-} \quad (6)$$

Dissociation of water:

$$H_2O \Leftrightarrow H^{+} + OH^{-} \quad (7)$$

2.2 Equilibrium model

The equilibrium constant associated with the above independent reactions (other than reaction 2) can be thermodynamically expressed in terms of the activities of the reacting species. Henceforth the non-reacting part ($^{-}O_3S$-R-) of the amino acid anion will be expressed as $^{-}$R in its structural formula.

$$K_{carb} = \frac{[{}^{-}RNH_2][HCO_3^{-}]}{[{}^{-}RNHCOO^{-}]} \frac{\gamma_{{}^{-}RNH_2}\gamma_{HCO_3^{-}}}{a_w\,\gamma_{{}^{-}RNHCOO^{-}}} \quad (8)$$

$$K_{AmA} = \frac{[{}^{-}RNH_2][H^{+}]}{[{}^{-}RNH_3^{+}]} \frac{\gamma_{{}^{-}RNH_2}\gamma_{H^{+}}}{\gamma_{{}^{-}RNH_3^{+}}} \quad (9)$$

$$K_{CO_2} = \frac{[HCO_3^{-}][H^{+}]}{[CO_2]} \frac{\gamma_{HCO_3^{-}}\gamma_{H^{+}}}{a_w\,\gamma_{CO_2}} \quad (10)$$

$$K_{HCO_3^{-}} = \frac{[CO_3^{2-}][H^{+}]}{[HCO_3^{-}]} \frac{\gamma_{CO_3^{2-}}\gamma_{H^{+}}}{\gamma_{HCO_3^{-}}} \quad (11)$$

$$K_w = [H^+][OH^-]\frac{\gamma_{H^+}\gamma_{OH^-}}{a_w} \quad (12)$$

The concentrations in the above definitions of the equilibrium constants are in molal units. Since the liquid phase is an aqueous solution, the activity of water a_w, was set equal to its mole fraction (Deshmukh & Mather, 1981). The equilibrium constant for reaction (2), which was left out from the reaction scheme, can be expressed in terms of the equilibrium constant of reactions (3), (4) and (5).

$$K_{ov} = \frac{K_{CO_2}}{K_{AmA}\,K_{carb}} \quad (13)$$

The chemical reactions in the liquid phase are accompanied by the vapor-liquid equilibria of CO_2 and water. The equilibrium vapor pressure of CO_2 in the gas phase was related to the liquid phase concentration using the experimental (physical) solubility data obtained in an earlier study, which was described using the model of Weisenberger and Schumpe (1996).

$$P_{CO2} = RT\, m_{CO2}\, [CO_2] \quad (14)$$

where,

$$\log (m_{CO2,w}/m_{CO2}) = K_s\, C_s \quad (15)$$

Here $m_{CO2,w}$ is the physical solubility of CO_2 in water, C_s is the molar amino acid salt concentration and K_s is the Sechenov constant which is defined in terms of ion specific (h_i) and gas specific (h_G) constants.

$$K_s = \Sigma\,(h_i + h_G)\, z_i \quad (16)$$

Here z_i is the charge number of the ion. The numerical values of the temperature independent ion specific constants were obtained from the work of Kumar et al. (2001) and the temperature dependent gas (CO_2) specific constant was obtained from the work of Weisenberger and Schumpe (1996).

For water, the vapor-liquid equilibrium is given by:

$$P_w = a_w\, P_w^{sat} \quad (17)$$

Since the amino acid salt present in the liquid phase is in ionic form, it was assumed to be non-volatile. The gas phase total pressure in the present work was approximately 100 kPa. Therefore the non-ideality in the gas phase was neglected. In addition to the above equations, the following mass conservation and charge balance equations were also used in the equilibrium model.

Amine mass balance:

$$[^-RNH_2]_0 = [^-RNH_2] + [^-RNH_3^+] + [^-RNHCOO^-] \quad (18)$$

CO_2 mass balance:

$$\alpha_{CO2}\,[^-RNH_2]_0 = [CO_2] + [^-RNHCOO^-] + [HCO_3^-] + [CO_3^{2-}] \quad (19)$$

The principle difference between the VLE model of aqueous alkanolamines and amino acid salts is mostly related to the charge of the ionic species present in the liquid phase. The following remarks apply for an amino acid salt system:

1. The deprotonated amino acid that reacts with CO_2 is an anion with a single negative charge.
2. The protonated amino acid is a zwitterion and was considered electrically neutral like a molecular species.
3. The concentration of the cation (K^+) of the amino acid salt is the same as that of the initial amino acid salt concentration ($[^-RNH_2]_0$).
4. The carbamate anion of the amino acid salt has a charge of -2.

The above remarks were incorporated and the result is the following charge balance equation:

$$[K^+] + [H^+] = [^-RNH_2] + [OH^-] + [HCO_3^-] + 2\,[^-RNHCOO^-] + 2\,[CO_3^{2-}] \qquad (20)$$

2.3. Liquid Phase Non-ideality

The above set of equations can be solved by neglecting the non-ideality in the liquid phase (by setting the value of the activity coefficients in all equilibrium relations to one) and force fitting the thus obtained simplified model to the experimental data. In this procedure, the equilibrium constants of reactions (3) (carbamate hydrolysis reaction; K_{carb}) and (4) (amine deprotonation reaction; K_{AmA}) are used as fit parameters. The equilibrium constants obtained this way are rather apparent constants. This is also the basic approach of the equilibrium model proposed by Kent and Eisenberg (1976), which was found to fit very well for single alkanolamine-acid gas systems, in the range of CO_2 loading between 0.2 and 0.7 mole CO_2 per mole of amine.

A number of semi-empirical excess Gibbs free energy or activity coefficient models for aqueous electrolyte systems and valid for ionic strengths representative of those found in industrial applications are available in the literature. These models basically account for the non-idealities in the liquid phase by taking into account various short range and long range interactions between different ionic and molecular species present in the solution. The most relevant ones from the point of view of simplicity and thermodynamic soundness are the models based on the extended Debye-Hückel theory (Deshmukh & Mather, 1981) and the electrolyte-NRTL theory (Chen & Evans, 1986; Austgen et al., 1989). For a single amine-acid gas system, the Deshmukh-Mather model was found to be thermodynamically rigorous as well as simple from the computational point of view (Weiland et al., 1993) and therefore will be considered here. The model uses the following equation for the activity coefficient of a solute species and was proposed originally by Guggenheim (1935):

$$\ln \gamma_i = \frac{-2.303\, A\, z_i^2\, I^{0.5}}{1 + Ba\, I^{0.5}} + 2 \sum_{j \neq w} \beta_{ij}\,[j] \qquad (21)$$

This model takes into account the long-range electrostatic (first term of Eq 21) and short-range van der Waals (second term of Eq 21) forces. The long-range electrostatic forces are

taken into account by the Debye-Hückel term, whereas the short range forces are accounted for by the binary interaction (parameters, β_{ij}) between different molecular and ionic solutes. The Debye-Hückel limiting slope, A and the parameter, B are related to the dielectric constant of the solvent (water) according to the following relations (Butler, 1964):

$$A = 1.825 \times 10^6 (\varepsilon T)^{-3/2} \quad (22)$$

$$B = 50.3 (\varepsilon T)^{-1/2} \quad (23)$$

Though the parameter "a" in Eq (21) is an adjustable parameter in Angstrom units, a constant value of 3 as proposed by Guggenheim (1935) was used in the present work for all ionic species. Any associated errors due to this assumption are automatically accounted for while fitting the binary interaction parameters. The ionic strength of the solution, I is defined as,

$$I = \frac{1}{2} \sum_j [j] z_j^2 \quad (24)$$

Here z_j is the charge number of the ion. The binary interaction parameters, β_{ij} in Eq (21) cannot be computed theoretically and therefore the values of these parameters need to be obtained by fitting the model to the experimental VLE data. For the present amino acid salt-CO_2 system comprising nine solute species in the liquid phase, the number of possible binary interactions is too large to be able to make a meaningful estimation of all of them. However, the following rules of thumb were used to reduce the number of interaction parameters and they are described in detail by Weiland et al. (1993):

1. The interactions between the ions of similar charge were neglected.
2. The interactions of all ionic and molecular species with water and its ionisation products were neglected.
3. The interactions between CO_2 and other solute species were neglected.
4. The interactions with CO_3^{2-} were neglected.

Basically, the last two assumptions are related to the very low concentrations of these species that occur in the liquid phase. By this procedure, the number of interaction (parameters; β_{ij}) to be considered in the regression reduces to the following eight::

$^-RNH_3^+$ - HCO_3^- ; HCO_3^- - K^+ ; $^-RNH_2$ - $^-RNH_3^+$; $^-RNH_2$ - K^+ ; $^-RNH_3^+$ - $^-RNH_3^+$;
$^-RNH_3^+$ - $^-RNHCOO^-$; $^-RNHCOO^-$ - K^+ ; $^-RNH_3^+$ - K^+

The set of equations including the activity coefficient model was numerically solved using commercially available MATLAB software, in which the following objective function for minimisation was used (Weiland et al., 1993).

$$F_i = \frac{\left(P_{CO_2}^{exp} - P_{CO_2}^{m}\right)^2}{P_{CO_2}^{exp} P_{CO_2}^{m}} \quad (25)$$

*Table **(1)** Literature source for the various equilibrium constants used in the VLE model.*

Constant	Temperature Range (K)	Reference
K_w	273-498	Tsonopoulos et al. (1976)
K_{CO2}	273-498	Edwards et al. (1978)
K_{HCO3}	273-498	Edwards et al. (1978)
K_{AmA}	283-323	Perrin (1965)

The initial guess values for the concentration of the 9 solute species in the liquid phase were obtained by setting all the interaction parameters in Eq (21) to zero (the model then reduces to the Debye - Hückel expression). The equilibrium constants in equation (9) to (12) were obtained from literature and are shown in Table 1. In addition, the experimentally determined (in the present work; see section 4.1) value of the carbamate hydrolysis equilibrium constant, K_{carb} (Eq 8) was used. Already at this stage, the calculated values of P_{CO2} were reasonably accurate. Some "bad" data points in the experimental data set (data for a single amino acid salt concentration) were eliminated using the methodology described in detail by Weiland et al. (1993). This procedure involves that any data point for which the predicted vapor pressure of CO_2 deviates from the experimental value by more than a factor 2 was eliminated from the data set. This avoided problems in the convergence of the fitting procedure in the subsequent step when the binary interaction parameters were taken into account in the expression for the activity coefficient. However, the present experimental data were obtained in a relatively narrow range of partial pressures of CO_2 (compared to 5-6 orders variation studied by Weiland et al., 1993) and hence the number of bad data points was insignificant. In the second step, the binary interaction parameters (β_{ij}) as well as K_{carb} (depending upon the availability of the experimental values) were used as fit parameters in the model and the experimental data were regressed with the complete model to determine the above constants.

3.0. Experimental

3.1. Chemicals

The potassium salt solution of taurine was prepared by neutralising the amino acid (Merck) dissolved in deionised water, with a slightly less than equimolar (known) quantity of potassium hydroxide (Merck) in a standard flask. The remaining amount of KOH was added precisely by potentiometrically titrating the solution with an aqueous KOH solution of known strength. The concentration of the aqueous amino acid salt (or deportonated amino acid) solution prepared was cross-checked by titrating it with standard HCl solutions.

3.2. Experimental Setup & Procedure

The schematic diagram of the experimental setup is shown in Figure 1. The principle part of the setup was a double walled, stirred (glass) reactor of approximately 1.6 liter in volume. The reactor was provided with a high intensity gas-inducing stirrer in the liquid

phase and a propeller type impeller in the gas phase. Also, the reactor was equipped with a digital pressure transducer, thermocouple and a pH electrode. A continuous dilute CO_2 gas stream of known composition was prepared by mixing desired flowrates of pure CO_2 and N_2 using the mass flow controllers. Two double walled water vapor (glass) saturators were used to saturate the N_2 and CO_2 gas streams separately before mixing them to prepare the feed gas. While the nitrogen stream was saturated with an identical amino acid salt solution as that used in the reactor, the CO_2 stream was saturated with water. The gas stream was fed to the reactor using a sintered stainless steel sparger located below the impeller of the liquid phase. The outlet gas stream from the reactor was led to a cold trap to condense all the water vapor and the concentration of CO_2 in the gas stream from the cold trap was subsequently analysed using an infrared CO_2 analyser. Before the experiment, the feed gas stream was passed through a two-way valve that was used to bypass the reactor to determine the concentration of CO_2 in the feed gas. The contents of the stirred reactor and vapor saturators were maintained at a constant temperature using a thermostatic water bath. The measurements of all the instruments were recorded in a computer using a data acquisition system.

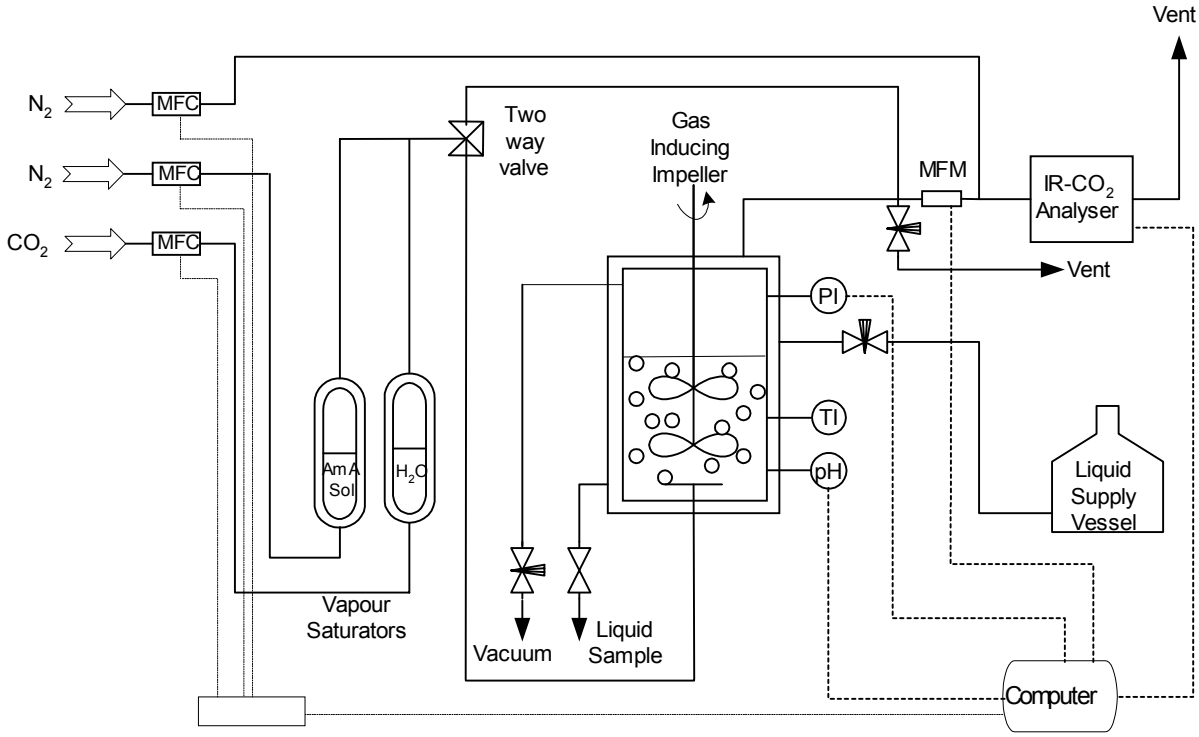

Figure (1) *Schematic diagram of the experimental setup*

In a typical experimental run, a known volume (≅ 500 ml) of the amino acid salt solution was charged into the reactor. It was stirred for 30 minutes to reach the desired absorption temperature. The mass flow controllers were adjusted to obtain the desired flowrates of N_2 and CO_2. The concentration of CO_2 in the feed gas stream was measured in the gas analyser by bypassing the stirred reactor (using the two-way valve). Subsequently,

the gas stream was allowed to flow through the reactor and the outlet gas stream CO_2 concentration was monitored in the IR gas analyser. Equilibrium was attained when the outlet and feed gas stream CO_2 concentration were the same. Since dilute (< 6.0 vol. % CO_2) gas streams were used for absorption, it generally took very long times to reach equilibrium. Therefore a known amount of pure CO_2 from a calibrated gas supply vessel was used to pre-load the amino acid salt solution before the above described equilibrium experiments. This considerably reduced the experimental time. Since several (max: 4-5) experiments were conducted in succession with the same solution (stepwise loading), the concentration of the amine in the reactor was checked by titration as described previously. The change in the amino acid salt concentration during one set of experiments (consisting of max 4-5 experiments) was within 2.5 percent. After equilibrium between the gas and liquid phase was attained in the reactor, a liquid sample of known volume was collected in a known volume of standard alkali (NaOH) solution. The pH of the loaded solution in the reactor was measured at the time of sampling. The sample was subsequently analysed for CO_2 loading using an analytical method similar to the one described in detail by Blauwhoff et al. (1984). All the experiments were conducted at near atmospheric pressure in the reactor and for two absorption temperatures, namely 298 and 313 K. Crystallisation was observed in the loaded solutions for potassium taurate concentrations of 2000 mol m^{-3} and above. In these situations, a clear liquid that is free of solids present in the reactor was used for determining the liquid CO_2 loading.

3.3. Carbamate Hydrolysis

The carbamate hydrolysis equilibrium constant (K_{carb} in Eq 8) for the potassium salt of taurine was independently measured using an experimental technique identical to the one reported by Danckwerts & Chan (1981). A reaction mixture containing an equimolar quantity of amine and potassium bicarbonate was prepared in a reaction flask and was allowed to equilibrate for 24 hrs in a thermostatic shaker at 298 K. After equilibration, the bicarbonate in the solution was precipitated as $BaCO_3$ by the addition of an excess alkaline $BaCl_2$. The reaction mixture was immediately filtered and washed with a known amount of deionised water. The filtrate was quickly titrated with a standard HCl solution. From the amount of HCl consumed in the titration, the carbamate hydrolysis equilibrium constant, K_{carb} was calculated using the procedure described in detail by Danckwerts and Chan (1981). The precipitation of the bicarbonate and subsequent filtration was done very fast in order to avoid a change in the equilibrium composition of the reaction mixture due to the removal of HCO_3^-. Therefore, only very low concentrations of the amino acid salt and bicarbonate were used (< 300 mol m^{-3}) in the reaction mixture. The experimental technique was initially standardised for monoethanolamine, for which a limited number of experimental data on K_{carb} is available in literature. The influence of the ionic strength on the carbamate hydrolysis constant of monoethanolamine was studied at 298 K by performing the above experiments in the presence of a known amount of an inert and strong electrolyte (KCl). For MEA, the experiments were conducted for two initially equimolar concentrations of the amine and bicarbonate in the reaction mixture, namely 100 mol m^{-3} and 200 mol m^{-3}.

4.0 Results and Discussion

4.1. Carbamate Hydrolysis Equilibrium Constant (K_{carb})

The K_{carb} is one of the constants in the earlier described equilibrium model, which is usually obtained by fitting the VLE model to the experimental equilibrium CO_2 solubility data. If K_{carb} can be estimated independently for experimental conditions of interest in the actual gas treating processes (data at high ionic strength of the solution), the number of fit parameters in the VLE model can be reduced. This way, the simple Kent-Eisenberg equilibrium model for the primary and secondary amines can be used to quantitatively describe the vapor-liquid equilibria of a given CO_2-amine system without any fit parameters. The information on the values of the other equilibrium constants, such as K_{AmA} and K_{CO2} can be obtained from literature at different temperatures (see Table 1). In general, the sensitivity of the predicted CO_2 vapor pressure to the carbamate hydrolysis constant is at its maximum for liquid CO_2 loadings between 0.1 and 0.4.

It has been shown for primary and secondary alkanolamines (however only with a limited number of experimental data) that K_{carb} has a more or less strong dependence on the ionic strength of the solution (Danckwerts & Chan, 1981). The information on the stability of the carbamates (inversely proportional to K_{carb}) of amino acids is scarce and very old, with no published data on the K_{carb} of taurine.

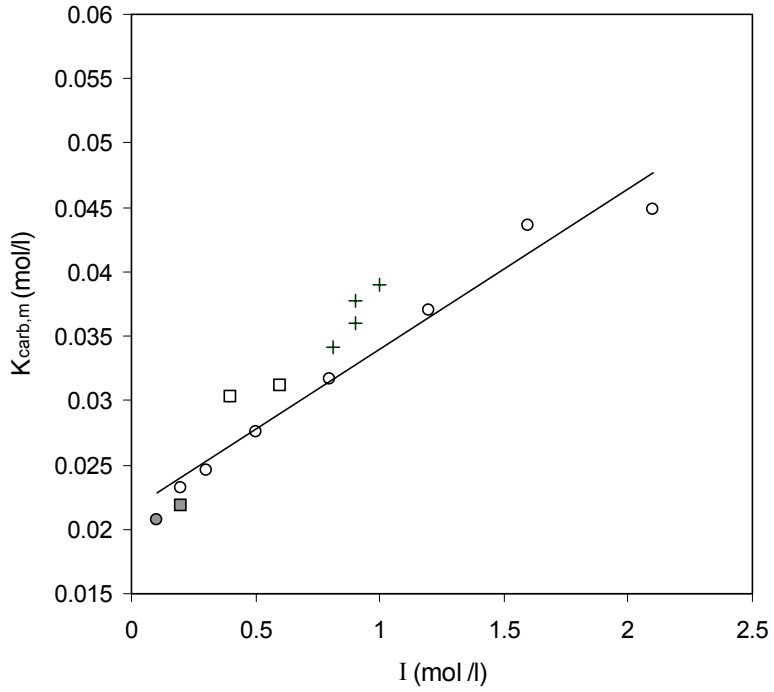

Figure (2) *Influence of Ionic strength on the Carbamate hydrolysis equilibrium constant of MEA at 298 K (+ Danckwerts & Chan (1981); o Present work, $[MEA]_0 = [HCO_3^-]_0 = 100$ mol m^{-3}; □ Present work, $[MEA]_0 = [HCO_3^-]_0 = 200$ mol m^{-3}). The dark points in the figure indicate the measurements done without KCl in the reaction mixture.*

To start with, the influence of the ionic strength of the solution on K_{carb} was studied for monoethanolamine at 298 K, as only a limited amount of experimental data for solutions of

low ionic strength is available in literature. Two different initial equimolar concentrations of amine and bicarbonate in the reaction mixture were used along with different concentrations of KCl. The results for K_{carb} are shown in Figure 2 as a function of the ionic strength of the reaction mixture. The $K_{carb,m}$ shown in the figure is based on molar concentration units and is defined as:

$$K_{carb,m} = \frac{[RNH_2]_m\,[HCO_3^-]_m}{[RNHCOO^-]_m} \qquad (27)$$

The experimental results of Danckwerts and Chan (1981) are also shown in Figure 2. It should be noted that these authors did also use Na_2CO_3 along with the amine and bicarbonate in the initial reaction mixture. Though the range of amine and bicarbonate concentrations studied in the present work (with no KCl in the reaction mixture) is comparable to that of Danckwerts and Chan, the ionic strength of the solutions in their experiments was higher due to the presence of carbonate. The results as shown in the Figure 2 indicate that K_{carb} is strongly influenced by the ionic strength of the solution and the results of Chan and Danckwerts fall in line with the present experimental results. For MEA solutions with high ionic strength as usually encountered in industrial applications, the value of K_{carb} could differ significantly from the experimental values as reported for low ionic strengths. Linear regression of the experimental data obtained from the present work gave the following expression.

$$K_{carb,m} = 0.0124\ I + 0.0216 \qquad (28)$$

Table (2) *Carbamate hydrolysis equilibrium constants of aqueous potassium taurate at 298 K*

$[^-RNH_2]_0$ (mol m^{-3}) x 10^{-3}	$[HCO_3]_0$ (mol m^{-3}) x 10^{-3}	$K_{carb,m}$ (mol m^{-3}) x 10^{-3}
0.10	0.10	0.0531
0.15	0.15	0.0532
0.20	0.20	0.0482
0.30	0.30	0.0509

Using the above experimental procedure, the carbamate hydrolysis equilibrium constant of the potassium salt of taurine was also measured at 298 K and the results are shown in Table 2. From these results, it is clear that the carbamate of taurine is reasonably stable (comparable to primary amines), but somewhat less stable than that of MEA. Though the variation in the experimental initial concentrations of the amino acid salt and bicarbonate was limited, there does not seem to be a significant influence of the ionic strength of the solution on the equilibrium constant. However, the range of experimental data is rather limited to make definitive conclusions. In Table 3, $K_{carb.m}$ of some similar amino acids (with a single primary amino functional group) as reported in the literature (Rochelle et al., 2000) are given. The experimental measurements were done for very low amino acid concentrations,

as in the present study. The values reported by Rochelle et al for 298 K were estimated (using the information on the heat of reaction of the carbamate hydrolysis reaction, $-\Delta H_R$) from the original data, which were measured at 291 K. There does not seem to be any clear trend between $K_{carb,m}$ and the basicity of the amine (pKa). Nevertheless, the stability of the carbamate of all amino acids, except α-alanine is comparable to that of primary alkanolamines. It is a well established theory that substitution at the α- carbon atom adjacent to the amino group of an amine reduces the stability of the carbamate, resulting in enhanced hydrolysis of the carbamate to bicarbonate/carbonate (Chakraborty et al., 1988). This could explain the relative instability (or high $K_{carb,m}$) of the carbamate of α-alanine.

Table (3) *Carbamate hydrolysis constants for various amino acids reported in literature (Rochelle et al., 2000).*

Amino acid	$K_{carb,m}$ at 291 K (mol m^{-3}) x 10^{-3}	$K_{carb,m}$ at 298 K (mol m^{-3}) x 10^{-3}	pKa at 298 K -	Original Source of Data for $K_{carb,m}$ at 291 K
Glycine ($H_2NCH_2CO_2H$)	0.033	0.042	9.78	Jensen et al. (1952)
α - Alanine ($CH_3CH(NH_2)CO_2H$)	0.108	0.125	9.87	Jensen & Faurholt (1952)
β - Alanine ($H_2NCH_2CH_2COOH$)	0.031	0.039	10.41	Jensen & Faurholt (1952)
Taurine ($H_2NCH_2CH_2SO_3H$)	-	0.051	9.08	Present work

4.2. CO_2 - Aqueous Potassium Taurate Vapor-Liquid Equilibria

Table 4 and 5 (given in the Appendix) contain the experimental CO_2 solubility data measured at 298 and 313 K respectively. The experimental measurements were carried out in the range of partial pressures of CO_2 varying between 0.1 and 6.0 kPa, which is the range typically encountered in the removal of CO_2 from flue gas. The experimental VLE data obtained from the present study, as shown in Figure 3 indicate that the equilibrium absorption capacity of CO_2 in aqueous potassium taurate solutions, for a given P_{CO2} seems to be comparable to that of the primary alkanolamines (say monoethanolamine) of similar concentration. For MEA, only a limited amount of experimental data is available in literature for 298 K, especially for amine concentrations less than 2500 mol m^{-3}. As mentioned earlier, crystallisation was observed in the higher range of P_{CO2} for solutions with a high amino acid salt concentrations (2 molar and above). However, the initial analysis and discussion of the experimental VLE data will be focussed for situations where no crystallisation has occurred; the rest will considered in the subsequent section 4.3.

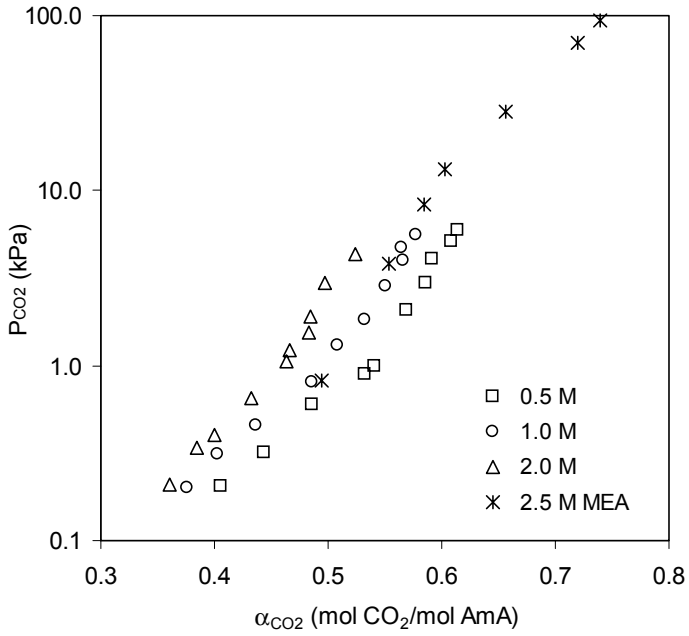

Figure (3) *Equilibrium solubility of CO_2 in aqueous potassium taurate solutions at 298 K. Also shown is the solubility of CO_2 in 2.5 M aqueous monoethanolamine solutions at 298 K (Muhlbauer & Monaghan, 1957). The legend of the figure indicates the total molar amine concentration ($[RNH_2]_o$).*

The experimental data were regressed with the VLE model to obtain the binary interaction parameters in the extended Debye-Hückel expression as well as K_{carb}. The experimental values of K_{carb} obtained in the present study are valid only for solutions of low ionic strengths and therefore, it was also used as a fit parameter in the data regression (to study the influence of the amino acid salt concentration or ionic strength on K_{carb}). As mentioned in section 2.3, in the initial regression of the experimental data, the β_{ij}'s were set to zero and only K_{carb} was used as a fitting parameter. Analysis of the calculated equilibrium concentrations of the nine species in the liquid phase (as predicted by the model) indicated that the change in the ionic strength of the solution for the range of α_{CO2} studied in the present work varied between 3 and 6 % for different amino acid salt concentrations (see also Figure 4). In such a situation, the first term (Debye-Hückel) in the extended Debye-Hückel expression will become essentially constant. This means that Eq (21) basically reduces to:

$$\ln \gamma_i = C + 2 \sum_{j \neq w} \beta_{ij} [j] \qquad (29)$$

Such a remarkable behavior can be understood from the following arguments that will use the asymptotic situations in the absorption of CO_2 in aqueous alkaline salt solutions of amino acids and alkanolamines. In the following discussion, the subscript AmA and AA refer to the amino acid salt and alkanolamine respectively.

1. Unlike aqueous alkanolamines (for which the ionic strength is near zero for unloaded solutions), the ionic strength of unloaded aqueous amino acid salt solutions is the molal salt concentration.

   For $\alpha_{CO2} = 0$; $I_{AmA} = [^-RNH2]_0$

$I_{AA} \cong 0$

2. For an asymptotic situation of a complete conversion of the amine, but negligible hydrolysis of the carbamate as described by reaction (2), the CO_2 loading of the solution is 0.5. Then the ionic strengths of the aqueous amino acid salt and alkanolamine solutions are:

For $\alpha_{CO2} = 0.5$; $I_{AmA} = ½ \{[^-RNHCOO^-] (-2)^2 + [^-RNH_3^+] (0)^2 + [K^+] (1)^2\}$

$= ½ \{0.5 [^-RNH_2]_0 (-2)^2 + 0.5 [^-RNH_2]_0 (0)^2 + [^-RNH_2]_0 (1)^2\}$

$= 1.5 [^-RNH_2]_0$

$I_{AA} = ½ \{[RNHCOO^-] (-1)^2 + [RNH_3^+] (1)^2\} = 1.0 [RNH_2]_0$

3. Assuming a complete hydrolysis of the carbamate, the absorption capacity of the amine solutions can reach the theoretical maximum of 1.0 mole CO_2 per mole amine as per the following overall reaction for amino acids:

$$^-RNH_2 + CO_2 + H_2O \Leftrightarrow HCO_3^- + {}^-RNH_3^+$$

For $\alpha_{CO2} = 1.0$; $I_{AmA} = ½ \{[HCO_3^-] (-1)^2 + [^-RNH_3^+] (0)^2 + [K^+] (1)^2\}$

$= 1.0 [^-RNH_2]_0$

$I_{AA} = ½ \{[HCO_3^-] (-1)^2 + [RNH_3^+] (1)^2\} = 1.0 [RNH_2]_0$

.

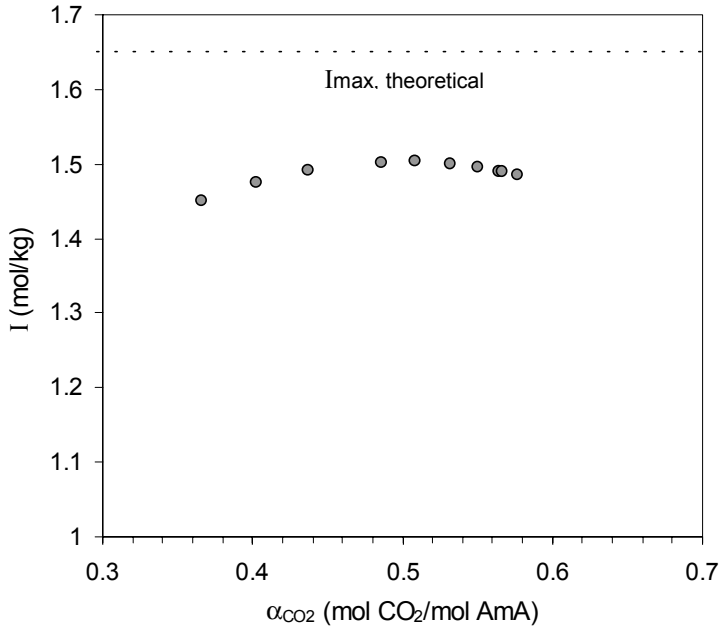

Figure (4) *Influence of CO_2 absorption on the ionic strength of 1.0 molar (≅ 1.1 molal, aqueous potassium taurate solution at 298 K. Ionic strength calculated based on the results obtained with the Debye-Hückel model.*

Therefore during the absorption of CO_2 in aqueous amino acid salt solutions, the ionic strength changes from the initial amino acid salt concentration ($[^-RNH_2]_{0)}$ to the maximum possible value (I_{max}) of $1.5[^-RNH_2]_0$ corresponding to the asymptotic case 2. For

CO_2 loadings larger than 0.5, the ionic strength decreases with increase in α_{CO2} and eventually reaches the value of an unloaded solution. In reality the carbamate hydrolysis becomes significant even at α_{CO2} as low as 0.1 and therefore the maximum value is less than the theoretical value (1.5 $[R\text{-}NH_2]_0$; see also Figure 4). This behavior is very different from that of aqueous alkanolamines. Figure 4 shows the ionic strength of a 1.0 molar aqueous potassium taurate solution as function of CO_2 loading. The ionic strength of the solution given in the figure was calculated from the individual species concentration predicted by the VLE model neglecting the interaction parameters, β_{ij}'s.

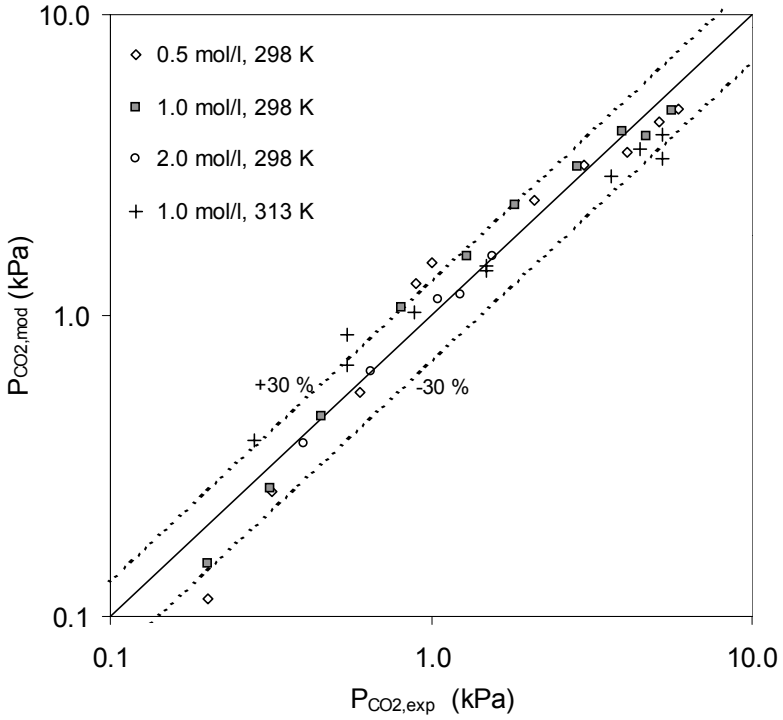

***Figure (5)**. Parity plot of predicted and experimental values of vapor pressure of CO_2 above aqueous potassium taurate solutions at 298 and 313 K.*

This indeed shows that the extended Debye-Hückel expression (Eq 21) essentially reduces to Eq (29) for the experimental data obtained in the present work. However, Eq (29) loses the thermodynamic soundness of the extended Debye-Hückel expression and simply becomes an empirical fitting equation, in which the activity coefficients are related to the molal concentration of various species in the liquid phase along with a number of associated constants. Now the choice of the interaction parameters among the seven β's mentioned in section 2.3 becomes rather empirical. Considering the above facts, it was decided to regress the experimental data with a VLE model neglecting the binary interaction parameters in the extended Debye-Hückel expression (Eq 21). Since the ionic strength does not change significantly within the range of the present experimental data, this simplification makes the model similar to the Kent-Eisenberg model as the activity coefficient can now be calculated explicitly. Similar to the Kent-Eisenberg model, the amine deprotonation equilibrium constant (K_{AmA}) was also made an adjustable fit parameter as the experimental data available in the literature are rather old (Perrin, 1965) and the information about its accuracy is not known. So the final form of the VLE model used consisted of two fitting parameters, namely K_{carb} and

K_{AmA}. Table 5 shows the optimal values of the fitting parameters obtained in the regression for different experimental data sets.

Table (5) *Fitted Equilibrium constants for different data sets.*

T (K)	$[^{-}R\text{-}NH_2]_0$ (mol m^{-3})	K_{AmA}^{m} (mol kg^{-1})	K_{carb}^{m} (mol kg^{-1})	$K_{AmA,m}^{m}$ (mol m^{-3}) x 10^{-3}	$K_{carb,m}^{m}$ (mol m^{-3}) x 10^{-3}	$K_{AmA,m}$ – lit* (mol m^{-3}) x 10^{-3}
298	500	4.40 x 10^{-10}	0.021	1.27 x 10^{-9}	0.019	8.91 x 10^{-10}
298	1000	4.39 x 10^{-10}	0.053	1.18 x 10^{-9}	0.048	8.91 x 10^{-10}
298	2000	3.74 x 10^{-10}	0.105	9.05 x 10^{-10}	0.085	8.91 x 10^{-10}
313	1000	1.15 x 10^{-10}	0.937	3.07 x 10^{-9}	0.847	1.94 x 10^{-9}

* From literature; Perrin (1965)

The K_{carb}^{m} and K_{AmA}^{m} given in Table 5 are the apparent equilibrium constants (in molar units) obtained by lumping the activity coefficients of the species involved in the reactions (and the activity of water, a_w, in case of K_{carb}^{m}) with K_{carb} and K_{AmA} respectively. The amine dissociation constant, K_{AmA}^{m} is within 35 % of the experimental value reported in literature. The carbamate hydrolysis constant shows a strong dependence on the initial amino acid salt concentration (or ionic strength of the solution). However, such a trend could not be clearly observed from the measured K_{carb} data, though they are limited in number and range (see Table 2). Infact, the observed dependence of K_{carb}^{m} on the ionic strength seems to be much larger than that for MEA, for which the experimental values are reported as a function of ionic strength of the solution in section 4.1.

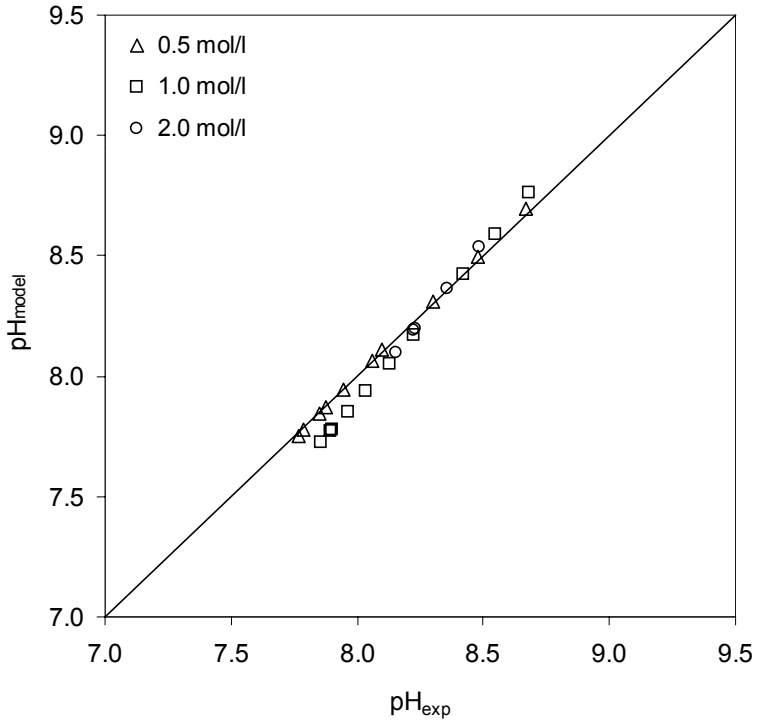

Figure (6)*. Parity plot of the predicted and experimental values of the pH of CO_2 loaded aqueous potassium taurate solutions (corresponding to the solubility data at 298 K). The legend of the figure indicates the total molar amino acid salt concentration ($[RNH_2]_o$).*

Finally, the most important aspect of a VLE model is the accuracy of its prediction of the experimental data. Figure 5 shows the parity plot for the experimental as well as predicted value of the partial pressure of CO_2. The average error in the prediction of P_{CO2} is 16.5 %. Figure 6 shows the parity plot of the predicted and experimentally determined value of the pH of the loaded potassium taurate solutions at 298 K. The average error in the prediction of the solution pH is 0.54%.

3.3. Crystallisation in Aqueous Potassium Taurate Solutions and its influence on the Vapor-Liquid Equilibria

Hook (1997) reported that the products of the reaction between CO_2 and certain aqueous alkaline salts of amino acids (say alanine), and especially C_α-substituted amino acids (like 2-methyl glycine), undergo crystallisation at moderate to high conversions of the amino acid salt. In a recent study, Kumar et al. (2002b) reported crystallisation during the absorption of CO_2 in aqueous potassium taurate solutions as well. The following are some important conclusions made from that investigation.

1. For aqueous potassium taurate solutions, crystallisation of the reaction product occurs even at moderate CO_2 loadings (0.20 - 0.5 mol CO_2 per mole AmA), depending upon the total amino acid salt concentration ($[^{-}RNH_2]_0$) .
2. The crystallising reaction product is the protonated amine (or zwitterionic form of amino acid).

$$2\ {}^{-}O_3S\text{-}R\text{-}NH_2 + CO_2 \Leftrightarrow {}^{-}O_3S\text{-}R\text{-}NHCOO^{-} + {}^{-}O_3S\text{-}R\text{-}NH_3^{+} \downarrow \quad (30)$$

3. There is a clear relationship between the critical CO_2 loading value ($\alpha_{CO2,crit}$) at which crystallisation of the reaction product occur and the solubility of the zwitterionic form of taurine.

$$\alpha_{CO_2,\,crit} = \frac{S}{[^{-}RNH_2]_0} \quad (31)$$

   Here S is the solubility of the amino acid in the solution and $[^{-}RNH_2]_0$ is the total amino acid salt concentration. The inverse relationship between $\alpha_{CO2,crit}$ and $[^{-}RNH_2]_0$ signifies that the crystallisation will occur much earlier (in terms of CO_2 loading) for higher amino acid salt concentrations.
4. The formation of crystals in the liquid phase was semi-qualitatively found to reduce the volumetric mass transfer coefficient (k_La) of the gas-liquid contactor.

The results presented in this section are related to another important aspect of the crystallisation phenomenon that was not dealt with in the earlier work, i.e., the influence of crystallisation of the reaction product on the vapor-liquid equilibrium of the CO_2-aqueous potassium taurate system. For equilibrium limited liquid phase reactions, the selective removal of a reaction product from the reaction mixture will essentially shift the equilibrium towards the product side (Westerterp et al., 1984). This technique is widely used in industry to enhance the equilibrium conversion of reversible reactions. For the present CO_2-amino acid salt system also, crystallisation of the reaction product (protonated amine) can be

expected to increase the CO_2 absorption capacity of the aqueous amino acid salt solutions for a given partial pressure of CO_2 in the gas phase. Therefore, this phenomenon was also investigated in the present work.

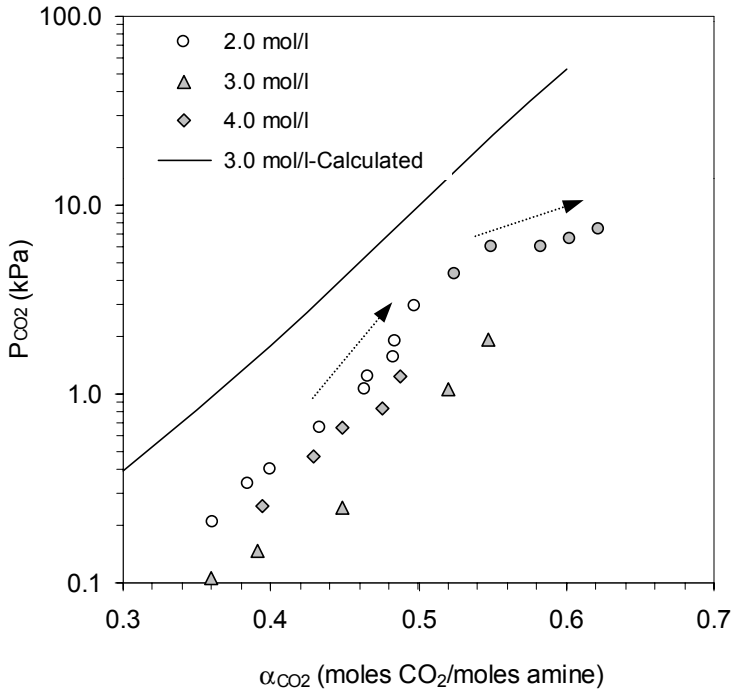

Figure (7) *Influence of crystallisation of the reaction product on the solubility of CO_2 in concentrated aqueous potassium taurate solutions. The dark points in the figure indicate the presence of solids in the liquid phase at equilibrium. The continuous line in the figure indicates the hypothetical calculated partial pressure of CO_2 for a 3 molar solution using the VLE model and neglecting precipitation. The legend of the figure indicates the total amino acid salt concentration ($[RNH_2]_o$).*

Figure 7 shows the experimental CO_2 solubility data for concentrated aqueous potassium taurate solutions (≥ 2 molar). For 2 molar solutions, crystallisation was observed halfway in the range of partial pressures studied in the present work. The remarkable influence of crystallisation on the equilibrium CO_2 absorption capacity of the salt solution can be clearly observed from the drastic decrease in the slope of the experimental trend. However, for the 3 molar and 4 molar solutions crystallisation was observed even for partial pressures of CO_2 as low as 0.1 kPa. This was expected because the critical CO_2 loading value ($\alpha_{crit,CO2}$) measured in an earlier work (Kumar et al., 2002b) was approximately 0.30 and 0.17 mole CO_2 per mole amino acid salt for 3 and 4 molar salt solutions respectively. The equilibrium partial pressure of CO_2 (P_{CO2}) for the 3 and 4 molar salt solutions (and for a given value of CO_2 loading) is less than that of a 2 molar amino acid salt solution. In order to understand the magnitude of the influence of crystallisation on the CO_2 absorption capacity of 3 and 4 molar potassium taurate solutions, the VLE model developed earlier was used to predict the hypothetical partial pressure of CO_2 for a 3 molar aqueous potassium taurate solution assuming no crystallisation had occurred. In the model, the value of K_{AmA}^{m} as reported in Table 5 was used, whereas the K_{carb}^{m} values obtained for solutions of lower

amino acid salt concentrations were linearly extrapolated. For a given value of α_{CO2}, the equilibrium vapor pressure of CO_2 predicted by the model that would have occurred in the absence of crystallisation is more than an order of magnitude higher than the experimental values of P_{CO2} measured with crystallisation in the loaded solution. This is a significant improvement in the capacity of the acid gas treating process, though it has some negative implications associated with the handling of slurries in gas-liquid contactors. It should be noted however that the present equilibrium model can be extended to a situation in which the protonated amine is allowed to crystallise in the solution. In that case, the mole balance for the amine in the liquid phase (Eq 18) becomes redundant as the protonated amine ($[RNH_3^+]$) crystallises and the concentration of the protonated amine becomes equal to the solubility of the amino acid in a saturated aqueous salt solution. As the amount of reliable experimental data for the conditions where crystallisation occurred is limited in the present work, that model extension is not presented in this work.

5.0 Conclusions

The solubility of CO_2 in aqueous potassium taurate solutions was measured at 298 and 313 K and for the range of CO_2 partial pressure between 0.1 and 6.0 kPa. In the present work, the Deshmukh-Mather model, based on the extended Debye-Hückel theory was adopted to describe the experimental VLE data of aqueous alkaline salt solutions of amino acids. Inspite of the fact that aqueous alkanolamines and amino acid salt solutions undergo similar reactions with CO_2 in the liquid phase (formation of carbamate and subsequent hydrolysis of the carbamate to bicarbonate or carbonate), the thermodynamic characteristics of the two solutions differ significantly. This is due to the difference in the ionic charges associated with the reactants and reaction products. In the range of partial pressures of CO_2 that covers the present experimental measurements, the change in the ionic strength of the loaded amino acid salt solution was found to be insignificant. Therefore, the Debye-Hückel term in the extended Debye-Hückel expression became essentially a constant for the conditions studied and the expression for the activity coefficient became an empirical fitting equation consisting of various interaction parameters. Consequently, the interaction parameters in the extended Debye-Hückel were neglected and the resulting model was used to describe the experimental data. The accuracy of the predictions of VLE model with reference to the experimental solubility data was reasonably good and the fitting parameters, namely the amine deprotonation constant as well as the carbamate hydrolysis equilibrium constant, are in agreement with the experimental values measured independently in the present study.

The equilibrium constant of the carbamate hydrolysis reaction is an important fit parameter in the VLE model. The above parameter was also experimentally measured for aqueous monoethanolamine and potassium taurate solutions at 298 K. For monoethanolamine, the equilibrium constant was found to show a strong dependence on the ionic strength of the solution. For low ionic strengths, the experimental values were in good agreement with the values reported in literature. Similarly for potassium taurate, the experimental carbamate hydrolysis constant was found to be comparable to the data available in the literature for similar amino acids like glycine and alanine.

During the absorption of CO_2 in aqueous potassium taurate solutions, crystallisation of the reaction products was observed, especially for concentrated solutions. The crystallisation phenomenon was found to remarkably increase the equilibrium CO_2 absorption capacity of the potassium taurate solutions, for a given partial pressure of CO_2 in the gas phase.

Acknowledgement

This research is part of the research programme performed within the Centre for Separation Technology (CST), which is a co-operation between the Netherlands Organisation for Applied Scientific Research (TNO) and the University of Twente. We acknowledge Sven Timmer for his assistance to the experimental work and H.J. Moed for the construction of the experimental setups.

6.0 Nomenclature

a_w	activity of water, dimensionless
K	Equilibrium constant, various units, but based on mol/kg
P	Partial pressure, kPa
m	Physical solubility $([CO_2]_{liq}/[CO_2]_{gas})_{eq}$, dimensionless
C_s	Concentration of amino acid salt, mol m^{-3}
K_s	Sechenov constant, m^3 mol^{-1}
h_-	Anion specific constant, m^3 mol^{-1}
h_G	Gas specific constant, m^3 mol^{-1}
z	Valency of the ion, dimensionless
P_w^{sat}	Saturation pressure of water, kPa
R	Universal gas constant, J $mole^{-1}$ K^{-1}
T	Absolute temperature, K
A	Debye-Hückel limiting slope
B	Constant in Eq (21)
a	Ionic size in Eq (21), Å
I	Ionic strength, mol kg^{-1}
F_i	Error of the i^{th} measurement, dimensionless
S	Solubility of amino acid, mol kg^{-1}

Greek

γ	Activity coefficient, dimensionless
α_{CO2}	CO_2 loading, mole CO_2 mole AmA^{-1}
β_{ij}	Parameter for the interaction of species I with species j, kg $mole^{-1}$

Subscript

carb	Carbamate
AmA	Amino acid Salt
ov	Overall

w	Water
m	Expressed in molar units
0	Initial or total

Superscript

exp	Experimental
m	Model
crit	Critical, related to CO_2 loading

7.0 References

Austgen, D.M., Rochelle, G.T., Peng, X., & Chen, C.C. (1989). Model of vapor-liquid equilibria for aqueous acid gas-alkanolamine systems using the Electrolyte-NRTL equation. *Industrial & Engineering Chemistry Research*, **28**, 1060-1073.

Blauwhoff, P.M.M., Versteeg, G.F., & van Swaaij, W.P.M. (1984). A study on the reactions between CO_2 and alkanolamines in aqueous solutions. *Chemical Engineering Science*, **39(2)**, 207-225.

Butler, J.N. (1964). *Ionic Equilibrium: A Mathematical Approach*. London: Addison-Wesley Publishing Company.

Chakraborty, A.K., Bischoff, K.B., Astarita, G., & Damewood, J.R., Jr. (1988). Molecular orbital approach to substituent effects in amine-CO_2 interactions. *Journal of American Chemical Society*, **110(21)**, 6947-6954.

Chen, C.C., & Evans, L.B. (1986). A local composition model for the excess Gibbs energy of aqueous electrolyte systems. *AIChE Journal*, **32**, 444-454.

Danckwerts, P.V., & Chan, H.M. (1981). Equilibrium of MEA and DEA with bicarbonate and carbamate. *Chemical Engineering Science*, **36**, 229-330.

Deshmukh, R.D., & Mather, A.E. (1981). A mathematical model for equilibrium solubility of hydrogen sulfide and carbon dioxide in aqueous alkanolamine solutions. *Chemical Engineering Science*, **36**, 355-362.

Edwards, T.J., Maurer, G., Newman, J., & Prausnitz, J.M. (1978). Vapor-liquid equilibrium in multicomponent aqueous solutions of volatile weak electrolytes. *AIChE Journal*, **24(6)**, 966-972.

Greenstein, J.P., & Winitz, M. (1961). *Chemistry of the amino acids*. New York: Wiley.

Guggenheim, E.A. (1935). The specific thermodynamic properties of aqueous solutions of strong electrolytes. *Philosophical Magazine*, **19**, 588-591.

Hook, R.J. (1997). An investigation of some sterically hindered amines as potential carbon dioxide scrubbing compounds. *Industrial & Engineering Chemistry Research,* **36(5)**, 1779-1790.

Jensen, A., & Faurholt, C. (1952). Studies on carbamates V. The carbamates of α-Alanine and β-Alanine. *Acta Chemica Scandinavica*, **6**, 385-394.

Jensen, A., Jensen, J.B., & Faurholt, C. (1952). Studies on carbamates VI. The carbamate of Glycine. *Acta Chemica Scandinavica*, **6**, 395-397.

Kent, R., & Eisenberg, B. (1976). Better data for amine treating. *Hydrocarbon Processing*, **55**, 87-90.

Kohl, A. L., & Nielsen, R.B. (1997). *Gas Purification*: 5th ed. Houston: Gulf Publishing Company.

Kumar, P.S., Hogendoorn, J.A., Feron, P.H.M., & Versteeg, G.F. (2001). Density, viscosity, solubility and diffusivity of N_2O in aqueous amino acid salt solutions. *Journal of Chemical & Engineering Data,* **46**, 1357-1361 (Chapter 1 of this thesis).

Kumar, P.S., Hogendoorn, J.A., Feron, P.H.M., & Versteeg, G.F. (2002a). New absorption liquids for the removal of CO_2 from dilute gas streams using membrane contactors. *Chemical Engineering Science* (In Press - Chapter 5 of this thesis).

Kumar, P.S., Hogendoorn, J.A., Feron, P.H.M., & Versteeg, G.F. (2002b). Crystallisation in CO_2 loaded aqueous alkaline salt solutions of amino acids (To be published; Chapter 3 of this thesis).

Kumar, P.S., Hogendoorn, J.A., Feron, P.H.M., & Versteeg, G.F. (2002c). On kinetics of reaction between CO_2 and aqueous amino acid salt solutions. *AIChE Journal* (In review; Chapter 2 of this thesis).

Muhlbauer, H.G., & Monaghan, P.R. (1957). New equilibrium data on sweetening of natural gas with ethanolamine solutions. *Oil & Gas Journal*, **55(17)**, 139-145.

Penny, D.E., & Ritter, T.J. (1983). Kinetic study of the reaction between carbon dioxide and primary amines. *Journal of Chemical Society Faraday Society*, **79**, 2103-2109.

Perrin, D.D. (1965). *Dissociation of organic bases in aqueous solutions*. London: Butterworth.

Rochelle, G.T., Bishnoi, S., Chi, S., Dang, H., & Santos, J. (2000). Research Needs for CO_2 Capture from Flue Gas by Aqueous Absorption/Stripping. U.S. Department of Energy Report No. DE-AF26-99FT01029, Federal Energy Technology Center, Pittsburgh.

Tsonopolous, C., Coulson, D.M., & Inman, L.B. (1976). Ionisation constants of water pollutants. *Journal of Chemical & Engineering Data*, **21(2)**, 190-193.

Weiland, R.H., Chakravarty, T., & Mather, A.E. (1993). Solubility of carbon dioxide and hydrogen sulfide in aqueous alkanolamines. *Industrial & Engineering Chemistry Research*, **32**, 1419-1430.

Weisenberger, S., & Schumpe, A. (1996). Estimation of gas solubilities in salt solutions at temperatures from 273K to 363K. *AIChE Journal*, ***42***, 298-300.

Westerterp, K.R., van Swaaij, W.P.M., & Beenackers, A.A.C.M. (1984). *Chemical reactor design and operation*. New York: Wiley and Sons.

Appendix

Table (4) *Solubility of CO_2 in Aqueous Potassium Taurate solutions at 298 K*

$[^{-}RNH_2]_0$: 500 mol m^{-3}

α mol CO_2/mol AmA	P_{CO2} kPa
0.396	0.203
0.405	0.204
0.444	0.318
0.486	0.598
0.532	0.892
0.541	1.003
0.569	2.087
0.586	2.999
0.592	4.083
0.608	5.117
0.614	5.887

$[^{-}RNH_2]_0$: 1000 mol m^{-3}

α mol CO_2/mol AmA	P_{CO2} kPa
0.366	0.202
0.376	0.201
0.403	0.314
0.437	0.456
0.486	0.811
0.509	1.297
0.532	1.824
0.550	2.847
0.565	4.701
0.567	3.951
0.577	5.623

$[^{-}RNH_2]_0$: 2000 mol m^{-3}

α mol CO_2/mol AmA	P_{CO2} kPa
0.353	0.221
0.385	0.318
0.400	0.401
0.433	0.658
0.466	1.232
0.464	1.054
0.483	1.560
0.497	2.938
0.524	4.336*
0.525	5.198*
0.549	6.008*
0.583	5.978*
0.602	6.586*
0.622	7.396*

$[^{-}RNH_2]_0$: 3000 mol m^{-3}

α mol CO_2/mol AmA	P_{CO2} kPa
0.360	0.107*
0.391	0.147*
0.449	0.252*
0.520	1.058*
0.547	1.950*

$[^{-}RNH_2]_0$: 4000 mol m^{-3}

α mol CO_2/mol AmA	P_{CO2} kPa
0.394	0.256*
0.429	0.463*
0.449	0.659*
0.476	0.847*
0.487	1.241*

* For these experimental conditions, crystallisation was observed in the stirred reactor

Table (5) *Solubility of CO_2 in Aqueous Potassium Taurate solutions at 313 K*

$[^{-}RNH_2]_0$: 1000 mol m^{-3}

α mol CO_2/mol AmA	P_{CO2} kPa
0.225	0.280
0.276	0.546
0.317	0.886
0.351	1.483
0.355	1.489
0.410	3.063
0.435	3.639
0.461	4.488
0.475	5.286

Chapter 5

Performance of the New Absorption Liquids in CO_2 Removal by Membrane Gas Absorption Process

Abstract

A new absorption liquid based on amino acid salts has been studied for CO_2 removal in membrane gas-liquid contactors. Unlike conventional gas treating solvents like aqueous alkanolamines solutions, the new absorption liquid does not wet polyolefin microporous membranes. The wetting characteristics of aqueous alkanolamines and amino acid salt solutions for a hydrophobic membrane was studied by measuring the surface tension of the liquid and the breakthrough pressure of the liquid into the pores of the membrane. The dependence of the breakthrough pressure on surface tension follows the Laplace-Young equation. The performance of the new absorption liquid in the removal of CO_2 was studied in a single fiber membrane contactor over a wide range of partial pressures of CO_2 in the gas phase and amino acid salt concentrations in the liquid. A numerical model to describe the mass transfer accompanied by multiple chemical reactions occurring during the absorption of CO_2 in the liquid flowing through the hollow fiber was developed. The numerical model gives a good prediction of the CO_2 absorption flux across the membrane for the absorption of CO_2 in the aqueous amino acid salt solutions flowing through the hollow fiber.

1.0 Introduction

Membrane gas-liquid (G-L) contactors make use of a porous membrane to separate the gas and liquid phase. Ideally, the micro-pores of the membrane should be completely gas filled, to minimise any mass transfer resistance due to the presence of the membrane. Hence, the membranes themselves usually do not offer any selectivity for the gases to be separated; this role is fulfilled by the absorption liquid. Reactive absorption liquids are preferably used above physical absorption liquids as their absorption rate and capacity are generally much better. This not only results in a reduction in the size of the contactor, but also the solvent circulation rate. The principle advantages of membrane gas-liquid contactors are operational flexibility, high mass transfer rate and easy linear scale-up. The operational flexibility is due to the absence of interpenetration of the phases in the contactor and hence the liquid and gas phase flowrates can be manipulated independently of each other, without any consequences like flooding, entrainment and weeping, as encountered in column type contactors. The absorption rate depends among others on the interfacial area for the gas-liquid contact ($\underline{a}$) and mass transfer coefficient (k_L). The interfacial area for mass transfer in a membrane gas-liquid contactor is the membrane surface area. For commercially available hollow fiber membrane modules, it varies between 1500-3000 m^2/m^3 of contactor volume, depending on the diameter and packing density of the hollow fiber. This is much higher than the contact areas available in conventional contactors (100-800 m^2/m^3) like bubble columns, packed and plate columns (Westerterp et al., 1984). In the membrane contactors, the high interfacial area is obtained at the cost of the fiber side mass transfer coefficient, which is low due to the laminar flow of fluids inside the fiber. Nevertheless, the volumetric mass transfer coefficient ($k_L\underline{a}$) is several times higher, resulting in a considerable reduction in the size of the contactor. Especially for offshore applications this offers tremendous advantages.

These unparalleled advantages over conventional column contactors seem to make the membrane modules an ideal gas-liquid contactor in the recovery/removal of CO_2 from flue gas, natural gas and different industrial process gas streams. Since the first pioneering work of Cussler and his coworkers (Qi & Cussler, 1985), there has been considerable academic and industrial research work done on this gas-liquid contactor concept for the removal of CO_2 (Gabelman & Hwang, 1999). However, only very few of these processes have been successfully tested on a larger scale. Kvaerner Oil & Gas and W.L. Gore & Associates GmbH have been developing a membrane gas absorption process for the removal of acid gases from natural gas and exhausts of the offshore gas turbines (Hanisch, 1999). In this process, PTFE hollow fiber membranes are used in combination with physical (Morphysorb®) or chemical solvents (alkanolamines). TNO Environment Energy and Process Innovation (The Netherlands) have been developing a membrane gas absorption process for the removal of CO_2 from flue gases using commercially available and cheaper polypropylene hollow fiber membranes. As conventional absorption liquids like alkanolamines are not suitable for polypropylene membranes, new reactive absorption liquids have been developed (Feron & Jansen, 1995).

Long-term stable operation of the membrane contactor requires that the pores of the membrane remain completely gas filled (non-wetted) over prolonged periods of operational

time. This is because in case of wetted membranes, the gas to be absorbed also has to diffuse through the stagnant liquid inside the pores, thereby considerably increasing the overall mass transfer resistance. So, the prevention of wetting is an important criterion determining the operability of the contactor. Most of the absorption liquids used for the removal of gases like NH_3, SO_2, etc. are aqueous salt solutions and so membrane modules made of hydrophobic microporous membranes like polyolefin membranes were found to be ideally suitable. In case of reactive absorption of CO_2, conventional reactive absorption liquids like aqueous alkanolamine solutions were found to wet polyolefin membranes. However, many investigators had successfully used more hydrophobic membranes like Teflon (PTFE) to overcome wetting (Nishikawa et al., 1995). Unlike polypropylene hollow fibers, PTFE fibers are not available in small diameters (a few hundred microns) and they are more expensive, making CO_2 removal using membrane gas absorption (MGA) not so economically attractive in comparison to conventional absorption processes.

Thus, there is a need for the development of new absorption liquids for the removal of CO_2 using membrane contactors that can offer stable performance with relatively cheap polyolefin membrane. Also for oxygen rich gas streams like flue gas, it will be an added advantage if the new liquids have better thermal degradation properties than traditional alkanolamines. Amino acid salts can be a possible alternative to alkanolamines, though they are more expensive. The use of the salts of amino acids for acid gas removal has traditionally been restricted to using it as promoters for the conventional gas treating solvents (Kohl & Nielsen, 1997). Some of the noted amino acids used as promoters are glycine, alanine and diethyl or dimethyl glycine. TNO has developed and patented a range of absorption liquids based on amino acid salts and given them the trade name CORAL (CO_2 Removal Absorption liquid). These liquids offer similar absorption characteristics as aqueous alkanolamine solutions, have better degradation properties and above all, do not wet polypropylene membranes (Feron & Jansen, 1995). The present work deals with the above qualities of one such CORAL liquid as well as on the performance of this liquid in MGA, for the removal of CO_2. A numerical model involving mass transfer accompanied by multiple chemical reactions, occurring during the absorption of CO_2 into the absorption liquid flowing through the hollow fiber has been developed and the results of the numerical model have been compared with the experimental results.

2.0 Theory: Mass Transfer accompanied by chemical reactions

2.1 Reactive Absorption of CO_2 in Aqueous Amino Acid Salt Solutions

Amino acids dissolved in water exists as zwitter ion [form II in Eq. (1)] and the pH of the solution is equal to the isoelectric point of the given amino acid. The amino group should be deprotonated (form III) before it can react with CO_2. This is usually done by the addition of an equimolar amount of base.

$$\underset{\text{I}}{HOOC-R-NH_3^+} \overset{-H^+}{\rightleftharpoons} \underset{\text{II}}{^-OOC-R-NH_3^+} \overset{-H^+}{\rightleftharpoons} \underset{\text{III}}{^-OOC-R-NH_2} \quad (1)$$

Aqueous solutions of amino acid salts react with CO_2 similar to primary alkanolamines. Unlike alkanolamines, there is no reliable information available in open literature regarding the reaction mechanism/kinetics and physico-chemical constants (such as physical solubility, diffusivity of CO_2 in aqueous salt solution) necessary to interpret the experimental kinetic data or design of the gas-liquid contactor. In the present study, the potassium salt of taurine (2-aminoethanesulfonicacid) was used as a model amino acid salt and representative of the CORAL family of absorption liquids. To get reliable physico-chemical properties of the model component, several independent experimental studies were carried out (Kumar et al., 2001a,b). The data were used in the present study, for the modeling of the absorption of CO_2 in the aqueous amino acid salt solutions flowing through the hollow fiber (Section 2.2). The principle reactions occurring during the absorption of CO_2 in aqueous amino acid salt solutions are reaction (2) and (3) in the following scheme.

$$2\,RNH_2 + CO_2 \underset{k_{2,2}}{\overset{k_{2,1}}{\rightleftharpoons}} RNHCOO^- + RNH_3^+ \qquad (2)$$

$$CO_2 + OH^- \underset{k_{3,2}}{\overset{k_{3,1}}{\rightleftharpoons}} HCO_3^- \qquad (3)$$

$$RNH_3^+ \underset{k_{4,2}}{\overset{k_{4,1}}{\rightleftharpoons}} RNH_2 + H^+ \qquad (4)$$

$$H_2O \underset{k_{5,2}}{\overset{k_{5,1}}{\rightleftharpoons}} H^+ + OH^- \qquad (5)$$

Amino acid salts in aqueous solution react with CO_2, resulting in the formation of a carbamate and protonated amine. The mechanism of the reaction of CO_2 with the amino acid salts seems to be somewhat different from the well-known zwitterion mechanism proposed for the alkanolamines (Versteeg et al., 1996). The information on the forward reaction rate of the reaction (2) is given in the appendix. The contribution of reaction (3) to the overall reaction rate is usually not significant as the pH of the aqueous amino acid salt solutions is not high enough to have an appreciable concentration of OH^- ion in the liquid. Since the OH^- ion concentration is always in equilibrium with the amine concentration, the protonation/deprotonation (dissociation) reactions of the amino acid and water [given by reaction (4) and (5)] need to be considered also.

The experimental data on the physical solubility and diffusion coefficient of CO_2 in amino acid salt solutions were interpreted using appropriate mathematical models and are given in the Appendix. The kinetic, equilibrium and physico-chemical data related to the reactions (3)-(5) were obtained from the literature and they are also summarised in the Appendix. However, the experimental information on the equilibria of reaction (2) was only available for a narrow concentration range. The limited experimental data were regressed for the Kent-Eisenberg model and its value seems to be comparable to that of monoethanolamine (Kohl & Nielsen, 1997), the details of which are also given in the Appendix.

2.2 Numerical Model

Numerous mass transfer models such as film, penetration and surface renewal models are available in literature to describe the reactive absorption of a gas in a liquid

(Westerterp et al., 1984). The basic and common assumption of all these models is the presence of a well-mixed bulk phase adjacent to the gas-liquid interface. For the present case of the reactive absorption of a gas in the liquid flowing through a hollow fiber, the well-mixed liquid bulk is absent. Due to the laminar flow of liquid through the hollow fiber, there is a velocity profile in the liquid phase, which extends from the gas-liquid interface to the axis of the fiber. Hence, the mathematical treatment of the present problem to predict the enhancement factor for the effect of chemical reaction on absorption is not easy. However, for physical absorption and constant gas-liquid interface conditions, Kreulen et al. (1993a) proposed an approximate solution for the mass transfer coefficient analogous to the heat transfer coefficient in the constant wall temperature heat transfer problem of Graetz (1883) and Leveque (1928) and it was experimentally validated.

$$Sh = \sqrt[3]{3.67^3 + 1.62^3\ Gz} \tag{6}$$

The above equation was found applicable for the complete range of Graetz numbers in the laminar flow regime. Due to the limitations mentioned above, the mass transfer process involving chemical reaction in the liquid flowing inside the hollow fiber has to be described by a model based on first principles. The differential mass balance for any species, i, present in the liquid phase is given by,

$$v_z \frac{\partial C_i}{\partial z} = D_i \left[\frac{1}{r} \frac{\partial}{\partial r} \left(r \frac{\partial C_i}{\partial r} \right) \right] - R_i \tag{7}$$

In arriving at Eq. (7), the diffusion in the axial direction was neglected and axi-symmetry was assumed. The temperature effect during the absorption process was considered to be negligible. As the liquid flow inside the fiber is laminar, the velocity profile in the radial direction is given by,

$$v_z = 2\ v_L \left[1 - \left(\frac{r}{R} \right)^2 \right] \tag{8}$$

The entrance effects had been neglected as the liquid flows through the hollow fiber for considerable distance (> $100 d_{in}$, required for the velocity profile to be fully developed, see Perry & Green, 1984) before it contacts the gas phase. A generalised reversible reaction scheme to take into account the multiple reactions, as described in section 2.1, was incorporated in the model. The partial differential equation (7) requires one initial condition and two boundary conditions in the axial and radial directions respectively. For the axial direction, the inlet conditions/properties of the liquid are specified.

$$\text{At } z = 0, \qquad C_i = C_{i,o} \tag{9}$$

In the radial direction, symmetry was assumed at the axis of the cylindrical fiber,

$$\text{At } r = 0, \qquad \left(\frac{\partial C_i}{\partial r} \right) = 0 \tag{10}$$

At the gas-liquid interface, the conservation of mass with respect to the component that is absorbed from the gas phase (CO_2) was enforced.

$$\text{At } r = R \qquad D_A\left(\frac{\partial C_A}{\partial r}\right) = k_{ext}\,(C_{A,g} - C_{A,g,i}) \qquad (11)$$

All components other than the gas species absorbed are assumed to be non-volatile.

$$\text{At } r = R \qquad \left(\frac{\partial C_i}{\partial r}\right) = 0 \qquad \text{for } i \neq CO_2 \qquad (12)$$

The set of partial differential equations (the number depending on the number of chemical species involved in the reaction scheme) was solved numerically using a technique similar to the one described by Kreulen et al. (1993b). Also refer Chapter 6 (section 2.0 and 3.0) for more details on the external mass transfer coefficient, k_{ext}. From the concentration profile of CO_2 in the liquid phase obtained from the solution of mass balance equations, the local absorption flux of CO_2 along the length of the fiber was calculated using Fick's law. The average CO_2 absorption flux ($<J_{CO2}>$) was obtained from integration of the local fluxes across the length of the fiber.

2.3 Analogy with Conventional Mass Transfer Models

Kumar et al. (2002a) showed that under limiting conditions, an analogy exists between the present mass transfer problem as described by Eq. (7) and conventional mass transfer models like the penetration model. For sufficiently short gas-liquid contact time in the hollow fiber, the penetration depth [approximately $0.5(D_A\pi L/v_L)^{0.5}$, see Westerterp et al., 1984] is a few orders of magnitude less than the radius of the hollow fiber (R). As a consequence, the liquid far away from the gas-liquid interface is unaffected by the absorption process. Physically this implies that the liquid is of infinite depth in comparison to the penetration depth of the gas. This is similar to the situation where a gas is absorbed in a falling film (of finite thickness and with constant velocity distribution in the liquid film) of a wetted wall column (Westerterp et al., 1984). For this limiting situation, the Hatta number (Ha*) and infinite enhancement factor ($E_{i,\infty}$*) can be defined on the properties of the liquid far away from the interface (at the axis of the fiber) analogous to the bulk liquid properties in conventional gas-liquid contactors. For an (1,1)-order reaction, the dimensionless Hatta number and infinite enhancement factor can be defined as,

Modified Hatta Number:
$$Ha^*_A = \frac{\sqrt{k_1\, C_{B,r=0}\, D_A}}{k_L} \qquad (13)$$

Modified Infinite Enhancement Factor:
$$E_{a,\infty} = \left(1 + \frac{C_{B,r=0}}{\nu_B\, m\, C_{A,g,i}}\right)\left(\frac{D_B}{D_A}\right)^{1/2} \qquad (14)$$

Here the mass transfer coefficient (k_L) can be calculated from Eq. (6). Developing an analogy with the conventional mass transfer models as described above, provides a

convenient tool for the explanation of the experimental and numerical results in a simplistic way.

3.0 Experimental

3.1 Chemicals

The potassium salt of taurine was prepared by neutralising taurine (Merck), dissolved in deionised water, with an equimolar amount of potassium hydroxide (Merck). The concentration of the amino acid salt was determined potentiometrically by titrating with standard HCl. Aqueous alkanolamine solutions used for comparison were prepared by dissolving pure alkanolamines (Merck) in deionised water. The concentration was determined by titrating with standard HCl.

3.2 Experimental Setup and Procedure

3.2.1 Surface Tension and Breakthrough Pressure Measurements

The wettability of a hydrophobic microporous membrane by a liquid depends, among others, on the surface tension of the liquid. It can be quantified by measuring the breakthrough pressure of the liquid through the membrane. The experimental technique to measure the breakthrough pressure was similar to the liquid entry pressure method described by Franken et al. (1987). In this method, a dry membrane is brought into contact with a liquid after which the liquid pressure is increased. The pressure at which the liquid penetrates into the pores (this can be observed by the formation of the first liquid drop on the other side of the membrane) is measured. In the present study, the breakthrough pressure of various liquids was measured for a hydrophobic PTFE microporous membrane ($d_{p,max}$: 3.5 μm; Schleicher & Schuell, Germany). The surface tension of the liquid was measured using two techniques: the Wilhelmy plate method (Kruss Digital Tensiometer K9, Kruss GmbH) and the maximum bubble pressure method (SITA Online t60, SITA Messtechnik GmbH). With the maximum bubble pressure method, the values of the surface tension were measured for a long bubble lifetime (60s) inorder to obtain the equilibrium value of the surface tension. The values of the surface tension obtained with both methods were within ± 0.2 mN m^{-1}.

3.2.2 Absorption Measurements

Absorption experiments were carried out in a single hollow fiber membrane contactor. Figure 1 shows the single fiber contactor as well as the flowsheet of the experimental setup used for the absorption experiments. The contactor consisted of a jacketed, cylindrical glass tube with threaded ends as shown in Figure 1. The two ends of a membrane hollow fiber were passed through two small stainless steel (SS) tubes whose inside diameter was slightly larger than the outside diameter of the hollow fiber. The length of the fiber exposed to the gas during absorption measurements was the distance between the two SS tubes. So, the distance between the SS tubes was carefully adjusted and the fiber was potted to the SS tubes on both the ends of the two tubes. The length of the fiber inside the SS tube (> 0.07 m), on the liquid entry side provides sufficient distance (> $10d_{in}$)

for the laminar liquid flow inside the fiber to be fully developed, before it contacts the gas. The hollow fiber between the SS tubes was placed coaxial to the jacketed glass tube and the two SS tubes were fastened to the ends of the threaded glass tube (without stretching the fiber) with a special assembly as shown in the Figure 1. The liquid feed line was connected to the SS tube on the feed side of the contactor.

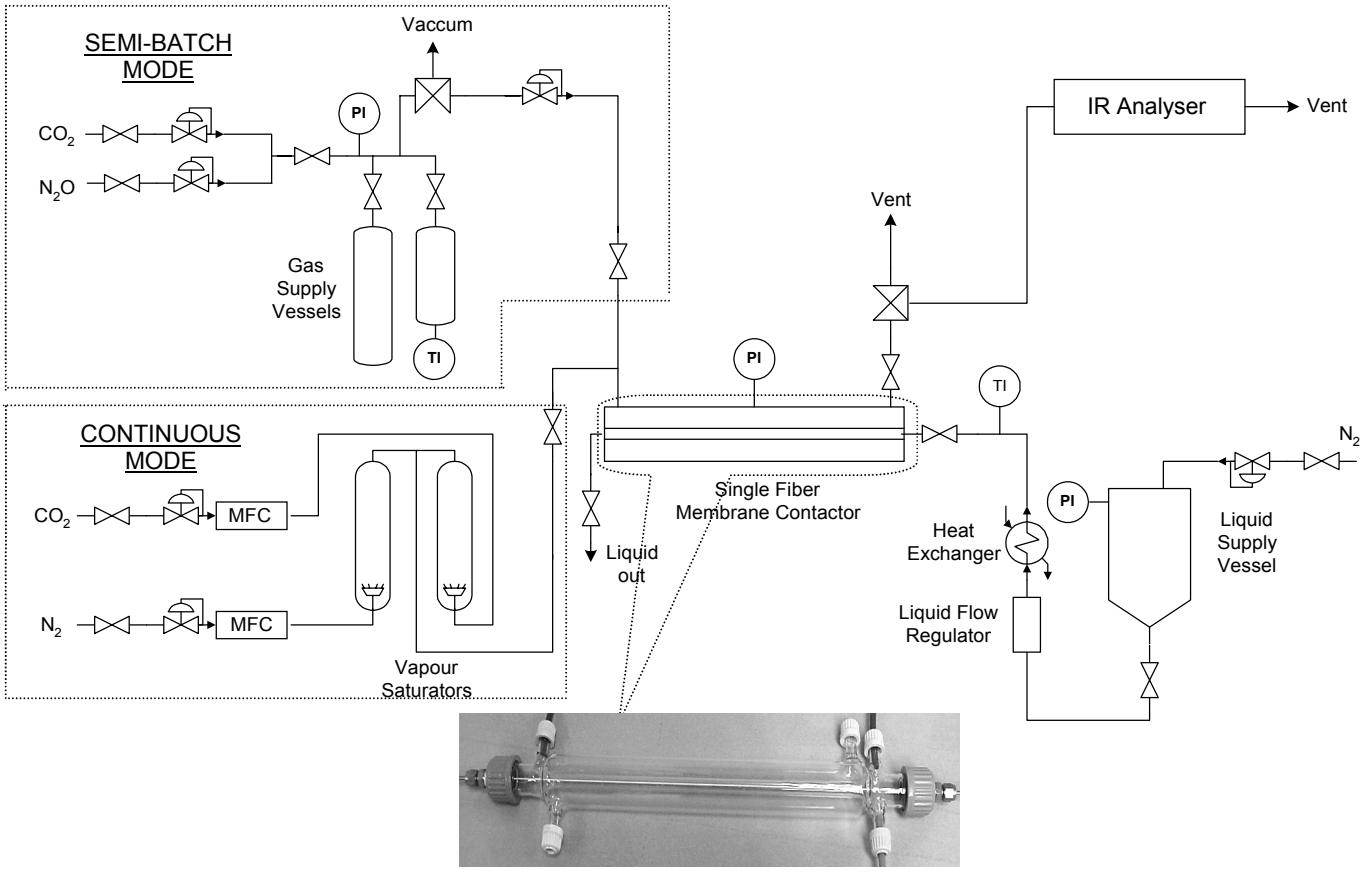

Figure (1) *Experimental setup to study the performance of new absorption liquids in a single fiber membrane gas-liquid contactor.*

Two modes of gas-liquid contacting operation were studied during the experiments. In both cases, the liquid flow through the fiber was continuous. The liquid was fed from a pressurised supply vessel to the membrane contactor via a flow controller. The inert gas (nitrogen) pressure above the liquid in the supply vessel was maintained constant using a precision pressure controller to enable a constant pulse-free flow of liquid through the fiber. The reactive liquids used in all the experiments were freshly prepared and degassed prior to the measurements. In the so-called semi-batch mode, the CO_2 partial pressure outside the hollow fiber in the contactor was maintained constant by feeding pure CO_2 from a gas supply vessel, through a pressure regulator. From the drop in the pressure of CO_2 in the gas supply vessel, the absorption rate and hence average CO_2 flux across the membrane was calculated. In case of the so-called continuous operation, nitrogen and CO_2 were premixed to a desired concentration using mass flow controllers and fed to the contactor after saturating the gas stream with water vapor. For all experiments studied, the gas flowed

cocurrently with respect to the liquid phase. The CO_2 concentration in the feed and outlet gas streams of the contactor was measured using an Infrared analyser. From this, the CO_2 absorption flux was estimated by making a mass balance over the reactor.

$$< J_{CO2} > = \frac{\phi_g \left(C_{A,g,in} - C_{A,g,out} \right)}{d_{in} L} \qquad (15)$$

It was assumed that the volumetric flowrate of the feed and exit streams are equal, as the concentration range of CO_2 in the feed stream studied was low (less than 6% by volume) and also, the fraction of the moles of CO_2 in the feed stream absorbed by the liquid was not high. For dilute gas streams flowing along the fiber, the contribution of the gas phase mass transfer resistance to the overall resistance can be significant. As the objective of the study is to understand the phenomenon of mass transfer with chemical reaction in the liquid phase, the gas phase resistance had to be minimised. The annular distance between the contactor glass wall and the outer surface of the fiber (through which the gas flows) was kept minimum and also the gas flowrate was increased till it had a negligible influence on the absorption rate. Absorption experiments were not conducted for high CO_2 concentrations in the gas stream, to avoid operating the contactor differentially (i.e., small concentration difference in the gas stream between inlet and outlet of the contactor). Differential operation can lead to large errors in the measurement of the absorption flux as the average flux is based on the inlet and outlet stream concentrations of CO_2 [Eq. (15)].

In the present work, the following systems were studied:

1. Physical Absorption
   a. N_2O - water (Semi-batch)
   b. CO_2 - water (Semi-batch)
2. Chemical Absorption
   a. CO_2 - NaOH(aq) (Semi-batch)
   b. CO_2 - amino acid salt(aq) (Semi-batch & Continuous)

The physical absorption experiments were studied to check the accuracy of the experimental setup for mass transfer measurements. Similarly, absorption of CO_2 in aqueous NaOH solution was chosen as a model reactive system, as accurate kinetic and physico-chemial data are available in literature. The hollow fiber membranes used for the experiments were supplied by Akzo Nobel (Accurel PP capillary membrane, Type Q3/2: average pore diameter: 0.2 μm; d_{in}: 600 μm).

4.0 Results and Discussion

4.1 Wetting Qualities of Aqueous Alkanolamines and Amino Acid Salt Solution for a Hydrophobic Microporous Membrane

Wetting of the membrane depends on the properties of the liquid as well as the membrane material. These influences can be quantified in terms of surface tension of the liquid (γ_L), contact angle of the liquid with the membrane material (θ) and the pore properties

of the membrane. A considerable amount of information is available in the literature on the criteria for wetting of microporous membranes (Franken et al., 1987). For low energy surfaces like polyolefin and PTFE, the relation between surface tension and contact angle is given by (Bargeman & Vader, 1973),

$$\gamma_L \cos\theta = -\gamma_L + c \qquad (16)$$

For a single known value of γ_L and θ (usually for pure water), the constant c can be calculated. The influence of the presence of pores on the contact angle can be corrected as indicated by Troger et al. (1997). With information on the values of surface tension, contact angle and pore properties, the minimum pressure to be applied on the liquid to enter the pores of the membrane (Breakthrough Pressure, BP) can be estimated using the Laplace-Young equation,

$$\Delta p = -\frac{4\gamma_L \cos\theta}{d_{max}} \qquad (17)$$

Here d_{max} is the maximum pore diameter in the microporous membrane. Table 1 shows experimental values of the surface tension of 2 molar primary, secondary and tertiary aqueous alkanolamine solutions measured at 295 $\pm$ 0.2 K. Aqueous solutions of alkanolamines are organic substances dissolved in water and their solubility is primarily due to the presence of the OH group. Hence their values of surface tension as shown in the table are significantly less than that of water. It can be observed that the surface tension progressively decreases from primary to tertiary amines or with increase in the molecular weight of the alkanolamines. Among tertiary amines, the surface tension of the aqueous MDEA solution is higher than that of the aqueous DMEA solution, due to the presence of an additional polar OH group in MDEA. For loaded solutions, the surface tension was found to increase with CO_2 loading and this can be explained by the presence of ionic reaction products formed during the reaction of CO_2 with alkanolamines as given below (Versteeg et al., 1996).

For Primary & Secondary Amines: $2\,RNH_2 + CO_2 \longleftrightarrow RNHCOO^- + RNH3^+$ (18)

For Tertiary Amines: $R_3N + CO_2 + H_2O \longleftrightarrow HCO_3^- + R_3NH^+$ (19)

The experimental breakthrough pressures for different loaded and unloaded aqueous alkanolamine solutions with a hydrophobic PTFE microporous membrane are shown in Table 1. These data are averaged values of at least five measurements with reproducibility within $\pm$ 1 kPa. It should be noted that the maximum pore diameter of the PTFE membrane used ($d_{p,max}$: 3.5 μm) was more than an order of magnitude higher than the pore diameter of the polypropylene membranes used in the actual absorption experiments (typically 0.2 μm). For polypropylene flat sheet membranes with a pore diameter of 0.2 μm, the breakthrough pressure for the liquids of high surface tension such as water and aqueous salt solutions are larger than the mechanical burst pressure of the membrane. Hence for a qualitative comparison of various alkanolamine solutions, a hydrophobic PTFE membrane with a larger pore diameter was used to measure the breakthrough pressure of all liquids having values of surface tension significantly higher (alkaline salts) and lower (amines) than that of water. As

can be seen in Table 1, the influence of the type of amine and CO_2 loading on the breakthrough pressure follows exactly the same trend as observed for the surface tension.

Table (1) *Surface tension and Breakthrough pressure of loaded and unloaded alkanolamine solutions at 295 K. The breakthrough pressure was measured for a PTFE membrane ($d_{p,max}$: 3.5 μm, Schleicher & Schuell).*

Alkanolamine	CO_2 Loading (mol CO_2/mol amine)	γ_L (mN m^{-1})	Breakthrough Pressure (kPa)
Water	Unloaded	72.3	25.4
Monoethanolamine (MEA)	Unloaded	68.2	18.2
Diethanolamine (DEA)	Unloaded	64.8	14.4
Methyldiethaolamine (MDEA)	Unloaded	57.2	13.1
Dimethylethanolamine (DMEA)	Unloaded	49.3	12.4
Monoethanolamine (MEA)	0.05	69.1	23.0
Monoethanolamine (MEA)	0.12	70.2	-
Monoethanolamine (MEA)	0.28	72.6	25.5

Eventhough the value of the surface tension of an aqueous MEA solution is close to that of water, the breakthrough pressure for this liquid is significantly less than that of water, indicating possible changes in the surface/pore morphology of the membrane similar to the theory proposed by Barbe et al. (2000). Barbe et al. experimentally demonstrated for a hydrophobic membrane in contact with a liquid of low surface tension (also for water) that the pore equivalent diameter increases due to the non-wetting intrusion of the liquid meniscus into some pores with a resulting enlargement of the pore entrances. This enlargement of pores could result in wetting of the membranes at liquid pressures much lower than those predicted by Eq. (17). Figure 2 shows the plot of experimental values of the breakthrough pressure measured for different alkanolamine solutions. The line in the figure indicates the calculated value of breakthrough pressure using the Laplace-Young equation. Except for aqueous DMEA solution, the prediction of the Laplace-Young equation is reasonably good.

Table (2) *Physical properties of Unloaded and Loaded Aqueous amino acid salt solutions at 295 K*

Concentration (mol m^{-3}) x 10^{-3}	CO_2 Loading (mol CO_2/mol amine)	Viscosity (cP)	γ_L (mN m^{-1})	Breakthrough Pressure (kPa)
1.0	Unloaded	1.18	72.9	25.4
2.0	Unloaded	1.59	74.4	25.9
4.0	Unloaded	3.27	77.5	-
2.0	0.04	-	74.8	27.7
2.0	0.17	-	75.3	-
2.0	0.32	-	76.1	-

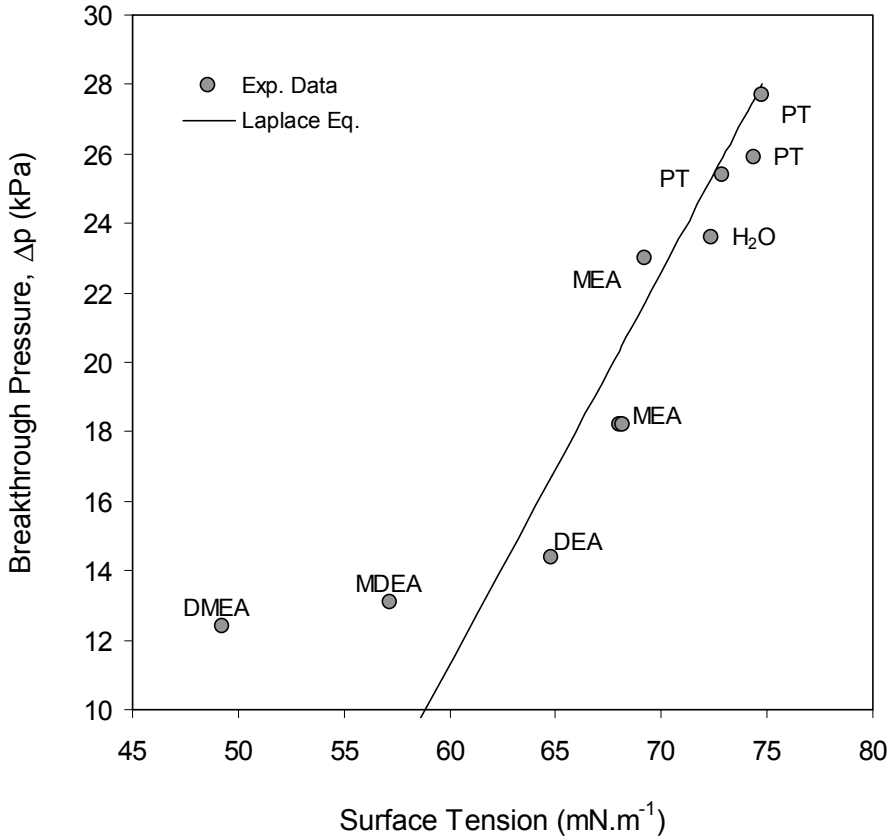

Figure (2) *Comparison of the experimental data of breakthrough pressure for a hydrophobic microporous PTFE membrane ($d_{p,max}$: 3.5 μm, Schleicher & Schuell) with the values predicted by the Laplace-Young equation. The abbreviation 'PT' in the figure denotes potassium salt of taurine.*

Table 2 gives some of the physical properties of unloaded and loaded aqueous amino acid salt solutions at 295 K. As expected, the surface tension of the aqueous amino acid salt solutions are higher than for water. Unlike aqueous alkanolamines solutions, the surface tension increases with concentration of the salt and also increases with the CO_2 loading of the solution. Some experimental breakthrough pressure data of the aqueous amino acid salt solutions with a hydrophobic PTFE membrane are also shown in Figure 2.

4.2 Absorption Experiments

Experiments were carried out in semi-batch and continuous mode with respect to the gas phase. The semi-batch experiments were performed using pure CO_2, with the objective to test the experimental setup and also to generate experimental data to validate the numerical model for idealised and simple test conditions. The accuracy of the numerical model in comparison to the experimental data for the model amino acid salt studied indirectly gives an indication of the accuracy of the physico-chemical data (reaction kinetics, equilibrium solubility, diffusion coefficients, etc. see Appendix and Kumar et al., 2001a,b), used as input parameters in the numerical model. The continuous mode of operation using dilute gas streams is of more practical relevance and therefore the concentration range of CO_2 removal from flue gas was simulated.

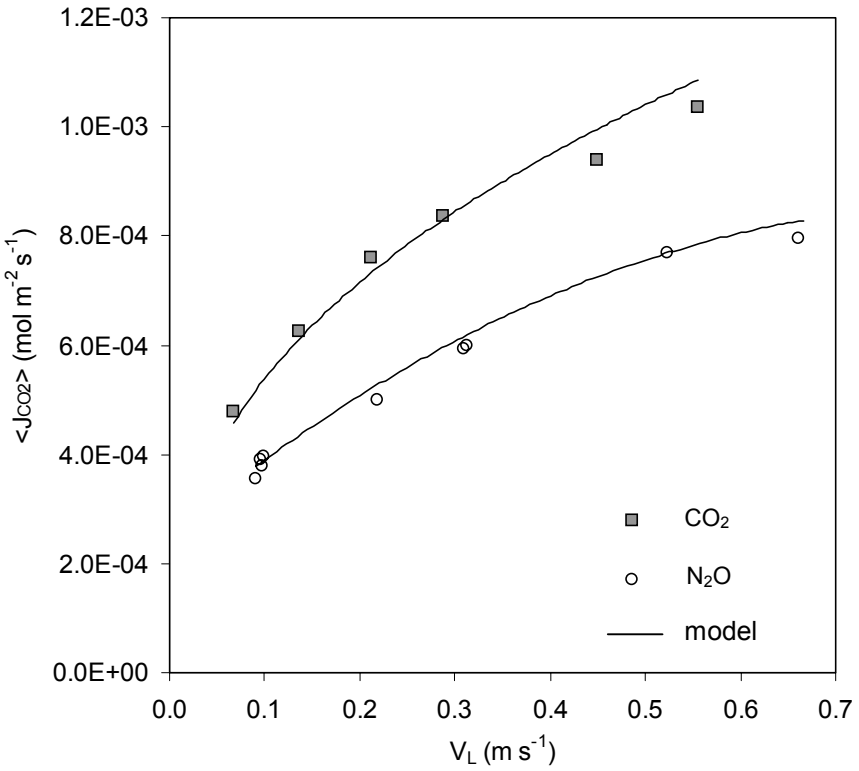

Figure (3) *Physical absorption of CO_2 and N_2O in water flowing through a hollow fiber. (Semi-batch; L: 0.38 m; P_{gas}: 107 kPa; T: 295 K)*

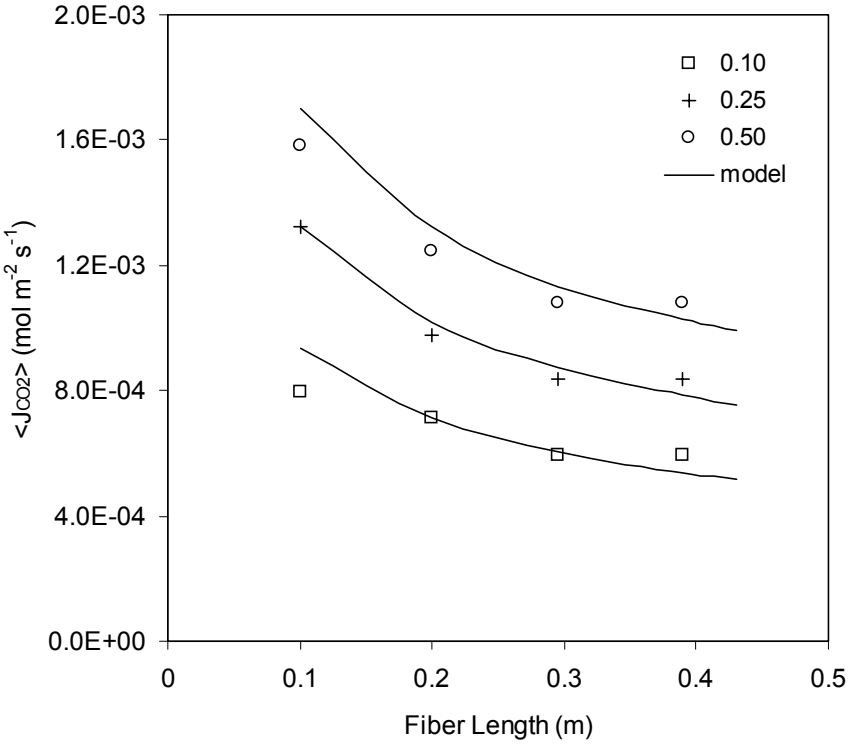

Figure (4) *Influence of fiber length on the absorption rate of CO_2 in water flowing through the hollow fiber. The legend of the figure indicates the liquid velocity in m s^{-1}. (Semi-batch; T: 293 K; P_{gas}: 107 kPa)*

4.2.1 Physical Absorption

Absorption of pure CO_2 and N_2O in degassed water was carried out in semi-batch mode. The results of the present experimental study are shown in Figure 3, which shows that the numerical model accurately predicts the experimental data for both gases. The difference in the absorption flux for N_2O and CO_2 can primarily be accounted for by the difference in the physical solubility of these gases in water. To further investigate the accuracy of the numerical model, the length of the fiber was varied and absorption experiments were again carried out with pure CO_2. The influence of the fiber length is shown in Figure 4 for different liquid velocities, which also shows a good agreement between theory and experiments. The accuracy of the liquid velocity in the experimental studies was within $\pm$ 0.005 m s^{-1}. It should be noted that for physical absorption, the influence of the length of the fiber on the absorption flux can also be theoretically quantified using the Graetz-Leveque solution [Eq. (6)]. The CO_2 absorption flux along the length of the fiber decreases due to saturation of the liquid by the gas and hence the average flux increases with decrease in length of the fiber exposed to gas.

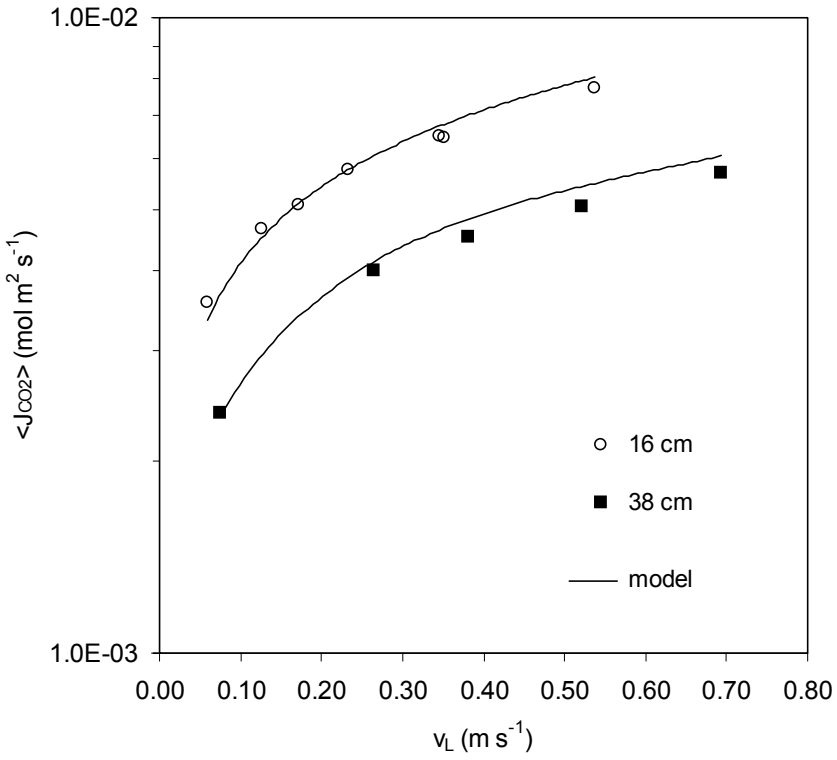

Figure (5) *Influence of liquid velocity on the absorption rate of CO_2 in aqueous NaOH solutions flowing through a hollow fiber. The numbers in the legend of the figure indicate the length of the fiber. (Semi-batch; C_{NaOH}: 0.24 M; P_{gas}: 107 kPa; T: 295 K)*

Absorption Enhanced by Chemical Reaction

4.2.2 Absorption of CO_2 in Aqueous NaOH Solution

Absorption of CO_2 in aqueous NaOH is widely used as a model system to investigate the performance of gas-liquid contactors. As the surface tension of these liquids is high (due

to their ionic nature), they do not wet polyolefin microporous membranes. Considerable and accurate information is available in the literature on the physico-chemical parameters required to model the absorption process. So, this system was used as a model system to study absorption enhanced by chemical reaction in a hollow fiber. In the numerical model only reaction (3) was considered for the simulations. The kinetic, solubility and diffusivity data used as input parameters in the model were obtained from literature (Pohorecki & Moniuk, 1988; Schumpe, 1993; Hikita et al., 1976). Electroneutrality in the liquid phase was maintained by using mean ion diffusion coefficients for the ionic species in the liquid phase. The results of the experimental study as well as that of the model are shown in Figure 5. It can be seen that the model predictions are in good agreement with experimental results.

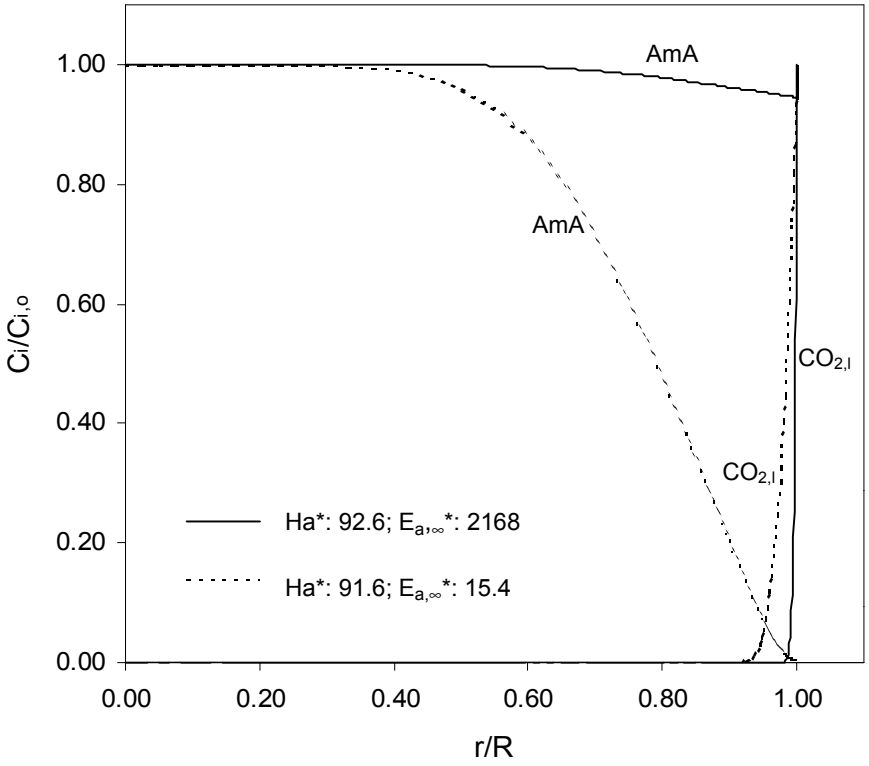

Figure (6) *The numerical radial concentration profile of the amino acid salt and CO_2 in the liquid phase during the absorption of CO_2 in the amino acid salt solution flowing through the fiber, for two asymptotic absorption regimes, namely fast ($2<Ha^*<E_{a,\infty}$) and instantaneous ($2<Ha^*>E_{a,\infty}$). The radial profile is at the liquid exit of the fiber (i.e., z=L). (L: 0.165 m; R: 300 μm, v_L: 0.10 m s^{-1}; $C_{AmA,o}$: 992 mol m^{-3}; P_{CO2}: 107 kPa for instantaneous regime and 0.77 kPa for fast regime; T: 295 K).*

4.2.3 Absorption of CO_2 in Aqueous Amino Acid Salt Solutions

Influence of Liquid Velocity

Liquid velocity is perhaps the most important operating variable in the membrane gas-liquid contactors because in general it has a large influence on the absorption flux. Depending on the liquid velocity (and hence Ha*) and $E_{a,\infty}$*, the absorption regime continuously changes from the liquid entrance to the exit. At the liquid inlet, there is no depletion of the amine at the gas-liquid interface and the absorption rate is influenced by the

chemical reaction rate (kinetics), while the liquid velocity has no effect on the local absorption rate (Fast regime; Ea = Ha*). Further, along the length of the fiber (depending on Ha* and $E_{a,\infty}$*), depletion of the amine may occur at the interface. For the extreme case of complete depletion of amine at the interface, the absorption rate is limited by the radial diffusion of the reacting species to the reaction plane and the flux is strongly influenced by the mass transfer coefficient (instantaneous regime; Ea = $E_{a,\infty}$*).

As an example, Figure 6 shows the numerically calculated radial concentration profiles of the amino acid salt and CO_2 in the liquid phase at the liquid exit of the fiber (z=L). The experimental conditions for which the simulations were carried out are given in the figure. It can be clearly observed that there is no significant depletion of the amino acid salt for 2<Ha*< $E_{a,\infty}$* (Fast regime). In the present study, the partial pressure of CO_2 in the gas stream is low and therefore the absorption in the continuous experiments fulfilled this condition. However for the case 2<Ha*> $E_{a,\infty}$*, the concentration of the amino acid salt at the gas-liquid interface approaches zero and a reaction plane is formed. This situation is analogous to the instantaneous regime described by the conventional mass transfer models. This example shows that the conventional mass transfer models can be used to describe the absorption of a gas in a liquid flowing through the hollow fiber. The necessary condition for the use of the conventional mass transfer model is that the gas-liquid contact time (residence time of the liquid) should be short enough to prevent the depletion of the amino acid salt at the axis of the fiber.

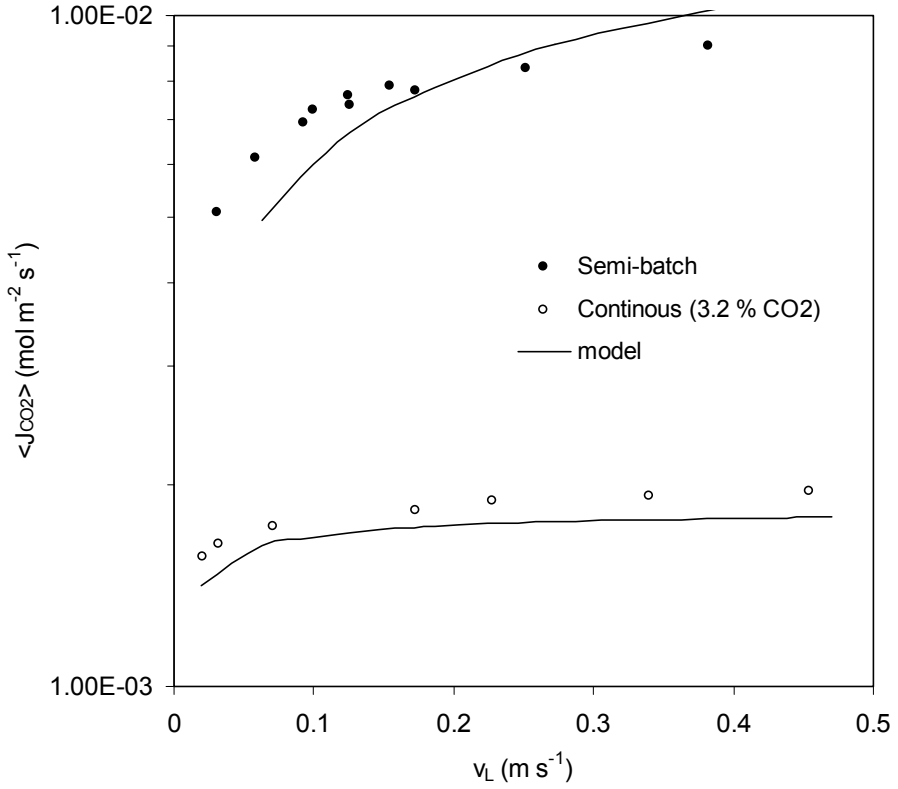

Figure (7) *Influence of liquid velocity on the absorption rate of CO_2 in aqueous amino acid salt solution flowing through the hollow fiber. (L: 0.426 m; C_{AmA}: 0.992 M; $P_{gas,\ s.batch}$: 107 kPa; $P_{gas,\ cont}$: 103 kPa; T: 295 K)*

Figure 7 shows the influence of the liquid velocity on the absorption rate of CO_2 from a gas phase, for two different partial pressures of CO_2. The numerical model predicts the experimental trend and data reasonably well. For the semi-batch experiments, where pure CO_2 is used, the absorption regime in a part of the fiber is instantaneous and hence absorption rate is influenced by the liquid velocity. During absorption from a gas stream containing a low partial pressure of CO_2, except at very low liquid velocity, the absorption rate is not influenced by v_L significantly. So, at a liquid velocity above few centimeters per second, the absorption regime is in the Ea = Ha* regime and this regime is ideally suitable for the operation of the membrane contactor.

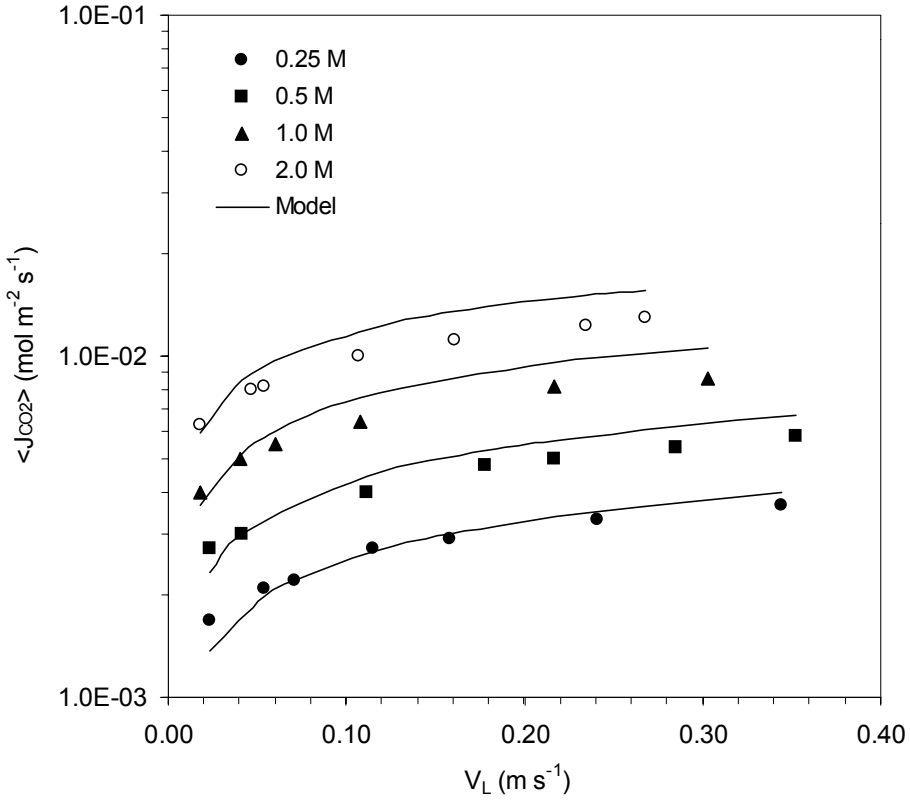

Figure (8) *Influence of amino acid salt concentration on the absorption rate of CO_2 in the semi-batch measurements. The legends in the figure indicate the molar concentration of the solution used (L: 0.165 m; P_{gas}: 107 kPa; T: 295 K)*

Influence of Amino Acid Salt Concentration and Partial Pressure of CO_2 (Semi-Batch and Continuous Experiments)

Absorption of pure CO_2 in aqueous amino acid salt solutions of different concentrations was investigated and the results are shown in Figure 8. For a CO_2 partial pressure of approximately 100 kPa in the gas phase and low amine concentration in the liquid phase, there is a significant depletion of the amine at the gas-liquid interface (indicating the instantaneous absorption regime) and hence the liquid velocity (i.e., k_L) significantly influences the absorption flux, as described earlier. As it can be seen in Figure 8, the numerical model predicts the experimental data within ± 20 %. The lower accuracy in the prediction of the numerical model in comparison to the aqueous NaOH-CO_2 system can

be partly due to the inaccuracy in the values of equilibrium constants used in simulations for reaction (2).

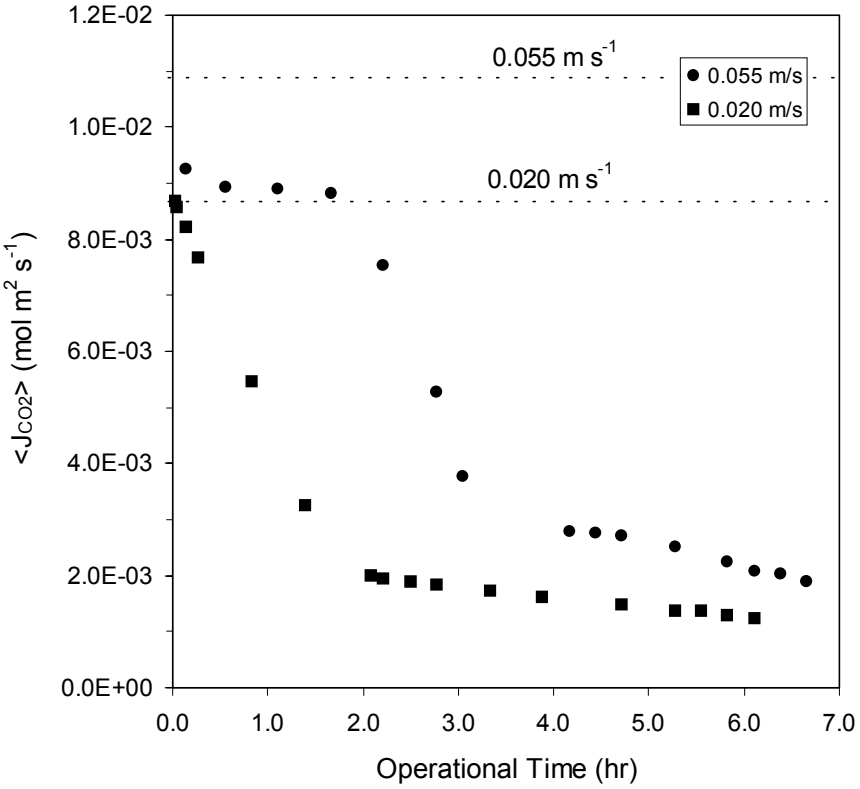

Figure (9) *The absorption rate of pure CO_2 as a function of operational time for a 4 molar amino acid salt solution. The legends of the figure indicate the velocity of the liquid flowing through the fiber. The dotted line represents the value of absorption flux predicted by the numerical model in the absence of mass transfer resistance due to the precipitate layer (Semi-batch; P_{gas}: 1.07 bar; L: 0.165 m; T: 295 K)*

An important feature in the absorption of CO_2 in aqueous alkaline salts of amino acid is the precipitation of the reaction products for liquids with a high amine concentration and high CO_2 loading. Hook (1997) reported qualitatively on the precipitation problem for different classes of amino acids. However, there is no generalised rule to predict the onset of crystallisation through some process variables like partial pressure of CO_2 in gas stream, amine concentration, CO_2 loading in the liquid, etc., for sterically and non-sterically hindered amino acid salts, reported in literature. Detailed study and discussion about this phenomenon is made in chapter 3 and 4. Also in the present study, precipitation was observed at high partial pressures of CO_2 and high amine concentrations. The implication of precipitation on the practical operation of the membrane contactor varies from a significant increase in the overall mass transfer resistance to a complete blockage of the fiber by the precipitate at very low liquid velocities. The influence of precipitation on the absorption flux for different liquid velocities is shown in Figure 9. After a few hours of operation, the flux drops by an order of magnitude and the entire mass transfer resistance is due to the precipitate layer at the gas-liquid interface (fiber wall). For liquid velocities less than 0.01 m s^{-1}, the solids completely blocked the flow of liquid, resulting in leakage of the absorption

liquid. The dotted lines in the figure indicate the CO_2 flux predicted by the numerical model in the absence of precipitation. It should be noted that the absorption of CO_2 in different types of amino acid salt solutions does not necessarily lead to precipitation (even at high CO_2 loading), as it strongly depends on the type of amino acid used (Hook, 1997).

Figure 10 shows the influence of the partial pressure of CO_2 in the feed gas stream for different amino acid salt concentrations in the liquid stream. For a given salt concentration, the flux increases linearly with the partial pressure of CO_2 in the feed stream and it is strongly dependent on the amino acid salt concentration. The experimental absorption flux is nearly proportional to $C_{AmA}^{n/2}$ (which is in accordance with the power in the Hatta number), where n is the order of the reaction with respect to the amino acid salt. Also, at these operating conditions (except for a 0.43 molar solution), the absorption was not significantly affected by the liquid velocity (see also Figure 7) and thus independent of k_L. Combining together these observations, it can be concluded that for those conditions the absorption rate is principally influenced by the reaction kinetics and there is no significant depletion of the amine at the gas-liquid interface (Ea = Ha*). The numerical model predicts the experimental data within ± 25 %.

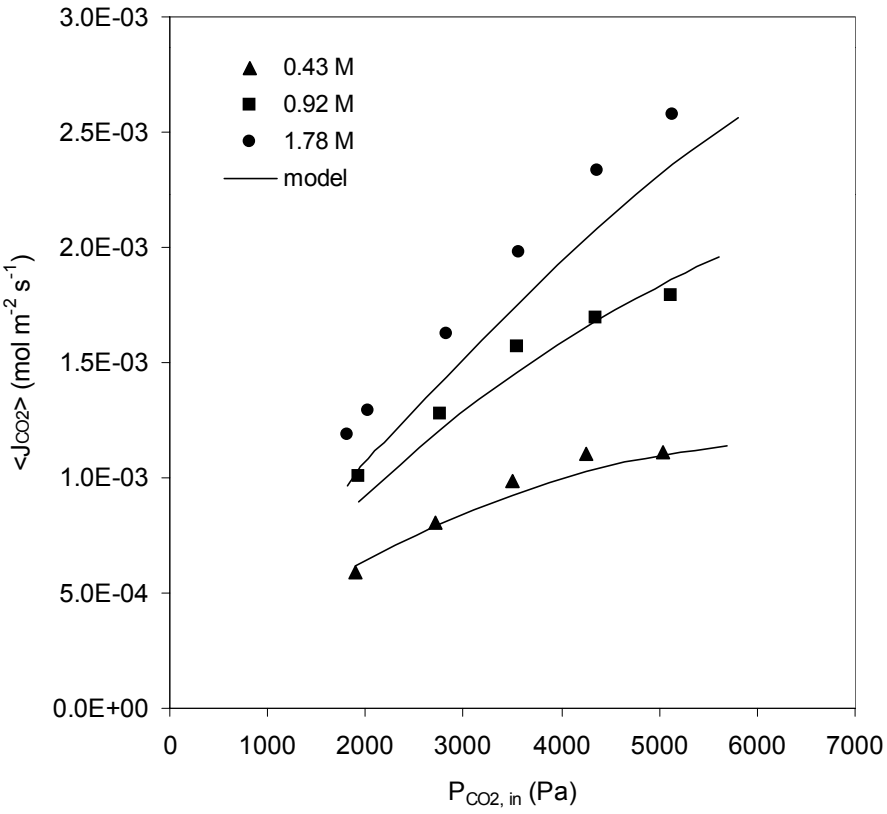

Figure (10) *Influence of the partial pressure of CO_2 in the feed gas stream on the absorption rate of CO_2 in aqueous amino acid salt solution flowing through the hollow fiber membrane. The legends in the figure indicate the molar concentration of the salt in liquid. (Continuous; L: 0.38 m; v_L: 0.025 m s^{-1}; $P_{gas.}$: 103 kPa; T: 295 K)*

As the stability of a membrane contactor is of paramount importance, additionally the CO_2 absorption flux was monitored in the single fiber reactor for 72 hrs for a 2 molar amino

acid salt solution. During this prolonged period of operation, the flux dropped by only 6% and this drop was mainly observed during the initial period of 30 minutes.

5.0 Conclusions

In the present study, a new absorption liquid based on the aqueous alkaline salts of amino acids was studied in an experimental, single fiber membrane gas-liquid contactor. The new liquid has suitable physical properties to prevent the wetting of commercially available polypropylene microporous membranes and also has good reactivity towards CO_2. The liquids based on amino acid salts seem promising for the removal of CO_2 in membrane contactors and are suited for stable gas-liquid contacting.

The wetting of the microporous membranes was studied by measuring the breakthrough pressure of the liquid for a hydrophobic membrane. Experimental results of the breakthrough pressure and surface tension for different classes of aqueous alkanolamines and amino acid salt solutions explain qualitatively the underlying reason for the wetting of polyolefin membranes by alkanolamines and also, the opposite phenomenon encountered for amino acid salts. The Laplace-Young equation could be conveniently used to predict the breakthrough pressure of various liquids for a microporous membrane.

Membrane gas absorption experiments were performed extensively to determine the performance of the non-wetting aqueous amino acid salt solutions in the removal of CO_2 from dilute gas streams. Absorption of CO_2/N_2O in water and aqueous NaOH solutions were used as model non-reactive and reactive experimental systems respectively, to establish the accuracy of the experimental setup and the applicability of the numerical model. Under limiting conditions, the experimental trends of the absorption flux with respect to the various operating parameters can be conveniently explained using traditional mass transfer models.

A numerical model has been developed to simulate mass transfer accompanied by multiple chemical reactions, occurring during the absorption of a gas in the liquid flowing through the hollow fiber. The numerical model provides good insights on the mass transfer process occurring in the liquid phase flowing through the fiber and it accurately predicts the experimental data of model reactive and non-reactive systems. For the absorption of CO_2 in aqueous amino acid salt solutions, the experimental data are predicted within $\pm$ 25 % for a wide range of experimental conditions.

Acknowledgement

This research is part of the research programme carried out within the Centre for Separation Technology, a cooperation between the University of Twente and TNO, the Netherlands Organisation for Applied Scientific Research. We also acknowledge L.H. Laagwater for his assistance to the experimental work and Wim Leppink for the construction of experimental setups.

6.0 Nomenclature

c	Constant in Eq. (16), mN m^{-1}
C	Concentration, mol m^{-3}
d_{in}	Inside diameter of the hollow fiber, m
$d_{p,max}$	Maximum pore diameter, μm
D	Diffusion coefficient, m^2 s^{-1}
d_{max}	Maximum pore size, m
Ea	Enhancement factor, dimensionless
$E_{a,\infty}$	Modified infinite enhancement factor, dimensionless
F	Faradays constant, C mol^{-1}
Gz	Graetz number, $v_L d^2/DL$, dimensionless
Ha*	Modified Hatta number, dimensionless
$<J_{CO2}>$	Average CO_2 absorption flux, mol m^{-2} s^{-1}
K_{sub}	Reaction equilibrium constant, sub: reaction number, $k_{subs,1}/k_{sub,2}$
$k_{sub,1}$	Reaction rate constant, sub: reaction number, forward, $(mol^{-1}\ m^3)^o\ s^{-1}$
$k_{sub,2}$	Reaction rate constant, sub: reaction number, backward, $(mol^{-1}\ m^3)^o\ s^{-1}$
k_{ext}	External mass transfer coefficient, m s^{-1}
k_L	Liquid side mass transfer coefficient, m s^{-1}
L	Length of the hollow fiber, m
m	Physical solubility, $(C_{A,l}/C_{A,g})_{eq}$, dimensionless
o	Overall order of the reaction, dimensionless
P_{gas}	Pressure in the gas phase, kPa
r	Distance in radial direction from the fiber axis, m
R	Radius of the fiber, m
R_i	Reaction rate, mol m^{-3} s^{-1}
Sh	Sherwood number, $k_L d/D$, dimensionless
T	Temperature, K
v_L	Average liquid velocity, m s^{-1}
v_z	Liquid velocity in the axial direction, m s^{-1}
z	Distance in the axial direction from the liquid inlet, m
z^+, z^-	Ionic charge

Greek

θ	Contact angle of the liquid with solid surface
ν	Stoichiometric coefficient
ϕ	Gas flowrate, m^3 s^{-1}
γ_L	Surface tension of liquid, mN m^{-1}
Δp	Breakthrough pressure, kPa

Subscript

A	Component in gas phase

AmA	Amino acid salt
B	Component in liquid phase
g	Gas phase
l	Liquid phase
i	Component i, interface
in	Feed stream
out	Outlet stream
o	Inlet condition

Abbreviations

BP	Breakthrough pressure
MGA	Membrane Gas Absorption
PTFE	Polytertraflouroethylene

7.0 References

Barbe, A.M., Hogan, P.A., & Johnson, R.A. (2000). Surface morphology changes during initial usage of hydrophobic, microporous polypropylene membranes. *Journal of Membrane Science*, **172**, 149-156.

Bargeman, D., & van Voorst Vader, F. (1973). Effect of surfactant on contact angles at non-polar solids. *Journal of Colloid & Interface Science,* **42(3)**, 467-472.

Edwards, T.J., Maurer, G., Newman, J., & Prausnitz, J.M. (1978). Vapour-liquids equilibria in multicomponent aqueous solutions of volatile weak electrolytes. *AIChE Journal*, **24**, 966-976

Feron, P.H.M., & Jansen, A.E. (1995). Capture of carbon-dioxide using membrane gas-absorption and reuse in the horticultural industry. *Energy Conversion & Management,* **36(6-9)**, 411-414.

Franken, A.C.M., Nolten, J.A.M., Mulder, M.H.V., Bargeman, D., & Smolders, C.A. (1987). Wetting criteria for the applicability of membrane distillation. *Journal of Membrane Science,* **33**, 315-328.

Gabelman, A., & Hwang, S.T. (1999). Hollow fiber membrane contactors. *Journal of Membrane Science,* **159(1-2)**, 61-106.

Graetz, L. (1883). Über die Wärmeleitungsfähigkeit von Flüssigkeiten, 1e Abhandlung, Annalen der Physik und Chemie, **18**, 79-84.

Greenstein, J.P., & Winitz, M. (1961). *Chemistry of the amino acids*. New York: Wiley.

Gubbins, K.E., Bhatia, K.K., & Walker, R.D. (1966). Diffusion of gases in electrolytic solutions. *AIChE Journal*, **12**, 548-552.

Hanisch, C. (1999). Exploring options for CO_2 capture and management. *Environmental Science & Technology*, **33(3)**, 66A-70A.

Hikita, H., Asai, S., & Takatsuka, T. (1972). Gas absorption with a two step chemical reaction. *Chemical Engineering Journal*, **4**, 31-40.

Hook, R.J. (1997). An investigation of some sterically hindered amines as potential carbon dioxide scrubbing compounds. *Industrial & Engineering Chemistry Research,* **36(5)**, 1779-1790.

Hovarth, A.L. (1985). *Handbook of aqueous electrolytic solutions: physical properties, estimation and correlation methods*. New York: John Wiley.

Kohl, A. L., & Nielsen, R.B. (1997). *Gas Purification*: 5th ed. Houston: Gulf Publishing Company.

Kreulen, H., Smolders, C.A., Versteeg, G.F., & van Swaaij, W.P.M. (1993a). Microporous hollow-fiber membrane modules as gas-liquid contactors. 1. Physical mass transfer processes - A specific application - Mass transfer in highly viscous liquids. *Journal of Membrane Science,* **78(3)**, 197-216.

Kreulen, H., Smolders, C.A., Versteeg, G.F., & van Swaaij, W.P.M. (1993b). Microporous hollow-fiber membrane modules as gas-liquid contactors. 2. Mass transfer with chemical reaction. *Journal of Membrane Science,* **78(3)**, 217-238.

Kumar, P.S., Hogendoorn, J.A., Feron, P.H.M., & Versteeg, G.F. (2001a). On kinetics of reaction between CO_2 and aqueous amino acid salt solutions. *AIChE Journal* (Under Review; Chapter 2 of this thesis).

Kumar, P.S., Hogendoorn, J.A., Feron, P.H.M., & Versteeg, G.F. (2001b). Density, Viscosity, Solubility and Diffusivity of N_2O in Aqueous Amino Acid Salt Solutions. *Journal of Chemical & Engineering Data,* **46**, 1357-1361. (Chapter 1 of this thesis)

Kumar, P.S., Hogendoorn, J.A., Feron, P.H.M., & Versteeg, G.F. (2002a). Approximate solution to predict the enhancement factor for the reactive absorption of a gas in a liquid flowing through a microporous hollow fiber. (To be published; Chapter 6 of this thesis).

Kumar, P.S., Hogendoorn, J.A., Feron, P.H.M., & Versteeg, G.F. (2002b). Equilibrium solubility of CO_2 in aqueous potassium taurate solutions. (To be published; Chapter 4 of this thesis).

Leveque, J. (1928). Les lois de la transmission de chaleur par convection, Annls. Mines, Paris (Series 12), 201.

Nishikawa, N., Ishibashi, M., Ohta, H., Akutsu, N., Matsumoto, H., Kamata, T., & Kitamura, H. (1995). CO_2 removal by hollow-fiber gas-liquid contactor. *Energy Conversion & Management,* **36(6-9)**, 414-418.

Perrin, D.D. (1965). *Dissociation of organic bases in aqueous solution*. London: Butterworth.

Perry, R.H., & Green, D. (1984). *Perry's chemical engineer's handbook*. Singapore: McGraw-Hill

Pohorecki, R., & Moniuk, W. (1988). Kinetics of the reaction between carbon dioxide and hydroxyl ion in aqueous electrolyte solutions. *Chemical Engineering Science*, **43**, 1677-1684.

Qi, Z., & Cussler, E.L. (1985). Microporous hollow fibers for gas absorption I. Mass transfer in the liquid. *Journal of Membrane Science*, **23**, 321-333.

Schumpe, A. (1993). The estimation of gas solubilities in salt solutions. *Chemical Engineering Science*, **48**, 153-158.

Troger, J., Lunktwitz, K., & Burger, W. (1997). Determination of the surface tension of microporous membrane using contact angle measurements. *Journal of Colloid & Interface Science,* **194(2)**, 281-286.

Versteeg, G.F., van Dijck, L.A.J., & van Swaaij, W.P.M. (1996). On the kinetics between CO_2 and alkanolamines both in aqueous and non-aqueous solutions. An overview. *Chemical Engineering Communications,* **144**, 113-158.

Versteeg, G.F., & van Swaaij, W.P.M. (1988). Solubility and diffusivity of acid gases (CO_2, N_2O) in aqueous alkanolamine solutions. *Journal of Chemical & Engineering Data*, **33**, 29-34.

Westerterp, K.R., van Swaaij, W.P.M., & Beenackers, A.A.C.M. (1984). *Chemical reactor design and operation*. New York: Wiley and Sons.

Appendix

The physical and chemical parameters for CO_2-aqueous amino acid salt system were obtained from independent experimental studies. Part of these studies have been published in the open literature (Kumar et al., 2001b) and others will be published shortly hereafter (Kumar et al., 2001a).

Physical solubility

As CO_2 reacts with the aqueous amino acid salt solutions, the physical solubility of CO_2 in the salt solutions was indirectly obtained from the solubility of N_2O. A model similar to that of Schumpe (1993) described the experimental data on the solubility of N_2O in aqueous potassium taurate solutions (Kumar et al., 2001b).

$$\log (m_w/m) = K C_s$$

where C_s is the salt concentration in kmol m^{-3}. For a single salt, the Sechenov constant, K based on the Schumpe model is given by the following relation,

$$K = \Sigma (h_i + h_G) n_I \qquad m^3\ kmol^{-1}$$

The anion and cation specific constants are,

h_+:	0.0922	$m^3\ kmol^{-1}$
h_-:	0.0249	$m^3\ kmol^{-1}$

The temperature dependent gas (CO_2) specific constant was obtained from the database of Schumpe (1993). The solubility of CO_2 and N_2O in water (m_w) were obtained from the work of Versteeg and van Swaaij (1988)

Diffusion Coefficient

An approach similar to the physical solubility was used to determine the diffusivity of CO_2 in aqueous salt solutions. The diffusion coefficient of N_2O in potassium taurate solution was obtained from Kumar et al. (2001b). A modified Stokes-Einstein equation was used for the estimation of the diffusion coefficient of N_2O in aqueous potassium taurate solutions.

$$D\mu^{0.74} = \text{constant}$$

The information on the dependence of viscosity on the amino acid salt concentration is available in Kumar et al. (2001b). The diffusion coefficient of CO_2 in aqueous potassium taurate solutions was estimated according to Gubbins et al. (1966):

$$(D/D_w)_{N2O} = (D/D_w)_{CO2}$$

The diffusion coefficients of CO_2 and N_2O in water were obtained from the work of Versteeg and van Swaaij (1989). The mean ion diffusion coefficient of the amino acid salt in aqueous solution at infinite dilution was estimated using the Nernst equation (Hovarth, 1985).

$$D_i^{\infty} = \frac{z^+ + z^-}{z^+ z^+} \frac{RT}{F^2} \frac{\lambda_+^{\infty}\, \lambda_-^{\infty}}{\lambda_+^{\infty} + \lambda_-^{\infty}}$$

The ionic conductivity at infinite dilution for the potassium ion (λ_+^∞) was fitted as a polynomial function of temperature from the data available in Howarth (1985). Similarly λ_-^∞ for the anion was obtained for 298 K from Greenstein and Winitz (1961). As information on the temperature dependence of λ_-^∞ was not available in the literature for the taurate ion, the dependence was assumed to be similar to that of the cation. At 295K, the values of λ_+^∞ and λ_-^∞ are 70.1and 28.9 $m^2\ \Omega^{-1}\ mol^{-1}$ respectively. The dependence of the diffusion coefficient of the amino acid salt in aqueous solution on the salt concentration was assumed to follow the modified Stokes-Einstein relation (Versteeg et al., 1996),

$$D\mu^{0.6} = \text{constant}$$

Diffusivities of protonated amine and carbamate were estimated from the amino acid salt diffusivities as no data are available in literature.

Kinetics and Equilibria Parameters

The forward reaction rate of the reaction between CO_2 and aqueous potassium taurate solution was obtained from Kumar et al. (2001a) and is given by the following relation:

$$R_{CO_2} = \frac{k_2\, C_{CO_2,I}\, C_{AmA}}{1 + \dfrac{1}{k_{AmA}\, C_{AmA} + k_{H_2O}\, C_{H_2O}}} \qquad \text{mol m}^{-3}\ \text{s}^{-1}$$

Here C_{Am}, C_{H2O} and $C_{CO2,I}$ are the concentration of amino acid salt, water and carbon dioxide in the absorption liquid respectively in mol m^{-3}. The values of k_2, k_{AmA} and k_{H2O} are given below:

$k_2 = 3.23 \times 10^9 \exp(-5700/T)$ $\quad m^3\ mol^{-1}\ s^{-1}$

$k_{AmA} = 2.36 \times 10^{-6} \exp(1225/T)$ $\quad m^3\ mol^{-1}$

$k_{H2O} = 2.29 \times 10^{-8} \exp(1483/T)$ $\quad m^3\ mol^{-1}$

The forward rate constant of reaction (3) as a function of ionic strength, I (mol m^{-3}) was obtained from Pohorecki and Moniuk (1988).

$$\log (k_{3,1}/k_{3,1}^\infty) = 2.21 \times 10^{-4}\, I - 1.6 \times 10^{-8}\, I^2$$

and the rate constant at infinite dilution is given by,

$$k_{3,1}^\infty = 8.895 - (2382/T) \qquad m^3\ mol^{-1}\ s^{-1}$$

As the reactions (4) and (5) were instantaneous, a large value of forward rate constant (10^6 m^3 mol s^{-1}) was used for $k_{4,1}$ and $k_{5,1}$.

The backward reaction rates were estimated by the assumption that at equilibrium conditions, forward and backward rates are equal. The equilibrium constant of reaction (2) was obtained from the work of Kumar et al. (2002b).

The equilibrium constant (K_3) of reaction (3) was obtained from Edwards et al. (1978). Similarly, the dissociation (equilibrium) constants of amino acid (K_4) and water (K_5) were obtained from Perrin (1965) and Edwards et al. (1978) respectively.

Chapter 6

Approximate Solution to Predict the Enhancement Factor for the Reactive Absorption of a Gas in a Liquid Flowing through a Microporous Membrane Hollow Fiber

Abstract

Approximate solutions for the enhancement factor (based on the traditional mass transfer theories) for gas-liquid systems with a liquid bulk have been adapted to situations where a liquid bulk may be absent and a velocity gradient is present in the mass transfer zone. Such a situation is encountered during the absorption a gas in a liquid flowing through a hollow fiber. The explicit solution of DeCoursey (1974) for a second order irreversible reaction has been used as a representative sample of the approximate solutions available in literature. It was chosen because of the accuracy of its predictions and the simplicity in use. The solution of DeCoursey was adapted, but still has limitations at long gas-liquid contact times. Under these conditions, the actual driving force for mass transfer of the gas phase species may not be identical for physical and reactive absorption. Also for these situations, there may be a significant depletion of the liquid phase reactant at the axis of the fiber (which is considered to be analogous to the liquid bulk in traditional mass transfer models). A criterion has been proposed for the applicability of the adapted DeCoursey's approximate solution for a second order irreversible reaction. Within the range of applicability, the approximate solution has been found to be accurate with respect to the exact numerical solution of the mass transfer model as well as the experimentally determined values of enhancement factor in a single hollow fiber membrane gas-liquid contactor. The single hollow fiber membrane contactor that has been used in this study has potential for use as a model gas-liquid contactor. This contactor can thus be used, along with the present approximate solution of the enhancement factor, to obtain the physico-chemical properties of a reactive gas-liquid system from the experimental absorption flux measurements or vice-versa, as described in the present work.

1.0 Introduction

Microporous hollow fiber membrane modules can be conveniently used for gas-liquid mass transfer operations and offer numerous advantages over conventional contactors like plate and packed columns (see Gabelman and Hwang, 1999). The design of membrane gas-liquid contactors is relatively simple and the scale-up is linear because of the modular nature of the contactor. For physical absorption of a gas in a liquid, important contactor specific design parameters are the mass transfer coefficients and the interfacial area for gas-liquid mass transfer. Since the liquid flow through the hollow fiber is laminar, the liquid side mass transfer coefficient can be estimated accurately using approximate solutions or correlations. The interfacial area for mass transfer (which is usually difficult to estimate within a reasonable accuracy for conventional contactors) is easy to determine, as it is simply the membrane surface area.

For well-known reasons, the reactive absorption of a gas in liquid is normally preferred over physical absorption (Kohl & Nielsen, 1997). In the reactive absorption of a gas in a liquid, the contribution of the chemical reaction to the enhancement of the mass transfer rate is traditionally quantified by a term called enhancement factor (E). This parameter needs to be quantified accurately for a good design of the gas-liquid contactor. Depending upon the degree of complexity in describing the absorption process, different approaches have been used by the membrane researchers to estimate the enhancement factor. The simplest approach is to use analytical solutions based on the traditional mass transfer theories described below, which are available for certain asymptotic conditions in the gas-liquid contactor (Qi & Cussler, 1985; Nii et al., 1992). Similarly, an approximate analytical solution of a mass transfer model based on the film theory (van Krevelen & Hoftijzer, 1948), applicable over a wider range of process conditions has also been used to qualitatively interpret the experimental data (Nii & Takeuchi, 1994; Li & Teo, 1998). It should be noted however that the traditional mass transfer models assume the presence of a well-mixed liquid bulk (relatively large compared to the mass transfer zone) adjacent to the mass transfer zone, which may not be present in case of the absorption of a gas in the liquid flowing through the hollow fiber, especially for small fiber diameters. Also, an additional feature of gas absorption in hollow fiber membranes is the presence of a velocity profile in the liquid side mass transfer zone. In addition to the above mentioned (approximate) analytical solutions, the absorption process in the membrane hollow fibers can be rigorously described using the differential mass balance equations. The exact numerical results of these equations can be used to accurately predict the enhancement factor (Kreulen et al., 1993a; Kumar et al., 2002).

While a large number of mass transfer models is available in literature to describe the absorption process in gas-liquid systems with a well defined liquid bulk (Westerterp et al., 1984), only three mass transfer models based on the film, penetration and surface renewal theories respectively are widely used to predict the contribution of the chemical reaction in enhancing the mass transfer rate (enhancement factor). Although for a wide range of operating conditions, the film model gives similar enhancement factors as those of the other two models, it is physically unrealistic and should therefore only be chosen because of its ease of use. The penetration and surface renewal models involve unsteady-state diffusion

with chemical reaction. As analytical solutions for the above mass transfer models are available for only certain asymptotic conditions, numerical solutions are generally required. Numerical solution of the mass transfer models is usually laborious and complex, necessitating the development of approximate solutions for calculating the enhancement factors based on one of the above mentioned mass transfer models. van Krevelen and Hoftijzer (1948) developed an approximate solution for the enhancement factor based on the film theory. Yeramian et al. (1970), Hikita and Asai (1964) proposed approximate solutions based on Higbie's penetration theory. Onda et al. (1970) and DeCoursey (1974, 1982) have provided approximate solutions based on Danckwert's surface renewal theory. It should be noted that the above-cited references for the approximate solutions to various mass transfer theories are only indicative, as considerably more information is available in literature.

In the present work, the applicability and limitations of the approximate solutions for the enhancement factor based on the traditional mass transfer models (with liquid bulk) are explored for their use in the design of membrane gas-liquid contactors (with no liquid bulk). The explicit approximate solution of DeCoursey (1974) was used as a test case and the results of it will be compared with the exact numerical results obtained for a membrane hollow fiber. For an irreversible second order reaction, the approximate results were also compared with the experimental results of a single fiber membrane gas-liquid contactor.

2.0 Theory

For a situation where a liquid flows inside the non-wetted hollow fibers of a membrane module, the mass transfer of a component A from the gas phase flowing outside the hollow fibers to the liquid can be described by the traditional "resistances in series" model, as given below. Here a reaction occurs between A and the species B present in the liquid phase.

$$\langle J_A \rangle = K_{ov}\, \Delta C_A \qquad (1)$$

Not only in gas-liquid systems with liquid bulk, but also in membrane gas absorption processes, the overall mass transfer coefficient (K_{ov}) is generally expressed as follows (Kreulen, 1993a),

$$\frac{1}{K_{ov}} = \frac{1}{k_g} + \frac{1}{k_m} + \frac{1}{m k_L E} \qquad (2)$$

The gas side mass transfer coefficient, k_g depends on the fluid hydrodynamics in the "shell side" of the membrane module and is module specific due to the high packing density and non-uniform spacing of the hollow fibers within the membrane module (Gabelman & Hwang, 1999). This may result in maldistribution of the gas flow around the fibers (like channeling). A number of correlations of the form of Eq (3) to predict k_g, based on dimensionless numbers, is available in literature (Gabelman & Hwang, 1999).

$$Sh_g = b\, (Re_g)^c\, (Sc_g)^{0.33} \qquad \text{b and c are constants} \qquad (3)$$

Assuming that there is no convective transport of A through the microporous membrane, the mass transfer across the membrane can be described using Fick's law and the mass

transfer coefficient related to the transport process through the membrane can be defined as,

$$k_m = \frac{D_{A,e}}{\delta} = D_A \frac{\varepsilon}{\delta \tau} \quad (4)$$

Depending upon the pore diameter (d_p) of microporous membrane and the gas phase pressure, the diffusion through the pores can be due to bulk diffusion ($d_p > 1.0 \times 10^{-5}$ m) or Knudsen diffusion ($d_p < 1.0 \times 10^{-7}$ m) or both in the intermediate region. A detailed description on the mass transport process through a microporous membrane can be found elsewhere (Mulder, 1996). For a binary gas mixture, the diffusion coefficient, D_A in a porous structure is calculated as given below:

$$\frac{1}{D_A} = \frac{1}{D_{A,j}} + \frac{1}{D_{K,A}} \quad (5)$$

The Knudsen diffusion coefficient is given by,

$$D_{K,A} = K_0 \sqrt{\frac{8 R T}{\pi M_w}} \quad (6)$$

For a (ideal) membrane with cylindrical pores, K_0 is equal to $4\varepsilon d_p/3\tau$. In reality, the parameter K_0 depends on the morphology of the membrane and the interaction between the molecules and porous structure. For single gas permeation, the values of K_0 for various commercial polyolefin membranes and gases respectively were experimentally determined by Guijt et al. (2000). The bulk diffusion coefficient can be calculated from the kinetic theory of gases. The liquid side mass transfer coefficient can be obtained from Leveque's solution derived from the analogous case of Graetz's heat transfer problem of laminar flow of a liquid through a circular duct (Leveque, 1928). The assumptions involved in Leveque's solution are constant gas-liquid interface conditions and a fully developed laminar flow of liquid through the fiber. The following correlations are available for the asymptotic regions of the Graetz number (Gz):

For Gz < 10, $Sh_L = 3.67$ (7)

For Gz > 20, $Sh_L = 1.62\ (Gz)^{1/3}$ (8)

Kreulen et al. (1993b) presented a correlation valid over the entire range of Graetz numbers (Gz).

$$Sh = \frac{k_L d}{D_A} = \sqrt[3]{3.67^3 + 1.62^3 Gz} \quad (9)$$

The above correlations (7-9) are based on the following definition of the average mass transfer coefficient, k_L (Leveque, 1928),

$$k_L = \frac{< J_A >}{(C_{A,l} - < C_{m,L} >)} \quad (10)$$

Here $<C_{m,L}>$ is the mixing cup (analogous to average bulk) concentration of A averaged over the length of the hollow fiber. For laminar flow of liquid through a hollow fiber, with a fully developed velocity profile, the mixing cup concentration of A in the liquid, at any axial distance, z from the liquid inlet side of the fiber is as follows (Kreulen et al., 1993b):

$$C_{m,z} = C_{A,I}\left[1 - \exp\left(-\frac{4k_L z}{<v>d}\right)\right] \tag{11}$$

The average bulk concentration of A ($<C_{m,L}>$) in the fiber can be obtained from the integration of $C_{m,z}$ over the length of the fiber.

$$<C_{m,L}> = \frac{C_{A,I}}{L}\left\{L + \frac{<v>d}{k_L}.\left[\exp\left(-\frac{4k_L L}{<v>d}\right) - 1\right]\right\} \tag{12}$$

The enhancement factor E that describes the influence of a chemical reaction on the mass transfer rate in Eq (2) can be obtained either from the exact numerical solution of the mass transfer models or analytical/approximate solutions of the mass transfer models. The enhancement factor affects the mass transfer rate significantly and thus the design of membrane gas-liquid contactors and will be the subject of further discussion.

3.0 Numerical model

For the reactive absorption of a gas in a liquid flowing through a microporous hollow fiber, the differential mass balance for any species, i, present in the liquid phase is given by,

$$v_z \frac{\partial C_i}{\partial z} = D_i\left[\frac{1}{r}\frac{\partial}{\partial r}\left(r\frac{\partial C_i}{\partial r}\right)\right] - R_i \tag{13}$$

In arriving at Eq. (13), the diffusion in axial direction was neglected and axi-symmetry of the hollow fiber was assumed. The temperature effect during the absorption process was considered to be negligible. Since the liquid flow inside the fiber is laminar, the velocity profile in the radial direction is given by,

$$v_z = 2 <v>\left[1 - \left(\frac{r}{R}\right)^2\right] \tag{14}$$

For a hypothetical situation where a gas is absorbed in a liquid flowing through a fiber under plug flow conditions, the differential mass balance equation (13) reduces to the following form,

$$\frac{\partial C_i}{\partial t} = D_i\left[\frac{1}{r}\frac{\partial}{\partial r}\left(r\frac{\partial C_i}{\partial r}\right)\right] - R_i \qquad \text{where } t = z/<v> \tag{15}$$

This is similar to the unsteady state mass balance equation of the penetration theory described in cylindrical co-ordinates and the important physical difference in the present case is the absence of a well-mixed bulk as described earlier. In this work, an irreversible second order reaction of the following type was assumed to occur in the liquid phase.

$$A + \gamma_b B \Rightarrow C + D \quad (16)$$

The partial differential equations (13) (laminar flow) and (15) (plug flow) require the following initial and boundary conditions in the axial and radial directions respectively and they are described in detail by Kreulen et al. (1993a).

At z = 0; for all r; $C_i = C_{i,0}$ (17)

For z > 0; at r = 0; $\left(\frac{\partial C_i}{\partial r}\right) = 0$ (18)

For z > 0; at r = R; $\left(\frac{\partial C_i}{\partial r}\right)_{i \neq A} = 0$ (19)

$$D_A\left(\frac{\partial C_i}{\partial r}\right) = k_{ext}\left(C_{A,g,bulk} - C_{A,g,l}\right) \quad (20)$$

The external mass transfer coefficient (k_{ext}) is a lumped parameter comprising of the resistances to mass transport of species A due to the gas phase and microporous membrane.

i.e., $$\frac{1}{k_{ext}} = \frac{1}{k_g} + \frac{1}{k_m} \quad (21)$$

The set of partial differential equations (the number depends on the number of chemical species involved in the reaction scheme) was solved numerically using a technique similar to the one described by Versteeg et al. (1989). In the numerical solution of the differential equations, the value of k_{ext} was kept very high (10^6 m s^{-1}) to focus completely on the mass transfer with chemical reaction occurring in the liquid phase (by neglecting the resistance due to the membrane and gas phase). The concentration profile of the absorbed gas (A) in the liquid phase was obtained from the solution of the mass balance equations. The local absorption flux of A along the length of the fiber was subsequently calculated using Fick's law. The average absorption flux ($<J_A>$) was obtained from the integration of the local fluxes along the length of the fiber.

$$< J_A > = \frac{1}{L}\int_0^L J_A(z)\,dz \quad (22)$$

The exact numerical enhancement factor (E) is defined as the ratio of the absorption rate/flux of a gas in the liquid in the presence of a chemical reaction to the absorption rate/flux in the absence of a reaction.

$$E_{num} = \frac{< J_{A,Chem} >_{num}}{< J_{A,Phys} >_{num}} \quad (23)$$

It should be noted that the above definition for the enhancement factor traditionally applies to a situation where the driving force (of A) for mass transfer is identical in the presence and absence of a chemical reaction. However, the above conditions may not be satisfied for large gas-liquid contact time in a membrane contactor (or at low Graetz numbers). In these

situations, there will be a significant concentration (<$C_{m,L}$>) of A in the liquid "bulk" for the case of physical absorption (Eq 12). Nevertheless, this definition will be used to calculate the overall enhancement factor for a membrane contactor and instead the enhancement factor predicted by the approximate solutions of traditional mass transfer models will be adapted to incorporate the change in the concentration of A in the liquid "bulk".

4.0 Approximate Solutions for Enhancement Factor

Numerous approximate solutions to the earlier described mass transfer models are available in the literature that are applicable over a wide range of process conditions, reactions of differing complexity and chemical solute loadings. However, all the models assume the presence of a well mixed liquid bulk adjacent to the mass transfer zone and therefore the dimensionless Hatta number and infinite enhancement factor used in these approximate solutions are based on the conditions existing in the liquid bulk. Depending upon the gas-liquid contact time, the mass transfer zone in the liquid phase of the hollow fiber may actually extend upto the axis of the fiber and the centerline concentration may be disturbed. Under the limiting condition of short gas-liquid contact time, the penetration depth of the gas phase species diffusing from the gas-liquid interface is small in comparison to the fiber radius. Consequently, the liquid far from the interface (say at the axis of the fiber) is essentially undisturbed (analogous to the liquid bulk that is assumed to be present at infinite distance from the gas-liquid interface in traditional mass transfer models) and the concentration of the liquid phase reactant B at the centerline (axis) is the same as the concentration of B in the liquid entering the fiber. For that case, the dimensionless Hatta number and asymptotic enhancement factor, adopted for a hollow fiber can be described based on the conditions at the liquid inlet (z = 0).

Hatta Number:
$$Ha^{*} = \frac{\sqrt{k_{m,n}\ D_A\ C_{A,I}{}^{m-1} C_{B,0}{}^{n}}}{k_L} \qquad (24)$$

Here m and n are the partial reaction order with respect to A and B respectively. The mass transfer coefficient for the laminar flow conditions was estimated using the Leveque's solution (Eqs 7 to 9). For plug flow of liquid through the hollow fiber, k_L was estimated using the following equation (Westerterp et al., 1984).

$$k_{L,Plug} = 2\sqrt{\frac{D_A}{\pi\,\tau}} = 2\sqrt{\frac{D_A\,L}{\pi < v >}} \qquad (25)$$

The asymptotic infinite enhancement factor for an irreversible reaction is defined as:

$$E_{\infty}^{*} = \left(1 + \frac{C_{B,0}\,D_B}{\nu_B\,m\,C_{A,g,I}\,D_A}\right)\left(\frac{D_A}{D_B}\right)^{q} \qquad (26)$$

The value of q varies depending upon the type of mass transfer model chosen and is given below.

Film model	q = 0
Penetration model	q = 1/2

Leveque model (presence of a velocity gradient in the mass transfer zone) q = 1/3

In the present work, the applicability and limitations of using an approximate solution of one of the mass transfer models (all developed originally for the case where a well defined liquid bulk is present) to predict the enhancement factor for the reactive absorption of a gas in a liquid flowing through a hollow fiber were investigated. The explicit approximate solution of DeCoursey based on Danckwert's surface renewal theory, developed originally for an irreversible second order chemical reaction (DeCoursey, 1974), was used as an example.

$$E_{app} = \frac{-Ha^{*2}}{2\left(E_{\infty}^{*}-1\right)} + \sqrt{\left[\frac{Ha^{*2}}{4\left(E_{\infty}^{*}-1\right)^{2}} + \frac{E_{\infty}^{*}\,Ha^{*2}}{\left(E_{\infty}^{*}-1\right)} + 1\right]} \qquad (27)$$

DeCoursey (1982) later extended the above expression to a reversible reaction that is second order in both directions and for equal diffusivities of reactants and products. The definition of the infinite enhancement factor (E_{∞}) was suitably modified for a reversible reaction. Later DeCoursey and Thring (1989) presented an implicit expression for the enhancement factor for a reversible reaction and unequal diffusivities of reactants/products. Recently, Hogendoorn et al. (1997) have shown that with a suitable adaptation for E_{∞}, Eq (27) can be used to predict the enhancement factor for a reversible reaction of finite rate and unequal diffusivity of reactants. An adapted analytical solution for the infinite enhancement factor for film model as derived by Secor and Beutler (1967) for an instantaneous reversible reaction, was used by the authors to calculate E_{∞}. To conclude, though the present work is based on Eq (27) for an irreversible reaction type of (16), it can be easily extended to other situations in line with the work of Hogendoorn et al. (1997).

The approximate solution for the enhancement factor (E_{app}) is usually obtained by developing an approximate solution for the time averaged (in the present case length averaged) absorption flux ($<J_{A,Chem}>_{app}$) in the presence of a chemical reaction. Further, E_{app} is obtained as per definition by dividing $<J_{A,Chem}>_{app}$ by the time/length averaged absorption flux in the absence of a chemical reaction. For an unloaded solution,

$$< J_{A,Phys} >_{app} = k_L C_{A,I} \qquad (28)$$

The enhancement factor as per the traditional definition is (for $C_{A,bulk}$ = 0),

$$E_{app} = \frac{< J_{A,Chem} >_{app}}{k_L\, C_{A,I}} \qquad (29)$$

However, the Leveque solution that provides an accurate estimate of k_L for the mass transfer in a hollow fiber is related to the absorption flux according to Eq (10). For physical absorption, the effective driving force for the mass transfer of A is reduced for long gas-liquid contact time, due to the saturation of the liquid by the gas absorbed. Therefore, the traditional approximate solutions for the enhancement factor available in the literature, which assume a negligible concentration of A in the liquid bulk, need to be adapted to the present situation to enable a proper comparison with the exact numerical solution.

$$E_{app,l} = E_{app} \frac{C_{A,l}}{(C_{A,l} - < C_{m,L} >)} \quad (30)$$

For large Graetz numbers (Gz), the saturation of the liquid by the solute gas is insignificant ($C_{A,l}$ >> <$C_{m,L}$>). Therefore,

$$E_{app,l} = E_{app} \quad (31)$$

It should be remembered that Eq (27) is an approximate solution for the penetration model in rectangular co-ordinates and therefore its simple extension to the present case (cylindrical geometry) essentially means that the curvature effects were neglected.

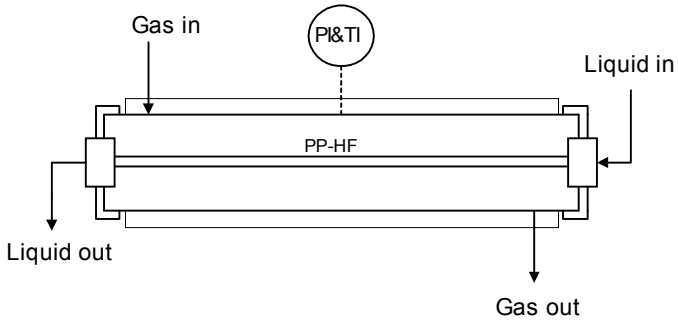

Figure (1) *Experimental single fiber membrane gas-liquid contactor*

5.0 Experimental Setup & Procedure

The reactive absorption of a gas in a liquid flowing through a hollow fiber was studied in a single fiber membrane gas-liquid contactor. The schematic diagram of the membrane contactor is shown in Figure 1. The details regarding the experimental set-up can be obtained from Kumar et al. (2002). A microporous polypropylene hollow fiber (Accurel PP: Type Q3/2; average pore diameter: 0.2 μm; d_{in}: 600 μm) was used in the membrane contactor. Two modes of gas-liquid contacting operation, namely the semi-batch and continuous mode, were studied in the present work. The liquid flow through the hollow fiber was continuous in both modes. In the semi-batch mode, pure gas present outside the hollow fiber was absorbed in the liquid flowing through the fiber. The gas phase pressure outside the hollow fiber was maintained constant by feeding pure gas from a supply vessel to the membrane contactor *via* a pressure regulator. From the drop in gas pressure in the supply vessel, the gas absorption rate/flux was calculated. In the continuous mode, a gas stream of known composition was fed to the membrane contactor and the composition of the gas stream entering and leaving the contactor was measured using an Infra-red (IR) gas analyser. The gas stream (CO_2/N_2) flowed cocurrent with respect to the liquid flow direction. By making a mass balance over the gas phase of the membrane contactor, the absorption rate/flux was calculated. Further information about the experimental procedure can be obtained in Kumar et al. (2002). The accuracy of the experimental setup was tested by measuring the physical absorption flux of N_2O and CO_2 in water. For physical absorption, the solubility (m) and diffusion coefficient (D_A) of the gas in liquid are the required (absorption) system specific input parameters for the numerical model and accurate information on these parameters is available in literature (Versteeg & van Swaaij, 1988). Therefore, the numerical

model should provide an accurate prediction of the absorption flux if compared to the experimental data. The absorption of CO_2 in aqueous NaOH solutions was used as a model reactive system, as accurate information on the physico-chemical parameters of this system is available in literature and the reaction also fits into the reaction scheme given by (16).

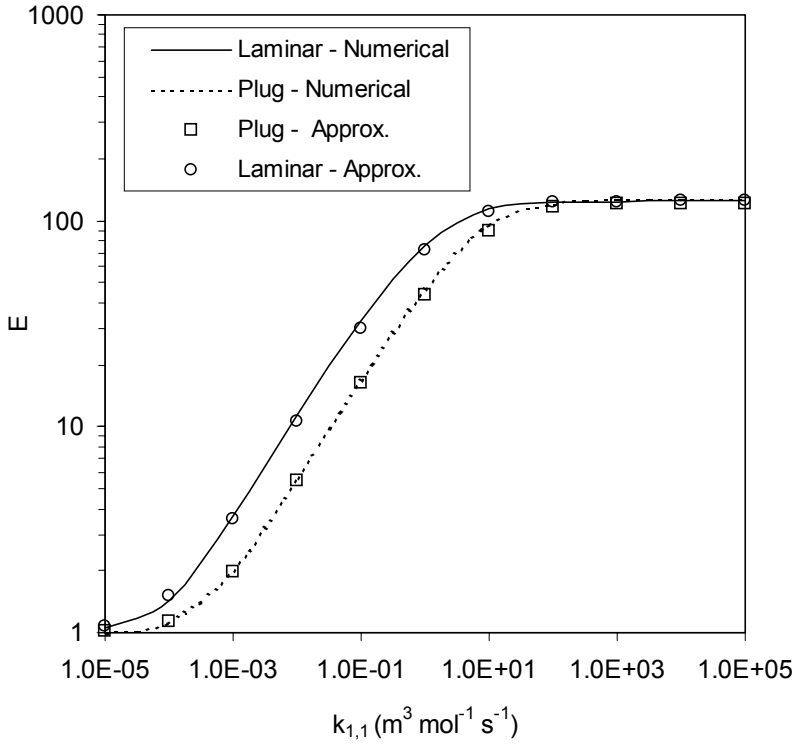

Figure (2) *The influence of the reaction rate constant on the enhancement factor for a second order irreversible reaction (Eq 16). Simulation conditions: L = 0.38 m; d = 600 x 10^{-6} m; <v> = 0.5 m s^{-1}; $C_{A,0}$ = 41.6 mol m^{-3}; $C_{B,0}$ = 5000 mol m^{-3}; $D_A = D_B$ = 1 x 10^{-9} m^2 s^{-1}; m = 1.0; ν_B = 1.0.*

6.0 Results and Discussion

6.1 Comparison of the Exact Numerical Solution and Approximate Solution for the Enhancement Factor

It should be noted that the DeCoursey's approximate solution is based on the surface renewal theory while the numerical model (at least for the situation where the liquid flow is plug) is related to the penetration theory. However, the difference in the prediction of E between the numerical model and approximate solution based on the two different theories is less than 2% for an irreversible first order reaction (Versteeg et al., 1989) and less than 6 % for an irreversible second order reaction with equal diffusivities of the reactants (DeCoursey, 1974). Figure 2 shows the enhancement factor predicted by the DeCoursey equation (adapted as per Eq 30) as well as the numerical model for the reactive absorption of a gas in liquid, flowing under plug and laminar conditions inside the hollow fiber as a function of the reaction rate constant. To avoid disturbance in the centerline concentration of A and B, the average residence time of the liquid was kept small enough to have an identical driving force of A for physical and chemical absorption (so that $E_{app,l}$ is identical to E_{app}). The

predictions of the approximate solution were in good agreement (within ± 5.5% for plug flow and ± 7.45% for laminar flow) with the exact solutions of the numerical model [% Error = (E_{num} – $E_{app,I}$) x 100/E_{num}]. The larger error for the laminar flow conditions is perhaps due to the error introduced by Leveque's solution (basically a correlation) in the prediction of the mass transfer coefficient for a situation where there is a velocity gradient in the mass transfer zone. The mass transfer coefficient (k_L) predicted by the Leveque solution for asymptotic conditions (Eq 7 & 8) is within ± 2 % of the exact numerical solution of the mathematical model (for the situation where there is no chemical reaction) described in section 3.0. The difference in E for the two flow conditions, at identical reaction rate constant, is due to the difference in the hydrodynamics of the mass transfer zone (presence and absence of a velocity gradient in the liquid) or more specifically on the numerical value of the mass transfer coefficient (k_L). These can be calculated for the two situations using Eqs (7 & 8) and (25) respectively.

For short gas-liquid contact time as considered in the above simulations, the mass transfer zone is thin and is restricted to the gas-liquid interface and therefore, there should be a negligible error due to the curvature of the fiber. This can be observed from similar values of the maximum error of the approximate solution for the present case (5.5% for plug flow and 7.5% for laminar flow) and the errors reported in literature for the penetration model (6%) in rectangular coordinates (Decoursey, 1974).

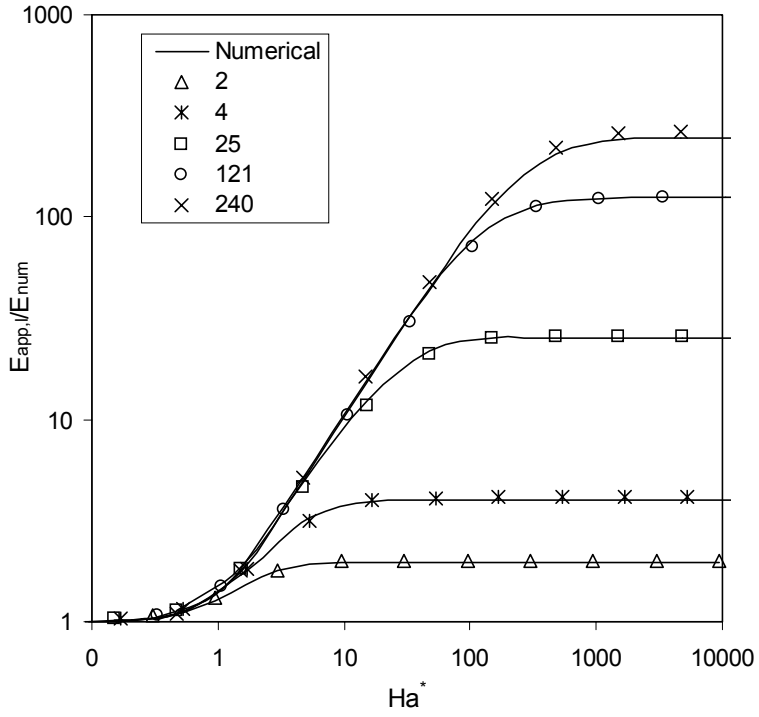

Figure (3) *E Vs Ha^* plot for the absorption of a gas in liquid (laminar flow) of finite depth accompanied by an irreversible second order reaction (Eq 16). Simulation conditions: L = 0.38 m; d = 600 x 10^{-6} m; <v> = 0.5 m s^{-1}; $C_{A,0}$ = 41.6 mol m^{-3}; $C_{B,0}$ = 40-9940 mol m^{-3}; $k_{1,1}$ = 1 x 10^{-5}-1 x 10^{5} m^3 mol^{-1} s^{-1}; D_A = D_B = 1 x 10^{-9} m^2 s^{-1}; m = 1.0; ν_B = 1.0. The legends of the figure indicate the value of E_∞^* for the conditions used in the numerical simulations as well as in the calculation of $E_{app,I}$.*

While a number of plots similar to Figure 2 can be generated for laminar flow conditions using the numerical model and approximate solutions, one can find a remarkable similarity between Figure 2 and the traditional E versus Ha plots. In fact, changing the reaction rate constant in Figure 2 is the same as changing the Ha^* for a given E_∞^*. Figure 3 shows the more generalised E versus Ha^* plot based on DeCoursey's approximate solution as well as the numerical results for the case of laminar flow of liquid through the fiber. The Ha^* and E_∞^* numbers were calculated using the definitions given by Eq (24) and (26) respectively. The Ha^* for a given E_∞^* was varied by changing the second order reaction rate constant, $k_{1,1}$ and E_∞^* itself was changed by varying the concentration of the reactant, B in the liquid phase. The accuracy of the enhancement factor predicted by the adapted DeCoursey's approximate solution is within ± 8.2% of the exact numerical solution of the model equations. As can be expected, the maximum error is in the transition region of Ha^* between the asymptotic absorption regimes [such as "$E = Ha^*$" (fast, $2<Ha^*< E_\infty^*$) and "$E = E_\infty^*$" (Instantaneous, $2<Ha^*> E_\infty^*$)]. In the asymptotic absorption regimes, the approximate solution reduces to the analytical solution of the mass transfer model and therefore the errors of the approximate solutions are minimal in the asymptotic regimes. Though the remarkably accurate prediction of E by the DeCoursey's solution is well known (DeCoursey, 1974; Hogendoorn et al., 1997) for the situation where a liquid bulk is present, the accuracy in the present case is also related to the accuracy of the Leveque solution in describing the physical mass transfer process for laminar flow conditions.

6.2 Influence of Graetz number on the applicability of the approximate solutions

6.2.1 1,1 Irreversible reaction, laminar flow; $D_A = D_B = 1x\ 10^{-9}\ m^2\ s^{-1}$; $\nu_B = 1$

The Graetz number ($<v>d^2/D_AL$) is simply the ratio of the penetration time of the solute gas to reach the axis of the hollow fiber (from the gas-liquid interface), to the average residence time of the liquid in the fiber. The influence of Gz on the accuracy of the approximate solution was studied using the parameters shown in Table 1. For low Graetz numbers, there is a significant concentration of A ($<C_{m,L}>$) in the liquid "bulk" during physical absorption and in case of a moderate to fast reaction, the concentration of B at the axis of the hollow fiber is less than that of the inlet concentration due to depletion. The consequences due to this are as follows:

1. Due to a significant concentration of A at the centerline incase of physical absorption, the driving force for mass transfer is not necessarily the same for physical and reactive absorption, which makes the traditional definition of the enhancement factor rather trivial. However, the traditional approximate solution can be corrected to some extent using Eq (30) to have a proper basis for the comparison with the exact numerical solutions.

2. The Hatta number and infinite enhancement factor are based on the concentration of B at the liquid inlet ($C_{B,0}$) assuming that the concentration of B at the axis of the hollow fiber is the same as that of $C_{B,0}$. Due to depletion of B, the actual "bulk" concentration of B that should be used in Ha* and E_∞^* is less than $C_{B,0}$.

Table (1) *Numerical values of the parameters used in the simulations*

Parameters	Numerical Value
L	0.4 m
d	600 x 10^{-6} m
<v>	0.01-2.0 m s^{-1}
$C_{A,g}$	41.6 mol m^{-3}
$C_{B,0}$	10 - 10^4 mol m^{-3}
$k_{1,1}$	10^{-3} - 10^3 m^3 mol^{-1} s^{-1}
m	1.0

For Gz > 100, the values of $E_{app,I}$ were within ± 9.1% of the values predicted numerically. As can be expected, the error in the prediction of the approximate solution was relatively high at low Graetz numbers (Gz < 100) and the error increased rather exponentially for Gz < 20 (see Figure 4 in which the absolute errors as function of the Gz number are given for a few simulation conditions as examples). This is mostly due to a significant depletion of the concentration of B at the axis of the fiber. The numerical simulations indicated that the minimum value of Gz at which the concentration of the reactant, B is unaltered at the axis and end of the fiber was approximately 120.

$$Gz > 120 \tag{32}$$

On substituting the above number in the Leveque's equation,

$$Sh_L^* = 1.62\,(Gz)^{1/3} > \cong 8 \tag{33}$$

The above criterion on the applicability of the approximation (based on the Sherwood number) is in line with the criterion proposed by van Elk (2001) for gas absorption in a falling liquid film, a similar physical situation where a well defined liquid bulk is absent. Though the approximate solution is applicable for Gz greater than 120, it could nevertheless be used for values much lower than this without a significant loss of accuracy. As an example, for the range of process conditions mentioned in Table 1, the maximum error in the prediction of the $E_{app,I}$ for Gz equal to 45 was 21%.

For certain asymptotic conditions, the error in the prediction of the approximate solution can be reduced significantly by also making simple corrections to account for the depletion in the concentration of B at the axis of the fiber. For a condition in which the absorption rate of A is limited by the diffusion of the reactant species ($2<Ha^*> > E_\infty^*$), the depletion of B can be approximately related to the saturation of A (in the absence of a chemical reaction). Especially at very low Graetz numbers and for instantaneous reactions, the average "bulk" concentration of A, $<C_{m,L}>$ in the liquid can be related to the average reduced "bulk" concentration of B, $<C_B>$.

$$\frac{<C_B>}{C_{B,0}} \cong \frac{C_{A,I} - <C_{m,L}>}{C_{A,I}} \tag{34}$$

$<C_{m,L}>$ can be calculated using Eq (12). The adapted average "bulk" concentration, $<C_B>$ can now be used instead of $C_{B,0}$ to calculate Ha^* and E_∞^* and hence the enhancement factor. As an example, Figure 4 shows a few cases in which the correction for the "bulk" concentration of B has been implemented in the approximate solution for the instantaneous absorption regime ($2<Ha^*> > E_\infty^*$). As the k_L increases with increase in Graetz number, the Ha* decreases and the absorption regime gradually shifts away from the instantaneous regime. Consequently, the correction for the "bulk" concentration of B is found to be less suitable for high Gz numbers.

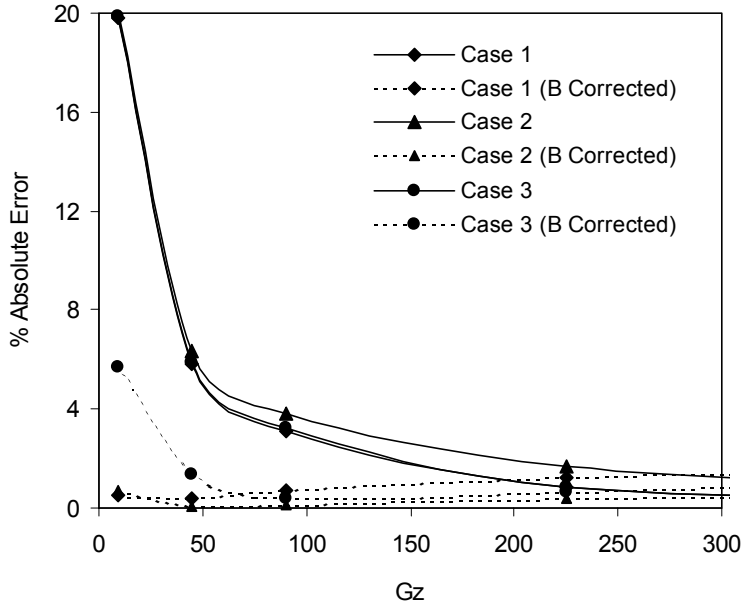

Figure (4) *The influence of the correction of "bulk" concentration of B using Eq (34) for the Instantaneous absorption regime (*$2<Ha^*> > E_\infty^*$*). Simulation conditions: L = 0.4 m; d = 600 x* 10^{-6} *m;* $<v>$ *= 0.01-1.5 m* s^{-1}*;* $C_{A,0}$ *= 41.6 mol* m^{-3}*;* $D_A = D_B = 1 \times 10^{-9}$ m^2 s^{-1}*; m = 1.0;* v_B *= 1. Case 1:* $C_{B,0}$ *= 1000 mol* m^{-3}*;* $k_{1,1}$ *= 10* m^3 mol^{-1} s^{-1}*. Case 2:* $C_{B,0}$ *= 1000 mol* m^{-3}*;* $k_{1,1}$ *= 100* m^3 mol^{-1} s^{-1}*. Case 3:* $C_{B,0}$ *= 100 mol* m^{-3}*;* $k_{1,1}$ *= 1* m^3 mol^{-1} s^{-1}*.*

6.2.2 1,1 Irreversible reaction, $D_A/D_B \neq 1$*;* $v_B = 1$

In the absence of a velocity gradient in the mass transfer zone, DeCoursey (1974) has shown that the approximate solution can be used for values of (D_B/D_A) other than one, with a maximum error of 9%. Though the present case is not identical to the above-described physical situation, the DeCoursey solution can still be conveniently used to predict the enhancement factor. Figure 5 shows the dimensionless concentration of B at the axis (r = 0) and end (z = L) of the fiber, for different values of D_B/D_A. Based on this information, the following empirical criterion provides the minimum value of the Graetz number above which the concentration of reactant B is undisturbed at the axis of the hollow fiber and the approximate solution can be used to predict the enhancement factor accurately.

$$Gz > 120\left(\frac{D_B}{D_A}\right) \qquad (35)$$

Expressing the criterion in terms of the Sherwood number,

$$Sh_L^* = \frac{k_L R}{D_A} > 4\left(\frac{D_B}{D_A}\right)^{1/3} \qquad (36)$$

In contrast to the above criterion, for the absorption of a gas in a falling liquid film, van Elk (2001) proposed a ½ power dependence of the Sherwood number on the ratio of diffusivities. For the instantaneous absorption regime ($2<Ha^*> > E_\infty^*$), Eq (34) can be used to account for the depletion in the "bulk" concentration of B, to reduce the error in the prediction of E by the adapted approximate solution.

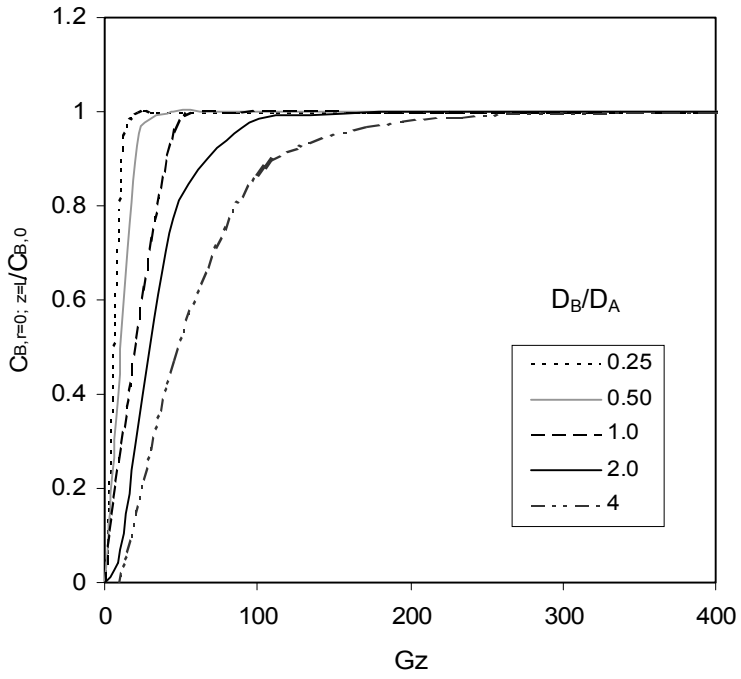

Figure (5) *Dimensionless concentration of B at the axis of the hollow fiber and z equal to L. Simulation conditions: L = 0.4 m; d = 600 x 10^{-6} m; <v> = 0.01-1.5 m s^{-1}; $C_{A,0}$ = 41.6 mol m^{-3}; $C_{B,0}$ = 1000 mol m^{-3}; $k_{1,1}$ = 1.0 m^3 mol^{-1} s^{-1}; D_A = 1 x 10^{-9} m^2 s^{-1}; m = 1.0; v_B = 1.0.*

While the present discussion is restricted to an irreversible second order reaction, the approximate solutions (DeCoursey solution, as in the present case) can be extended to other situations (like reversible reactions) as dealt with in detail by Hogendoorn et al. (1997) for systems with a well defined liquid bulk. However, necessary criteria (like Eq 32 & 35) to determine the range of applicability of the approximate solutions under various conditions need to be developed.

6.3 Comparison of the Experimental Enhancement Factor (E_{exp}) with the Prediction of DeCoursey's Approximation Solution ($E_{app,I}$).

Based on the conclusions drawn from the discussions in the previous sections, the following experimental conditions were used in the single fiber membrane contactor to

satisfy the assumptions/criteria (for applicability) used in the adaptation of the traditional approximate solution for the estimation of the enhancement factor in a hollow fiber.

1. Constant gas-liquid interface conditions (semi-batch mode; see also section 2.0).
2. The range of the liquid velocity was chosen such that the criterion given by Eq (35) was satisfied.

However, some experiments were also carried out relaxing the above criteria to verify its effect on the error between the $E_{app,l}$, predicted by the adapted approximate solutions and E_{exp}, the experimental enhancement factor. As mentioned earlier, absorption of CO_2 in an aqueous NaOH solution was used as a model reactive system. The physico-chemical data used for the calculation of the approximate enhancement factor were obtained from the references given in Table 2. The D_B (mean ion diffusivity of NaOH at infinite dilution) was calculated using the Nernst-Hartley equation. The influence of ionic strength of the aqueous NaOH solution on the reaction rate constant, $k_{1,1}$ was accounted.

Table (2) *Literature source of the physico-chemical data used in the calculation of Eapp,l.*

Property	System	Literature Source
D_A, m	CO_2 – water	Versteeg & van Swaaij (1988)
D_A, m	N_2O – water	Versteeg & van Swaaij (1988)
m	CO_2 – aq. NaOH	Weisenberger & Schumpe (1996)
D_A	CO_2 – aq. NaOH	Hikita et al. (1976)
D_B	CO_2 – aq. NaOH	Hovarth (1985)
$k_{1,1}$	CO_2 – aq. NaOH	Pohorecki & Moniuk (1988)

Table (3) *Experimental conditions for the data provided in the parity plot; semi-batch mode of operation*

Exp. Set No	L (m)	$C_{NaOH,0}$ (mol m^{-3})	$C_{CO2,g}$ (mol m^{-3})	No. of Exp.	Gz range	Avg. error* (Max error*) %	120 x $(D_B/D_A)^{\#}$	Avg. error** (Max error**) %
1	0.160	240	43.1	7	79 - 702	6.3 (8.9)	205	5.4 (7.3)
2	0.380	240	43.2	6	98 - 1080	7.3 (7.9)	205	4.3 (5.6)
3	0.165	500	43.1	7	40 - 473	7.4 (10.7)	212	5.9 (10.7)
4	0.165	950	43.1	7	23 - 386	9.1 (16.0)	226	6.2 (9.9)

Note: The % error is defined as $(E_{app,l} - E_{exp}) \times 100 / E_{app,l}$; *The maximum and average errors are based on $E_{app,l}$ calculated using $C_{B,0}$ or $C_{NaOH,0}$; ** The errors are based on $E_{app,l}$ calculated using $\langle C_B \rangle$ as per Eq (34) instead of $C_{B,0}$; # Criterion for the applicability of approximate solution - Eq (35).

In the semi-batch experiments, the physical absorption flux of N_2O/CO_2 in water was measured at 295 K and these experimental values were found to be within $\pm$ 4 % of the values predicted by the numerical model. This indirectly gives an indication of the accuracy of the experimental measurements (or setup). Some of the experimental results have already been reported in Kumar et al. (2002). Similarly, the reactive absorption of CO_2 in aqueous NaOH solutions was measured for four different experimental conditions as described in Table 3. For all the experimental data sets, the absorption temperature was

maintained at 295±0.2 K and the experimental Graetz number range is given in Table 3. Except for the experimental data set 3, the error in the prediction of $E_{app,I}$ by the present approximate solution was somewhat higher at low Graetz numbers (see Table 3) and it falls in line with the error behavior of the approximate solution as compared to the numerical model (as discussed in section 6.2). It should be noted that the reproducibility of the experimental data was within ± 5%. Due to the experimental conditions used for the semi-batch experiments, the numerical values of the Hatta number and infinite enhancement factor were such that the absorption was in the instantaneous regime (2<Ha*> E_∞*). Therefore, the correction for the depletion in the "bulk" concentration of B as given by Eq (34) was used. Figure 6 shows the parity plot of the values of experimental and approximate enhancement factor ($E_{app,I}$) for the four sets of experiments. Here the corrected or reduced "bulk" concentration of B was used in calculating, $E_{app,I}$. The $E_{app,I}$ predicted by the approximate solution was within ± 10.7% (maximum error) of the experimental values of enhancement factor and the average error was 5.4% (see also Table 4).

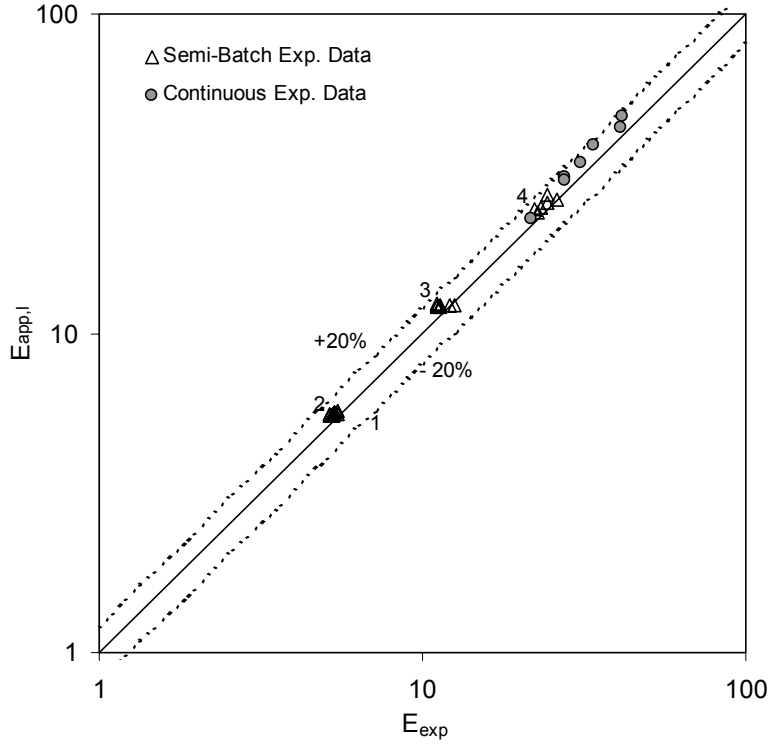

Figure (6) *Parity plot for the experimental and approximate enhancement factor for the absorption of CO_2 in aqueous NaOH solutions. Refer to Table 3 & 4 for the experimental conditions. The "bulk" concentration of B, used in $E_{app,I}$ has been corrected for the depletion as per Eq (34), for Gz <120 (D_B/D_A).*

A limited number of experiments was also conducted in the continuous mode for which a gas stream (CO_2 in N_2) flowed outside the hollow fiber in the single fiber membrane contactor. These experiments were performed with the objective to obtain experimental data in regimes other than the instantaneous absorption regime for which experimental data were obtained in the semi-batch mode of operation. The experimental conditions are summarised

in Table 4. Based on the conditions in the membrane contactor, the absorption is expected to be in the fast regime ($2<Ha^*< E_\infty^*$). Since the concentration of CO_2 in the gas phase changes (though not significantly; < 6% of $C_{CO2,g,in}$) along the length of the hollow fiber, a log mean concentration ($C_{CO2,g,LM}$) based on the inlet ($C_{CO2,g,in}$) and outlet gas stream concentration ($C_{CO2,g,out}$) was used in calculating the approximate infinite enhancement factor (E_∞^*). As $C_{CO2,g,out}$ is unknown, it was estimated (along with $E_{app,I}$) iteratively as follows:

1. To start with, $C_{CO2,g,out}$ was guessed and E_∞^* was calculated based on the $C_{CO2,g,LM}$.
2. The average CO_2 absorption flux was calculated using Eq (10), with the enhancement factor calculated using the adapted DeCoursey solution (Eq 30).
3. A mass balance over the gas phase provided a new value of $C_{CO2,g,out}$.

The above steps were repeated till $C_{CO2,g,out}$ converged. The values of the predicted enhancement factor along with the experimental values are also shown in the parity plot of Figure 6. The maximum and average errors were 13.6% and 9.5% respectively. The somewhat larger error (inspite of the fact that the Graetz numbers studied are higher than that of the semi-batch measurements) for the continous mode was expected because the k_L calculated from Leveque's solution assumes a constant gas-liquid interface concentration of A which is not true for the continuous experiments.

Table (4) *Experimental conditions for the data provided in the parity plot; continuous mode of operation.*

Operating Conditions	Numerical value
P	103 kPa
T	295 K
L	0.33 m
d	6.0×10^{-4} m
$C_{NaOH,0}$	100 mol m^{-3}
$C_{CO2,g,in}$	2.58 kPa
Gz	173 – 1336

Influence of Mass Transfer Resistance due to the Microporous Membrane

In the calculation of the experimental enhancement factor (E_{exp}) from the absorption flux measurements, the mass transfer resistances due to the gas phase ($1/k_g$) and microporous membrane ($1/k_m$) were neglected. Since pure CO_2 was used in the semi-batch measurements, the gas phase resistance can be neglected. Similarly, the gas phase resistance for the continuous measurements was minimised as described in Kumar et al. (2002). Depending upon the liquid side mass transfer resistance ($1/mk_LE$), the membrane resistance ($1/k_m$) can become significant. The pore diameter (d_p) of the polypropylene membrane used in the present work was relatively small (0.2 μm) and also the gas pressure was low. The membrane resistance was estimated for the continuous experiments. For the semi-batch experiments using pure gases, the resistance will be lower because, in that case,

a concentration gradient across the microporous membrane can only be present if a pressure gradient is present. A pressure gradient (and the resulting convective flow) causes much larger CO_2 fluxes (than those measured in the semi-batch absorption experiments), and therefore, the possibility of a membrane resistance is unlikely in case pure gases are used for absorption.

The k_m for the continuous experiments (binary diffusion) was estimated simply using Eq (4). The bulk diffusion coefficient was calculated from the kinetic theory of gases (Reid et al., 1987) and the Knudsen diffusion coefficient according to Eq (6). The overall mass transfer coefficient was calculated from the experimental absorption flux as given below.

$$K_{ov,exp} = \frac{< J >_{exp}}{m\, C_{CO_2,g}}$$

The estimated value of k_m was 4.62 x 10^{-2} m s^{-1} and the maximum value of $K_{ov,exp}$ for the continuous experiments was 1.07 x 10^{-3} m s^{-1}. Therefore the maximum contribution of the membrane resistance to the overall resistance is only 2.3 percent. Though the membrane does not offer any significant resistance for the present experiments, for a large enhancement in absorption rate due to chemical reaction, the mass transfer resistance due to the membrane can become significant and has to be taken into account.

7.0 Conclusions

In this contribution, it was shown that approximate solutions for the enhancement factor, developed originally for mass transfer with chemical reaction in the presence of a well defined liquid bulk can be adapted to situations where a liquid bulk may be absent and in addition a velocity gradient is present in the mass transfer zone. This was demonstrated using DeCoursey's explicit approximate solution for an irreversible second order reaction as an example. For long gas-liquid contact time in a hollow fiber, the driving force for the gas phase species absorbed was found not to be identical for physical and reactive absorption. Therefore, an overall enhancement factor ($E_{app,l}$) was introduced for a proper basis of comparison with the exact numerical results.

The exact numerical results of the mass transfer model for a membrane fiber indicate that the approximate solution fails for very low values of the Graetz number due to a significant depletion of the liquid phase reactant at the axis of the hollow fiber (analogous to liquid bulk in traditional mass transfer models). For a second order irreversible reaction, the use of approximate solutions is limited to Gz > 120 (D_B/D_A). Within the range of applicability, the approximate solutions were found to be very accurate in comparison to the exact numerical results as well as experimentally measured values of the enhancement factor. As shown with the experimental as well as numerical results, the approximate solution can be used for Graetz numbers lower than the above-mentioned criterion without a significant loss of accuracy. However, the error increases rather exponentially at very low values of the Graetz number.

The above prescribed lower limit for the Graetz number ($<v>d^2/DL$) is a serious limitation in terms of the applicability of the approximate solution in the design of membrane gas-liquid contactors that use very small diameter hollow fibers (usually of the order of few

hundred microns). The liquid velocity through these small diameter fibers is usually kept low to avoid a large pressure drop across the modules and therefore the operational Graetz numbers are usually lower than the prescribed criterion.

The absorption flux and enhancement factor measured in the single fiber membrane contactor, as described in this work and Kumar et al. (2002) are very well predicted by the numerical model as well as the adapted DeCoursey's approximate solution. Since the hydrodynamics of the liquid flowing inside the hollow fiber of a single fiber membrane contactor is well defined (like in a laminar jet or wetted wall column), it can be used also as a model gas-liquid contactor. The approximate solutions for the enhancement factor can then be conveniently used to interpret the experimental absorption data to estimate the physico-chemical or kinetic parameters for a reactive gas-liquid system. Conversely, if the above parameters are known from independent measurements, their accuracy can be independently verified by comparing the absorption fluxes predicted using the approximate solutions and the experimental absorption data, as was done in this work as well as that of Kumar et al. (2002).

Acknowledgement

This research is part of the research programme carried out within the Centre for Separation Technology, a cooperation between the University of Twente and TNO, the Netherlands Organisation for Applied Scientific Research. We acknowledge Wim Leppink for the construction of experimental setup.

8.0 Nomenclature

b	Constant in Eq (3), dimensionless
c	Constant in Eq (3), dimensionless
C	Concentration, mol m^{-3}
$C_{m,z}$	Mixed cup concentration at z, mol m^{-3}
$<C_{m,L}>$	Length averaged mixed cup concentration of A, mol m^{-3}
d	Inside diameter of the hollow fiber, m
d_p	Pore diameter, m
D	Diffusion coefficient, m^2 s^{-1}
E	Enhancement factor, dimensionless
E_∞	Asymptotic enhancement factor, dimensionless
Gz	Graetz number, $<v>d^2/DL$, dimensionless
Ha	Hatta number, dimensionless
J	Local absorption flux, mol m^{-2} s^{-1}
<J>	Length averaged absorption flux, mol m^{-2} s^{-1}
K_0	Constant in Eq (6), m
K_{ov}	Overall mass transfer coefficient, m s^{-1}
k_{ext}	External mass transfer coefficient, m s^{-1}
k	Mass transfer coefficient, m s^{-1}
$k_{1,1}$	Reaction rate constant, m^3 mol^{-1} s^{-1}
L	Length of the hollow fiber, m
M_w	Molecular weight, dimensionless
m	Physical solubility, $(C_{A,l}/C_{A,g})_{eq}$, dimensionless
r	Distance in radial direction from the axis of hollow fiber, m
P	Contactor pressure, kPa
R	Radius of the hollow fiber, m
Re	Reynolds number, $(d<v>\rho/\mu)$, dimensionless
R_i	Reaction rate, mol m^{-3} s^{-1}
Sc	Schmidt number, $(\mu/\rho D)$, dimensionless
Sh	Sherwood number (kd/D), dimensionless
t	time, s
T	Temperature, K
<v>	Average liquid velocity, m s^{-1}
v_z	Liquid velocity in the axial direction, m s^{-1}
z	Distance in the axial direction from the liquid inlet, m

Greek

δ	Thickness of the membrane, m
ε	Porosity, dimensionless
τ	Tortousity, dimensionless
γ	Stoichiometric coefficient, dimensionless

Superscript

*	Without well defined liquid bulk

Subscript

A	Gas phase species
app	approximation
bulk	Bulk phase conditions
Chem	Chemical absorption
e	effective
g	gas phase
I	Gas-liquid interface
i	chemical species
in	inlet gas stream
K	Knudsen
l	laminar
L	Liquid
LM	Log mean
m	membrane
num	Numerical
out	Outlet gas stream
Phys	Physical absorption
Plug	Plug flow of liquid
z	axial coordinate
0	Liquid inlet conditions

9.0 References

Guijt, C.M., Racz, I.G., Reith, T., & de Haan, A.B., (2000). Determination of membrane properties for use in the modelling of a membrane distillation module. *Desalination*, **132**, 255-261.

DeCoursey, W.J. (1974). Absorption with chemical reaction: development of a new relation for the Danckwerts model. *Chemical Engineering Science*, **29**, 1867-1872.

DeCoursey, W.J. (1982). Enhancement factor for gas absorption with reversible chemical reaction. *Chemical Engineering Science*, **37**, 1483-1489.

DeCoursey, W.J. & Thring, R.W. (1989). Effects of unequal diffusivities on enhancement factors for reversible and irreversible reaction. *Chemical Engineering Science*, **44(8)**, 1715-1721.

Gabelman, A., & Hwang, S. (1999). Hollow fiber membrane contactors. *Journal of Membrane Science*, **159**, 61-106.

Hikita, H., & Asai, S. (1964). Gas absorption with (m,n)-th order irreversible chemical reaction. *International Journal of Chemical Engineering*, **4**, 332-340.

Hikita, H., Asai, S., & Takatsuka, T. (1976). Absorption of carbon dioxide into aqueous sodium hydroxide and sodium carbonate-bicarbonate solutions. *Chemical Engineering Journal*, **11**, 131-141.

Hogendoorn, J.A., Vas Bhat, R.D., Kuipers, J.A.M., van Swaaij, W.P.M., & Versteeg, G.F. (1997). Approximation for the enhancement factor applicable to reversible reactions of finite rate in chemically loaded solutions. *Chemical Engineering Science*, **52(24)**, 4547-4559.

Hovarth, A.L. (1985). *Handbook of aqueous electrolytic solutions: Physical properties, estimation and correlation methods*. New York: John Wiley & Sons.

Kohl, A. L., & Nielsen, R.B. (1997). *Gas Purification*; 5th ed. Houston: Gulf Publishing Company.

Kreulen, H., Smolders, C.A., Versteeg, G.F., & van Swaaij, W.P.M. (1993a). Microporous hollow fiber membrane modules as gas-liquid contactors. Part 2. Mass transfer with chemical reaction. *Journal of Membrane Science*, **78**, 217-238.

Kreulen, H., Smolders, C.A., Versteeg, G.F., & van Swaaij, W.P.M. (1993b). Microporous hollow fiber membrane modules as gas-liquid contactors. Part 1. Physical mass transfer processes. *Journal of Membrane Science*, **78**, 197-216.

Kumar, P.S., Hogendoorn, J.A., Feron, P.H.M., & Versteeg, G.F. (2002). New Absorption Liquids for the Removal of CO_2 from Dilute Gas Streams using Membrane Contactors. *Chemical Engineering Science*, In press. (Chapter 5 of this thesis)

Leveque, J. (1928). Les lois de la transmission de chaleur par convection, Annls. Mines, Paris (Series 12), 201.

Li, K., & Teo, W.K. (1998). Use of permeation and absorption methods for CO_2 removal in hollow fiber membrane modules. *Separation and Purification Technology*, **13**, 79-88.

Mulder, M. (1996). *Basic Principles of Membrane Technology*. Kluwer Academic: Dordrecht, The Netherlands.

Nii, S., & Takeuchi, H. (1994). Removal of CO_2 and/or SO_2 from gas streams by a membrane absorption method. *Gas Separation & Purification*, **8(2)**, 107-114.

Nii, S., Takeuchi, H., & Takahashi, K. (1992). Removal of CO_2 by gas absorption across a polymeric membrane. *Journal of Chemical Engineering of Japan*, **25(1)**, 67-72.

Onda, K., Sada, E., Kobayashi, T., & Fujine, M. (1970). Gas absorption accompanied by complex chemical reaction – I. Reversible chemical reactions. *Chemical Engineering Science*, **25**, 753-760.

Pohorecki, R., & Moniuk, W. (1988). Kinetics of the reaction between carbon dioxide and hydroxyl ion in aqueous electrolyte solutions. *Chemical Engineering Science*, **43**, 1677-1684.

Qi, Z., & Cussler, E.L. (1985). Microporous hollow fibers for gas absorption II. Mass transfer across the membrane. *Journal of Membrane Science*, **23**, 333-345.

Reid, R.C., Prausnitz, J.M., & Poling, B.E. (1987). *The properties of gases & liquids*. Singapore: McGraw-Hill.

Secor, R.M., & Beutler, J.A. (1967). Penetration theory for diffusion accompanied by a reversible chemical reaction with generalised kinetics. *AIChE Journal*, **13**, 365-373.

van Krevelen, D.W., & Hoftijzer, P.J. (1948). Kinetics of gas-liquid reactions – I. General theory. *Rec. Trav. Chim.*, **67**, 563-586.

Versteeg, G.F., & van Swaaij, W.P.M. (1988). Solubility and diffusivity of acid gases (CO_2, N_2O) in aqueous alkanolamine solutions, *Journal of Chemical & Engineering Data*, **33**, 29-34.

Versteeg, G.F., Kuipers, J.A.M., van Beckum, F.P.M., & van Swaaij, W.P.M. (1989). Mass transfer with complex reversible chemical reactions - I. Single reversible chemical reaction. *Chemical Engineering Science*, **44**, 2295-2310.

Weisenberger, S., & Schumpe, A. (1996). Estimation of gas solubilities in salt solutions at temperatures from 273K to 363K. *AIChE Journal,* **42**, 298-300.

Westerterp, K.R., van Swaaij, W.P.M., & Beenackers, A.A.C.M. (1984). *Chemical reactor design and operation*. New York: Wiley and Sons.

Yeramian, A.A., Gottifredi, J.C. & Ronco, J.J. (1970). Mass transfer with homogenous second order irreversible reaction. A note on an explicit expression for the reaction factor. *Chemical Engineering Science*, **25**, 1622-1624.

van Elk, E.P. (2001). Gas-liquid reactions: Influence of liquid bulk and mass transfer on process performance. Ph.D. Thesis, University of Twente, The Netherlands.

Appendix

Thermal Stability and Degradation Products of Amino Acids

1.0 Thermal Stability of Amino acids

At this moment, interest on aqueous alkaline amino acid salt solutions is essentially directed towards CO_2 removal for small-scale, offshore applications such as ambient air control in submarines and spacecrafts (Hook, 1997). At this scale of operation, thermal regeneration of the CO_2 loaded aqueous amino acid salt solutions is mostly carried out in electrically heated strippers, as they are the most convenient ones to operate and maintain. However, these are high (heat) flux heat transfer devices in which the surface temperature of the heating element is much higher than the bulk liquid temperature. Under these conditions, the thermal stability of the amino acids used becomes a critical issue as the usual degradation products of amino acids like ammonia and nitriles are very toxic. Erga et al. (1995) and Feron (1998) have studied the use of amino acid salts in the CO_2 removal from gas streams in pilot scale absorber-desorber setups. In both studies, scaling was observed in the stripper and traces of ammonia and olefins were observed in the CO_2 obtained from stripper. This indicates the cracking of amino acid molecules due to some localised heating in the stripper or the heat exchanger which was used to raise the temperature of the liquid from the absorber to the stripper temperature. In case of the experiments at TNO, electrical heating was used in the stripper as well as in the heat exchanger. Erga et al. (1995) used direct steam contacting in the stripper and an electrically heated heat exchanger to raise the temperature of the liquid to the stripper temperature.

Table (1) *Thermal Degradation (Pyrolysis) Products of amino acid at 500 °C, in % of pyrolysate (Simmonds et al., 1974).*

Degradation Product	Glycine (H_2N-CH_2-CO_2H)	Alanine (H_2N-CH_2-CH_2-CO_2H)	Leucine $(CH_3)_2CHCH_2CH(NH_2)CO_2H$	Valine $(CH_3)_2CHCH(NH_2)CO_2H$
CO_2	39.8	43.2	30.8	27.9
NH_3	20.5	13.5	11.6	12.5
H_2O	22.7	17.0	8.8	5.3
Nitriles	14.6	3.7	17.7	13.7
Aliphatic amines	0.5	17.3	21.0	19.3
Aliphatic Amides	0.8	0.4	-	-
Aliphatic Aldehydes	-	< 0.1	< 0.1	1.9
N- Alkyl Aldimine	-	3.4	7.8	13.8
CH_4	0.6	0.8	0.4	0.2
Olefins	< 0.1	0.5	1.8	1.7
Aldehydes & Ketones	-	< 0.1	< 0.1	0.2-0.3

Considerable information is available in the literature on the thermal stability and degradation products of the biological amino acids at 500 °C (Simmonds et al., 1972; Ratcliff et al., 1974; Douda and Basiuk, 2000). However, there is not much information in literature on the temperature range in which degradation of the amino acid begins and also on the degradation products of synthetic amino acids like taurine. Table 1 shows the typical composition of the degradation products of some simple amino acids. It can be found that

the principle reaction products are CO_2, water, NH_3, aliphatic amines and nitriles compounds. The detailed discussion on the reaction mechanism can be obtained elsewhere (Simmonds et al., 1972; Ratcliff et al., 1974).

In the present work, differential scanning calorimetry (DSC) was performed to study the temperature at which decomposition of taurine begins. The analysis was done in a Mettler DSC12E calorimeter and the taurine samples were heated from room temperature (20 °C) to 400 °C at a rate of 10 °C/min. Figure 1 (presented at the end of the appendix) shows the DSC results of Taurine, for the experiments carried under helium and air atmosphere. The first endothermic peak observed at 332 °C is due to the decomposition of the amino acid molecule. This is typical for many other organic molecules as most of them do no have a melting point and usually decompose upon heating. Table 2 indicates the temperature range of decomposition for some amino acids which show promise in acid gas treating processes. The temperatures given in the bracket are the endothermic peak temperatures as shown in Figure 1. Although the thermal stability of taurine is better than that of monoamino monocarboxylic acids, its vulnerability to degradation in electric heated heat transfer equipments is still present.

Table (2) *Thermal decomposition temperature range (based on Differential Scanning Calorimetry) of some important amino acids.*

Amino acid	Temperature range (°C)
Glycine	215-220 (260)
Alanine	190-195 (265)
Taurine	320-325 (332)
Proline	200-205 (244)

2.0 Degradation Products of Taurine

To obtain qualitative information on the thermal decomposition of taurine, decomposition products of taurine were analysed using Mass Spectroscopy (Balzers Omnistar) and Gas Chromatography (Varian 3700, Column: HayeSep R, HayeSep C). The experimental procedure used is as follows: the taurine sample was heated in a temperature programmable furnace, in an inert atmosphere of Helium. The degradation products were analysed directly in a mass spectrometer, similarly to Simmonds et al. (1972). The sample was heated to 250 °C (at 10 °C/min) and subsequently, the temperature was raised at a rate of 2 °C/min upto 400 °C. The masses less than the molecular mass of taurine (125.15) were monitored and recorded as a function of sample temperature. From the mass spectra, the degradation of the amino acid could be clearly observed between 325 and 340 °C. This is in agreement with the results of the DSC measurements. The identification of the degradation products was done by comparison of the captured mass spectra with published spectra (RSC, 1983). Independent chromatographic analyses were also carried out with a gas chromatograph (GC) to identify the degradation products. The taurine sample was heated in a temperature programmable tubular furnace, with helium flowing over the sample. At temperatures above 320 °C, the gas stream from the furnace containing the helium along

with the degradation products was collected in a large leak proof glass syringe. The gaseous content of the syringe was analysed in a GC to identify the degradation products. The identified degradation products along with the possible degradation paths, based on the reaction mechanism proposed by Simmonds et al. (1972) are shown in Figure 2. Apart from the degradation products proposed by the mechanism, a few other secondary degradation products like H_2S and CO_2 could also be found in appreciable amounts.

From the above study, it can be concluded that some of the principle contaminants in the stripped gas, in case of degradation of taurine in the stripper, should be NH_3, SO_2, olefins, H_2S and trace amount of nitriles.

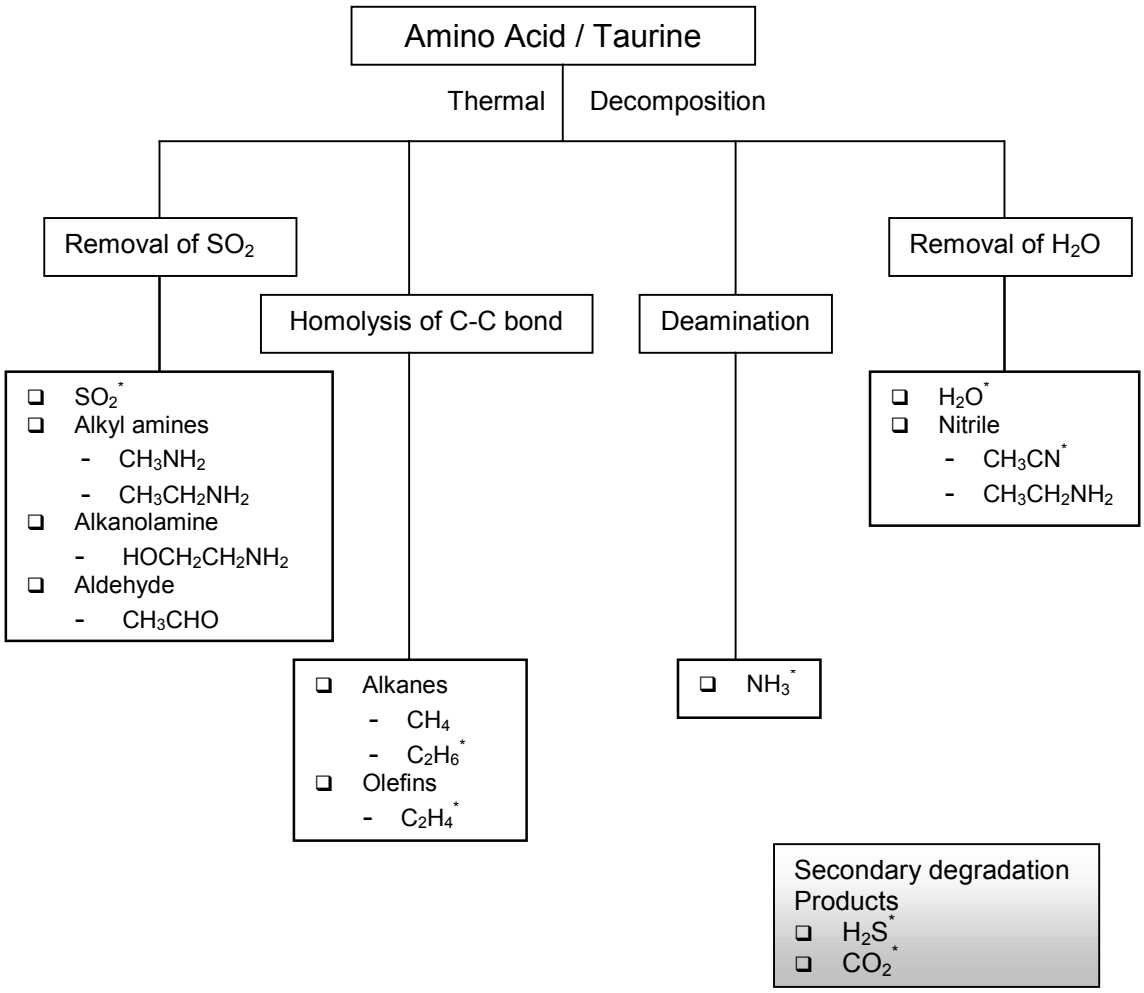

Figure (2) *Proposed thermal decomposition paths of taurine with the decomposition products identified in the present study using Mass Spectroscopy. The * indicates the species identified independently by chromatographic analysis of gaseous products (pyrolysate).*

Acknowledgement

This research is part of the research programme performed within the Centre for Separation Technology (CST), which is a cooperation between the Netherlands Organisation for Applied Scientific Research (TNO) and the University of Twente. The authors would like to acknowledge Dr. K. Seshan (CPM, UT), Drs. F.J. Franqueira Valo (CPM, UT) for the

support in carrying out MS and DSC analysis and Ing. A. Hovestad (OOIP, UT) for GC analysis.

3.0 References

Douda, J., & Basiuk, V.A. (2000). Pyrolysis of amino acids: recovery of starting materials and yields of condensation, *Journal of Analytical & Applied Pyrolysis*, **56(1)**, 113-121.

Eighth Peak Index of Mass Spectra. (1983), Volume 1 Part 1, Third Edition, Nottingham: The Royal Society of Chemistry (RSC).

Erga, O., Juliussen, O., & Lidal, H. (1995). Carbon dioxide recovery by means of aqueous amines, *Energy Conversion & Management*, **36(6-9)**, 387-392.

Feron, P.H.M. (1998). Personal Communications, TNO Environment Energy and Process Innovation, The Netherlands.

Hook, R.J. (1997). An Investigation of some sterically hindered amines as potential carbon dioxide scrubbing compounds. *Industrial & Engineering Chemistry Research,* **36(5)**, 1779-1790.

Ratcliff, Jr., M.A., Medley, E.E., & Simmonds, P.G. (1974). Pyrolysis of amino acids. Mechanistic considerations, *Journal of Organic Chemistry*, **39(11)**, 1481-1490.

Simmonds, P.G., Medley, E.E., Ratcliff Jr., M.A., & Shulman, G.P. (1972). Thermal decomposition of aliphatic monoamino monocarboxylic acids, *Analytical Chemistry*, **44(12)**, 2060-2066.

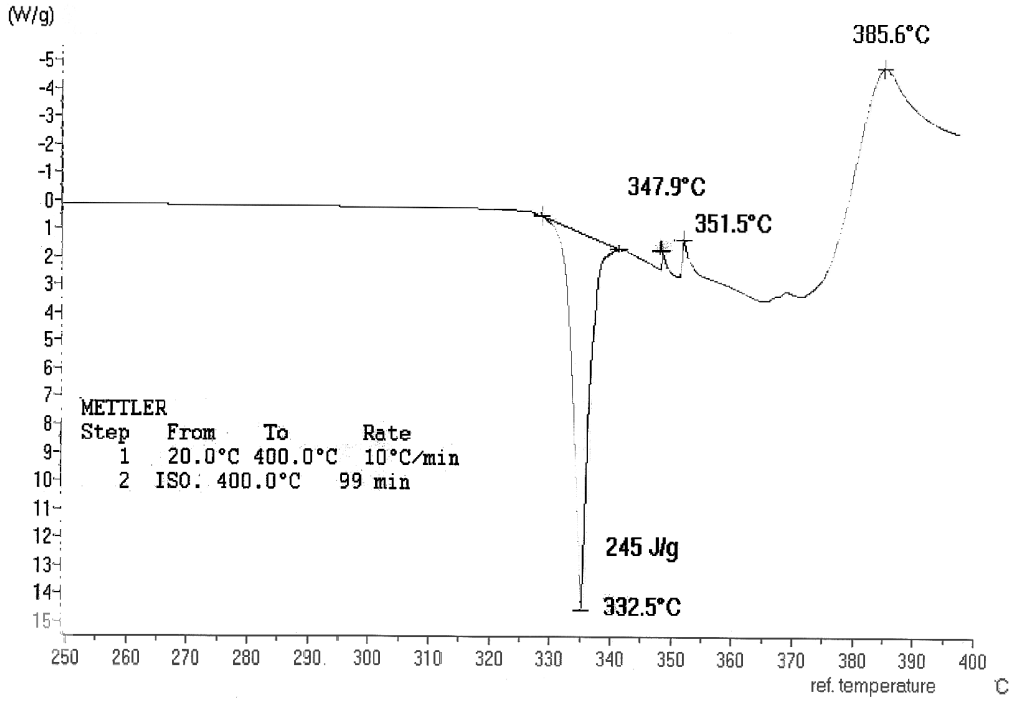

Figure (1a) *Differential Scanning Calorimetery (DSC) results of Taurine in air atmosphere.*

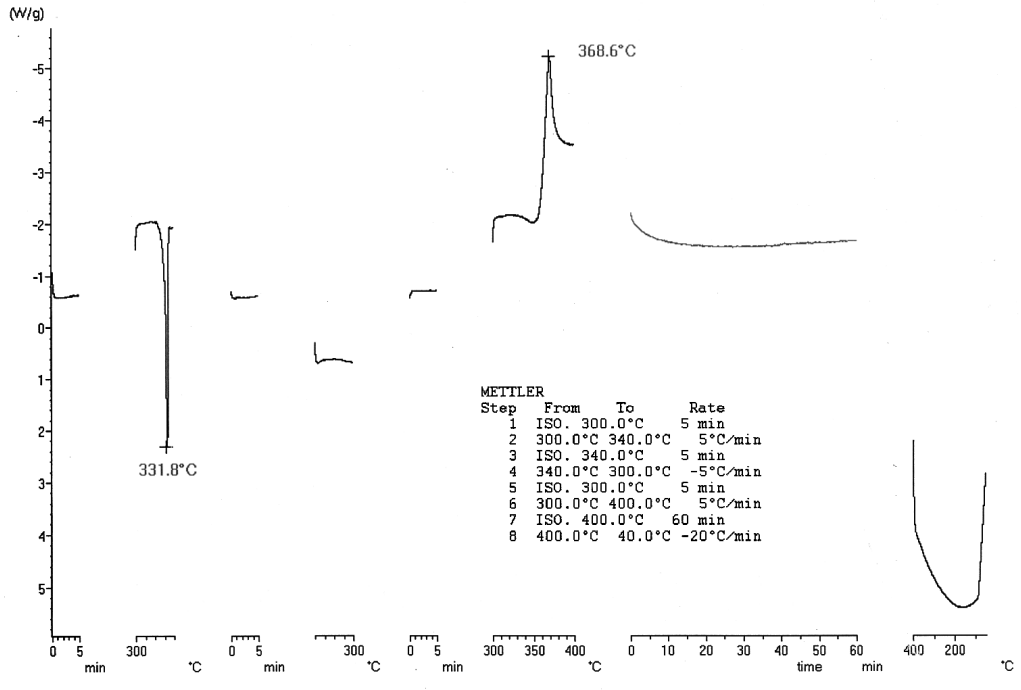

Figure (1b) *Differential Scanning Calorimetery (DSC) results of Taurine in argon atmosphere.*

Summary

Bulk or selective removal of CO_2 from industrial gas streams, by reactive absorption in a liquid has been and is an important operation in the chemical process industry. Lately, the bulk removal of CO_2, especially from effluent gas streams, has received wide attention due to the presumed role of CO_2 in the greenhouse effect, a phenomenon related to global warming. Traditionally CO_2 is removed from gas streams by absorption, either physically or chemically, in column type gas-liquid contactors such as plate and packed columns. This is a very energy intensive operation and therefore is only attractive if the separation results in (economic) value addition of the products, as in natural gas processing. In certain instances, as in the removal of CO_2 from flue gas of a power generation plant, the separation is done for environmental reasons. In such situations, the energy and separation efficiency of the CO_2 removal process may become vital to the economic viability of the entire manufacturing process (Gottlicher & Pruschek, 1997).

Membrane based separation processes such as ultrafiltration, nanofiltration and reverse osmosis are known for its separation as well as energy efficiency. It is widely expected that membrane based separation processes will also play a larger role in the selective removal of CO_2 from industrial gas streams in the near future. Gas separation using dense membranes does not seem to be an economically attractive option at present due to the low CO_2/N_2 selectivity of the commercially available membranes. It should be noted that the partial pressure of CO_2 in gas streams of interest such as flue gas is usually low and this necessitates a large improvement in the selectivity (Gottlicher & Pruschek, 1997).

In a recent development, modules of microporous membranes (usually hollow fibers) are being used as gas-liquid contactors in absorption processes. In this hybrid process (known as membrane gas absorption), the separation selectivity (even at low driving force of the gas that is absorbed) of the traditional absorption process is combined with the flexibility, modularity and compactness of the devices used in the membrane based separation processes. In the development of membrane gas absorption processes, the strategy that has been widely followed in the past is to use the traditional absorption liquids that have proven to be efficient in a conventional contactor, in combination with the cheapest and commercially available microporous membranes. There is a wealth of information on the physico-chemical properties of these liquids in literature, which is required among others for the design of the membrane gas absorption (MGA) processes. The important prerequisite for the success of the membrane gas absorption process is that the absorption liquid should not wet the pores of the membrane under all operating conditions, as the wetted membranes significantly raises the overall mass transfer resistance of the separation process. This was successfully realised in the development of MGA processes for the removal of gases such as SO_2 and NH_3 in a short span of time. In the bulk or selective removal of CO_2, aqueous

alkanolamine solutions are the widely used absorption liquids in the traditional absorption processes. However, they were found to wet the commercially attractive and available polyolefin microporous membranes (Kreulen, 1993).

The present project was initiated with the objective to develop stable membrane gas-liquid contactors for the removal of CO_2 from gas streams, especially flue gas. As mentioned earlier, the stability of the gas-liquid contacting in a membrane contactor depends on the non-wetting characteristics of the microporous membrane and absorption liquid. Among the various possibilities available to overcome wetting that are discussed in the *introduction* of this thesis, it was decided to develop/use reactive absorption liquids other than aqueous alkanolamines in combination with the commercially available microporous polypropylene membranes. TNO Environment Energy and Process Innovation (The Netherlands) has developed and patented dedicated absorption liquids called CORAL (CO_2 Removal Absorption Liquid) based on aqueous alkaline salts (Feron & Jansen, 1998). In the present work, aqueous alkaline salts of amino acids were chosen and used, as they are known (though qualitatively) for their reactive properties similar to that of aqueous alkanolamines. Also, aqueous alkaline salt solutions of amino acids do have a much better resistance to degradation in oxygen bearing gas streams (e.g. flue gas) than aqueous alkanolamine solutions and therefore have potential for use in traditional absorption processes as well. Among the available amino acids, taurine was chosen as model amino acid for detailed investigation because of its high thermal stability. However, the potassium salt of glycine was also investigated to determine some of its physico-chemical properties for comparison with that of taurine. In the removal of CO_2 from gas streams by absorption, the principle resistance to mass transfer usually lies in the liquid phase, which normally flows in the lumen side of the membrane contactor. Therefore, one of the primary aims of the project was to investigate the gas-liquid mass transfer process accompanied by chemical reaction that occurs during the absorption of CO_2 in aqueous amino acid salt solutions.

In contrast to aqueous alkanolamines, there is a very limited amount of data in literature on the physico-chemical parameters that are required for the design of the MGA process. A large number of physical and transport parameters such as density, viscosity of the amino acid salt solutions and physical solubility and diffusivity of CO_2 in aqueous salt solutions was required in the interpretation of the data from the kinetic experiments. However, there are no published data on these properties. Since CO_2 reacts with amino acid salt solutions, the solubility and diffusivity had to be estimated indirectly. The physical solubility of N_2O in aqueous potassium salt solutions was measured in a stirred reactor for a wide range of amino acid salt concentrations and temperatures. As the solutions contain electrolytes, the solubility data could be described accurately with the model of Schumpe (Schumpe, 1993). Using Schumpe's extensive data on the ion and gas specific constants, the temperature independent ion specific constant was estimated for the anion of the potassium salt of taurine and glycine. This was used to indirectly estimate the physical solubility of CO_2 in aqueous potassium taurate and glycinate solutions using the above-mentioned model.

The diffusion coefficient of N_2O in aqueous salt solutions was determined in a diaphragm cell and the experimental data were related to the viscosity of the salt solution, using a modified Stokes-Einstein relation. Gubbins et al. (1966), based on an extensive experimental study, had concluded that the ratio of diffusion coefficient of a gas in an electrolyte solution to that in water is independent of the gas. Using this conclusion, the diffusion coefficient of CO_2 in the amino acid salt solution was calculated from the experimentally estimated values of N_2O.

The kinetics of the reaction of CO_2 with aqueous amino acid salts was studied in a stirred reactor with a flat gas liquid interface. The experiments at temperatures ranging from 285 to 305 K were carried out with aqueous potassium taurate solutions for concentrations between 100 mol m^{-3} and 4000 mol m^{-3}. For comparison, a limited number of kinetic experiments was also carried out for aqueous potassium glycinate solutions at 298 K. At low amino acid salt concentrations, the reactivity of the amino acid salt solutions based on the apparent rate constants seems to be comparable to that of primary alkanolamines of similar basicity. Contrary to aqueous primary alkanolamines, the partial reaction order was found to change from one at low concentration to approximately 1.5 at salt concentrations as high as 3000 mol m^{-3}, a behavior typically exhibited by aqueous secondary alkanolamines. Such a behavior was distinctly observed for the aqueous potassium salt of taurine as well as glycine for different reaction temperatures. The kinetic data could be well described by a zwitterion mechanism proposed originally by Caplow (1968) for the reaction of CO_2 with secondary amines. However, the second order forward reaction rate constant for the zwitterion formation step (an acid-base reaction) was found to be much higher than that for alkanolamines of similar basicity. This indicates that the Brønsted plot for amino acids could be different from that of alkanolamines. Also, the contribution of water in the zwitterion deprotonation was found to be significantly higher in comparison to the reported values for secondary alkanolamines.

The equilibrium solubility of CO_2 in aqueous potassium taurate solutions is important for the design of a membrane gas absorber. The solubility data were measured at 298 K for amino acid salt concentrations between 500 mol m^{-3} and 4000 mol m^{-3}, in the range of CO_2 partial pressures between 0.1 and 7.0 kPa. A limited number of experimental measurements was also carried out at 313 K. Crystallisation of one of the reaction products was encountered during the equilibrium measurements, for potassium taurate concentrations higher than 2000 mol m^{-3} at 298 K. The solubility data measured in the absence of crystallisation were found to be comparable to the reported data for primary alkanolamines (say monoethanolamine). However, there is a significant difference in the thermodynamic characteristics of the unloaded and loaded solutions of aqueous alkanolamines and amino acid salts. This is basically due to the differences in the ionic charges associated with the reactant and product species involved in the reaction equilibria. The Deshmukh-Mather model (Deshmukh & Mather, 1981), originally proposed to accurately describe the acid gas-alkanolamine equilibrium was adapted to the present system. In the range of CO_2 loadings studied in the present work (0.35-0.63 mole CO_2 per mole salt; for measurements at 298K), the change in the ionic strength of the solution was found to be insignificant. Consequently,

the Deshmukh-Mather model basically reduced to a model similar to the one proposed by Kent and Eisenberg (1976). This model was used to further analyse the experimental solubility data, measured in the absence of crystallisation, to obtain the carbamate hydrolysis and amine deprotonation equilibrium constant.

As mentioned earlier, crystallisation was encountered during the equilibrium measurements, for potassium taurate concentrations higher than 2000 mol m^{-3} at 298 K. The analysis of the crystallised solids in the reactor indicated that it is the protonated amine (or the zwitterionic form of taurine), which is formed during the reaction of CO_2 with aqueous potassium taurate solutions. The experimentally measured critical CO_2 loading value at which crystallisation occurred was found to be inversely proportional to the initial amino acid salt concentration. A simple relation was found to exist between the critical CO_2 loading value, the initial amino acid salt concentration and the solubility of the amino acid in the solution.

The influence of crystallisation of the protonated amine (a reaction product) on the equilibrium CO_2 absorption capacity of the potassium taurate solution was quantitatively investigated. The crystallisation of the reaction product from the solution was found to significantly enhance the equilibrium solubility of CO_2 due to the shift in the reaction equilibrium towards the product side. Crystallisation during CO_2 absorption, occurring already at moderate loadings in solutions of high potassium taurate concentrations, can seriously limit their use in membrane contactors due to plugging of the hollow fibers by the solids formed. However, this phenomenon can also be advantageously used in other types of gas-liquid contactors for the bulk removal of CO_2.

The influence of crystallisation of a reaction product on the gas-liquid mass transfer characteristics of a stirred reactor was semi-quantitatively investigated. The volumetric mass transfer coefficient (k_La) was determined from the physical absorption rate of N_2O in potassium taurate solutions with different CO_2 loading (in the presence and absence of crystals). Since the solids formed do not have any specific physical or chemical interaction with the gas absorbed, the k_La was found to decrease in the presence of the crystals.

The carbamate hydrolysis equilibrium constant, used in prediction of the equilibrium solubility of CO_2 in aqueous amine solutions was measured experimentally for the potassium salt of taurine and monoethanolamine. The stability of the carbamate (inversely related to the carbamate hydrolysis constant) of taurine at low ionic strengths was found to be comparable to the reported values for similar amino acids like glycine, β-alanine and primary alkanolamines. Though the ionic strength of the solution was found to have a significant influence on the carbamate hydrolysis constant of monoethanolamine, the same could not be established for aqueous potassium taurate due to limited range of experimental data. However, the carbamate hydrolysis constant obtained by fitting the vapor-liquid equilibrium model to the experimental data was found to show a very strong dependence on the ionic strength of the solution.

The wetting and non-wetting characteristics of aqueous alkanolamines and amino acid salt solutions respectively were investigated for a hydrophobic membrane by measuring the breakthrough pressure of the liquid into the pores of the membrane. The surface tension of the above two classes of liquids was also measured. The dependence of the breakthrough pressure on the surface tension of the liquid followed the Laplace-Young equation.

The performance of the new absorption liquid in the CO_2 removal was studied in a single fiber membrane gas-liquid contactor over a wide range of partial pressures of CO_2 as well as amino acid salt concentrations. The reliability of the experimental set-up was tested by performing experiments with model non-reactive (absorption of CO_2/N_2O in water) and reactive (absorption of CO_2 in aqueous NaOH solutions) absorption systems. A numerical model to describe the mass transfer accompanied by multiple chemical reactions occurring during the absorption of CO_2 in aqueous amino acid salt solutions flowing through the hollow fiber was developed. The physico-chemical parameters such as physical solubility, diffusion coefficient and reaction kinetics obtained independently in the present project were used in the numerical model to predict the absorption flux of CO_2. The model predicted the experimental absorption flux measurements reasonably well and it gave an indirect indication on the accuracy of these physico-chemical parameters also. The stability of gas-liquid contacting with a microporous polypropylene membrane and aqueous potassium taurate solutions was shown by long duration experiments.

Approximate solutions for the enhancement factor, developed originally to quantify the influence of a chemical reaction in enhancing the mass transfer rate over physical absorption, for a gas-liquid system with a well mixed bulk were adapted to situations where a liquid bulk may be absent and, in addition, a velocity gradient is present in the mass transfer zone. The later described situation is present during the reactive absorption of a gas in a liquid flowing through a hollow fiber. The approximate solution of DeCoursey (1974) was used as a representative from the traditional approximate solutions. The limitations and the range of applicability of the approximate solution were discussed and also experimentally verified.

The single fiber membrane contactor in which the liquid flows through a hollow fiber can be used as a model gas-liquid contactor due to its well-defined liquid hydrodynamics (similar to a laminar jet or wetted wall column). It was demonstrated with a model gas-liquid reaction that the above contactor can be used (in combination with the approximate solutions for the enhancement factor) to conveniently determine the physico-chemical parameters from the experimental absorption flux or vice-versa.

References

Caplow, M., (1968). Kinetics of carbamate formation and breakdown, *Journal of American Chemical Society*, **90(24)**, 6795-6803.

DeCoursey, W.J. (1974). Absorption with chemical reaction: development of a new relation for the Danckwerts model. *Chemical Engineering Science*, **29**, 1867-1872.

Deshmukh, R.D., & Mather, A.E. (1981). A mathematical model for equilibrium solubility of hydrogen sulfide and carbon dioxide in aqueous alkanolamine solutions. *Chemical Engineering Science*, **36**, 355-362.

Feron, P.H.M. & Jansen, A.E. (1998). Method for gas absorption across a membrane. US Patent No. US5749941.

Gottlicher, G., & Pruschek, R. (1997). Comparison of CO_2 removal systems for fossil fueled power plant processes. *Energy Conversion & Management*, **38**, S173-S178.

Gubbins, K.E., Bhatia, K.K., & Walker, R.D. (1966). Diffusion of gases in electrolytic solutions. *AIChE Journal*, **12**, 548-552.

Kent, R., & Eisenberg, B. (1976). Better data for amine treating. *Hydrocarbon Processing*, **55**, 87-90.

Kreulen, H. (1993). Microporous membranes in gas separation processes using a liquid phase. Ph.D. Thesis, University of Twente, The Netherlands.

Schumpe, A. (1993). The estimation of gas solubilities in salt solutions. *Chemical Engineering Science*, **48**, 153-158.

Samenvatting

De selectieve of bulkverwijdering van CO_2 uit industriële gasstromen door middel van reactieve absorptie in een vloeistof is sinds lange tijd een belangrijke stap in de procesindustrie. Recentelijk staat met name de bulkverwijdering van CO_2 uit rookgassen sterk in de belangstelling vanwege de vermoedelijke rol die dit gas speelt bij het zogenaamde broeikaseffect, een term waarmee de geleidelijke opwarming van de aarde wordt aangeduid. Traditioneel wordt CO_2 uit gasstromen verwijderd middels (chemische dan wel fysische) absorptie in een vloeistof en uitgevoerd in absorptiekolommen die al dan niet gepakt zijn. Dit is een zeer energie-intensief proces en is economisch dan ook alleen maar aantrekkelijk indien de CO_2 verwijdering tot een duidelijke toename van de waarde van het eindprodukt leidt zoals bij de productie van aardgas. In andere gevallen, zoals bij de verwijdering van CO_2 uit de rookgassen van een electriciteitscentrale, is de verwijdering milieutechnisch gezien wenselijk. In zulke gevallen kan de energie en scheidingsefficiency van het scheidingsproces een zeer bepalende factor worden in de economische haalbaarheid van het integrale produktieproces (Gottlicher & Pruschek, 1997).

Scheidingsprocessen die gebaseerd zijn op het gebruik van membranen, zoals ultrafiltratie, nanofiltratie en omgekeerde osmose, staan mede bekend vanwege hun efficiënte gebruik van energie. Het wordt dan ook verwacht dat processen die gebruik maken van membranen in de nabije toekomst een wezenlijke rol gaan spelen in het (selectief) verwijderen van CO_2 uit verschillende gasstromen. Het gebruik van dichte membranen lijkt daartoe niet economisch haalbaar als gevolg van de lage CO_2/N_2 selectiviteit van de nu commercieel verkrijgbare membranen. Voordat zulke dichte membranen succesvol kunnen worden toegepast voor de verwijdering van CO_2 uit rookgassen moet er dan ook een aanzienlijke toename van de selectiviteit bereikt worden aangezien het gehalte van CO_2 in deze rookgassen laag is en dat van N_2 hoog (Gottlicher & Pruschek, 1997).

In een meer recente ontwikkeling worden modules die bestaan uit micro-poreuze membranen (gewoonlijk holle vezels) gebruikt als gas-vloeistof contactoren. In dit hybride proces (bekend staand als Membraan Gas Absorptie) wordt de hoge scheidingsselectiviteit (zelfs bij lage concentraties van het gas dat verwijderd moet worden) zoals die optreedt bij traditionele wasprocessen gecombineerd met de hoge flexibiliteit, modulaire opschaling en compactheid van de modules die in de membraanscheidingswereld gebruikt worden. Bij de ontwikkeling van Membraan Gas Absorptie (MGA) processen heeft men zoveel mogelijk getracht de traditionele wasvloeistoffen te gebruiken (die hun geschiktheid al lange tijd bewezen hebben in traditionele contactoren) in combinatie met goedkope en alom verkrijgbare microporeuze membranen. Er is in de literatuur een grote hoeveelheid kennis beschikbaar over de chemisch/fysische parameters van deze wasvloeistoffen, welke tevens nodig is voor het ontwerpen van een MGA module. Een zeer belangrijke voorwaarde voor het succesvol kunnen toepassen van de wasvloeistoffen is dat de wasvloeistof het

membraan niet mag bevochtigen aangezien in dat geval een aanzienlijke toename van de overall stofoverdrachtsweerstand wordt verkregen. Dit heeft men in een relatief korte periode weten te realiseren bij de ontwikkeling van MGA processen voor de verwijdering van SO_2 en NH_3. Voor de verwijdering van CO_2 wordt traditioneel gebruik gemaakt van alkanolamine oplossingen, maar deze blijken de commercieel aantrekkelijke en beschikbare polyolefine membranen te bevochtigen (Kreulen, 1993).

Het huidige project is geïnitieerd met als doel stabiele membraan gas-vloeistof contactoren te ontwikkelen die gebruikt kunnen worden voor de verwijdering van CO_2 uit met name rookgassen. Zoals eerder vermeld kan het membraan gas-vloeistof proces alleen dan stabiel opereren indien de gebruikte wasvloeistof het geselecteerde membraan niet bevochtigt. Als één van de opties die beschikbaar is voor het vermijden van deze bevochtiging (alle andere opties worden besproken in de introductie) is het gebruik van wasvloeistoffen anders dan alkanolamines in combinatie met commercieel verkrijgbare polypropyleen membranen bestudeerd. TNO-MEP heeft verschillende CO_2 absorptievloeistoffen ontwikkeld en het gebruik ervan in combinatie met MGA modules gepatenteerd. Deze vloeistoffen worden CORAL (CO_2 Removal Absorption Liquid) genoemd en zijn gebaseerd op waterige basische zoutoplossingen van aminozuren (Feron & Jansen, 1998). Van deze zouten is kwalitatief bekend dat ze in water een soortgelijke CO_2 absorptiecapaciteit en snelheid vertonen als vergelijkbare alkanolamines. Als additioneel voordeel hebben deze CORAL zoutoplossingen ook nog eens een verhoogde oxidatieve stabiliteit, wat ze potentieel geschikt maakt als vervanger van alkanolamines in traditionele gaswassers voor het behandelen van gasstromen die veel zuurstof bevatten (bijv. rookgassen). Als representant van de alkalische zouten van de aminozuren is in dit onderzoek het gedrag van met name kaliumtauraat bestudeerd omdat dit naast de eerder genoemde voordelen ook nog eens een hoge thermische stabiliteit bezit. Om een indicatieve vergelijking tussen de verschillende aminozuren mogelijk te maken is daarnaast ook nog een aantal experimenten uitgevoerd met het kaliumzout van glycine.

Bij de verwijdering van CO_2 uit gasstromen middels absorptie ligt de voornaamste stofoverdrachtsweerstand normaliter in de vloeistof. Het belangrijkste doel van dit onderzoek is dan ook geweest de bestudering en beschrijving van het gas-vloeistof stofoverdrachtsproces met chemische reactie welke optreedt tijdens de absorptie van CO_2 in een aantal geselecteerde CORAL oplossingen.

In tegenstelling tot waterige alkanolamines is er voor CORAL vloeistoffen slechts een zeer beperkte hoeveelheid data beschikbaar over de fysisch/chemische parameters. Deze data zijn niet alleen benodigd voor een betrouwbaar ontwerp van een MGA module. Een groot aantal fysisch/chemische data -zoals dichtheid, viscositeit, fysische oplosbaarheid en de diffusiecoëfficiënt van CO_2 in deze CORAL oplossingen- is ook nodig voor het bepalen van o.a. kinetiek en de evenwichtsligging. Er zijn echter geen data beschikbaar voor het systeem kaliumtauraat/CO_2 en dus zijn deze bepaald. Omdat CO_2 met CORAL vloeistoffen reageert moet de fysische oplosbaarheid en de diffusiecoëfficiënt van CO_2 via een indirecte weg worden bepaald. Daartoe is de fysische oplosbaarheid van N_2O in waterige

kaliumtauraat oplossingen over een brede range van temperaturen en concentraties gemeten. Omdat de oplossingen electroliet oplossingen zijn, kon voor de beschrijving van de experimentele data succesvol gebruik worden gemaakt van het model van Schumpe (Schumpe, 1993). Aan de hand van de ionspecifieke constanten die in een uitgebreide databank van Schumpe worden genoemd, kon de temperatuur onafhankelijke ionspecifieke constante voor het anion (in dit geval dus het tauraat of het glycinaat ion) worden vastgesteld. Door nu wederom gebruik te maken van het model van Schumpe kon de fysische oplosbaarheid van CO_2 in de kaliumtauraat en kaliumglycinaat oplossingen worden afgeschat.

De diffusiecoëfficiënt van N_2O in waterige kaliumtauraat oplossingen is bepaald in een diafragmacel. De verkregen data zijn gecorreleerd aan de viscositeit van de oplossingen door gebruik te maken van een gemodificeerde Stokes-Einstein relatie. Gubbins et al. (1966) heeft met een uitgebreide experimentele studie aangetoond dat de verhouding van de diffusiecoëfficiënt van een gas in een electrolietoplossing en die in water onafhankelijk is van het gas. Op basis van deze conclusie is het nu mogelijk de diffusiecoëfficiënt van CO_2 in CORAL oplossingen af te schatten aan de hand van de diffusiecoëfficiënt van N_2O in deze CORAL oplossingen en de diffusiecoëfficiënt van beide gassen in water.

De kinetiek van de reactie van CO_2 met de geselecteerde CORAL oplossingen is in een geroerde cel reactor met vlak gas-vloeistof grensvlak bestudeerd. De temperatuur is daarbij gevarieerd tussen de 285 K en 305 K en de kaliumtauraatconcentratie tussen de 100 mol m^{-3} en 4000 mol m^{-3}. Een beperkt aantal experimenten is tevens uitgevoerd met kaliumglycinaat bij 298 K om een onderlinge vergelijking tussen de twee CORAL representanten mogelijk te maken. Bij lage concentraties blijkt de reactiviteit van de bestudeerde CORAL oplossingen vergelijkbaar met die van oplossingen van alkanolamines met soortgelijke pK_a. In tegenstelling tot primaire alkanolamines blijkt de reactieorde in het aminozuur echter niet constant, maar neemt van 1 bij lage concentraties toe tot 1.5 bij concentraties vanaf 3000 mol m^{-3}. Dit gedrag, dat kenmerkend is voor secundaire alkanolamines, is zowel voor het de tauraat als de glycinaat oplossingen bij alle bestudeerde temperaturen waargenomen. De verkregen data konden goed worden beschreven met het zwitterion mechanisme dat oorspronkelijk door Caplow (1968) is voorgesteld voor de reactie van CO_2 met secundaire alkanolamines. De tweede-orde reactiesnelheidsconstante voor de vorming van het zwitterion blijkt echter aanzienlijk hoger dan de uit de literatuur bekende reactiesnelheidsconstanten voor vergelijkbare alkanolamines. Dit geeft aan dat de Brønsted plot voor de bestudeerde CORAL mogelijkerwijs anders is dan die voor alkanolamines. Hiernaast is tevens vastgesteld dat de bijdrage van water aan de deprotonatiesnelheid van het zwitterion beduidend hoger ligt dan de in de literatuur vermelde waarden voor secundaire alkanolamines.

De evenwichtsoplosbaarheid van CO_2 in waterige CORAL oplossingen is een belangrijke parameter in het ontwerp van een MGA module die gebruik maakt van deze oplossingen. De CO_2 oplosbaarheidsdata bij 298 K zijn gemeten voor kaliumtauraatoplossingen met een concentratie tussen de 500 mol m^{-3} en 4000 mol m^{-3} en

bij CO_2 partiaaldrukken tussen de 0.1 en 7.0 kPa. Tevens is een beperkt aantal metingen bij 313 K uitgevoerd. Bij de experimenten is voor concentraties hoger dan 2000 mol m^{-3} kristallisatie van één van de reactieprodukten geconstateerd. De oplosbaarheidsdata die in afwezigheid van het neerslag verkregen zijn, zijn vergelijkbaar met de data zoals die voor primaire alkanolamines in de literatuur vermeld staan (zoals bijvoorbeeld voor Monoethanolamine). Er blijkt echter een belangrijk onderscheid te zijn in het thermodynamische gedrag van de alkanolamine oplossingen enerzijds en de kaliumtauraat oplossingen anderzijds. Dit wordt voornamelijk veroorzaakt door het verschil dat tussen de twee oplossingen voor de ladingen van reactanten/produkten aanwezig is. Het Deshmukh-Mather model (Deshmukh & Mather, 1981) dat oorspronkelijk ontwikkeld is voor CO_2/H_2S-alkanolamine systemen is toegepast op het huidige systeem. In de range van CO_2 beladingen die bestudeerd is (bijvoorbeeld 0.35-0.63 mol CO_2 per mol zout bij 298 K), bleek de ionensterkte van de oplossing nagenoeg constant. Dientengevolge kan het Deshmukh-Mather model vereenvoudigd worden tot een model dat gelijk is aan dat van Kent en Eisenberg (1976). Dat model is dan ook gebruikt om de in afwezigheid van kristallisatie verkregen experimentele evenwichtsdata te interpreteren. Vervolgens zijn met het model de carbamaat hydrolyseconstante en de amine deprotonatieconstante bepaald.

Zoals eerder vermeld trad er bij 298 K bij kaliumtauraat concentraties hoger dan 2000 mol m^{-3} neerslagvorming op. Analyse van het neerslag wees uit dat dit het geprotoneerde amine is dat overall electroneutraal is (dit komt overeen met de zwitterion vorm van taurine). De experimenteel bepaalde kritische CO_2 belading (dit is de belading waar net neerslagvorming optreedt) bleek omgekeerd evenredig met de initiële kaliumtauraat concentratie. De kritische CO_2 belading kan middels een eenvoudige relatie berekend worden uit de initiële kaliumtauraat concentratie en de oplosbaarheid van taurine in de desbetreffende oplossing.

De invloed van de kristallisatie van het geprotoneerde amine (een reactieprodukt) op de CO_2 absorptiecapaciteit is kwantitatief bestudeerd. De neerslagvorming bleek een aanzienlijke stijging van de CO_2 absorptiecapaciteit te bewerkstelligen doordat het evenwicht naar de produktkant wordt gedreven. De neerslagvorming die blijkens de experimenten al bij relatief lage CO_2 belading kan optreden, kan de toepassing van de deze CORAL vloeistof in holle vezel membraancontactoren ernstig beperken als gevolg van mogelijke verstopping van de vezels met het gevormde neerslag. Daarentegen kan van de neerslagvorming in andere type contactoren die geen hinder ondervinden van een neerslag (bijvoorbeeld slurryreactoren) in positieve zin gebruik worden gemaakt voor een efficiënte CO_2 verwijdering aangezien de neerslagvorming een extra absorptiecapaciteit voor CO_2 creëert.

De invloed van de kristallisatie van een reactieprodukt op de stofoverdrachtskarakteristieken is semi-kwantitatief bestudeerd in een geroerde cel reactor met vlak gas-vloeistof grensvlak. De volumetrische stofoverdrachtscoefficient (k_La) is daarbij bepaald uit de fysische absorptiesnelheid van N_2O in kaliumtauraat oplossingen beladen met verschillende hoeveelheid CO_2 (in aan en afwezigheid van neerslag). Vanwege het feit dat het neerslag geen specifieke interactie vertoont met het geabsorbeerde gas, bleek

overeenkomstig de theoretische verwachtingen voor zulke systemen de k_La af te nemen in de aanwezigheid van het neerslag.

De carbamaathydrolyse evenwichtsconstante zoals die gebruikt wordt in de voorspelling van de CO_2 absorptiecapaciteit in amineoplossingen is experimenteel gemeten voor kaliumtauraat en Monoethanolamine. De stabiliteit van het carbamaat (die omgekeerd evenredig is met de carbamaat hydrolyseconstante) van kaliumtauraat bleek bij lage ionensterkte van de oplossing vergelijkbaar met de literatuurwaarden voor primaire alkanolamines en soortgelijke aminozuren als glycine en β-alanine. Alhoewel de ionensterkte van de oplossing een aanzienlijke invloed had op de carbamaathydrolyseconstante van Monoethanolamine, bleek dit effect voor de kaliumtauraatoplossing niet op te treden. Dit is mogelijk te verklaren door de beperkte experimentele range waarin deze constante voor kaliumtauraat is bepaald. Bij het fitten van de carbamaathydrolyseconstante aan de verkregen evenwichtsdata bleek namelijk dat deze constante wel degelijk een sterke afhankelijkheid van de ionensterkte van de oplossing vertoonde.

Het bevochtigingsgedrag van waterige alkanolamines en CORAL oplossingen is bestudeerd door voor een hydrofoob membraan de drukval over het membraan te bepalen waarbij het membraan begint door te lekken. Als onderdeel van deze studie is tevens de oppervlaktespanning van de gebruikte vloeistoffen bepaald. Er bleek dat de drukval over het membraan waarbij het membraan begint door te lekken volgens de Laplace-Young vergelijking van de oppervlaktespanning van de gebruikte vloeistof afhangt.

In een membraan gas-vloeistof contactor die bestaat uit één enkele vezel is het absorptiegedrag van CO_2 over een breed gebied van CO_2 partiaalspanningen en kaliumtauraat concentraties gemeten. Om de geschiktheid van de experimentele set-up te bestuderen zijn er eerst experimenten uitgevoerd met niet-reactieve (absorptie van CO_2/N_2O in water) en reactieve (absorptie van CO_2 in waterige NaOH oplossingen) wasvloeistoffen. Voor de beschrijving van de stofoverdracht en simultane reactie die tijdens de absorptie van CO_2 in de door de holle vezel stromende kaliumtauraatoplossing optreedt, is een model ontwikkeld. In het model zijn de verschillende fysisch/chemische parameters zoals in dit onderzoek onafhankelijk bepaald (o.a. diffusiecoëfficiënten, oplosbaarheden, kinetiek) in het model geïmplementeerd om zodoende de flux zonder te fitten te kunnen voorspellen. Het model bleek een redelijk accurate voorspelling van de experimentele flux op te leveren, wat een impliciet bewijs is voor de bruikbaarheid van de in de deelstudies verkregen data. Er zijn met de één-vezel opstelling lange duur experimenten uitgevoerd met een polypropyleen membraan en waterige kaliumtauraat oplossingen, waarbij de performance over de gehele periode constant bleef.

De in de literatuur voorkomende uitdrukkingen voor de versnellingsfactor (welke een maat geeft voor de versnelling van de stofoverdracht in situaties waarin reactie optreedt ten opzichte van situaties waarin fysische absorptie optreedt) zijn aangepast voor situaties waarin geen vloeistofbulk aanwezig is en bovendien een snelheidsgradiënt in de

stofoverdrachtszone aanwezig is. Het ontbreken van een vloeistofbulk en de aanwezigheid van een snelheidsgradiënt in de stofoverdrachtszone is van toepassing indien een vloeistof door een holle vezel stroomt. De benaderende oplossing van DeCoursey (1974) is bij deze studie als representatief voorbeeld van de benaderende oplossingen van de traditionele stofoverdrachtsmodellen gebruikt. De bruikbaarheid en de begrenzingen van de aangepaste oplossing van DeCoursey is bediscussieerd en ook experimenteel geverifieerd.

Tijdens dit onderzoek is gebleken dat de één-vezel membraanreactor een geschikte model reactor is vanwege de goed gedefinieerde vloeistof hydrodynamica in de vezel (vergelijkbaar met de natte wand kolom en laminaire jet). Voor een model gas-vloeistof reactie is aangetoond dat met gebruik van deze één-vezel membraanreactor een nauwkeurige bepaling van de fysisch/chemisch parameters mogelijk is.

Referenties

Caplow, M., (1968). Kinetics of carbamate formation and breakdown, *Journal of American Chemical Society*, **90(24)**, 6795-6803.

DeCoursey, W.J. (1974). Absorption with chemical reaction: development of a new relation for the Danckwerts model. *Chemical Engineering Science*, **29**, 1867-1872.

Deshmukh, R.D., & Mather, A.E. (1981). A mathematical model for equilibrium solubility of hydrogen sulfide and carbon dioxide in aqueous alkanolamine solutions. *Chemical Engineering Science*, **36**, 355-362.

Feron, P.H.M. & Jansen, A.E. (1998). Method for gas absorption across a membrane. US Patent No. US5749941.

Gottlicher, G., & Pruschek, R. (1997). Comparison of CO_2 removal systems for fossil fueled power plant processes. *Energy Conversion & Management*, **38**, S173-S178.

Gubbins, K.E., Bhatia, K.K., & Walker, R.D. (1966). Diffusion of gases in electrolytic solutions. *AIChE Journal*, **12**, 548-552.

Kent, R., & Eisenberg, B. (1976). Better data for amine treating. *Hydrocarbon Processing*, **55**, 87-90.

Kreulen, H. (1993). Microporous membranes in gas separation processes using a liquid phase. Ph.D. Thesis, University of Twente, The Netherlands.

Schumpe, A. (1993). The estimation of gas solubilities in salt solutions. *Chemical Engineering Science*, **48**, 153-158.

Kumar, P.S., Hogendoorn, J.A., Feron, P.H.M., & Versteeg, G.F. (2001). Density, Viscosity, Solubility and Diffusion Coefficient of N_2O in Aqueous Amino acid Salt Solutions, *Journal of Chemical & Engineering Data*, **46**, 1357-1361.

Kumar, P.S., Hogendoorn, J.A., Feron, P.H.M., & Versteeg, G.F. (2002). New Absorption Liquids for the Removal of CO_2 from Dilute Gas Streams using Membrane Contactors, *Chemical Engineering Science,* **57(9)**, 1639-1651.

Kumar, P.S., Hogendoorn, J.A., Feron, P.H.M., & Versteeg, G.F. (2002). Kinetics of the Reaction of Carbon Dioxide with Aqueous Potassium Salt Solutions of Taurine and Glycine, *AIChE Journal* (Accepted for publication).

Kumar, P.S., Hogendoorn, J.A., Feron, P.H.M., & Versteeg, G.F. (2002). Approximate Solution to Predict the Enhancement Factor for the Reactive Absorption of a Gas in a Liquid Flowing through a Hollow Fiber. *Chemical Engineering Research and Design* (Submitted).

Kumar, P.S., Hogendoorn, J.A., Timmer, S.J., Feron, P.H.M., & Versteeg, G.F. (2002). Equilibrium Solubility of CO_2 in Aqueous Potassium Taurate Solutions (To be published).

Kumar, P.S., Hogendoorn, J.A., Feron, P.H.M., & Versteeg, G.F. (2002). Crystallisation in CO_2 Loaded Aqueous Alkaline Salt Solutions of Amino Acids (To be published).

Oral Presentations

Kumar, P.S., Hogendoorn, J.A., Feron, P.H.M., & Versteeg, G.F. (2000). Membrane Gas Absorption Systems - Some recent developments, *International Seminar on Reactive Separation Technologies*, KVIV, 21st March, Antwerp (Belgium).

Kumar, P.S., Hogendoorn, J.A., Feron, P.H.M., & Versteeg, G.F. (2000). CO_2 recovery using Membrane Gas Absorption Systems, *Industrial Chemistry Awards Symposium honoring Guido Saratori*, Division of Industrial and Engineering Chemistry, American Chemical Society, 26-30 March, San Francisco (USA).

Kumar, P.S., Hogendoorn, J.A., Feron, P.H.M., & Versteeg, G.F. (2001). New Absorption Liquids for the Removal of CO_2 from Dilute Gas Streams using Membrane Contactors, *International Symposium on Multifunctional Reactors (ISMR-2)*, EFCE, 26-28 June, Nuremberg (Germany).

Kumar, P.S., Hogendoorn, J.A., Feron, P.H.M., & Versteeg, G.F. (2001). Absorption Liquids for the Removal of CO_2 from Dilute Gas Streams using Stable Membrane Contactors, *Nederlands Processtechnologie Symposium (NPS)*, OSPT, 17-18 September, Lunteren (The Netherlands).

Patent

Versteeg, G.F., Kumar, P.S., Hogendoorn, J.A., & Feron, P.H.M. (2002). Methode voor absorptie van zure gassen (NL Patent; Application Filed).

Acknowledgements

It was a wonderful and satisfying experience gained at the University of Twente in general and OOIP/PK group in particular. Professionally, I am happy to have worked in a green field project of industrial relevance in close cooperation with TNO-MEP, an institute of international reputation. The project overlapped multiple disciplines of chemical engineering science and therefore the objectives were broad enough to steer it in a direction of personal interest without compromising the interest of the research group as well as TNO. I am grateful to my promotor, Prof. Geert Versteeg for offering me an opportunity to work in this project and providing the maximum possible freedom in the research work as well as helping me to keep focussed to finish it well in time. His expertise in reactive absorption, especially amine-CO_2 systems was very valuable at every stage of the project. It was a great time to work with Dr. Hogendoorn as my assistant promotor. As a person with whom I had the maximum professional interaction at Twente, I greatly admire his two of his best qualities, i.e., sharp analytical skills and plain speaking. In spite of his many commitments, the extra effort he took in correcting the chapters of the thesis towards the end resulted in a comfortable finish. Thank you, Kees!

A great part of this thesis has been crafted from the valuable work of many undergraduate students from UT and HTS, Enschede. It was a pleasant experience to work with these guys with different personalities and educational backgrounds. Pieter Derksen measured the diffusion coefficients in a diaphragm diffusion cell, a challenging experimental task requiring a lot of patience. Nanne Ongena in a brief time measured a part of the reaction kinetics. Leon Laagwater did experimental work in the single fiber membrane contactor. Sven Timmer did the CO_2-amine equilibria measurements and came out with some interesting experimental results. Thanks lot guys. Thanks to Praveen for the cooperation, which led to the development of VLE model for CO_2-amine systems. Special thanks go to Paul Feron for his enthusiastic interest in my research work. He shared a lot of useful information/data from his independent experiments at TNO and the numerous discussions we had during his trips to Twente on various occasions were very supportive. Many thanks to Nicole for managing many things beyond my control and all with a smile.

It's practically not possible to conduct experimental research work in reaction engineering without the skilled hands of the technicians. I had the luxury of utilising the amazing ideas and skills of all the four technicians of the OOIP and FAP group. In the initial days in Twente, Wim Leppink provided an excellent support with practical ideas and speedy construction of the kinetics and membrane contactor setups. Gerrit Schorfhaar built the diaphragm diffusion cell. Henk Jan constructed the equilibrium cell and helped me in solving many mysterious problems associated with the instrumentation. Benno provided the crucial back up with quick solutions for the problems during the experiments. Above all, it was a great time talking to them during many informal dinners. Thanks also goes to Robert Meijer for helping me in solving the problems related to the data acquisition systems and Wim Lengton for guiding me in developing the analytical techniques (especially for determining the CO_2 loading in the liquid phase).

The wonderful interaction with the staff members of the OOIP and FAP group needs special mention. I am grateful to Hans Kuipers for his generous help in the numerical work, in the initial phase of the project and also for being instrumental in my selection to the present project in the erstwhile PK group. Also thanks to Wim (Brilman) for his spontaneous help in various issues concerning the research work. It was always pleasant to talk to Bert (Heesink) on all issues and in particular I thank him for the counseling on the various aspects of career development.

Most gratitude goes to all the AiOs, TWAiOs and undergrad students of the Vlugter lab, with whom I spent most of my time in Twente. The cultural diversity in the Vlugter lab provided a vibrant life lab and has no comparison. It was great time sharing the office with Toine for the last couple of years. Many technical discussions, especially the one on zwitterion mechanism was wonderful. Gerhard, Vishwas and Mousa, it was a nice time with all of you. Thanks to Esther for the cooperation and the initiatives in organising the Vlugter lab lecture series.

Friends around us make the world wonderful. Special thanks to Kapil, Pranay and Mujeeb with whom my friendship goes back to the days in UDCT. They have always been a source of fun, inspiration and motivation. Thanks to Uli and Ivayla for the many gaming evenings, informal dinners and wine feasts. In addition, thanks also go to members of the “Tadka group” namely Parasu, Vishwas, Dhanya, Salim, Aseesh, Amrish, Kalyani, Ranjit, Lilia and Jay. I also owe a lot to my former and current flat-mates in Calslaan and Matenweg for giving me a memorable stay in Twente.

Thanks to Dr. Seshan and Jayanthi for their hospitality and motivation during the last three years in Twente. I greatly enjoyed the innumerous evenings and weekend trips to many near by and far off places. Thanks to Dr. Lenin and his family for their hospitality in Enschede and Antwerp. My interest in research was stimulated by Prof. Pandit at UDCT and I still cherish the days in UDCT. I thank him and Prof. Joshi for recommending me to Twente and the continuous motivation thereafter.

The greatest are those souls who think and act for your welfare behind the scenes. I wish to extend the deepest sense of gratitude to my parents who missed me at home for nearly a decade and always inspired and motivated me to go for best, in spite of many testing times at their end. Their blessings and immense belief in my ability had helped me to sail through many turbulent times. I also owe hearty thanks to my sister, Uma and Uncle, Kandaswamy for their continuous support. I had always waited for the Friday evenings when I usually called them and spoke to their kids, Anitha and Vishnu. It was very refreshing. Thanks also go to Velusamy anna’s family and Dr. Somasundaram’s family for their continuous inspiration.

I thank all those whom I missed to mention explicitly for helping me to see this day. Thank you everybody.

Senthil

Résumé

Paramasivam Senthil Kumar was born on February 9, 1974 in Velur, India. After completing his higher secondary schooling at Bharathiya Vidya Bhavan School, Erode, he joined Coimbatore Institute of Technology, an autonomous institution affiliated to Bharathiyar University, Coimbatore to obtain his Bachelors in Chemical Technology.

Subsequently, he received a Junior Research Fellowship (JRF) from the University Grants Commission, New Delhi and joined the Department of Chemical Technology (UDCT), University of Bombay in August 1995 for his Masters in Chemical Engineering. He worked on a dissertation titled “Modeling and Scale-up of Cavitational Reactors” with the guidance of Prof. Dr. A.B. Pandit.

From May 1997, he worked as a research associate in the group of Prof. A.B. Pandit in a project titled “Effect of Soaker Geometry and Internals on Visbreaking Process”, funded by Center for High Technology (CHT), Ministry of Petroleum, Government of India, New Delhi. From May 1998, he worked for a short time with Elf Atochem Peroxides India Ltd., Madras as a Process Engineer in the Process Development group.

In November 1998, he joined a Ph.D. project in the OOIP group, University of Twente, The Netherlands, to conduct research on the development of membrane gas-liquid contactors for the removal of carbon dioxide from industrial gas streams. He was guided in his research work by Prof. dr. ir. G.F. Versteeg. From August 2002, he will be working for Shell Global Solutions International NV, Den Haag, as a research staff in the LNG business group.